Phenomena in Mixed Surfactant Systems

ACS SYMPOSIUM SERIES **311**

Phenomena in Mixed Surfactant Systems

John F. Scamehorn, EDITOR

University of Oklahoma

Developed from a symposium sponsored by
the ACS Division of Colloid and Surface Chemistry
at the 59th Colloid and Surface Science Symposium
and the 5th International Conference
on Surface and Colloid Science,
Potsdam, New York,
June 24–28, 1985

American Chemical Society, Washington, DC 1986

ACS Symposium Series

M. Joan Comstock, *Series Editor*

Advisory Board

FOREWORD

The ACS SYMPOSIUM SERIES was founded in 1974 to provide a medium for publishing symposia quickly in book form. The format of the Series parallels that of the continuing ADVANCES IN CHEMISTRY SERIES except that, in order to save time, the papers are not typeset but are reproduced as they are submitted by the authors in camera-ready form. Papers are reviewed under the supervision of the Editors with the assistance of the Series Advisory Board and are selected to maintain the integrity of the symposia; however, verbatim reproductions of previously published papers are not accepted. Both reviews and reports of research are acceptable, because symposia may embrace both types of presentation.

PREFACE

$\mathbf{M}$IXED SURFACTANT SYSTEMS are of scientific interest as well as technological value. Surfactants are used in numerous applications, including detergents, flotation, enhanced oil recovery, surface-wetting modification, foaming control, emulsification, controlled-release, and surfactant-based separation processes. Commercial surfactants are almost always composed of mixtures of surfactants. The production of single-component surfactants is generally expensive, and the properties of monoisomerically pure surfactants are rarely better than the surfactant mixtures. Often, the mixture may exhibit superior behavior compared to the pure surfactant components. It is an enormous challenge to understand the interactions between different surfactant components in the various applications in which surfactants are used.

This book presents chapters that discuss research on surfactant mixture behavior from a variety of active researchers around the world. I am grateful to the organizing committee of the symposium on which this book is based for allowing me to organize and chair sessions on this topic and especially to Josip Kratohvil for organizing the logistics of the program in such an efficient fashion.

I thank departmental staff Polly Dvorak, Sherry Childress, and Rick Wheeler for their efficient help with correspondence associated with the book. Kevin Stellner and Jim Rathman helped me by proofreading the first draft of the manuscripts. Cuong Nguyen provided the figure upon which the drawing on the cover of this book is based. I would also like to thank the authors who participated in this effort and the reviewers who must remain anonymous. Finally, I would like to thank my colleagues and graduate students at the University of Oklahoma for stimulating interactions and for helping to keep my perspective fresh and my interest in surfactants high.

JOHN F. SCAMEHORN
School of Chemical Engineering
   and Materials Science
University of Oklahoma
Norman, OK 73019

January 6, 1986

An Overview of Phenomena Involving Surfactant Mixtures

John F. Scamehorn

School of Chemical Engineering and Materials Science, University of Oklahoma, Norman, OK 73019

        The effect of using mixtures of surfactants
        on micelle formation, monolayer formation,
        solubilization,   adsorption, precipitation,
        and cloud point phenomena is discussed.
        Mechanisms of   surfactant   interaction and
        some   models   useful   in   describing   these
        phenomena   are   outlined.   The   use   of
        surfactant mixtures to solve   technological
        problems is also considered.

Surfactants used in   practical   applications   essentially
always   consist of a mixture of surface-active compounds.
Isomerically pure   surfactants   are   often   expensive   to
produce   and   generally   have   only   a   small   potential
advantage   in   performance   over   the   less   expensive
surfactant   mixtures.   In many applications,   mixtures of
dissimilar surfactants can have   superior   properties   to
those   of   the individual surfactant components involved.
These synergistic properties of surfactant mixtures   have
provided impetus for much of the research on interactions
between surfactants.
     Individual   surfactants   vary   'in   their tendency to
form aggregated structures.   Examples of such   aggregates
are micelles, precipitate, and monolayers.   In solutions
containing mixtures of surfactants,   the tendency to form
aggregated structures can be substantially different than
in   solutions   containing   only   the   pure   surfactants
involved.   For example,   precipitation may not occur in a
surfactant   mixture   whose   components   individually
precipitate   when   present   as   single   components.   The
tendency for components to distribute themselves between
the unaggregated state and an   aggregate   may   vary   from
component   to   component   for   mixtures.   Therefore,   for

example, the surfactant composition of a micelle may differ greatly from that of the surfactant monomer with which it is in equilibrium. This is important because the processes of interest may depend only on either monomer composition or on aggregate composition. For example, adsorption of surfactant on solids such as minerals depends only on monomer composition and concentration, not micellar properties. On the other hand, solubilization of compounds into micelles depends only on micellar composition.

The surfactant technologist needs to be able to predict and manipulate the tendency for surfactant mixtures to form aggregates, the properties of these aggregates, and the distribution of surfactant components between monomer and aggregate. A central theme of this paper is that mixtures of surfactants can achieve great synergisms in various processes by manipulation of the relative tendency to form various aggregated structures. Often, the formation of a certain aggregate will inhibit the formation of a less desirable aggregate. For example, addition of nonionic surfactants to anionic surfactants enhances the formation of micelles, resulting in a reduced tendency for the anionic surfactant to precipitate.

This overview will outline surfactant mixture properties and behavior in selected phenomena. Because of space limitations, not all of the many physical processes involving surfactant mixtures can be considered here, but some which are important and illustrative will be discussed: these are micelle formation, monolayer formation, solubilization, surfactant precipitation, surfactant adsorption on solids, and cloud point phenomena. Mechanisms of surfactant interaction will be discussed, as well as mathematical models which have been shown to be useful in describing these systems. Practical applications will be covered as part of the consideration of individual phenomena.

This overview will attempt to outline the state of current knowledge, without much comment on the areas in which further research is needed, the direction the field is taking, and the impact of the other chapters in this book. These are reserved for the Future Perspectives Chapter (last chapter of the book).

Micelle Formation

The structure and thermodynamics of formation of mixed micelles is of great theoretical interest. Micelles are also present and often integrally involved in practical processes. For example, in a small pore volume surfactant flooding process (sometimes called micellar flooding), the solution injected into an oil field generally contains 5-12 weight % surfactant ([1]) and the surfactant is predominately in micellar form in the reservoir water. In detergency, solubilization can be

important (2), so micelles are generally present in the
detergent   solution.   In   micellar-enhanced
ultrafiltration, a   separation   technique to remove
dissolved organic from water (3), micelles effect the
separation.

<u>Monomer-Micelle   Equilibria.</u> The   distribution   of
surfactant   components   between   micelles   and   monomeric
state   in   aqueous   solutions   depends   on   surfactant
structures   as   well   as on overall solution composition.
For example, for a binary system of surfactants A and B
in solution, the micelle may contain 50 mole % A/50 % B
while the monomer may be 90 % A/10 % B. Since either the
monomer or the micelle composition may be crucial to
behavior of the system, the ability to predict the
relative distribution of surfactant components between
monomer   and   micelle,   given   the   overall   solution
composition, is an important one.
     Except for some anionic/cationic surfactant mixtures
which form ion pairs, in a typical surfactant solution,
the   concentration   of   the   surfactant   components   as
monomeric   species   is   so dilute that no significant
interactions   between   surfactant   monomers   occur.
Therefore, the monomer-micelle equilibria is dictated by
the   tendency of the surfactant components to form
micelles and the interaction between surfactants in the
micelle.   Prediction   of   monomer-micelle   equilibria
reduces to modeling of the thermodynamics of mixed
micelle formation.
     The   behavior   of   mixed   micelles   is   commonly
approximated by using the pseudo-phase separation model
(4). This considers the micelles to be a separate
thermodynamic phase in equilibrium with the monomer.
Monomer-micelle equilibria then becomes analogous to
vapor-liquid equilibria; i.e., in both cases a dilute
phase   with   little   intermolecular   interaction   is   in
equilibrium with a   concentrated   phase   in   which
intercomponent interaction can be significant. The vast
array of solution thermodynamic models developed for
mixing in macroscopic phases can be utilized for mixed
micelles using the pseudo-phase approach.   The pseudo-
phase separation model is a good approximation when the
micellar aggregation number is greater than about 50 (5),
which is commonly the case for surfactants of commercial
importance.

<u>Ideal Mixed Micelles</u>. The Critical Micelle Concentration
(CMC) is the lowest surfactant concentration at which
micelles form; the lower the CMC, the greater the
tendency of a system to form micelles. When the total
surfactant concentration equals the CMC, an infintesimal
fraction of surfactant is present as micelles; therefore,
the CMC is equal to the total monomer concentration in
equilibrium with the micellar pseudo-phase. The CMC for
monomer-micelle equilibrium is analogous to the dew point
in vapor-liquid equilibrium.

The total monomer concentration of a binary mixture of two similarly structured surfactants of like charge (an ideal system) lies between the CMC's of the individual surfactants involved for total surfactant concentrations at or above the mixture CMC. Analogously, the vapor pressure of a mixed ideal liquid is intemediate between the vapor pressures of the components of which it is composed, whether there is substantial liquid present or the system is at the dew point (where an infintesimal amount of liquid is present).

For a binary system of surfactants A and B, the mixed micelle formation can be modeled by assuming that the thermodynamics of mixing in the micelle obeys ideal solution theory. When monomer and micelles are in equilibrium in the system, this results in:

$$C_M = CMC_A CMC_B / (y_A CMC_B + y_B CMC_A) \qquad (1)$$

$$x_A = y_A C_M / CMC_A \qquad (2)$$

where C_M is the total monomer concentration, CMC_A or CMC_B are the CMC values for the individual components, y_A or y_B are the monomer mole fractions of A or B, respectively, and x_A or x_B are the micellar mole fractions of A or B, respectively. The mole fractions are on a surfactant-only basis: i.e., y_A is the moles of A in monomer/ total moles of surfactant monomer. Therefore, $y_A + y_B = 1$ and $x_A + x_B = 1$. The values of CMC_A and CMC_B are needed at the same added electrolyte concentration as the mixture. If the total surfactant concentration in the mixed system is at the CMC (infintesimal number of micelles present), then C_M from Equation 1 is equal to the mixture CMC.

The mixture CMC is plotted as a function of monomer composition in Figure 1 for an ideal system. Equation 1 can be seen to provide an excellent description of the mixture CMC (equal to C_M for this case). Ideal solution theory as described here has been widely used for ideal surfactant systems (4,6-18). Equation 2 can be used to predict the micellar surfactant composition at any monomer surfactant composition, as illustrated in Figure 2. This relation has been experimentally confirmed (15-18). As seen in Figure 2, for an ideal system, if the ratio $x_A/y_A < 1$ at any composition, it will be so over the entire composition range. In classical phase equilibrium thermodynamic terms, the distribution coefficient between the micellar and monomer phases is independent of composition.

Equations 1 and 2 provide the ability to make a priori predictions of mixed micellar behavior for binary systems of similar surfactants (easily extended to more than 2 components(10)). No mixture data is necessary to use these equations. If the overall concentration of the individual surfactants in solution are known, Equations 1 and 2 can be combined with a material balance to
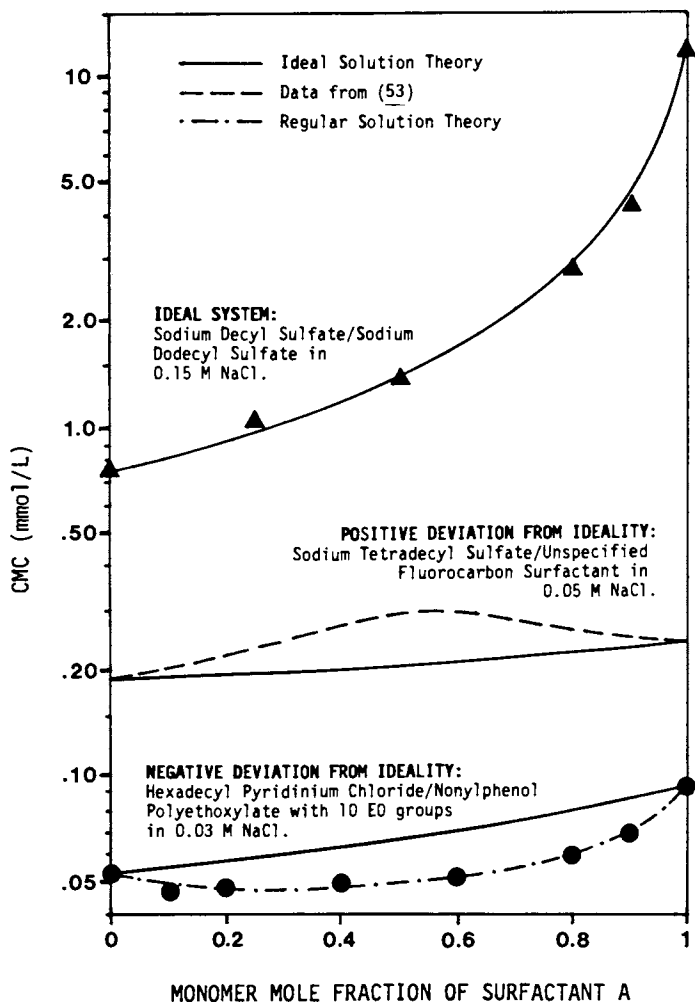
Figure 1. Mixed surfactant CMC values at 30°C (first surfactant listed is surfactant A).
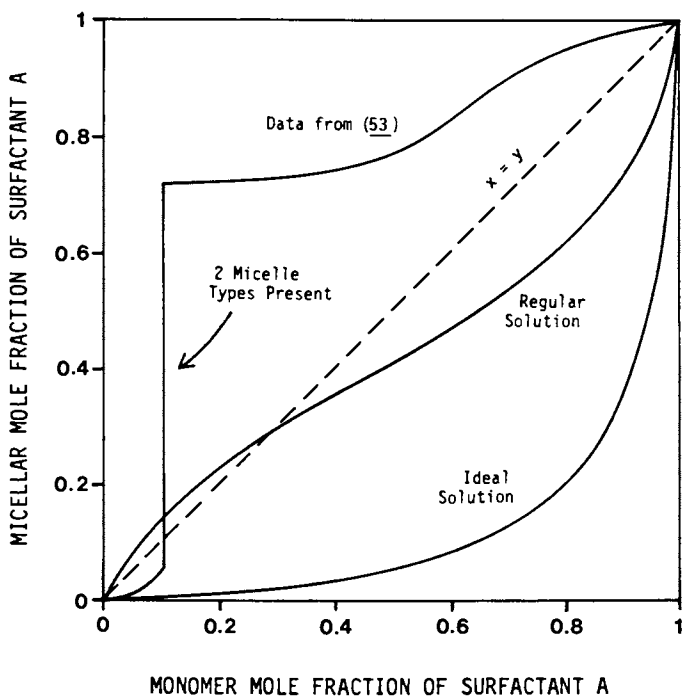
Figure 2.   Monomer-micelle equilibrium for systems in
Figure 1.

calculate the concentration of each surfactant in
monomeric form and micellar form. This predictive
capability is a powerful tool.

Mixed Micelles Showing Negative Deviation from Ideality.
In an aqueous solution containing a mixture of [1] an
ionic surfactant and a nonionic surfactant, or [2] an
anionic surfactant and a cationic surfactant, or [3] a
zwitterionic surfactant and an anionic surfactant, the
CMC of the mixed surfactant system exhibits a CMC which
is substantially less than that predicted by Equation 1
(9,12,18-37). This means that the mixed micelle
formation is enhanced and that the mixing process in the
micelle shows negative deviation from ideality. This is
demonstrated for a cationic/nonionic system in Figure 1.
      If the interactions between surfactants in the mixed
micelle can be described by regular solution theory, the
following equations apply for a binary system:

$$1 = \frac{y_A x_B CMC_B \exp[W(x_A^2 - x_B^2)/RT]}{y_B x_A CMC_A} \tag{3}$$

$$C_M = x_B CMC_B \exp[W x_A^2/RT])/y_B \tag{4}$$

where W is the interaction parameter, R is the gas
constant, and T is the absolute temperature. Once again,
C_M from Equations 3 and 4 is equivalent to the mixture
CMC when the total surfactant concentration is at the
CMC.
      Solution of Equation 3 at a given monomer
composition (y_A, y_B) result in predictions of values of
the the micellar composition (x_A, x_B). Then, solution of
Equation 4 predicts the value of the total monomer
concentration (C_M). However, this model does not give a
priori predictions. The adjustable parameter W is
needed. If a mixed CMC value is available, Equations 3
and 4 can be used to determine W by substituting the
measured CMC values for C_M. Then the model can predict
monomer-micelle equilibrium at any other system
composition. In fact, if multiple mixed CMC values are
available, a regression analysis is normally done to
determine the best value of W over the entire range of
measurements. Equations 3 and 4 have been widely used to
model CMC data for mixed surfactant systems showing
negative deviations from ideality (12,25-36). Equations
3 and 4 have been used to model the mixed
cationic/nonionic system in Figure 1. The model can be
seen to describe the data very well. The model can be
extended to include more than two surfactant components
(12). The predicted micellar compositions from Equations
3 (as illustrated in Figure 2) have also been
experimentally confirmed (25,34).
      The more negative the value of W (or W/RT which is
dimensionless), the greater the degree of nonideality of
the system. When W = 0, the system is ideal and

Equations 3 and 4 reduce to Equations 1 and 2. From tabulations of literature values of W/RT, some general conclusions about degree of interactions between dissimilar surfactants can be reached (31-34):

1. The deviation from ideality for binary pairs of surfactants increases in the order cationic/nonionic, anionic/nonionic, anionic/cationic.

2. The deviation from ideality decreases as added electrolyte concentration increases.

3. For an ionic/nonionic system, where the nonionic is a polyethoxylate, the greater the degree of polymerization of the polyoxyethylene hydrophilic group, the greater the deviation from ideality.

4. The deviation from ideality of a zwitterionic/anionic system can vary widely, from a value typical of a cationic/nonionic system to nearly that of a anionic/cationic system.

5. The deviation from ideality decreases as temperature increases for ionic/nonionic systems.

   Average values of W/RT from tabulated literature (33) at approximately room temperature and with no added electrolyte are -2.7 for cationic/nonionic systems; -3.4 for anionic/nonionic systems; and -19 for anionic/cationic systems.
   In order to illustrate the effect of micellar nonidealities of mixing on total surfactant monomer concentrations and micelle compositions in a system at the CMC, consider a hypothetical binary surfactant pair, A and B. Assume CMC_A = 1 mM and CMC_B = 2 mM. For a equimolar mixture of A and B as monomer, the values of C_M and micelle compositions are tabulated in Table I at various values of W/RT.

Table I. Total Monomer Concentrations and Micellar
Compositions for a Binary Surfactant System at
Various Deviations from Ideality

W/RT	C_M (mM)	x_A
0 (ideal system)	1.33	0.667
-2	0.83	0.586
-5	0.40	0.550
-25	0.0027	0.513

   As seen in Table I, for the ideal system, the values of C_M are between the CMC values of the two pure surfactant components. However, the systems showing

negative deviations from ideality could have mixture
monomer concentration values lower than either pure
surfactant. In fact, for a W/RT of −25 (possible for an
anionic/cationic mixture), the total surfactant monomer
concentration is less than 1% of that of either pure
component. Enormous monomer concentration depressions
are possible in these systems exhibiting negative
deviations from ideality. When it is desirable to
minimize monomer concentrations, these mixture effects
can be useful.

    As also seen in Table I, the micellar composition
can be affected substantially by nonideality. In fact,
azeotropic behavior in the monomer-micelle equilibrium is
possible for these nonideal systems; i.e., as the monomer
composition varies from pure A to pure B, the micelle can
vary from $x_A > y_A$ to $x_A = y_A$ (azeotrope) to $x_A < y_A$.
This azeotrope formation is illustrated for the
cationic/nonionic system in Figure 2, where an azeotrope
forms at $x_A = y_A = 0.3$. The minimum CMC for a mixture
corresponds to the azeotropic composition if an azeotrope
is present (32,37). For an ideal system, azeotropic
behavior is not observed.

    Systems with low monomer concentrations are of value
when micelles are participating in useful processes
directly (e.g., solubilization), where monomer is
"wasted" surfactant. However, often the monomer
composition as well as total monomer concentration is
important, when the monomer is participating in important
processes and each component interacts differently (e.g.,
adsorption). The surfactant combinations discussed here
can result in low monomer concentrations and the model
outlined can predict the monomer concentration of each
surfactant species.

Mechanisms of Nonideality. Similarly structured
surfactants mix ideally because the environments for the
hydrophobic and the hydrophilic groups in the mixed
micelle are similar to those in the pure component
micelle. When a nonionic surfactant is inserted into a
micelle composed of ionic surfactant, the nonionic
hydrophilic group separates charged ionic hydrophilic
groups from each other, reducing the electrical repulsion
in the Stern layer of the micelle (18-20,23,29,31,38,39).
In other words, the charge density at the micelle surface
is reduced, which reduces the absolute value of the
electrical potential there (40). It requires less work
to insert a ionic surfactant into this mixed micelle than
into a pure ionic micelle because of this reduced
electrical repulsion. This charge separation effect
causes the mixed micelle to form more easily than an
ideal mixed micelle and so the CMC is less than that of
an ideal mixed micelle.

    In addition to electrostatic forces, another
contribution to nonideality is due to the formation of
oxonium salts in the hydrophilic group of the nonionic

polyethoxylated surfactant ($\underline{21,23}$). These result from the association of cations (e.g., H^+ or Na^+) from solution with the negatively polarized ether oxygen atoms. The resulting net positive charge of the nonionic surfactant can also contribute to the stabilization of anionic/nonionic mixed micelles. This is the probable explanation for the generally greater nonideality of the anionic/nonionic systems over the cationic/nonionic systems. However, the number of oxonium ions formed is probably small, as evidenced by the similarity of W/RT for these two types of systems. If an ionic surfactant has a benzene ring in its hydrophobic group, the polyethoxylate group in a nonionic surfactant can interact with the aromatic ring in ionic/nonionic mixed micelles, resulting in an additional stabilizing force for these mixed micelles ($\underline{41,42}$). Electrostatic stabilization via the charge separation effect is the main cause of mixed ionic/nonionic surfactant deviations from ideality, with oxonium ion formation and benzene/ethylene oxide group interactions being a secondary effect. The anionic/cationic systems exhibit the ultimate in electrostatically induced nonidealities, with the oppositely charged surfactants combining to form extremely stable micelles.

In a mixed micelle composed of a polyethoxylated nonionic and an anionic surfactant, solubilization results (to be discussed in a later section) indicate that for short polyoxyethylene chains, the nonionic hydophobic groups are less compact than in a pure nonionic micelle because of the space taken up by the anionic hydrophilic group. That is, the volume per ethylene oxide group is greater in the region outside the palisade layer in the mixed case. However, for longer polyoxyethylene chains, the mixed micelle is more compact than a pure nonionic micelle. This latter effect is probably due to the specific interactions between the anionic head group and the oxonium ion of the polyethoxylate chain reducing the extension of the long polyethoxylate chain into solution, which overcomes the steric effect of the space occupied by the anionic hydrophilic groups. As a result, a higher fraction of the ethylene oxide groups is in close proximity to the anionic head group (perhaps wrapped around it), causing the area per total hydrophilic groups in this region to be potentially higher in the mixed case than for either pure surfactant micelle. If the micelle shape did not change drastically, this would result in a lower aggregation number than calculated by a mole fraction weighted average of the pure component values. Anionic/nonionic mixed micelles have been reported to have an aggregation number intermediate between or less than the two pure component micelles ($\underline{43,44}$), consistent with this interpretation.

Cationic/nonionic mixed micelles do not seem to show this compaction effect (at least as readily) as

anionic/nonionic micelles from solubilization results,
again consistent with the lack of specific attraction (or
even small repulsion) between the two dissimilar
hydrophilic groups. Not unexpectedly, cationic/nonionic
mixed micelles have been shown to exhibit a higher
aggregation number than the pure component micelles at
some compositions (38).

Regular Solution Theory. If the surfactant mixing in the
micelle obeys regular solution theory, the following
relationships are valid for a binary surfactant system
(45):

$$\Delta H_M = \Delta G_E = x_A x_B W \qquad\qquad (5)$$

where ΔH_M is the heat of mixing in the micelle and ΔG_E is
the excess free energy of mixing in the micelle.
Equation 5 shows that the heat and excess free energy of
mixing are symmetrical with respect to micellar
composition; i.e., ΔH_M reaches as extremum when $x_A = x_B =$
0.5. Equation 5 also shows that the nonideality of
mixing is entirely accounted for in the heat or enthalpy
of mixing. The excess entropy of mixing is assumed to be
zero.

There is substantial evidence that regular solution
theory is not valid in describing the nonideal mixed
micelles. The heat of mixing obtained from fitting
regular solution theory to CMC data has been shown to
differ greatly from that measured by calorimetry (29,36).
The excess free energy of mixing upon mixed micelle
formation can be very unsymmetrical with respect to
composition (21), contrary to the prediction of Equation
5. The value of W should be independent of temperature
and micellar composition (46). It has been found to be
substantially temperature dependent (34) and slightly
dependent on composition (30). If regular solution
theory applies for ionic/nonionic mixed micelles, the
fractional counterion binding must be proportional to the
mole fraction of ionic surfactant in the micelle (39,47),
which is contrary to experimental observations (40,43,47–
49).

Equations 3 and 4 are derived from Equation 5 (31),
which has been found to be invalid for the systems of
interest. However, Equations 3 and 4 have been shown to
accurately describe mixture CMC values and monomer–
micelle equilibrium. The resolution is that Equations 3
and 4 should be considered as valuable empirical
equations to describe these nonideal systems. The fact
that they were originally derived from regular solution
theory is a historical coincidence.

Only one model to describe nonideal micelle
formation was described here. Regular solution theory in
a different form than that used here has been applied to
these systems (39). Alternative models have been
proposed based on statistical mechanics (37,50), the

mass-action model of micelle formation (5), a model
accounting for electrical effects (24), and a group
contribution method (51).

Mixed Micelles Showing Positive Deviations from Ideality.

For binary surfactant systems where one component has a
hydrocarbon-based hydrophobic group and the other
component has a fluorocarbon-based hydrophobic group, and
both individual surfactants have the same charge on the
hydrophilic group, the mixture CMC is greater than that
predicted from ideal solution theory (13,52-56). These
systems show positive deviation from ideality as
illustrated in Figure 1.

While anionic/cationic surfactant systems show
negative deviations from ideality of mixing because of
attractions between dissimilar surfactants in the mixed
micelle, hydrocarbon-based/fluorocarbon based surfactants
exhibit positive deviations from ideality because of
phobicity between the dissimilar hydrophobic groups in
the mixed micelle. The monomer-micelle equilibrium for
such a system is illustrated in Figure 2. At low monomer
mole fractions of the hydrocarbon-based surfactant
(surfactant A), the monomer is in equilibrium with
predominately fluorocarbon-based micelles. At a critical
monomer composition of y_A = 0.1, the monomer is in
simultaneous equilibrium with a mainly fluorocarbon-based
micelle (x_A = 0.057) and a mainly hydrocarbon-based
micelle (x_A = 0.71). At higher values of y_A, the
predominately hydrocarbon-based micelle only is present.
As the temperature increases, the mutual phobicity
decreases in these systems, until there is no micellar
phase transition, although there is still positive
deviation from ideality (53-55). This remarkable
behavior can have substantial impact on processes
involving these mixed surfactant sytems. For example, if
solubilization into the hydrocarbon-based micelle were
different than that in the fluorocarbon-based micelle, a
sharp change in this property would occur at the monomer
composition corresponding to the micellar phase change.

Having shown that ionic/nonionic surfactant mixtures
show negative deviations from ideality (when both
components are hydrocarbon-based) and
fluorocarbon/hydrocarbon-based surfactant mixtures show
positive deviations from ideality, what would a ionic
fluorocarbon/nonionic hydrocarbon surfactant pair be
expected to do? In one example of this case (57), the
electrostatic stabilization forces overcome the
hydrophobic group phobicity effects and negative
deviation from ideality is observed.

Counterion Binding.

The fractional counterion binding on
charged mixed micelles is of fundamental interest because
it gives an indication of surface charge density which is
related to the mechanism of mixing nonidealities in
ionic/nonionic micelles. It is also a necessary

component in any prediction of electrical potential at
the micellar surface.

The fractional counterion binding on micelles
composed of binary mixtures of similarly structured
surfactants of like charge varies monotonically between
the values for the two pure component micelles as the
micellar composition is varied (15,40). For
ionic/nonionic mixed micelles, the fractional counterion
binding decreases as the nonionic content of the micelle
increases (22,40,43,47-49,58). This is expected, since
the space taken up by the nonionic hydrophilic groups
causes the ionic hydrophilic groups to have a lower
density on the micellar surface, resulting in a reduction
in absolute surface electrical potential. Therefore,
there is a reduced driving force for counterion binding.
The binding decreases as the number of oxyethylene groups
in the nonionic surfactant increases (21,43,49) because
these larger nonionic hydrophilic groups occupy even a
larger fraction of the micelle surface area, reducing the
surface charge density even more.

Monolayer Formation

The adsorption of mixed surfactants at the air-water
interface (monolayer formation) is mechanistically very
similar to mixed micelle formation. The mixed monolayer
is oriented so that the surfactant hydrophilic groups are
adjacent to each other. The hydrophobic groups are
removed from the aqueous environment and are in contact
with other hydrophobic groups or air. Therefore, the
forces tending to cause monolayers to form are similar to
those causing micelles to form and the thermodynamics and
interactions between surfactants are similar in the two
aggregation processes.

The practical importance of monolayer formation is
generally because of its relationship to reduction of
surface tension. Air-water surface tension can affect
such important phenomena as contact angle with a solid
surface (affecting flotation), rate of wetting of a
solid, or foaming (with applications in enhanced oil
recovery or fire extinguishers), just to name a few.
Reduction of air-water surface tension could, for
example, cause a liquid to spread on a solid instead of
beading up on it.

At very low surfactant concentrations in solution,
the adsorption density at the air-water interface is so
low that individual adsorbed surfactants do not interact
significantly with each other. At a certain
concentration, the adsorption density increases sharply
as a phase transition occurs (59). The coverage on the
surface rapidly approaches a monolayer coverage as
concentration increases further. Essentially a complete
monolayer is formed at concentrations well below the CMC
(60). It is in this region of monolayer formation that a
rapid decrease in surface tension with increasing

surfactant concentration is observed. Therefore, the
tendency for the monolayer to form is intimately related
to surface tension reduction.

In mixed surfactant systems, the interactions
between surfactants affects the tendency for monolayer
formation. At concentrations above the CMC, the surface
tension may very slowly increase or decrease. The
surface tension at the CMC is close to the minimum
surface tension which a surfactant system can attain.
Therefore, in terms of surface tension reduction, the
surfactant concentration required to attain a specified
surface tension below the CMC and the surface tension at
the CMC are indicative of the usefulness of a system.

Below the CMC, the surfactant mixing in monolayers
composed of similarly structured surfactants
approximately obeys ideal solution theory. This means
that the total surfactant concentration required to
attain a specified surface tension for a mixture is
intermediate between those concentrations for the pure
surfactants involved. For mixtures of ionic/nonionic or
anionic/cationic surfactants, below the CMC, the
surfactant mixing in the monolayer exhibits negative
deviation from ideality (i.e., the surfactant
concentration required to attain a specified surface
tension is less than that predicted from ideal solution
theory). The same guidelines already discussed to select
surfactant mixtures which have low monomer concentrations
when micelles are present would also apply to the
selection of surfactants which would reduce surface
tension below the CMC.

The mixing in these monolayers have been modeled
using ideal solution theory or regular solution theory
(26-28,32,61-64). The resulting equations are similar to
those already presented for mixed micelle formation. The
regular solution theory interaction parameter for
monolayer formation is similar to that of micelle
formation. For example, from (28), the average
difference between the monolayer and micelle interaction
parameter is only about 20% for ten varied systems.
Since the structure of the two aggregates is similar,
this is expected. The mechanisms leading to the
nonideality of mixed micelles (already discussed) are
qualitatively the same for mixed monolayers.

The higher the negative deviation from ideality in
monolayer formation, the lower the concentration required
to attain a given surface tension below the CMC. The
higher this deviation for micelle formation, the lower
the CMC. Since the CMC is where the surface tension
approximately levels out at near a minimum value, the
minimum surface tension in such a system represents the
relative enhancement of monolayer formation over micelle
formation. This relative favorability of aggregate
formation is often an important factor in many
applications, as will be further discussed in this
article.

Solubilization

Solubilization of dissolved organic molecules into micelles is important in detergency (2), emulsion polymerization (65), and micellar-enhanced ultrafiltration (3), just to name a few applications. Solubilization also indirectly affects many other operations because it often affects monomer-micelle equilibrium, influencing surfactant adsorption, wetting, etc. when solubilizable, non-surfactant species are present in solution.

Yellow OB dye is an essentially water-insoluble organic and is convenient to use as a solubilizate. The studies discussed here use Yellow OB for solubilization studies in mixed surfactant systems. Yellow OB can solubilize in the hydrocarbon core of the micelle as well as among the polyoxyethylene chains in a micelle with nonionic surfactant.

Nishikido (21) has done a systematic study of mixed surfactant solubilization. In that study, solubilization in mixed systems was compared to that predicted by application of a linear mixing rule to the solubilizations in the pure surfactant component micelles. For example, in this "ideal" case, a micelle composed of a 50/50 molar mixture of two surfactants would have a solubilization capacity which is an average of that of the two pure surfactants involved. A system showing negative deviation from ideality would have less solubilization than this ideal system; a system having positive deviation from ideality would have more.

Except when both the hydrophobic and hydrophilic groups of two polyethoxylated nonionics are similar, a nonionic/nonionic system shows negative deviations from solubilization ideality. This is because the chains pack most efficiently when they are of the same length. For example, if one hydrophilic group had 5 ethylene oxide (EO) groups and the other had 50 EO groups, the first 5 EO groups in the longer chain might see approximately the same environment as in the pure 50 EO surfactant micelle. However, those EO groups beyond this will not form as tight a structure as in the pure micelle. If solubilization is significant in the polyethoxylate portion of the micelle as well as in the hydrophobic portion, this will cause a decrease in solubilization since the environment for the solubilizate will not be as favorable in the region of less compact oxyethylene groups in the mixed micelle.

The same effect is seen when a non-aromatic cationic surfactant/nonionic surfactant system is used. Since the nonideality of mixed micelle formation in this case is due almost entirely to the electrostatic effects and not to any specific interactions between the dissimilar hydrophilic groups, the geometrical effect just discussed will cause the EO groups to be less compactly structured

in the mixed micelle. In this system, negative
deviations from ideality in mixed micelle formation
(enhancement of micelle formation) do not lead to
enhancement of solubilization (i.e., negative deviations
from solubilization ideality are seen).

     In anionic/nonionic systems, for a short
polyoxyethylene chain length, negative deviation from
solubilization ideality is seen. However, for a large
number of EO groups, substantial positive deviation is
seen. In addition to the steric effects already
discussed tending to cause less solubilization in the
mixed system, in anionic/nonionic systems the attraction
between the anionic head group and the oxonium salts in
the polyoxyethylene chain tend to cause the micelle to
become more compact, tending to increase solubilization.
For a small number of EO groups (e.g., 6), the former
effect dominates and negative deviation from
solubilization ideality is seen; for a large number of EO
groups (e.g, >14), the latter effect dominates, leading
to positive deviation from ideality for solubilization.

     For an anionic/nonionic system with the anionic
surfactant containing a benzene ring in the hydrophobic
group, and 9 EO groups in the nonionic surfactant,
positive deviation from ideality is seen when the benzene
ring is attached to the anionic hydrophilic group at the
end of the linear alkyl chain (66). However, when the
benzene ring is positioned in the hydrophobic group away
from the hydrophilic group, negative or no deviation from
solubilization ideality is seen. This is consistent with
the attractive interaction between the benzene ring of
the anionic surfactant and the EO groups of the nonionic
surfactant leading to a more compact micelle when the
benzene ring is in the palisade layer of the micelle,
leading to increased solubilization.

     Negative deviation from ideality of micelle
formation does not lead to increased solubilization
unless there is a specific attraction between the
hydrophilic groups of the dissimilar surfactants, not
just electrostatic forces. The specific attraction can
lead to a more compact micelle and higher
solubilizations. As already discussed, this is
consistent with aggregation numbers of mixed micelles.
If a system which had large solubilization enhancement
were desired, an anionic/nonionic system would be chosen
with a benzene ring attached to the anionic hydrophilic
group and a large number of EO groups in the nonionic.
This discussion only applies to systems in which
solubilization in the polyethoxylate portion of the
nonionic surfactant is significant (e.g., Yellow OB dye).
If the solubilizate is located only in the hydrocarbon
core of the micelle (e.g., hydrocarbons), large
deviations from ideality would not be expected. This
discussion is consistent with other mixed surfactant
solubilization data (67,68).

Adsorption on Solids

The adsorption of surfactants on solids affects flotation, agricultural soil conditioning, formulation of pharmaceutical dispersions, and dyeing (69), just to name a few processes. More specifically, in enhanced oil recovery, adsorption of surfactant on reservoir minerals can result in a substantial loss of surfactant (1). Selective adsorption of certain surfactant components from the multicomponent mixture can lead to chromatographic separation of the slug (70,71), with subsequent disasterous results. In detergency, adsorption of surfactant components on both textiles and contaminants (polar or nonpolar dirts) is important (2).

When surfactants adsorb on metal oxide surfaces (e.g., minerals), at low concentrations, the adsorbate molecules are widely dispersed enough that no significant interactions between adsorbed surfactants occurs. Above a certain critical concentration, dense surfactant aggregates form on the surface (72). These are called admicelles. For ionic surfactants, the admicelles are bilayered structures (72). Above the CMC, the total adsorption of surfactant can increase or decrease slowly.

When two similarly structured anionic surfactants adsorb on minerals, the mixed admicelle approximately obeys ideal solution theory (11). Below the CMC, the total adsorption at any total surfactant concentration is intermediate between the pure component adsorption levels. Adsorption of each surfactant component in these systems can be easily predicted from pure component adsorption isotherms by combining ideal solution theory with an empirical corresponding states theory approach (73).

When an ionic/nonionic surfactant mixture adsorbs on a metal oxide surface, the admicelle exhibits negative deviation from ideality (74). This means that the adsorption level is higher than it would be if the admicelle were ideal, at a specific surfactant concentration below the CMC. Above the CMC, the adsorption level is dictated by the relative enhancement of micelle formation vs. admicelle formation. In this region, the level of adsorption can be viewed as the result of the competition between micelles and admicelles for surfactant. In analogy, the surface tension above the CMC can be viewed as competition between the monolayer and micelles for surfactant.

The relative tendency for surfactants or surfactant mixtures to form a micelle compared to a monolayer is approximately the same. However, the relative tendency to form an admicelle can be substantially different from that to form micelles or monolayers. This is because there can be specific interactions between the solid surface and the surfactants as well as intersurfactant interactions in the aggregate. The surfactant technologist can take advantage of this to design

minimally or maximally adsorbing systems. For example, as the number of ethylene oxides in a polyethoxylated surfactant increases, the adsorption on a mineral surface decreases (74-76). A polyethoxylate with a very large number of EO groups does not adsorb significantly (or even has negative adsorption). Yet the tendency of such nonionics to form pure component micelles or nonideal mixed micelles with anionic surfactants is only weakly dependent on the number of EO groups. As a result, above the CMC, a mixture of an anionic and nonionic surfactant shows high adsorption for a small number of EO groups. However, for a large number of EO groups, adsorption of both nonionic and anionic surfactant can be very low (74). This is because the formation of the nonideal mixed micelle reduces the anionic surfactant monomer concentration, tending the reduce its adsorption. The nonionic has so little tendency to adsorb because of negative interaction with the surface that even with the anionic surfactant in the admicelle, it still exhibits negligible adsorption. In a sense, the micelle has won the competition for the monomer and the adsorption is reduced as the surfactants prefer the mixed micelle to mixed admicelle. Similarly, on silica gel, anionic surfactant has very low adsorption. When anionic surfactant is added to nonionic surfactant above the CMC, it reduces the nonionic surfactant adsorption on the silica gel, without adsorbing significantly itself (77).

On hydrophobic surfaces, similar effects probably occur and can explain the difference in adsorption of an anionic surfactant in the absence and presence of a nonionic surfactant above the CMC on carbon (78).

In designing surfactant systems, if adsorption of a given component is to be minimized, an additional surfactant should be added to the system above the CMC. This surfactant should be selected so that it forms micelles with high negative deviations from ideality, using the guidelines already discussed, and so that it tends not to adsorb on the solid of interest. This will be very specific to the particular solid and may require empirical experiments to specify the surfactant.

Surfactant Precipitation

Precipitation of surfactants from aqueous solution is generally undesirable in many surfactant-based technologies. Often, either additives must be included with the surfactant or mixtures of surfactants must be used to prevent precipitation. For example, in enhanced oil recovery, alcohols are often added to an injected slug (79) or mixtures of surfactants (80) are used to permit flooding of high salinity or hardness reservoirs while avoiding surfactant precipitation. In detergency, builder is added to a formulation (2) or non-built heavy duty liquid laundry detergents may utilize mixtures of anionic and nonionic surfactants (35,81-83) to permit washing in hard water.

Precipitation of surfactant can be useful   in some applications, such as in selective plugging of oil reservoirs to improve mobility control (84) or to recover surfactant from surfactant-based separation processes (85).

There have been two general approaches to studying surfactant precipitation: measurement of the Krafft temperature   (temperature   below   which   surfactant precipitates) or by measuring the precipitation phase boundary (added electrolyte concentration required to cause surfactant precipitation). An increase in salinity or hardness tolerance is directly measured from phase boundary studies or can be inferred from a decrease in the Krafft temperature. Since precipitation below the CMC   is   governed   by   a simple solubility product relationship,   this discussion   will   only   consider surfactant solution above the CMC, where interesting effects occur.

Anionic/Anionic   or   Cationic/Cationic   Surfactant Precipitation. When two surfactants of like charge are mixed together, and the structures are very similar (e.g., close members of an homologous series) and containing the same counterion, the Krafft temperature of the mixture is intermediate between the pure components or shows only a very shallow minimum (86,87). The crystals are mixed (contain both surfactants) in this case (86,87).

If the surfactants have a more dissimilar structure or if the counterion is different with the same surfactant ion (e.g., sodium dodecyl sulfate and calcium dodecyl sulfate), the Krafft temperature of the mixture can be much less than either pure component (87-89). These systems show the classical eutectic type behavior and the crystals contain only one kind of surfactant or counterion in substantial amounts (87-89).

In the case of non-eutectic systems, the solid phase shows nearly ideal mixing, so that the surfactant components distribute themselves between the micelle and the solid in about the same relative proportions (i.e., both the mixed micelle and mixed solid are approximately ideal). However, in the case of the eutectic type system, the crystal is extremely non-ideal (almost a single component), while the micelle has nearly ideal mixing.   As seen in earlier calculations for ideal systems, even though the total surfactant monomer concentration is intermediate between that of the pure components, the monomer concentration of an individual component decreases as its total proportion in solution decreases. As the proportion of surfactant A decreases in solution (proportion of surfactant B increases) from pure A, there is a lower monomer concentration of A. Therefore, it requires a lower temperature or a higher added electrolyte level to precipitate it. At some

composition, surfactant B precipitates preferentially to
A - this is the minimum in the Krafft temperature. At
still higher proportions of B in the system, the monomer
concentration of B increases, increasing the Krafft
temperature. In the case of the systems with the same
surfactant ion, but different counterions, as the
proportion of surfactant with counterion A decreases,
there is a lower concentration of unbound A to
precipitate the surfactant ion. At some composition,
counterion B preferentially precipitates the surfactant
and the minimum in the eutectic occurs.

We may consider precipitation in these systems in
the context of competitive aggregate formation between
micelles and precipitate. Even systems forming ideal
mixed micelles can exhibit synergisms in
salinity/hardness tolerance; in such systems, the more
components present, the higher the tolerance. This is
the reason that mixtures of isomeric surfactants
generally have Krafft temperatures considerably lower
than those of the individual compounds (90).

Ionic/Nonionic Surfactant Mixtures. Since nonionic
surfactants are uncharged, they will not form a salt
precipitate with counterions like the ionic surfactants.
Also, a mixture of ionic and nonionic surfactants form
nonideal micelles, resulting in a reduced ionic
surfactant monomer concentration compared to ideal mixed
micelle formation. As a result of these effects, the
salinity/hardness tolerance increases (35,91,92) or the
Krafft temperature decreases (93) as nonionic surfactant
is added to anionic surfactant solutions in increasing
proportions.

If the mixed micelle model already presented is used
to predict the ionic surfactant monomer concentration,
and a simple concentration-based solubility product is
assumed to hold between the unbound counterion and
monomer, the salinity tolerance of an anionic/nonionic
surfactant mixture can be accurately predicted (91),
supporting this view of the mechanism of tolerance
enhancement by nonionic surfactant.

In order to define a ionic/nonionic surfactant
solution with high salinity/hardness tolerance, the
following criterion should be followed. The mixed
micelle should have as large of a negative deviation from
ideality as possible. Surfactant mixture characteristics
which result in this have already been discussed. The
nonionic surfactant should have a high cloud point.
Otherwise the amount of nonionic surfactant which can be
added to the system is limited to low levels before phase
separation occurs. If possible, a mixed ionic surfactant
should be used for reasons just discussed. There is no
such benefit to using mixed nonionic surfactants,
although this is not necessarily detrimental either.

Anionic/Cationic Surfactant Mixtures. Mixed micelles

formed between anionic and cationic surfactants have high
negative deviation from ideality, as already discussed.
Therefore, it might seem that surfactant would not tend
to precipitate easily from these solutions. However, the
electrostatic attractions between the anionic and
cationic surfactant can cause ion pairing formation or
coacervate phase formation in these systems (94). It is
beyond the scope of this article to discuss the complex
phase behavior of the anionic/cationic surfactant
systems, but use of these mixtures is generally not an
effective way to solve precipitation problems.
Conversely, if precipitation or phase separation is
desirable, these mixtures can be beneficial (84).

Cloud Point Phenomena

As the temperature of dilute aqueous solutions containing
ethoxylated nonionic surfactants is increased, the
solutions may turn cloudy at a certain temperature,
called the cloud point. At or above the cloud point, the
cloudy solution may separate into two isotropic phases,
one concentrated in surfactant (coacervate phase) and the
other containing a low concentration of surfactant
(dilute phase). As an example of the importance of this
phenomena, detergency is sometimes optimum just below the
cloud point, but a reduction in the washing effect can
occur above the cloud point (95). However, the phase
separation can improve acidizing operations in oil
reservoirs (96). For surfactant mixtures, of particular
interest is the effect of mixture composition on the
cloud point and the distribution of components between
the two phases above the cloud point.
      The cloud point is close to, but not necessarily
equal to the lower consolute solution temperature for
polydisperse nonionic surfactants (97). These are equal
if the surfactant is monodisperse. Since the lower
consolute solution temperature is like a critical point
for liquid-liquid mixtures, the dilute and coacervate
phases have the same composition, and the volume fraction
of solution which the coacervate comprises is a maximum
at this temperature (98). If a coacervate phase
containing a high concentration of surfactant is desired,
the solution should be at a temperature well above the
cloud point.
      The cloud point of a mixture of nonionic surfactants
is intermediate between the pure nonionic surfactants
involved (93,99). The cloud point of a dilute nonionic
surfactant solution increases upon addition of ionic
surfactant (93,98-104). The coacervate phase forms
because of attractive forces between the micelles in
solution. The incorporation of ionic surfactant into the
nonionic micelles introduces electrostatic repulsion
between micelles, causing coacervate phase formation to
be hindered, raising the cloud point.
      The anionic/nonionic surfactant mixing in the

coacervate phase can be approximated by equations
resulting from regular solution theory and the
nonideality of mixing is similar to that of mixed micelle
formation for the same system (98). This is reasonable
because, at the cloud point, both phases are identical
and the coacervate is just a micellar solution. The
coacervate can be viewed as simply a very concentrated
micellar solution. The concentration of surfactant in
the dilute phase is always well above the CMC, so
micelles are present. If the total surfactant
concentration in the initial solution is below that which
would be present in this dilute phase above the cloud
point, the solution will not exhibit the cloud point
phenomena.

The equilibrium in these systems above the cloud
point then involves monomer-micelle equilibrium in the
dilute phase and monomer in the dilute phase in
equilibrium with the coacervate phase. Prediction of the
distribution of surfactant component between phases
involves modeling of both of these equilibrium processes
(98). It should be kept in mind that the region under
discussion here involves only a small fraction of the
total phase space in the nonionic surfactant-water system
(105). Other compositions may involve more than two
equilibrium phases, liquid crystals, or other structures.
As the temperature or surfactant composition or
concentration is varied, these regions may be encroached
upon, something that the surfactant technologist must be
wary of when working with nonionic surfactant systems.

Conclusions

This brief review has attempted to discuss some of the
important phenomena in which surfactant mixtures can be
involved. Mechanistic aspects of surfactant interactions
and some mathematical models to describe the processes
have been outlined. The application of these principles
to practical problems has been considered. For example,
enhancement of solubilization or surface tension
depression using mixtures has been discussed. However,
in many cases, the various processes in which surfactants
interact generally cannot be considered by themselves,
because they occur simultaneously. The surfactant
technologist can use this to advantage to accomplish
certain objectives. For example, the enhancement of
mixed micelle formation can lead to a reduced tendency
for surfactant precipitation, reduced adsorption, and a
reduced tendency for coacervate formation. The solution
to a particular practical problem involving surfactants
is rarely obvious because often the surfactants are
involved in multiple steps in a process and optimization
of a number of simultaneous properties may be involved.
An example of this is detergency, where adsorption,
solubilization, foaming, emulsion formation, and other
phenomena are all important. In enhanced oil recovery,

adsorption, microemulsion formation, precipitation, liquid crystal formation, and other processes are simultaneously occurring. Solution to one problem in these complicated systems may introduce other problems. This paper has given some guidelines which should aid in selection of surfactant mixtures to achieve certain objectives, but the performance of proposed systems will generally need to be tested in real world applications.

Acknowledgments

Literature Cited

1. Gogarty, W.B. J. Pet. Technol. 1983, 35, 1581.
2. Cahn, A.; Lynn, J.L. Jr. In "Kirk-Othmer Encyclopedia of Chemical Technology", Third Edition; Wiley: New York, 1983; Vol. 22, p. 332.
3. Dunn, R.O.; Scamehorn, J.F.; Christian, S.D. Sep. Sci. Technol. 1985, 20, 257.
4. Shinoda, K. In "Colloidal Surfactants"; Shinoda, K.; Tamamushi, T.; Nakagawa, T.; Isemura, T., Eds.; Academic Press: New York, 1963; Chapter 1.
5. Kamrath, R.F.; Franses, E.I. J. Phys. Chem. 1984, 88, 1642.
6. Shinoda, K. J. Phys. Chem. 1954, 58, 541.
7. Mysels, K.J.; Otter, R.J. J. Colloid Sci. 1961, 16, 474.
8. Barry, B.W.; Morrison, J.C.; Russell, G.F. J. Colloid Interface Sci. 1970, 33, 554.
9. Lange, H.; Beck, K.H., Kolloid Z.Z. Polym. 1973, 251, 424.
10. Nishikido, N.; Moroi, Y.; Matuura, R. Bull. Chem. Soc. Jpn. 1975, 48, 1387.
11. Scamehorn, J.F.; Schechter, R.S.; Wade, W.H. J. Colloid Interface Sci. 1982, 85, 479.
12. Holland, P.M.; Rubingh, D.N. J. Phys. Chem. 1983, 87, 1984.
13. Funasaki, N.; Hada, S. J. Phys. Chem. 1982, 86, 2504.
14. Clint, J.H. J. Chem. Soc. Faraday Trans. 1 1975, 71, 1327.
15. Shedlovsky, L.; Jakob, C.W.; Epstein, M.B. J. Phys. Chem. 1963, 67, 2075.
16. Tokiwa, F.; Ohki, K.; Kokubo, I. Bull. Chem. Soc. Jpn. 1968, 41, 2845.
17. Iwadare, Y. Bull. Chem. Soc. Jpn. 1970, 43, 3364.
18. Funasaki, N.; Hada, S. J. Phys. Chem. 1979, 83, 2471.
19. Schick, M.J. J. Am. Oil Chem. Soc. 1966, 43, 681.
20. Schick, M.J.; Manning, D.J. J. Am. Oil Chem. Soc. 1966, 43, 133.

21. Nishikido, N., J. Colloid Interface Sci. 1977, 60, 242.

22. Moroi, Y.; Akisada, H.; Saito, M.; Matuura, R. J. Colloid Interface Sci. 1977, 61, 233.

23. Kurzendorfer, C.P.; Schwuger, M.J.; Lange, H. Ber. Bunsen. Ges. Phys. Chem. 1978, 82, 962.

24. Moroi, Y.; Nishikido, N.; Saito, M.; Matuura, R. J. Colloid Interface Sci. 1975, 52, 356.

25. Rubingh, D.N. In "Solution Chemistry of Surfactants"; Mittal, K.L., Ed.; Plenum Press: New York, 1979; Vol. I, p. 337.

26. Hua, X.Y.; Rosen, M.J. J. Colloid Interface Sci. 1982, 90, 212.

27. Rosen, M.J.; Zhu, B.Y. J. Colloid Interface Sci. 1984, 99, 427.

28. Zhu, B.Y.; Rosen, M.J. J. Colloid Interface Sci. 1984, 99, 435.

29. Holland, P.M. In "Structure/Performance Relations in Surfactants"; Rosen, M.J., Ed.; ACS Symposium Series: Washington, D.C., 1984; p. 141.

30. Kamrath, R.F.; Franses, E.I. Ind. Eng. Chem. Fundam. 1983, 22, 230.

31. Scamehorn, J.F.; Schechter, R.S.; Wade, W.H. J. Dispersion Sci. Technol. 1982, 3, 261.

32. Rosen, M.J.; Hua, X.Y. J. Am. Oil Chem. Soc. 1982, 59, 582.

33. Holland, P.M. Adv. Colloid Interface Sci. In Press.

34. Nguyen, C.M.; Rathman, J.F.; Scamehorn, J.F., J. Colloid Interface Sci., In Press.

35. Cox, M.F.; Borys, N.F.; Matson, T.P. J. Am. Oil Chem. Soc. 1985, 62, 1139.

36. Hey, M.J.; MacTaggart, J.W.; Rochester, C.H. J. Chem. Soc. Faraday Trans. 1 1985, 81, 207.

37. Osborne-Lee, I.W.; Schechter, R.S. J. Colloid Interface Sci. In Press.

38. Birdi, K.S. Proc. Int. Conf. Colloid Surf. Sci. 1975, 1, 473.

39. Hall, D.G.; Huddleston, R.W. Colloids Surf. 1985, 13, 209.

40. Rathman, J.F.; Scamehorn, J.F. J. Phys. Chem. 1984, 88, 5807.

41. Tokiwa, F.; Tsujii, K. J. Phys. Chem. 1971, 75, 3560.

42. Tokiwa, F.; Tsujii, K. J. Colloid Interface Sci. 1972, 41, 343.

43. Tokiwa, F; Aigami, K. Kolloid Z. Z. Polym. 1970, 239, 687.

44. Kuriyama, K.; Inoue, H.; Nakagawa, T. Kolloid Z. Z. Polym. 1962, 183, 68.

45. Balzhiser, R.E.; Samuels, M.R.; Eliassen, J.D. "Chemical Engineering Thermodynamics"; Prentice-Hall: Englewood Cliffs, N.J., 1972; p. 403-405.

46. Modell, M.; Reid, R.C. "Thermodynamics and Its Applications"; Prentice-Hall: Englewood Cliffs, N.J., 1974; p. 279.

47. Hall, D.G.; Price, T.J. J. Chem. Soc. Faraday Trans.

1 1984, 80, 1193.
48. Corkill, J.M.; Goodman, J.F.; Tate, J.R. Trans. Faraday Soc. 1964, 60, 986.
49. Tokiwa, F; Moriyama, N. J. Colloid Interface Sci. 1969, 30, 338.
50. Nagarajan, R. Langmuir 1985, 1, 331.
51. Asakawa, T.; Johten, K.; Miyagishi, S.; Nishida, M. Langmuir 1985, 1, 347.
52. Mukerjee, P.; Yang, A.Y.S. J. Phys. Chem. 1976, 80, 1388.
53. Funasaki, N.; Hada, S. J. Phys. Chem. 1980, 84, 736.
54. Funasaki, N.; Hada, S.; Neya, S. Bull. Chem. Soc. Jpn. 1983, 56, 3839.
55. Funasaki, N.; Hada, S. J. Phys. Chem. 1983, 87, 342.
56. Shinoda, K.; Nomura, T. J. Phys. Chem. 1980, 84, 365.
57. Funasaki, N.; Hada, S. J. Colloid Interface Sci. 1980, 78, 376.
58. Meyer, M.; Sepulveda, L. J. Colloid Interface Sci. 1984, 99, 536.
59. Aratono, M.; Uryu, S.; Hayami, Y.; Motomura, K.; Matuura, R. J. Colloid Interface Sci. 1984, 98, 33.
60. Rosen, M.J. "Surfactants and Interfacial Phenomena"; Wiley: New York, 1978; Ch. 2.
61. Rosen, M.J.; Hua, X.Y. J. Colloid Interface Sci. 1982, 86, 164.
62. Rosen, M.J.; Zhao, F. J. Colloid Interface Sci. 1983, 95, 443.
63. Ingram, B.T. Colloid Polym. Sci. 1980, 258, 191.
64. Lucassen-Reynders, E.H. In "Progress in Surface and Membrane Science"; Cadenhead, D.A.; Danielli, J.F., Eds.; Academic Press: New York, 1976; p. 253.
65. Dunn, A.S. In "Emulsion Polymerization"; Piirma, I., Ed.; Academic Press: New York, 1982; p. 221.
66. Tokiwa, F.; Tsujii, K. Bull. Chem. Soc. Jpn. 1973, 46, 1338.
67. Tokiwa, F. J. Colloid Interface Sci. 1968, 28, 145.
68. Saito, H.; Shinoda, K. J. Colloid Interface Sci. 1967, 24, 10.
69. Hough, D.B.; Rendall, H.M. In "Adsorption from Solution at the Solid/Liquid Interface"; Parfitt, G.D.; Rochester, C.H., Eds.; Academic: New York, 1983; p. 247.
70. Harwell, J.H.; Helfferich, F.G.; Schechter, R.S. AICHE J. 1982, 28, 448.
71. Harwell, J.H.; Schechter, R.S.; Wade, W.H. AICHE J. 1985, 31, 415.
72. Scamehorn, J.F.; Schechter, R.S.; Wade, W.H. J. Colloid Interface Sci. 1982, 85, 463.
73. Scamehorn, J.F.; Schechter, R.S.; Wade, W.H. J. Am. Oil Chem. Soc. 1983, 60, 1345.
74. Scamehorn, J.F.; Schechter, R.S.; Wade, W.H. J. Colloid Interface Sci. 1982, 85, 494.
75. Furlong, D.N.; Aston, J.R. Colloids Surf. 1982, 4, 121.
76. Rouquerol, J.; Partyka, S.; Rouquerol, F. In "Adsorption at the Gas-Solid and Liquid-Solid Interface";

Rouqerol, J.; Sing, K.S.W., Eds.; Elsevier: Amsterdam,
1982; p. 69.
77. Gao, Y.; Yue, C.; Lu, S.; Gu, W.; Gu, T. J. Colloid
Interface Sci. 1984, 100, 581.
78. Schwuger, M.J.; Smolka, H.G. Colloid Polym. Sci.
1977, 255, 589.
79. LaLanne-Cassou, C.; Carmona, I.; Fortney, L.; Samii,
A.; Schechter, R.S.; Wade, W.H.; Weerasooriya, U.;
Weerasooriya, V.; Yiv, S., SPE Paper No. 12035, Presented
at the 58th Annual Technical Conference and Exhibition of
the Society of Petroleum Engineers, San Francisco,
October, 1983.
80. Novosad, J.; Maini, B.; Batycky, J. J. Am. Oil Chem.
Soc. 1982, 59, 833.
81. Cox, M.F.; Matson, T.P. J. Am. Oil Chem. Soc. 1983,
60, 1170.
82. Matson, T.P.; Berretz, M. Soap Cosmet. Chem. Spec.
1980, 56, 41.
83. Kravetz, L.; Scharer, D.H.; Stupel, H. Tr. Mezhdunar.
Kongr. Poverkhn. Akt. Veshchestvam, 7th 1978, 3, 192.
84. Arshad, S.A.; Harwell, J.H. SPE Paper No. 14291,
Presented at the 60th Annual Technical Conference of the
Society of Petroleum Engineers, Las Vegas, September,
1985.
85. Scamehorn, J.F.; Christian, S.D. In "Surfactant-Based
Separation Processes"; Scamehorn, J.F.; Harwell, J.H.,
Eds.; Marcel Dekker, In Press.
86. Murata, Y.; Motomura, K.; Matuura, R. Mem. Fac. Sci.
Kyushu Univ. Ser. C 1978, 11, 225.
87. Tsujii, K.; Saito, N.; Takeuchi, T. J. Phys. Chem.
1980, 84, 2287.
88. Hato, M.; Shinoda, K. J. Phys. Chem. 1973, 77, 378.
89. Moroi, Y.; Oyama, T.; Matuura, R. J. Colloid
Interface Sci. 1977, 60, 103.
90. Rosen, M.J. "Surfactants and Interfacial Phenomena";
Wiley: New York, 1978; p. 160.
91. Stellner, K.L.; Scamehorn, J.F. J. Am. Oil Chem.
Soc. submitted for publication.
92. Gerbacia, W.E.F. J. Colloid Interface Sci. 1983, 93,
556.
93. Nishikido, N.; Akisada, H.; Matuura, R. Mem. Fac.
Sci. Kyushu Univ. Ser. C 1977, 10, 91.
94. Tomlinson, E.; Davis, S.S.; Mikhayer, G.I. In
"Solution Chemistry of Surfactants, Vol. 1"; Mittal,
K.L., Ed; Plenum Press: New York, 1979; p. 3.
95. Wirth, W. Tenside Deterg. 1975, 12, 245.
96. Iaks, C.G. U.S. Patent 4 163 727, 1979.
97. Smith, D.H.; Fleming, P.D. J. Colloid Interface Sci.
1985, 105, 80.
98. Yoesting, O.E.; Scamehorn, J.F. Colloid Polym. Sci.,
In Press.
99. Maclay, W.N. J. Colloid Sci. 1956, 11, 272.
100. Saito, H.; Shinoda, K. J. Colloid Interface Sci.
1967, 24, 10.
101. Nakagawa, T.; Shinoda, K. In "Colloidal

Surfactants"; Shinoda, K.; Tamamushi, B.; Nakagawa, T.;
Isemura, T., Eds; Academic Press: New York, 1963; p. 130.
102.   Kuriyama, K.; Inoue, H.; Nakagawa, T. <u>Kolloid Z. Z.
Polym.</u> 1962, 183, 68.
103.   Tadros, ThF. <u>J. Colloid Interface Sci.</u> 1974, 46,
528.
104.   Corti, M.; Minero, C.; Degiorgio, V. <u>J. Phys. Chem.</u>
1984, 88, 309.
105.   Mitchell, D.J.; Tiddy, G.J.T.; Waring, L.; Bostock,
T.; McDonald, M.P. <u>J. Chem. Soc. Faraday Trans. 1</u> 1983,
79, 975.

2

Nonideal Mixed Micelles

Thermodynamic Models and Experimental Comparisons

Irvin W. Osborne-Lee[1] and Robert S. Schechter

Department of Chemical Engineering, The University of Texas at Austin, Austin, TX 78712

The variation of the mixture critical micelle concentration (CMC_M) with temperature and with overall surfactant composition has been studied using ultrafiltration for two binary mixed nonionic/anionic systems. The data are then compared to predictions based on a new model which includes an excess enthalpy of mixing and two contributions to the excess entropy of mixing. One of the contributions to the excess entropy of mixing is related to the order-disorder problem associated with strong interactions and the second is associated with the greater freedom accorded the ethylene oxide chain because of the greater area per chain in a mixed micelle as compared to the pure nonionic micelle. The latter contribution, which represents a configurational one, tends to increase the entropy whereas the former tends to decrease it. The new model predicts monomer and micellar compositions as a function of temperature when the ethylene oxide chain is relatively short ($\sim$ 10 units) but requires some modification of the parameters to predict the behavior of mixed micelles with nonionic components of relatively long chain length ($\sim$ 50 units). A method of extracting the enthalpy of mixing from knowledge of the variation of mixture CMC with temperature is developed. It is shown that the micellar composition must be known to calculate the enthalpic changes. The procedure is described. The comparison between calculated and predicted enthalpies of mixing is not satisfactory.

In most applications surfactant mixtures rather than pure species are used. These mixtures are usually composed of homologous surfactants, but in some cases mixtures of different surfactant types have

[1]Current address: Oak Ridge National Laboratory, Building 4500N, MS-228, P.O. Box X, Oak Ridge, TN 37831.

also proved advantageous.   Kurzendorfer et al. ($\underline{1}$) have noted that
mixtures of alkyl sulfates and octyl phenol ethoxylates exhibit ex-
cellent powers of detergency.   Other applications of nonionic-anion-
ic mixtures have been reported ($\underline{2},\underline{3}$).   In addition to being of con-
siderable practical interest, mixed micelles composed of both
nonionic and anionic surfactant mixtures are scientifically inter-
esting because of the strong interaction which attends their forma-
tion.   The existence of this interaction is evident when the mixture
critical micelle concentration is compared with that predicted
assuming the mixed micellar pseudophase to be an ideal mixture
($\underline{4},\underline{5}$).   The deviations from ideality are large and in any thermody-
namic treatment forces the introduction of activity coefficients to
correlate the data ($\underline{6-9}$).

    Recently, Rubingh ($\underline{7}$) and Scamehorn et al. ($\underline{9}$) have shown that
the activity coefficients obtained by fitting the mixture CMC data
can be correlated by assuming the mixed micelle to be a regular so-
lution.   This model proposed by Rubingh for binary mixtures has been
extended to include multicomponent surfactant mixtures by Holland
and Rubingh ($\underline{10}$).   Based on this concept Kamrath and Frances ($\underline{11}$)
have made extensive calculations for mixed micelle systems.

    While activity coefficients based on the regular solution theo-
ry model are adequate for representing the mixture CMC, it has been
shown that the monomer composition is not well predicted by such a
model ($\underline{12}$) and that the heat of mixing of sodium dodecylsulfate with
ethylene glycol monodecylether does not compare favorably with the
value predicted by the regular solution model ($\underline{13}$).   These discre-
pancies make clear the inadequacies in considering the micellar
pseudophase to consist of a regular solution of nonionic-anionic
surfactants. Osborne-Lee et al. ($\underline{12}$) have proposed that these dif-
ficulties arise primarily because the excess entropy of mixing does
not vanish as is assumed by the regular solution model.   There are
two contributions to the excess entropy; namely, the nonrandom ar-
rangement of nonionic and anionic surfactants in the mixed micelle
and the conformational entropy changes of the long-chain hydrophilic
group for the polyethylene oxide surfactants.   This latter contribu-
tion will be significant for longer ethylene oxide chains.   The for-
mer contributions must always be significant since reduction of
charge density by arranging anionic surfactants interspersed among
nonionics is thought to be the primary mechanism responsible for the
strong interaction ($\underline{14-15}$).   Because the arrangements increasing the
number of contacts are only a fraction of the total possible
arrangements, the entropy in such mixed micelles is, then, less than
that for micelles which result from random mixing.

    Osborne-Lee et al. ($\underline{12}$) have accounted for the additional con-
tribution to the excess entropy of mixing and found the following
excess free energy of mixing per amphiphile

$$f^E = z\bar{\phi}_{12}w - \frac{zkT}{2}\left\{2\ell n\frac{\phi_{12}{}^*}{\bar{\phi}_{12}} + (y_1 - \phi_{12}{}^*)\ell n(y_1 - \phi_{12}{}^*)\right.$$

$$+ (y_2 - \phi_{12}{}^*)\ell n(y_2 - \phi_{12}{}^*) - (y_1 - \bar{\phi}_{12})\ell n(y_1 - \bar{\phi}_{12})$$

$$\left. - (y_2 - \bar{\phi}_{12})\ell n(y_2 - \bar{\phi}_{12})\right\} - kTny_2(\chi_f - \chi_o) \qquad (1)$$

where z is the average coordination number between surfactant mole-
cules in a micelle, w is the interaction energy parameter, y_1 and
y_2 are the nonionic and anionic micellar mole fractions, respective-
ly, and n is the number of repeating units in the head group chain
(3 times the number of ethylene oxide units). The subscript f de-
notes the mixed micelle and the subscript o denotes the pure nonion-
ic micelle. ϕ_{12} represents the fraction of the total number of z
contacts which are between nonionic and anionic surfactants. The
$\phi_{12}*$ is a fraction of such contacts in a random distribution; where-
as $\overline{\phi}_{12}$ is a fraction of contacts determined by the quasichemical
approximation (16)

$$\overline{\phi}_{12} = \frac{1 - \sqrt{1 + 4y_1y_2[\exp(-\frac{zw}{kT}) - 1]}}{2[1 - \exp(-\frac{2w}{kT})]} \tag{2}$$

The quantity χ is given by

$$\chi = -2\,\ell n(1 - f) \tag{3}$$

where f represents the fraction of the available space occupied by
an ethylene oxide unit composing a portion of the surfactant hydro-
phile. Using a selfconsistent approximation (17), f can be deter-
mined as follows:

$$f\sqrt{-\frac{2}{3}\,\ell^2\ell n(1 - f)} = \nu\zeta_2 \tag{4}$$

where ζ_2 is the chain density given by $y_2/(y_1A_1 + y_2A_2)$, ℓ is the
length of each step taken in the positioning of the chain, the ex-
cluded volume per repeating unit, ν, is equal to the volume of a
sphere with radius $\ell/2$ and A_1 and A_2 are, respectively, the area per
amphiphile of nonionic and anionic components.
    The development of these equations has been reported elsewhere
(12), and it has also been shown using ultrafiltration techniques
that the composition of the monomer is well predicted by the equa-
tion (12)

$$y_i\gamma_iCMC_i = x_iCMC_{MIX} \quad , \quad i=1,2 \tag{5}$$

which have been developed based on the phase separation model. The
γ_i are obtained from the excess free energy expression, Equation 1,
and the classical equation

$$\gamma_i = f^E + (1 - y_i)\frac{df^E}{dy_i} \tag{6}$$

    Equation 1 has proved to be a better predictor of the equili-
brium which exists between monomer and micelles for mixed surfactant
systems than is the regular solution theory model. It also predicts
well the mixture CMC and shows the heat of mixing to be smaller than
that predicted by the regular solution theory in agreement with the
experiment (13). The purpose of this paper is to further explore

the validity of the thermodynamic model for mixed micelles as
expressed by Equation 1. Using ultrafiltration techniques, the
equilibrium between monomer and micelles has been measured for mix-
tures of an alkylbenzene sulfonate and two ethoxylated nonyl phenols
as a function of temperature. It will be seen that when the average
number of ethylene oxide units is modest ($\approx$ 10), the theory
accurately predicts the changing monomer composition without chang-
ing any of the physical parameters. However, for long ethylene
oxide chains ($\approx$ 50), the prediction deviates from the measured val-
ues indicating additional factors and must be incorporated into the
free energy expression. These additional terms are believed to be
related to the changing hydration of the ethylene oxide chains with
changing temperature. There have been few reports on the effect of
temperature on the CMC of surfactant mixtures, and to the authors'
knowledge none have reported the monomer compositions in equilibrium
with micelles.

Thermodynamics of Mixed Micelle Formation

A brief accounting of the thermodynamics of mixed micelle formation
is given here primarily to clarify certain important issues which
appear to have been previously overlooked. The necessity for mea-
suring the monomer and micellar composition will be demonstrated.

Consider the formation of a mixed micelle in aqueous solution
from a binary surfactant solution consisting of a nonionic and an
anionic surfactant. The process is depicted as the aggregation of
n_B molecules of nonionic surfactant B, of n_A molecules of anionic
surfactant A^-, and in addition there will be counterions, C^+, of the
anionic surfactant in the amount of αn_A where α is the fraction of
the counterions associated or bound with the surfactant anions in
the micelle. The process as depicted is

$$n_A A^- + n_B B + \alpha n_A C^+ \rightleftarrows A_{n_A} B_{n_B} C_{\alpha n_A} \tag{7}$$
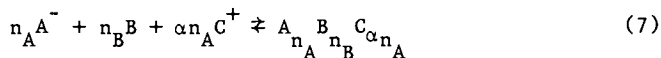
For this reversible process

$$\mu_{MIC} = n_A \mu_A + \alpha n_A \mu_C + n_B \mu_B \tag{8}$$

Assuming that the CMC is small, so that the activity coefficients
may be neglected, the monomer phase chemical potentials are given
by Equations 9-11.

$$\mu_A = \mu_A^o + kT \ln \frac{C_A}{C_w} \tag{9}$$

$$\mu_B = \mu_B^o + kT \ln \frac{C_B}{C_w} \tag{10}$$

$$\mu_C = \mu_C^o + kT \ln \frac{C_C}{C_w} \tag{11}$$

where C_w is the molar concentration of water and γ_C is an activity coefficient. Based on the phase separation model, the micellar phase activity coefficient is the chemical potential of the micellar standard state, or

$$\frac{\mu_{MIC}}{n} = \mu^o_{MIC} \tag{12}$$

In the presence of added electrolyte $C_C = C_S + CMC$. For $C_S \gg CMC$, C_C is very closely given by C_S. Noting that $y_1 = n_A/(n_A + n_B)$ and $y_2 = n_B/(n_A + n_B)$, and that $C_A = x_1 CMC_M$ and $C_B = x_2 CMC_M$, Equation 8 becomes, after rearrangement

$$\Delta G^o_{MIC,M} = (\mu^o_{MIC} - y_1\mu^o_A - y_2\mu^o_B - \alpha y_1\mu^o_C)$$

$$= kT\{\ell n[(\frac{CMC_M}{C_w} x_1)^{y_1} (\frac{CMC_M}{C_w} x_2)^{y_2} (\frac{\gamma_C C_S}{C_w})^{\alpha y_1}]\} \tag{13}$$

where the bracketed term on the left side of the equation may be defined as the standard free energy for the formation of the micelle (per surfactant chain in the micelle). An equilibrium constant K can be defined as

$$K(T,\alpha,y_1) = [\frac{CMC_M}{C_w}][x_1]^{y_1}[x_2]^{y_2}[\frac{\gamma_s C_s}{C_w}]^{\alpha y_1} \tag{14}$$

The standard free energy is therefore determined by measurement of the mixture CMC holding the micellar composition fixed. This analysis assumes that α is known as a function of temperature and micellar composition and is independent of the electrolyte composition. The heat of micellization cannot be determined from measurement of the temperature dependence of CMC_M without knowledge of the micellar composition and of α. Interpretation of calorimetric data is not possible without information regarding micellar composition. Ultrafiltration techniques designed to measure micellar compositions take an added importance when considering heats of micellization.

Experimental

The experimental methods have been described in previous publications (12,18). The decyl benzene sulfonate used in this study is isomerically pure with the benzene ring attached to the third carbon of the alkyl chain. This surfactant is designated as $3\phi C_{10}$. The nonyl phenol ethoxylates were of the Igepal CO series, donated by GAF Corporation. The particular species used were the CO660 and the CO970 surfactants. These commercial surfactants are each a polydispers mixture, the average number of ethylene oxide units being 10 and 50, respectively. These surfactants are abbreviated as NPE_{10} and NPE_{50}.
Sodium chloride, 0.17 M, was added to all surfactant solutions studied to prevent electrostatic forces from becoming significant

across the membrane. This also is a sufficient electrolyte concentration so that the approximation $C_S \gg CMC_M$ is satisfied.

The concentration and composition of the filtrand and filtrate were determined by reverse-phase liquid chromatography with an estimated error of less than 5%.

Results and Discussion

The CMC can be determined using ultrafiltration ($\underline{18}$). Figure 1 shows the CMC of NPE_{10} as a function of temperature and the thermodynamic properties determined using these data are given in Table I together with those of the other surfactants studied. The values are subject to some uncertainty because the complex CMC/temperature behavior renders differentiation of the data inaccurate. The values are, however, comparable to those for similar surfactants reported by others.

Table I.   Thermodynamic Properties of Surfactant Micellization in Aqueous Solutions at 300°K

Surfactant	$\Delta G^o{}_{MIC}$ (kcal/mol)	$\Delta H^o{}_{MIC}$ (kcal/mol)	$T\Delta S^o{}_{MIC}$ (kcal/mol)
NPE_{10}	-8.15	3.0	11.10
NPE_{50}	-7.23	5.0	12.00
$3\phi C_{10}$	-8.13	-7.5	+ 1.38

Figure 2 compares the mixture CMC to the values calculated using both Equation 1 and the regular solution model. This comparison is similar to those for other systems which we have studied and reported elsewhere ($\underline{12}$). The parametric values used in calculating the mixture CMC, as well as the micellar composition presented in Figure 3 are listed in Table II. Their significance has been discussed elsewhere; however, it is relevant to note that w, the interaction parameter, is related to the heat of mixing micelles which will be investigated here. Experiments conducted on a large number of mixtures all at 27°C have suggested w to be independent of EON.

The micellar composition shown in Figure 3 agrees well with predictions based on Equation 1 and reasonably well with the regular solution model. Similar agreement has been found at 37 and 50°C for the $3\phi C_{10}/NPE_{10}$ system without any modification of the parameters. This is reflected by the values shown in Table II for the $3\phi C_{10}/NPE_{10}$ system which apply over the temperature range between 27 and 50°C. Both the mixture CMC and the micellar composition are well fit using these parameters.

The $3\phi C_{10}/NPE_{50}$ system did not yield a similar agreement. Shown by Figures 4 and 5 are the CMC_M and micellar compositions at 50°C. To force Equation 1 to fit these results, it was necessary to modify the parameters. These changes are reflected by the temperature dependence shown in Table II for the system $3\phi C_{10}/NPE_{50}$. Note that both the interaction parameter, w, and the molecular area ratio, R, change as the temperature is changed. No definite trend is indicated. The value of w first increases and then decreases and R is somewhat increased. The increase in temperature is known to influence the hydrogen bonding between water and the polyethylene
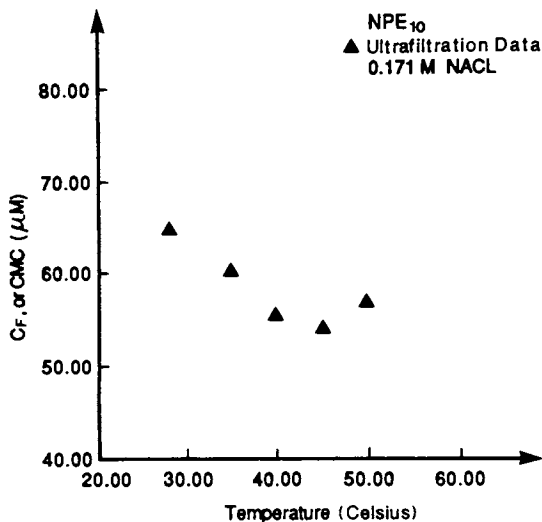
Figure 1.   CMC   versus   temperature   for   NPE$_{10}$:
             effect of temperature on the CMC for
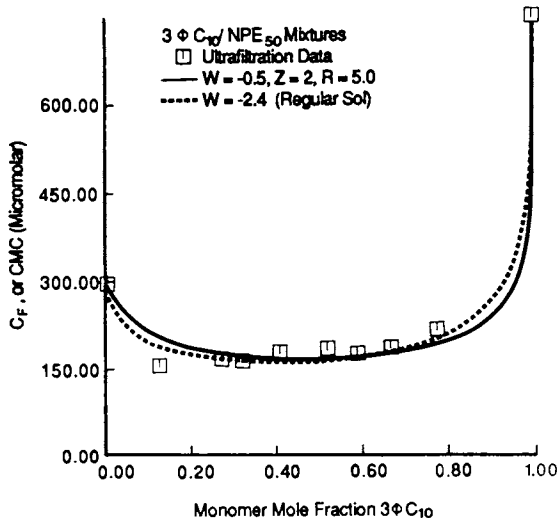   NPE$_{10}$ in 0.171 M NaCℓ.

Figure 2.   CMC's for 3ϕC$_{10}$/NPE$_{50}$ mixtures: vari-
             ation of the mixture critical micelle
             concentration with monomer phase compo-
             sition for mixtures of decyl benzene
             sulfonate with a nonyl phenol ethyoxy-
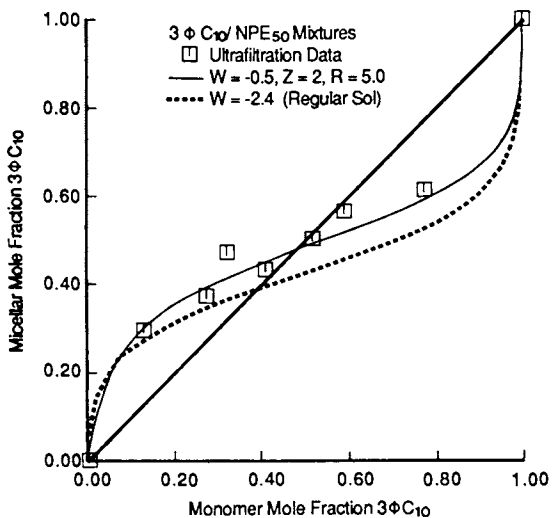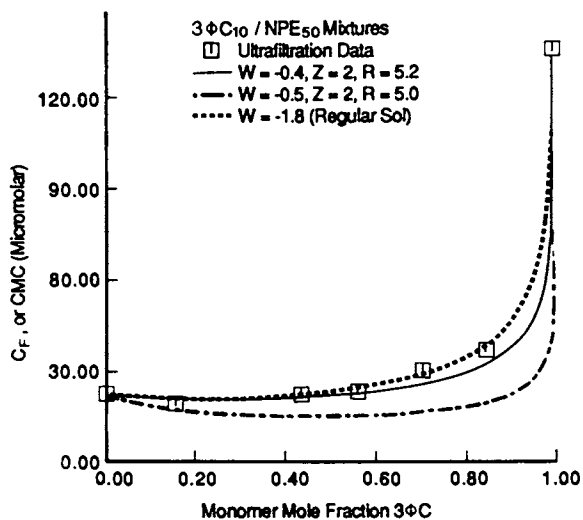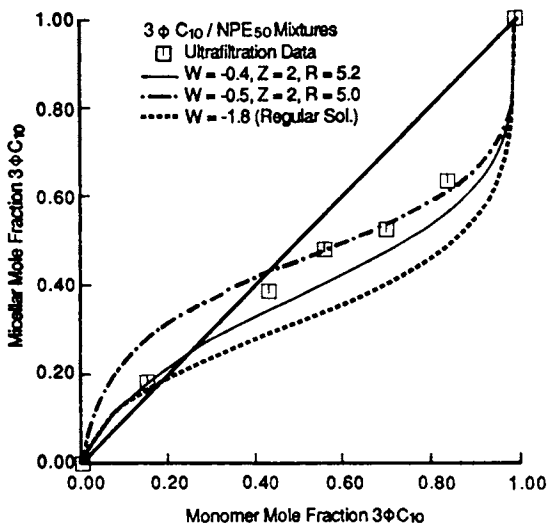   late having an ethylene oxide chain
             length of 50, at 27 °C.

Figure 3.   Phase compositions for $3\phi C_1\text{-}/NPE_{50}$ mix-
tures: variation of the micellar phase
composition with monomer phase composi-
tion for mixtures of decyl benzene sul-
fonate with a nonyl phenol ethoxylate
having an ethoxylate having an ethylene
oxide chain length of 50, at 27 $^{\circ}$C.

Figure 4.   CMC's for $3\phi C_{10}$/NPE$_{50}$ mixtures: varia-
tion of the mixture critical micelle
concentration with monomer phase compo-
sition for mixtures of decyl benzene
sulfonate with a nonyl phenol ethoxy-
late having an ethylene oxide chain
length of 50, at 50 °C.

Figure 5.   Phase compositions for $3\phi C_{10}/NPE_{50}$ mix-
tures: variation of the micellar phase
composition with monomer phase composi-
tion for mixtures of decyl benzene sul-
fonate with a nonyl phenol ethoxylate
having an ethylene oxide chain length
of 50, at 50 °C.

oxide chain and will cause conformational changes in the arrangement
of the hydrophile. One would anticipate a decrease in the radius
of gyration which should increase the area occupied by the molecules
at the micellar surface. This should also tend to decrease the
charge density and thereby decrease w (make it more negative).
These trends are not incorporated into the theory; and therefore,
it is necessary to alter the parameters to obtain a reasonable cor-
respondence with the results.

Table II. Parametric Values Used for Micellar Pseudo Activity

Surfactant Combination	Temperature ($^\circ$C)	Z	R (kcal/mol)	w	w_{RS} (kcal/mol)
$3\phi C_{10}/NPE_{10}$	27 - 50	2	3.0	-0.5	-1.5
$3\phi C_{10}/NPE_{50}$	27	2	5.0	-0.5	-2.4
$3\phi C_{10}NPE_{50}$	37	2	5.0	-0.5	-2.4
$3\phi C_{10}/NPE_{50}$	50	2	5.2	-0.4	-1.8

Selections Valid for All Combinations

$$\ell = 1.5 \text{ A}$$

$$\nu = \frac{4}{3}(1.5 \text{ A})^3$$

$$N_s = 3N_{EO}$$

$$\zeta_2 = \frac{y_2}{y_1 A_1 + y_2 A_2}$$

$$R = \frac{A_2}{A_1}$$

Although these parameter modifications are consistent with the
expected increase in the hydrophobicity of the ethylene oxide units
expected with increasing temperature, no relationship exists which
quantifies the model parameters as a function of temperature. Fig-
ures 4 and 5 taken together with others available elsewhere there-
fore serve to show that the new model does not accurately represent
the thermodynamic behavior of the long ethylene oxide chain surfac-
tants in aqueous solutions. It is adequate for shorter chain non-
ionic surfactants. The origin of the difference between the model
predictions and those measured can be further investigated by delv-
ing into thermodynamics of mixed micelle formation. This is possi-
ble for the first time since monomer and micellar compositions are
available through the use of ultrafiltration. Schick and Manning
(19) calculated the partial molal heats of micelle formation for
binary mixtures of dodecanol ethoxylates with n-dodecyl sulfate,
from measurements of mixture CMC, by the surface tension method, as
a function of temperature. The surface tension method, however,
yields no information about the pseudophase compositions which are
required in the calculation of the free energy and enthalpy of mi-
cellization (see Equation 14). Calculation of heats of micelliza-
tion based on knowledge of CMC_M alone requires an assumption of the
pseudophase compositions, which can introduce considerable error.
The standard free energy of micellization for mixed micelles in

which the mole ratio of surfactant types is equal ($y_1 = y_2 = 0.5$) have been calculated from data similar to that shown by Figures 1, 2, 3, 4, and 5.

To calculate the free energy one must assign a value to α, the degree of counterion binding. The theoretical development admits the possibility that α can depend on temperature and on micellar composition, but it must be independent of the salt concentration. The α used in the calculations presented here is 0.42. This value has been determined at 27°C by measuring the variation of the CMC with added electrolyte concentration. It has been used in all free energy calculations. A more comprehensive study would necessarily include determination of α by several methods including, for example, electrical conductivity and sodium ion activity measurements as well as direct calorimetric determination of the enthalpy of mixing. In the presence of large quantities of electrolyte which characterize this study, many of these methods are ineffective. Thus, the value of α determined by measuring the variation of CMC with electrolyte has been used.

The activity coefficient for the counterions was taken to be a constant value of 0.862. This value was derived from the experimental value of 0.745 for NaCl, which was reported by Moore (20). The sodium ion activity coefficient was obtained as the square root of the sodium chloride activity coefficient.

The values for $\Delta G^o{}_{MIC,M}$ (the subscript M now denotes mixture standard free energy) determined using Equation 13 along with the corresponding mixture CMC's and monomer compositions are given in Table III. It is observed that $\Delta G^o{}_{MIC,M}$ are smaller (more negative) for mixtures containing NPE_{10} than for those with NPE_{50}. This could reflect configurational entropy changes on micellization which would be larger in mixtures containing NPE_{50} than those containing NPE_{10} and which disfavor micellization. Standard enthalpies and entropies of micellization are also given in Table IV. It is seen that the formation process is exothermic for these 1:1 mixed micelles and that the entropy of formation is positive and intermediate between that of the pure components.

Table III.   Free Energy of Micellization for ABS/NPE Mixtures

Surfactant Combination	Temperature (°K)	CMC	x^1	$\Delta G^o{}_{MIC}$ kcal/mol
$3\phi C_{10}/NPE_{10}$	300	176	0.899	-9.04
$3\phi C_{10}/NPE_{10}$	310	276	0.939	-9.21
$3\phi C_{10}/NPE_{10}$	323	315	0.948	-9.55
$3\phi C_{10}/NPE_{50}$	300	170	0.543	-8.76
$3\phi C_{10}/NPE_{50}$	310	200	0.671	-8.99
$3\phi C_{10}/NPE_{50}$	323	272	0.744	-9.22

[1]$3\phi C_{10}$ monomer mole fraction.

The importance of entropic considerations in the formulation of a thermodynamic model for micelle formation in mixtures of ionic and nonionic surfactants has been demonstrated by the ability of the

Table IV.   Enthalpy and Entropy of Micellization for ABS/NPE
Mixtures

Surfactant Combination	Temperature ($^{\circ}K$)	ΔH°_{MIC} (kcal/mol)	$T\Delta S^{\circ}_{MIC}$ (kcal/mol)
$3\phi C_{10}/NPE_{10}$	305	-4.0	13.1
$3\phi C_{10}/NPE_{10}$	313	-0.9	10.1
$3\phi C_{10}/NPE_{50}$	305	-1.9	10.7
$3\phi C_{10}/NPE_{50}$	313	-3.6	12.6

Note: Enthalpies and entropies for formation of a micelle of equi-
molar proportions of $3\phi C_{10}$ and $NPE_x(x = 10$ or $50)$.

new model to fit both the mixture CMC and the pseudophase composi-
tional data at different temperatures with little change in param-
eters. A further test of the model would be to compare its predic-
tions for the heat of mixing with that obtained by other means. The
best source for heat of mixing data is calorimetry, but no measure-
ments including micellar compositions and counterion binding have
been reported. Heat of mixing data derived from measurement of the
variation of CMC with temperature are less reliable but can provide
some test of the model. The enthalpy of mixing ΔH°_{MIX} is related
to the enthalpies of micellization as follows:

$$\Delta H^{\circ}_{MIX} = \Delta H^{\circ}_{MIC,M} - y_1 \Delta H^{\circ}_{MIC,1} - y_2 \Delta H^{\circ}_{MIC,2} \qquad (15)$$

These are tabulated in Table V along with the model predictions

Table V.   Enthalpy of Mixing Decyl Benzene Sulfonate Micelles with
Nonyl Phenol Ethoxylate Micelles

Surfactant Combination	Temperature ($^{\circ}K$)	$\Delta H_{MIX}{}^1$ (kcal/mol)	$\Delta H_{MIX}{}^2$ (kcal/mol)	$\Delta H_{MIX}{}^3$ (kcal/mol)
$3\phi C_{10}/NPE_{10}$	305	-1.98	-0.574	-0.375
$3\phi C_{10}/NPE_{10}$	316	-0.50	-0.571	-0.600
$3\phi C_{10}/NPE_{50}$	305	-0.85	-0.574	-0.375
$3\phi C_{10}/NPE_{50}$	316	-2.88	-0.571	-0.600

[1]Derived from CMC and compositional data.
[2]Model calculation from Equation 1.
[3]Regular solution model.

obtained by

$$\Delta H^{\circ}_{MIX} = Z\phi_{12}w \qquad (16)$$

which is the enthalpic contribution to the free energy defined by
Equation 1. It is seen that little variation with temperature is
predicted for ΔH°_{MIX} by the model whereas the values derived from
temperature dependence of the CMC show considerable change with tem-
perature. The source of the discrepancy is uncertain. There are
indications that the hydration effects, which should be accounted

for by the pure component $\Delta H_{MIC,2}$, may differ between the pure component and mixed component micelles. Much more data of the type reported here will be required to fully evaluate the new thermodynamic model or to discern the origin of the apparent difference.

Acknowledgments

Literature Cited

1. Kurzendorfer, C. P.; Schwuger, M. J.; Lange, H. Ber. Bunsenges. Phys. Chem. 1978, 82, 962.
2. McCoy, D. R.; Naylor, C. G. U.S. Patent 4 288 344, 1981.
3. Hinkamp, P. E.; Tomkins, D. C.; Byth, N. J.; Thompson, J. L. Europe Patent Application 32 072.
4. Lange, H. Kolloid Z.-Z. Polym. 1953, 131, 96.
5. Shinoda, K. J. Phys. Chem. 1954, 58, 541.
6. Lange, H.; Beck, K.-H. Kolloid Z.-Z. Polym. 1973, 251, 424.
7. Rubingh, D. N. ACS Colloid Surf. Sci. Symp. 1978, 1, 185.
8. Funasaki, N.; Hada, S. J. Phys. Chem. 1979, 83, 2471.
9. Scamehorn, J. F.; Schechter, R. S.; Wade, W. H. J. Disp. Sci. Tech. 1982, 3, 261.
10. Holland, P. M.; Rubingh, D. N. J. Phys. Chem. 1983, 87, 1984.
11. Kamrath, R. F.; Franses, E. I. Ind. Eng. Chem. Fundam. 1983, 22, 230.
12. Osborne-Lee, I. W.; Schechter, R. S.; Wade, W. H. J. Colloid Interface Sci. 1985 (in press).
13. Holland, P. M. In "Relation Between Structure and Performance of Surfactants"; Rosen, M. F., Ed.; ACS SYMPOSIUM SERIES No. 253, American Chemical Society: Washington, D.C., 1984; pp. 141-151.
14. Nishikido, N. J. Colloid Interface Sci. 1969, 30, 338.
15. Tokiwa, F.; Aigama, K. Kolloid Z.-Z. Polym. 1969, 239, 687.
16. Prigogine, I. "The Molecular Theory of Solutions"; North Holland Publishing Company: Amsterdam, Holland, 1957.
17. Kox, A. J.; Wiegel, F. W. Physica 92A 1978, 466.
18. Osborne-Lee, I. W.; Schechter, R. S.; Wade, W. H. J. Colloid Interface Sci. 1983, 94, 179.
19. Schick, M. J.; Manning, D. J. J. Am. Chem. Soc. 1966, 43, 133.
20. Moore, W. "Physical Chemistry"; Prentice Hall Inc.: Englewood Cliffs, 1972; Table 10.6.

3

New Mathematical Models of Mixed Micellization

Robert F. Kamrath[1] and Elias I. Franses

School of Chemical Engineering, Purdue University, West Lafayette, IN 47907

The mass action model (MAM) for binary ionic or nonionic surfactants and the pseudo-phase separation model (PSM) which were developed earlier (I & EC Fundamentals 1983, 22, 230; J. Phys. Chem. 1984, 88, 1642) have been extended. The new models include a micelle aggregation number and counterion binding parameter which depend on the mixed micelle composition. Thus, the models can describe mixtures of ionic/nonionic surfactants more realistically. These models generally predict no azeotropic micellization. For the PSM, calculated mixed cmc's and especially monomer concentrations can differ significantly from those of the previous models. The results are used to estimate the Redlich-Kister parameters of monomer mixing in the mixed micelles from data on mixed cmc's of Lange and Beck (1973), Funasaki and Hada (1979), and others.

Many models have appeared in the literature describing interactions of surfactants in mixed micelles (1-14). For nonionic surfactants mixing nonideally, the key references up to 1984 have been recently summarized (15). Comparatively few models have been developed for ionic surfactants (5,6,10-12) and fewer models which acknowledge ionic/nonionic interactions are available (5-7). Since many practical surfactant mixtures involve ionic and nonionic surfactants which interact with each other and with added salts, it is important to develop explicit ionic/nonionic models.

The purpose of this paper is to develop realistic specific models of mixed micellization which (i) can describe properties of ionic/nonionic surfactant mixtures and effects of salt; (ii) lead to tractable calculations; and (iii) can be used for extracting information on micelle mixing and monomer concentrations from the limited experimental data which are usually

---

[1]Current address: 3M, Commercial Chemicals Division, Building 53–4N–02, 367 Grove Street, St. Paul, MN 55101.

available on cmc's, micelle sizes, and counterion binding. The mixed ionic surfactant pseudo-phase separation model (PSM) which has been previously published (10,12) has been extended to include the counterion binding parameter β (see Equation 1 later) which depends on the micelle composition x. The mass action model ((11), MAM) has also been extended to include $\beta(x)$ and aggregation number N also varying with the micelle composition. In the following sections the key aspects of the two models are discussed. Sample calculations are given for the PSM to illustrate the importance of $\beta(x)$ on the calculated cmc's and inventories. Finally, the PSM model is applied for interpreting experimental results, mostly from the literature on mixed nonionic/ionic and ionic/ionic binary surfactants with the same counterion.

Mass Action Model (MAM)

The equation which formally describes the micellization of binary surfactants is

$$xNR_1 + (1-x)R_2 + \beta NM^+ \overset{K_x}{\rightleftharpoons} (R_1R_2M)_{N,\beta,x} \tag{1}$$
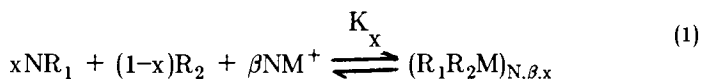
where R_1 and R_2 are monomers of surfactants 1 and 2, M^+ is the surfactant counterion, $(R_1R_2M)_{N,\beta,x}$ is a charged mixed micelle composed of N surfactant monomers and βN counterions, x is the fraction of monomers of surfactant 1 in the mixed micelle, and K_x is the micellization equilibrium constant; 1 is the component with the lower cmc. The degree of counterion binding β is taken to depend on x such that at $x = 0$ $\beta = \beta_2$ and at $x = 1$ $\beta = \beta_1$. The aggregation number N is taken to depend on x such that at $x = 0$ $N = N_2$ and at $x = 1$ $N = N_1$. We take that β_1, β_2, N_1, and N_2 are independent of concentration and ionic strength and that at any given concentration x, N, and β are the same for all micelles except for cases of demixing in micelles (10-12). The solution is taken to be ideal in the sense of Denbigh's convention III (16); hence, the activity coefficients of solvent, monomers, and micelles are taken equal to unity (10,11). For concentrated solutions a solution model such as Debye-Hückel's (14) or others (3,4) should be used for more accurate results.

The MAM described here is a generalization of the model previously published (10). Hence, only a summary of the derivation will be given here. Details can be found elsewhere (17). The basic equations are the surfactant and counterion material balances and the minimization of the Gibbs free energy of the system with respect to the micelle concentration c_m and mole fraction x (11). Equation 4 from Ref. (11) has been changed to

$$c_{M^+} + \beta N c_m = P c_T + c_s \tag{2}$$

where c_T is the total concentration of the surfactant and c_s is the concentration of salt with common counterion; the parameter P is the ratio of the total ionic surfactant concentration to the total surfactant

concentration. P allows one to model either purely ionic systems, $P = 1$, or ionic/nonionic, $P = \alpha$ or $P = 1 - \alpha$, where α is the mole fraction of 1 in the binary surfactant mixture. Only anionic/anionic or cationic/cationic mixtures can be described by the present models.

Equations (6) and (7) from Ref. (11) are modified to

$$\frac{\partial \mu_m^o}{\partial x} = \left[N + x\frac{\partial N}{\partial x}\right]\mu_1 - \left[N - (1-x)\frac{\partial N}{\partial x}\right]\mu_2 + \left[\beta\frac{\partial N}{\partial x} + N\frac{\partial \beta}{\partial x}\right]\mu_{M^+} \quad (3)$$

and

$$\mu_m^o = x\,\frac{N}{N_1}\,\mu_{1N_1}^o + (1-x)\,\frac{N}{N_2}\,\mu_{2N_2}^o + [\beta(x) - x\beta_1 - (1-x)\beta_2]N\mu_{M^+}^o$$

$$+ RTN\,\{x\ell nx + (1-x)\ell n(1-x) + x(1-x)w(x)\} \quad (4)$$

where μ_m^o, $\mu_{1N_1}^o$, and $\mu_{2N_2}^o$ are the reference chemical potentials of the mixed micelles and pure micelles of sizes N, N_1, and N_2 respectively. As before (10), w(x) is a function which measures the excess free energy of mixing in the mixed micelle. The $\beta(x)$... term accounts for additional counterions needed for a mixed micelle with $\beta(x)N(x)$counterions. The mixed micelle is produced from xN micelles of 1 which have $x\beta_1N$ counterions and $(1-x)N$ micelles of 2 which have $(1-x)\beta_2N$ counterions. Of course, if $\beta(x) = \beta_1x + \beta_2(1-x)$, this term vanishes (see also PSM section).

After algebraic manipulations, the model reduces to the solution of the following four nonlinear equations for x and the monomer and counterion concentrations c_1, c_2, and c_{M^+}:

$$\frac{x^{[N + x\frac{\partial N}{\partial x}]}}{(1-x)^{[N-(1-x)\frac{\partial N}{\partial x}]}} = \frac{c_1^{[N + x\frac{\partial N}{\partial x}]}}{c_2^{[N-(1-x)\frac{\partial N}{\partial x}]}}\, c_{M^+}^{[\beta\frac{\partial N}{\partial x} + N\frac{\partial \beta}{\partial x}]}$$

$$\cdot \left[\frac{\epsilon}{N_1(1-\epsilon)^{N_1}(1-\beta_1\epsilon)^{\beta_1 N_1}}\,\frac{1}{c^{\bullet}_{1}^{[N_1(1 + \beta_1)-1]}}\right]^{\frac{1}{N_1}[N + x\frac{\partial N}{\partial x}]}$$

$$\cdot \left[\frac{\epsilon}{N_1(1-\epsilon)^{N_2}(1-\beta_2\epsilon)^{\beta_2 N_2}}\,\frac{1}{c^{\bullet}^{[N_2(1 + \beta_2)-1]}}\right]^{-\frac{1}{N_2}[N-(1-x)\frac{\partial N}{\partial x}]}$$

$$\cdot \exp\left[-(1-2x)Nw(x) - x(1-x)N\frac{\partial w}{\partial x} - x(1-x)\frac{\partial N}{\partial x}w(x)\right] \quad (5)$$

$$c_1 + \left\{ xN\left[\frac{\epsilon}{N_1(1-\epsilon)^{N_1}(1-\beta_1\epsilon)^{\beta_1 N_1}}\right]^{\left[x\frac{N}{N_1} + (1-x)\frac{N}{N_1}\left[\frac{N + x\frac{\partial N}{\partial x}}{N-(1-x)\frac{\partial N}{\partial x}}\right]\right]} \right.$$

$$\cdot \left(\frac{c_1}{xc_1^*}\right)^{\left[xN + (1-x)N\left[\frac{N + x\frac{\partial N}{\partial x}}{N-(1-x)\frac{\partial N}{\partial x}}\right]\right]} \cdot c_M^{\left[\beta N + \left[\frac{(1-x)N[\beta\frac{\partial N}{\partial x} + N\frac{\partial \beta}{\partial x}]}{N-(1-x)\frac{\partial N}{\partial x}}\right]\right]}$$

$$\cdot c_1^{\left[(1-\beta_1 N_1)\left[x\frac{N}{N_1} + (1-x)\frac{N}{N_1}\left[\frac{N + x\frac{\partial N}{\partial x}}{N - (1-x)\frac{\partial N}{\partial x}}\right]\right]\right]} \cdot \exp\left[-x(1-x)Nw(x)\right]$$

$$- \left[\frac{N}{N-(1-x)\frac{\partial N}{\partial x}}\right]\left[(1-2x)(1-x)Nw(x)-x(1-x)^2 N\frac{\partial w}{\partial x}-x(1-x)^2\frac{\partial N}{\partial x}w(x)\right]\right\} = \alpha c_T$$

$$(6)$$

$$c_2 + \left\{(1-x)N\left[\frac{\epsilon}{N_2(1-\epsilon)^{N_2}(1-\beta_2\epsilon)^{\beta_2 N_2}}\right]^{\left[(1-x)\frac{N}{N_2} + \frac{N}{N_2}\left[\frac{N-(1-x)\frac{\partial N}{\partial x}}{N + x\frac{\partial N}{\partial x}}\right]\right]}\right.$$

$$\cdot \left(\frac{c_2}{(1-x)c_2^*}\right)^{\left[(1-x)N + xN\left[\frac{N-(1-x)\frac{\partial N}{\partial x}}{N + x\frac{\partial N}{\partial x}}\right]\right]} \cdot c_M^{\left[\beta N - \left[\frac{xN[\beta\frac{\partial N}{\partial x} + N\frac{\partial \beta}{\partial x}]}{N + x\frac{\partial N}{\partial x}}\right]\right]}$$

$$\cdot c^\bullet \left[(1-\beta_2 N_2) \left[(1-x)\frac{N}{N_2} + x\frac{N}{N_2} \left[\frac{N-(1-x)\frac{\partial N}{\partial x}}{N + x\frac{\partial N}{\partial x}} \right] \right] \right]$$

$$\cdot \exp \left[-x (1-x)Nw(x) + \left[\frac{N}{N + x\frac{\partial N}{\partial x}} \right] \left[x(1-2x)Nw(x) + x^2(1-x) N \frac{\partial w}{\partial x} \right. \right.$$

$$\left. \left. + x^2 (1-x)\frac{\partial N}{\partial x} w(x) \right] \right] \right\} = (1-\alpha)c_T \tag{7}$$

$$c_{M^+} + \left\{ \beta N \left[\frac{\epsilon}{N_1(1-\epsilon)^{N_1}(1-\beta_1\epsilon)^{\beta_1 N_1}c_{1\bullet}^{(\beta_1 N_1 - 1)}} \right] x \frac{N}{N_1} \right.$$

$$\cdot \left[\frac{\epsilon}{N_2(1-\epsilon)^{N_2}(1-\beta_2\epsilon)^{\beta_2 N_2} c^{\bullet (\beta_2 N_2 - 1)}} \right]^{(1-x)\frac{N}{N_2}}$$

$$\left. \cdot \left[\frac{c_1}{x c_1^*} \right]^{xN} \left[\frac{c_2}{(1-x) c_2^*} \right]^{(1-x)N} c_{M^+}^{\beta N} \exp\left[-x(1-x)Nw(x) \right] \right\} + Pc_T + c_s \tag{8}$$

These four equations reduce to the equations of Ref. (11) if N and β are fixed. The micelle concentration is then calculated from a mass action model expression as before, where (17)

$$K_x = K_1^{x \frac{N}{N_1}} K_2^{(1-x) \frac{N}{N_2}} x^{-xN} (1-x)^{-(1-x)N} \exp[-x(1-x)Nw(x)] \tag{9}$$

The parameter ϵ is defined in Ref. (11) and is usually taken to be 0.02. The mixed cmc c^* can be calculated as a function of c_1^*, c_2^*, α, β_1, β_2, $\beta(x)$, N_1, N_2, $N(x)$, P, and c_S (17). Given these parameters and c_T, one can calculate all pertinent parameters if there is only one type of mixed micelles. If there is demixing, the model can be extended as previously described (11). No specific calculations on the MAM model are yet available.

<u>Azeotrope Micellization.</u> Here the micelle mole fraction of 1 is the same as that of the monomers (10,11). For fixed $\alpha = \alpha_{AZ}$, the monomer and micelle compositions are equal to α for all total surfactant concentrations. If an azeotrope exists, this azeotropic condition and Equation 5 imply that

$$
(c_1+c_2)^{\frac{\partial N}{\partial x}} c_{M^+}^{[\beta\frac{\partial N}{\partial x} + N\frac{\partial \beta}{\partial x}]} \left[\frac{\epsilon}{N_1(1-\epsilon)^{N_1}(1-\beta_1\epsilon)^{\beta_1 N_1}} \frac{1}{c_{1^\bullet}^{[N_1(1+\beta_1)-1]}} \right]^{\frac{1}{N_1}[N+\alpha\frac{\partial N}{\partial x}]}
$$

$$
\cdot \left[\frac{\epsilon}{N_2(1-\epsilon)^{N_2}(1-\beta_2\epsilon)^{\beta_2 N_2}} \frac{1}{c_{\bullet}^{[N_2(1+\beta_2)-1]}} \right]^{-\frac{1}{N_2}[N-(1-\alpha)\frac{\partial N}{\partial x}]}
$$

$$
\cdot \exp\left[-(1-2\alpha)Nw(\alpha) - \alpha(1-\alpha)N\frac{\partial w}{\partial x} - \alpha(1-\alpha)\frac{\partial N}{\partial x}w(\alpha) \right] = 1 \quad (10)
$$

where β, N, w, $\partial\beta/\partial x$, $\partial N/\partial x$, and $\partial w/\partial x$ are evaluated at $x = \alpha$. But this equation contains the monomer and counterion concentrations c_1, c_2, and c_{M^+} which change with the total surfactant concentration. Thus α cannot be constant, which means that the assumption of azeotropy ($x = \alpha_{AZ}$) is contradicted. Hence, if $N_1 \neq N_2$ and $\beta_1 \neq \beta_2$, there are no conditions such that $x = \alpha$ for all finite total surfactant concentrations. If N and β are fixed and $N_1 = N_2$ and $\beta_1 = \beta_2$, then Equation 10 reduces to equations previously derived (11).

Pseudo-Phase Separation Model (PSM)

We take the limit of the MAM as $N \to \infty$ and $\epsilon \to 0$ (10,11). The resulting equations, which reduce to equations previously published if β is fixed, are the following:

$$
c_1 = x\gamma_1(x)c_{1}^{\bullet 1+\beta_1} c_{M^+}^{-[(1-x)\frac{\partial\beta}{\partial x} + \beta]} \quad (11)
$$

$$
c_2 = (1-x)\gamma_2(x)c_{2}^{\bullet(1+\beta_2)} c_{M^+}^{[x\frac{\partial\beta}{\partial x} - \beta]} \quad (12)
$$

where (17)

$$
\gamma_1(x) = \exp[(1-x)^2 w(x) + x(1-x)^2\frac{\partial w}{\partial x}] \quad (13)
$$

$$\gamma_2(x) = \exp[x^2 w(x) - x^2(1-x) \frac{\partial w}{\partial x}] \tag{14}$$

The mixed cmc $c^*(c_S)$ at salt concentration c_S, the micellar mole fraction x^* at the cmc, and c_{M^+} at the cmc are found from the following equations:

$$c_1 = \alpha c^*(c_s) = x^* \gamma_1(x^*) c_1^{*(1+\beta_1)} \; c_{M^+}^{-[(1-x^*)\frac{\partial \beta}{\partial x} + \beta(x^*)]} \tag{15}$$

$$c_2 = (1-\alpha)c^*(c_s) = (1-x^*)c_2^{*(1+\beta_2)} \; c_{M^+}^{[x^*\frac{\partial \beta}{\partial x} - \beta(x^*)]} \tag{16}$$

$$c_{M^+} = Pc^*(c_s) + c_s \tag{17}$$

If there is no added salt, $c_s = 0$, then we define simply $c^*(c_s = 0) \equiv c^*$. Above the cmc, the quantities c_1, c_2, c_m, c_{M^+}, and x are found from Equations 11 through 14 and the three mass balances. By eliminating c_1, c_2, and c_m from these equations we obtain a system of two nonlinear equations with unknowns x and c_{M^+}.

$$x(1-x)\left[\gamma_1(x)c^*_1{}^{(1+\beta_1)} \; c_{M^+}^{-[(1-x)\frac{\partial \beta}{\partial x} + \beta]} \right.$$

$$\left. - \gamma_2(x)c^*_2{}^{(1+\beta_2)} \; c_{M^+}^{[x\frac{\partial \beta}{\partial x} - \beta]}\right] = (\alpha-x)\,c_T \tag{18}$$

$$x c_{M^+} - x\beta\gamma_1(x)c^*_1{}^{(1+\beta_1)} \; c_{M^+}^{-[(1-x)\frac{\partial \beta}{\partial x} + \beta]} = (Px-\alpha\beta)c_T + xc_s \tag{19}$$

To this point we have used no specific mixing rule to describe the interactions of monomers of surfactants 1 and 2 in the micellar pseudo-phase. We have assumed, however, that only one micellar pseudo-phase exists. For our calculations we have used the Redlich-Kister expansion for $w(x)$ with up to two parameters (10,12). Moreover, we have not yet specified the form of the function $\beta(x)$, which can be varied for modeling specific counterion association behavior. For our calculations we have used the following linear function for $\beta(x)$:

$$\beta(x) = f_1(x)\beta_1 + f_2(x)\beta_2 = x\beta_1 + (1-x)\beta_2 \tag{20}$$

This simple relationship is probably more appropriate for ionic/ionic

systems, whose counterion binding capacities differ little, than for nonionic/ionic systems. Furthermore, the values of β_1 and β_2 should depend on the aggregation number, the total surfactant concentration, and the ionic strength of the solution. Stigter (18,19) has examined the elec-trostatic interactions between charged micelles and ions in solution. He used the Stern-Gouy-layer model to describe the ionic atmosphere sur-rounding a charged micelle. He concluded that although the counterion association depends on the micellar surface charge and the ionic strength of the solution, there is no clear relationship between these quantities. Stigter observed that a plot of the natural logarithm of the cmc versus the natural logarithm of the counterion concentration was linear. Possibly the effects of the aggregation number, the total surfactant concentration and the ionic strength on the counterion association to the micelle cancel each other. For simplicity of calculations and for lack of concrete evidence, we have taken β_1 and β_2 to be constant. Two recent papers have provided additional data on counterion binding (20,21). In the limit $\beta_1 = \beta_2 = 0$ (where P = 0), this model is the same as the nonionic/nonionic model described previously (10). If $\beta_1 = \beta_2 \neq 0$ (P = 1), the model is the same as the ionic/ionic model (11).

Azeotrope Micellization. Again, if azeotrope exists, $x = \alpha = \alpha_{AZ}$. Then for all total surfactant concentrations above the cmc this condition and Equations 15 and 16 imply that

$$\frac{c_1^{*(1+\beta_1)}}{c_2^{*(1+\beta_2)}} \, c_{M^+}^{\left(\frac{\partial\beta}{\partial x}\right)_{x=o}} \exp\left[(1-2\alpha)w(\alpha) + \alpha(1-\alpha)\left(\frac{\partial w}{\partial x}\right)_{x=\alpha}\right] = 1 \quad (21)$$

This equation contains the counterion concentration c_{M^+} which depends on the total surfactant concentration. It follows that x would depend on c_{M^+} and hence would vary above the cmc. This contradiction implies that azeotrope micellization cannot occur if $\beta = \beta(x)$. Of course, if $c_s \gg c_T$, the c_{M^+} would be constant and azeotropy can again occur. If $\partial\beta/\partial x = 0$, azeotropy can be also possible. For $\beta_1 = \beta_2 = 0.7$, $c_s = 0$, $c_2^*/c_1^* = 3.0$, and $w(x) = A + B (2x-1)$, which is the Redlich-Kister expansion (12), with A = -3 and B = 0, one finds from Equation 21 that $\alpha_{AZ} = 0.8113$. No value of α_{AZ} can be calculated if $\beta_1 = 0.7$, $\beta_2 = 0.3$, and $\beta(x) = \beta_1 x + \beta_2(1-x)$. Figures 1 and 2 illustrate this point showing monomer and micelle concentrations (or inventories) for $\alpha = 0.8113$. In the ionic/ionic case, the micelle composition x and the ratio c_1/c_2 are con-stant above the cmc. In the ionic/nonionic case (Figure 2) the micelle composition varies with total surfactant concentration. Osborne-Lee and Schechter (22) have found evidence of azeotrope micellization for
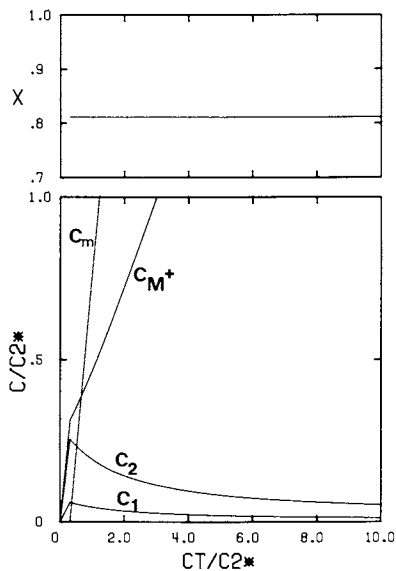
Figure 1. Inventories and micelle compositions for azeotrope micell-
ization of mixed ionic surfactants. $c_2^*/c_1^* = 3.0$, A $= - 3.0$, B $= 0.0$,
$\beta_1 = \beta_2 = 0.7$ and $\alpha = \alpha_{AZ} = 0.8113$.
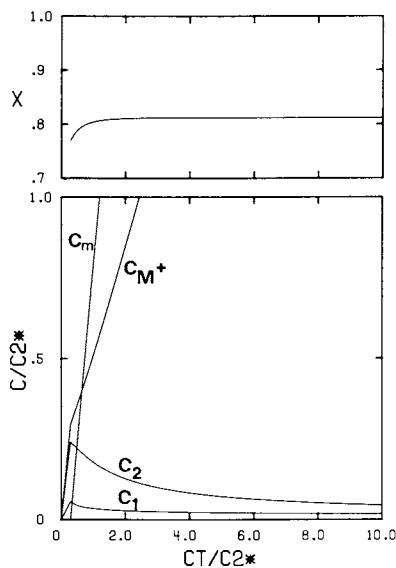
Figure 2. Inventories and micelle compositions for the same param-
eters as Figure 1 except that $\beta_1 = 0.7$ and $\beta_2 = 0.3$.

ionic/nonionic mixtures, for which surely $\beta = \beta(x)$. They have used high concentration of electrolyte and estimated mixed micelle compositions from ultrafiltration experiments. These results are consistent with the model presented here because c_s is high. It would be interesting to see whether in those systems the azeotrope composition or its very existence depend on the salt concentration as Equation 21 suggests.

Sample Calculations. For the PSM model, computer-calculations have been done (17). All concentrations are normalized with respect to c_2^*. In Figure 3 we show mixed cmc's versus overall surfactant composition calculated for mixed surfactants with $c_2^*/c_1^* = 3.0$, A = 0.0, B = 0.0, $c_s/c_2^* = 0.0$, and varying values of β_1, β_2 and P. For a given value of α, the calculated cmc for the nonionic/ionic system ($\beta_1 = 0.6$, $\beta_2 = 0.00$ and P = α) is larger than the cmc for the nonionic/nonionic case ($\beta_1 = \beta_2 = 0.3$, P = 0.0). Therefore if a nonionic/nonionic model is used to determine the interaction parameters A and B for mixed nonionic/ionic surfactant systems from cmc-versus-composition data, the determined values would be larger than those calculated with the nonionic/ionic model. The calculated c^*/c_2^* versus α curve for the nonionic/ionic system exhibits a maximum. Such a maximum can be observed for both positive and negative values of A. For the ionic/ionic and nonionic/nonionic models, the c^*/c_2^* versus α curves only exhibit a maximum if the surfactant chains within the micelles interact with positive deviations from ideal mixing, A > 0. Hence, the estimation of nonideality of mixing parameters from cmc-composition diagrams depend significantly on the model one uses to match the data.

In Figure 3, the curves for the ionic/ionic systems are all below the curve for the nonionic/nonionic case. As the degree of counterion binding increases, i.e. as β_1 and β_2 increase, the value of c^*/c_2^* decreases for a given value of α. The bottom curve in Figure 3 corresponds to the ionic/ionic system with $\beta_1 = 0.6$, $\beta_2 = 0.0$, and P = 1.0. This case is probably physically unrealistic, inasmuch as these parameters correspond to a system in which both surfactants 1 and 2 are ionic and contribute counterions to the system but surfactant 2 in the micelles acts as a nonionic surfactant and therefore has a zero degree of counterion binding.

In Figures 3.9 and 3.10 of Ref. (17) we show how the calculated cmc varies when β_1 is constant and β_2 is varied from 0.0 to 1.0 and for the case when β_2 is constant and β_1 is varied. For fixed β_1 or β_2, the calculated cmc decreases as the other counterion binding parameter decreases for the ionic/ionic cases. The cmc's calculated for the nonionic/ionic systems are larger than those calculated for the ionic/ionic systems. For the nonionic/ionic systems, a maximum occurs in the cmc-versus-α curve at values of α close to that of the pure nonionic surfactant. The maximum becomes greater as the value of α for the ionic surfactant increases.

Inventory and x-plots for an ionic/ionic system are shown in Figure 4 for $\beta_1 = \beta_2 = 0.6$. If $\beta_1 = \beta_2 = 0.3$ or $\beta_1 = 0.7$ and $\beta_2 = 0.5$, the plots are quite similar. In both surfactant monomer concentrations c_1 and c_2 there are maxima which are due to both mixture and ionic effects [10]. For the nonionic/ionic system (Figure 5) there is only a maximum in the monomer concentration of surfactant 1 (the ionic surfactant). The same is observed for $\beta_1 = 0.6$, $\beta_2 = 0.0$, and $P = 1.0$. The maximum in the surfactant 1 monomer concentration is more abrupt than for the system in Figure 5 due to the increased counterion concentration. The ratio of the concentration c_1 for the various models to c_1 for the ionic/ionic system with $\beta_1 = \beta_2 = 0.6$ is plotted in Figure 6 versus total surfactant concentration. Clearly, the calculated monomer concentrations depend significantly on the counterion binding parameters.

We have used our model to interpret mixed cmc data for nonionic/ionic systems. The mixed cmc versus composition data are used to determine the mixing parameters A and B. For each α only one parameter (A or B) can be calculated. Hence the calculated value of A depends on B and for each α a function of A versus B is calculated. The pair of values A and B which best fits the entire data set is determined graphically by plotting the A versus B for each data point on the same plot. In Figure 7 A-versus-B plot which are calculated using the nonionic/nonionic and the nonionic/ionic model are shown for the system $C_{15}OSO_3^-Na^+/C_8E_6$ [1]. No pair of A and B values can fit all of the data points exactly for either model. Hence, either the model is inadequate to predict exactly the observed behavior, or there are substantial experimental errors. Using the values which appear to fit most of the data one finds $A = -7.0$ and $B = -4.0$ for the nonionic/ionic model and $A = -5.0$ and $B = -1.0$ for the nonionic/nonionic model. We plot cmc versus composition curves for this system in Figure 8. Both models appear to fit the data to within experimental error, with one point as an exception. Thus, based on this fit, there is no compelling reason to use the more complex nonionic/ionic model. Nevertheless, the large differences in the calculated c_1-values (Figure 6) argue for using the more precise nonionic/ionic model. Two other applications of the nonionic/ionic model to mixed cmc data [23,24] are shown in Figure 9 and 10. In both cases, the model is able to adequately predict the observed behavior.

Conclusions

1. A mass action model (MAM) with monodisperse aggregation number N which depends on the micelle mole fraction x and the counterion binding parameter $\beta(x)$ has been developed for binary surfactants either ionic/ionic or nonionic/ionic.
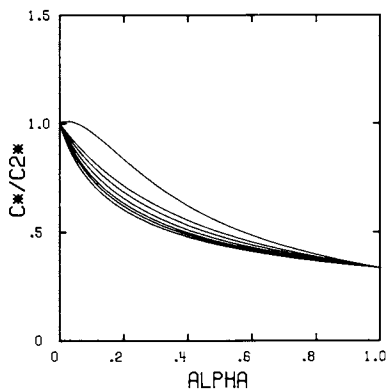
Figure 3. Mixed cmc's of binary surfactants. $c_2^*/c_1^* = 3.0$, $A = 0$, $B = 0$, $c_s/c_2^* = 0.0$ and variables β_1, β_2, and P. The values of (β_1,β_2,P) for the curves from top to bottom are: $(0.6, 0.0, \alpha)$, $(0.0, 0.0, 0.0)$, $(0.3, 0.3, 1.0)$, $(0.6, 0.6, 1.0)$, $(0.7, 0.5, 1.0)$, $(1.0, 1.0, 1.0)$, and $(0.6, 0.0, 1.0)$.
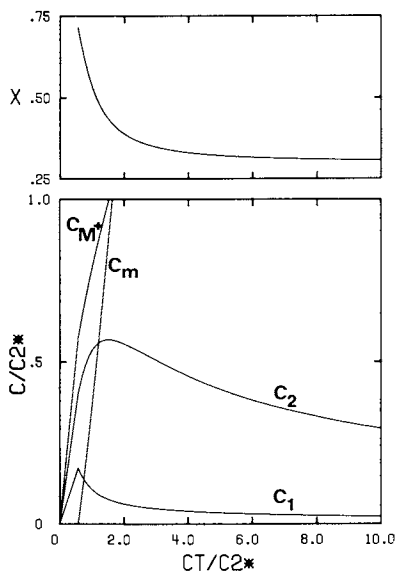
Figure 4. Surfactant 1 monomer (c_1), surfactant 2 monomer (c_2), counterion (c_{M^+}) and micelle (c_m) inventories and micelle compositions (x) for binary surfactants with $c_2^*/c_1^* = 3.0$, $A = 0$, $B = 0$, $c_s = 0.0$, $\alpha = 0.3$, $\beta_1 = \beta_2 = 0.6$, and $P = 1.0$.
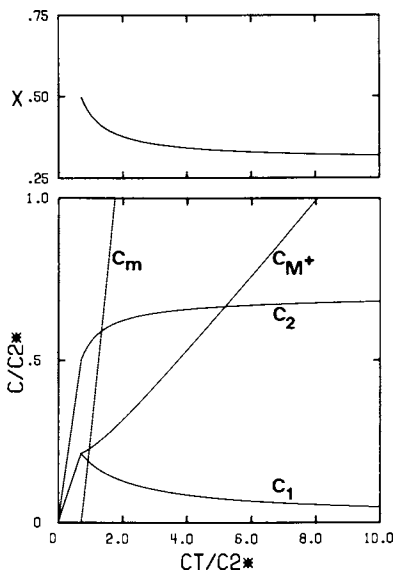
Figure 5. Same as Figure 4, except that $\beta_1 = 0.6$, $\beta_2 = 0.0$, and P $= 0.3$ (nonionic/ionic model).
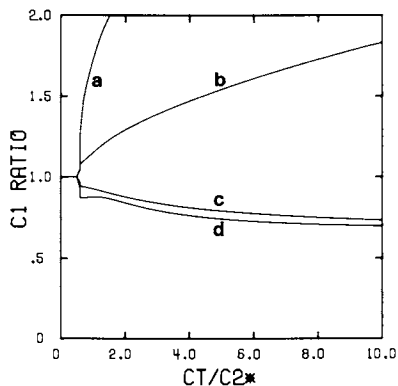
Figure 6. Ratio of the surfactant 1 monomer concentration for $c_2^*/c_1^* = 3.0$, A = 0, B = 0, $c_s/c_2^* = 0.0$, $\alpha = 0.3$. (a) $\beta_1 = 0.6$, $\beta_2 = 0.0$, P $= 0.3$; (b) $\beta_1 = 0.3$, $\beta_2 = 0.3$, P $= 1.0$; (c) $\beta_1 = 0.7$, $\beta_2 = 0.5$, P $= 1.0$; and (d) $\beta_1 = 0.6$, $\beta_2 = 0.0$, P $= 1.0$ to the surfactant 1 monomer concentration calculated for $\beta_1 = \beta_2 = 0.6$ and P $= 1.0$.
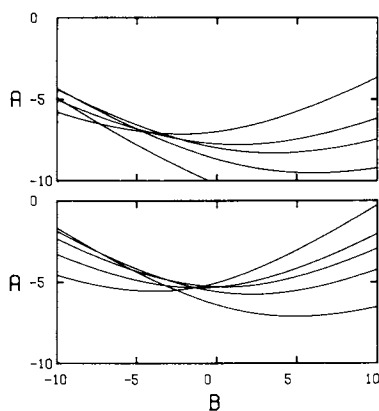
Figure 7. Calculated values of interaction parameters A versus B for $C_{15}OSO_3^-Na^+/C_8E_6$ mixed cmc data. $c_2^*/c_1^* = 1.315$, $c_s/c_2^* = 0.0$, with (a) $\beta_1 = 0.0$, $\beta_2 = 0.7$, P = 1 - α and (b) $\beta_1 = 0.0$, $\beta_2 = 0.0$, P = 0.0, where C_8E_6 is surfactant 1. The curves on each figure are for different values of overall mole fraction C_8E_6 in the mixture, α, and from top to bottom at B = 10 correspond to α values of 0.1, 0.3, 0.5, 0.7, and 0.9. The cmc versus mole fraction data are taken from Lange and Beck (1).
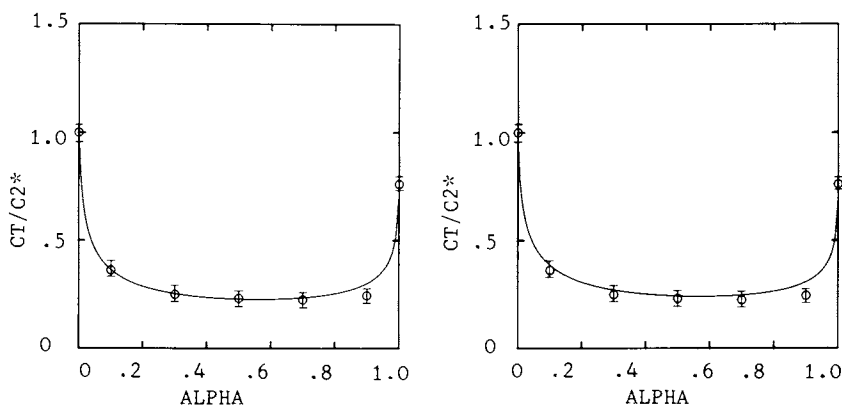
Figure 8. Mixed cmc's for $C_{15}OSO_3^-Na^+/C_8E_6$ versus mole fraction of C_8E_6. The circles are the experimental data of Lange and Beck (1). The curves are calculated values for $c_2^*/c_1^* = 1.315$, $c_s/c_2^* = 0.0$ with (a) $\beta_1 = 0.0$, $\beta_2 = 0.7$, P = 1 - α, A = - 7.0 and B = - 4.0 and (b) $\beta_1 = \beta_2 = 0.0$, P = 0.0, A = - 5.0, and B = - 1.0, where C_8E_6 is surfactant 1.
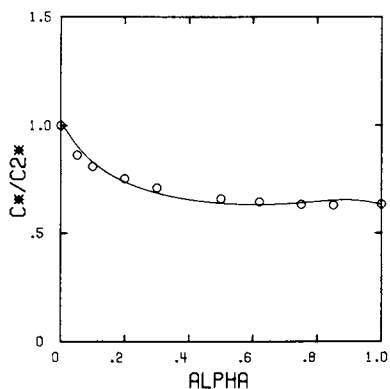
Figure 9. Mixed cmc's for decyl methyl sulfoxide (DeMS)/cetyltrimethylammonium bromide (CTAB) in lmM KBr versus overall mole fraction of CTAB. The circles are the experimental data of Funasaki and Hada (23). The curves are calculated values for $c_2^*/c_1^* = 1.581$, $c_s/c_2^* = 0.0$, $\beta_1 = 0.7$, $\beta_2 = 0.0$, P = α, A = - 1.7, and B = 1.4, where CTAB is surfactant 1.
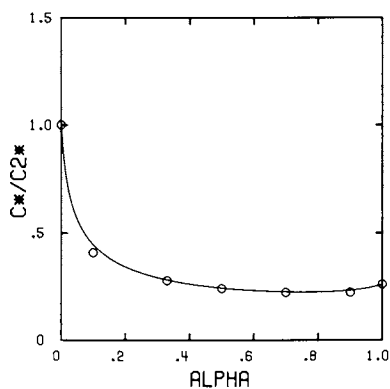
Figure 10. Mixed cmc's for the system sodium dodecylsulfate (SDS)/mono-octyltetraethylene glycol (C_8E_4) in 100 mM NaCl versus overall mole fraction of C_8E_4. The circles are the experimental data of Jayson et al. (24). The curves are calculated for $c_2^*/c_1^* = 3.857$, $c_s/c_2^* = 0.0$, $\beta_1 = 0.7$, $\beta_2 = 0.0$, P = α, A = - 4.0 and B = 1.0, where C_8E_4 is surfactant 1.

2. A pseudo-phase separation model (PSM) with $\beta(x)$ has been developed as the limit of the MAM as $N \rightarrow \infty$.

3. Although cmc's calculated based on the ionic/ionic model can differ little from those based on the nonionic/nonionic model, the monomer and counterion concentrations c_1, c_2, and c_{M^+} and the micelle composition x as calculated from the two models can differ substantially from each other.

4. For $\beta = \beta(x)$ and $N = N(x)$, the MAM predicts no azeotrope micellization. For $\beta = \beta(x)$, the PSM predicts no azeotrope micellization unless the salt concentration is substantially higher than the surfactant concentration.

5. The nonionic/ionic model rather than the nonionic/nonionic or the ionic/ionic model should be used for more precise determination of the nonideality-of-mixing parameters in the mixed micelles in nonionic/ionic mixtures.

6. Even with the used detail, both the MAM and the PSM models need some improvements for more realistic representation of available data. They could be refined to account for micelle size distribution (the MAM) and nonideal mixing with the solvent, once data on x, c_1, c_2, $N(x)$, and $\beta(x)$ become available.

Acknowledgments

Literature Cited

1. Lange, H.; Beck, K.H. Kolloid Z.-Z. Polym. 1973, 251, 424.

2. Clint, J., J. Chem. Soc. Faraday Trans. I, 1975, 71, 1327.

3. Hall, D.G. J. Chem. Soc., Faraday Trans. 2, 1977, 73, 897.

4. Hall, D.B. J. Chem. Soc., Faraday Trans. 2, 1972, 68, 668.

5. Moroi, Y.; Nishikido, N.; Saito, M.; Matuura, R. J. Colloid Interface Sci. 1975, 52, 356.

6. Nishikido, N. J. Colloid Interface Sci. 1977, 60, 242.

7. Scamehorn, J.F.; Schechter, R.S.; Wade, W.H. J. Dispersion Sci. Technol. 1982, 3, 261.

8. Rosen, M.J.; Hua, X.Y. J. Colloid Interface Sci. 1982, 86, 164.

9. Holland, P.M.; Rubingh, D.N. J. Phys. Chem. 1983, 87, 1984.

10. Kamrath, R.F.; Franses, E.I. Ind. Eng. Chem. Fundam. 1983, 22, 230.

11. Kamrath, D.F.; Franses, E.I. J. Phys. Chem. 1984, 88, 1642.

12. Kamrath, R.F.; Franses, E.I. In "Surfactants in Solution"; Mittal, K.L., Ed.; Plenum Press: New York, 1984; p. 129.

13. Stecker, M.M.; Benedek, G.B. J. Phys. Chem. 1984, 88, 6519.

14. Nagarajan, R. Langmuir 1985, 1, 331.

15. Holland, P.M. Adv. Colloid Interface Sci., in press, 1985.

16. Denbigh, K., "The Principles of Chemical Equilibrium," 3rd ed., Cambridge University Press, Cambridge, 1971, p. 276.

17. Kamrath, R.F. Ph.D. Thesis, Purdue University, W. Lafayette, Indiana, 1984.

18. Stigter, D. J. Phys. Chem. 1975, 79, 1008.

19. Stigter, D. J. Phys. Chem. 1975, 79, 1015.

20. Hall, D.G.; Price, T.J. J. Chem. Soc. Farad. Trans. I, 1984, 80, 1193.

21. Rathman, J.F., Scamehorn, J.F. J. Phys. Chem. 1984, 88, 5807.

22. Osborne-Lee, I.C.; Schechter, R.S. This volume.

23. Funasaki, N.; Hada, S. J. Phys. Chem. 1979, 83, 2471.

24. Jayson, G.G.; Thompson, G.; Hull, M.; Smith, A.L. In "Adsorption from Solution"; Ottewill, R.H.; Rochester, C.H.; and Smith, A.L., Eds.; Academic Press: New York, 1983; p. 129.

A Study of Mixed Aqueous Solutions of Hydrocarbon and Fluorocarbon Surfactants

Using 8-Anilino-1-naphthalenesulfonic Acid Ammonium Salt

Kenjiro Meguro, Yasushi Muto, Fujio Sakurai, and Kunio Esumi

Department of Applied Chemistry and Institute of Colloid and Interface Science, Science University of Tokyo, Kagurazaka, Shinjuku-ku, Tokyo 162, Japan

The miscibility between hydrocarbon and fluorocarbon surfactants was studied by means of a steady-state fluorescence. Three mixed aqueous solutions of surfactants were employed; sodium dodecyl sulfate (SDS)-p-$[(CF_3)_2CF]_2C=C(CF_3)O(CH_2CH_2O)_7-CH_3$(NF), hexaoxyethylene-glycol dodecyl ether (6ED)-lithium fluorooctane sulfonate (LiFOS), and 6ED-NF. The fluorescence probe was 8-anilino-1-naphthalene sulfonic acid ammonium salt (ANS). Since ANS was not solubilized into fluorocarbon micelles, the existence of mixed micelles formed by the fluorocarbon and hydrocarbon surfactants can be discussed. (i) 6ED-LiFOS mixed system: When the concentration of 6ED was fixed, the fluorescence intensity of ANS decreased with increasing the concentration of LiFOS, indicating that mixed micelles are formed. (ii) 6ED-NF mixed system: The result was similar to that of (i). However, the mixed micelles are not formed at concentrations below the CMC of NF. (iii) SDS-NF mixed system: When the concentration of NF was fixed and the concentration of SDS was increased, the fluorescence intensity of ANS remained constant, suggesting that pure NF and pure SDS micelles are formed, Further, the above results are confirmed by conductivity measurements.

Recently, some studies on the mixture of fluorocarbon and hydrocarbon materials have been carried out by surface tension, interfacial tension, differential conductance, NMR and solubilization methods(1-9). Mukerjee(5) and Funasaki(2) reported that fluorocarbon and hydrocarbon mixtures exhibit departure from ideal solution theory.
      Suzuku and Meguro et al.(7,8) have been studying the interaction of fluorocarbon and hydrocarbon surfactants by the use of the keto-enol tautomerism of benzoylacetoanilide(BZAA) as a probe and they found the existence of a mixed micelle between lithium fluorooctane sulfonate(LiFOS) and hexaoxyethylene glycol dodecyl ether(6ED).
      As one of the probes, fluorescence compounds are known. The fluorescence probe such as 8-anilino-1-naphthalene sulfonic acid ammonium salt(ANS) has been used as an indicator of membrane

potential(10,11).   Further, this probe has been useful for
elucidating the properties of aqueous surfactant solutions(11-13),
since the quantum yield of fluorescence for ANS is enhanced in a
nonpolar environment.   From this fact, when a concentration of a
hydrocarbon surfactant is larger than its critical micelle
concentration(CMC) in the presence of the ANS probe, the fluorescence
intensity increases because ANS molecules adsorb at the outerlayer
of micelles.
     Further, we have observed that ANS is not solubilized into
fluorocarbon surfactant micelles, so the miscibility of the
fluorocarbon and hydrocarbon surfactants can be studied by using the
fluorescence probe, ANS.

Experimental
Materials.   Lithium fluorooctane sulfonate, $C_8F_{17}SO_3Li$(LiFOS) was
synthesized by a previous method(7).   Hexaoxyethylene glycol
dodecyl ether, $C_{12}H_{25}O(CH_2CH_2O)_6H$(6ED) was obtained from Nikko
Chemicals Company Ltd., Tokyo.   6ED was highly pure as confirmed by
gas-liquid chromatography(GLC), thin layer chromatography(TLC) and
surface tension measurements.   Sodium dodecyl sulfate, $C_{12}H_{25}SO_3Na$
(SDS) was purified by recrystallization from ethanol twice.
$p-[(CF_3)_2CF]_2C=C(CF_3)O(CH_2CH_2O)_7CH_3$(NF) was donated by Neos Co.
8-Anilino-1-naphthalene sulfonic acid ammonium salt(ANS) was obtained
from Wako Pure Chemical Industries, Ltd.   Perfluorocarbon oil(pp-1,
pp-2) was supplied by Dainippon Ink and Chemical Industry Company
Ltd.   The water used in all experiments was purified by passing
through Milli-Q system(Nihon Millipore Co.) until its specific
conductivity fell below $10^{-7}\Omega^{-1}cm^{-1}$.

Measurement
     The fluorescence spectrum of ANS in each sample was measured at
25°C with a fluorescence spectrophotometer(Hitachi 650-10S).   The
concentration of ANS was fixed at 1×10^{-5}mole/l.   The fluorescence
spectra were measured with excitation at 360 nm in water, 377 nm in
6ED micelles, and 370 nm in SDS micelles and with emission at 520 nm,
485 nm, and 500 nm, respectively.
     The surface tension measurement was done at 25°C by a modified
Wilhelmy plate method(Shimadzu ST-1).
     The conductivity measurement was performed at 25°C by a
conductivity meter MODEL CM-30ET(TOA Electronics Ltd.).

Results and Discussion
The behavior of the fluorescence probe, ANS in the aqueous single
surfactant solution
     Figure 1 shows the change in fluorescence intensity of ANS in
the aqueous surfactant solution.   In the case of the hydrocarbon
surfactant, the fluorescence intensity of ANS was proportional to the
surfactant concentration above the CMC.   Since the fluorescence
intensity of ANS had a constant value below the CMC, the inflection
point appeared at the CMC.   The surfactant concentration at the
inflection point nearly coincided with the CMC of 6ED and SDS(the
CMC was 6×10^{-5}mole/l for 6ED and 8.5×10^{-3}mole/l for SDS).   These
findings indicate that ANS is solubilized into the hydrocarbon
surfactant micelles.   Further, above the CMC, the fluorescence
intensity of ANS in 6ED solution was about ten-fold larger than in
SDS solution.   Since both ANS and SDS are anionic, the lower
solubility of ANS in SDS micelles is probably due to the electric

repulsion between ANS and SDS. Adding sodium chloride to the SDS aqueous solution, the fluorescence intensity of ANS was greater than the system with no added electrolyte. This suggests that by addition of electrolyte the electrical potential at the micelle surface reduces due to compression of the electrical double layer, resulting in increased solubilization of ANS into the SDS micelles. In both SDS and 6ED aqueous solutions above their CMCs, the band of the excitation maxima of ANS shifted to a longer wavelength, but the the band of the emission maxima of ANS shifted to a shorter wavelength with increasing surfactant concentration. In water, the wavelengths of excitation and emission maxima were 360 nm and 520 nm, respectively. Above the CMC of 6ED aqueous solution, the excitation and emission wavelength maxima changed gradually and the former shifted to 377 nm, and the latter to 485 nm. These wavelengths almost coincided with those of ethyleneglycol used as the solvent. Accordingly, it seems that this probe,ANS, in the aqueous surfactant solution exists at the outer layer of the micelle which would show an environment like ethyleneglycol.

Furthermore, above the CMC of SDS aqueous solution, the excitation and emission wavelength maxima are reached at 370 nm and 500 nm, respectively.

On the other hand, when the fluorocarbon surfactant(NF and LiFOS) concentrations were increased, even at concentrations above their CMC, the fluorescence intensity remained constant and the maximum excitation and emission wavelengths also remained constant. Further, the fluorescence intensity and the maximum excitation and emission wavelength of ANS in the fluorocarbon surfactant solution were the same as those in water. The CMC of NF was about 6×10^{-6} mole/l and that of LiFOS was about 5×10^{-3} mole/l. These CMCs were determined by surface tension measurements. ANS was found to be insoluble in fluorocarbon oil, supporting the results showing that ANS is not solubilized into fluorocarbon surfactant.

The behavior of the fluorescence probe, ANS in the mixed aqueous surfactant solutions

Figure 2 shows the fluorescence intensity of ANS in 6ED-LiFOS mixed aqueous solutions as a function of LiFOS concentration. Here, the 6ED concentrations were fixed above its CMC. The fluorescence intensity of ANS proportionally decreased with increasing the concentration of LiFOS. It seems that ANS is less soluble in the mixed 6ED-LiFOS micelle.

The equivalent conductivity of the 6ED-LiFOS mixed solutions was measured, with the concentrations of 6ED fixed below and above the CMC. The break point corresponding to the CMC in the graph of equivalent conductivity vs. concentration of LiFOS disappeared gradually. The values of equivalent conductivity decreased with increasing the fixed 6ED concentration.

From the measurement of the fluorescence and conductivity it is apparent that mixed micelles are formed in the 6ED-LiFOS mixed system.

Figure 3 shows the fluorescence intensity of ANS in the NF-6ED mixed aqueous solutions as a function of NF concentration. The fixed 6ED concentrations were above its CMC. The concentration of NF at the inflection point was the same value regardless of the fixed 6ED concentration. In addition, the concentrations at these
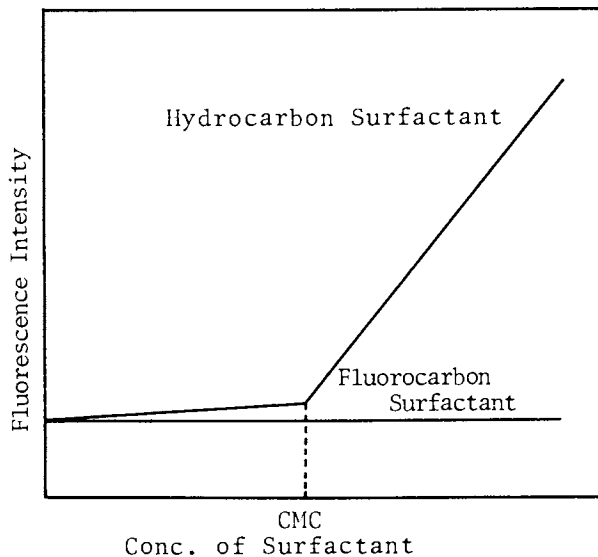
Figure 1. The relationship between fluorescence intensity vs.
           concentration of surfactant.
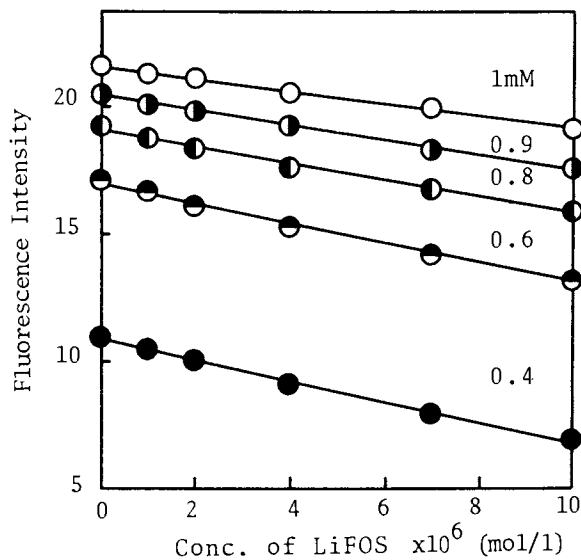
Figure 2. The relationship between fluorescence of ANS and
           concentration of LiFOS in 6ED-LiFOS mixed system.
           The fixed concentrations are 1mM, 0.9mM, 0.8mM,
           0.6mM and 0.4mM.

inflection points almost coincided with the CMC of NF and the fluorescence intensity of ANS was almost constant below its CMC. These results suggest that the NF molecules do not penetrate into the 6ED micelles below the CMC of NF. On the other hand, above the CMC of NF, the NF molecules penetrate into the 6ED micelles as observed for the 6ED-LiFOS mixed system.

It seems from the above results that NF molecules are not miscible with hydrocarbon surfactant below the CMC of NF, but above the CMC the miscibility of the NF and 6ED is similar to the LiFOS and 6ED system.

Figure 4 shows the fluorescence intensity of ANS in the SDS-NF mixed aqueous solutions as a function of NF concentration. The SDS concentrations were fixed below and above its CMC. The fluorescence intensity and maximum excitation and emission wavelength of ANS was kept constant even when the concentration of NF increased. This result means that the NF molecules do not penetrate into the SDS micelles.

The fluorescence intensity of ANS in the SDS-NF mixed aqueous solutions were measured as a function of SDS concentration. The NF concentration was fixed above its CMC. Several fluorescence intensities of ANS at the same SDS concentration agreed with that in the case of the single SDS solution. This result suggests that the mixed micelles can not be formed in the NF and SDS mixed solution, but,rather, that pure component micelles are formed.

Also, in the case of NF and SDS mixed aqueous systems, the conductivities were measured as a function of the SDS concentration. NF was fixed at several concentrations below and above the CMC. The break point corresponding to the CMC of SDS did not shift in several fixed NF concentrations, and the values of equivalent conductivity were almost the same at the same SDS concentration in the mixed solutions. Therefore, it is concluded that the NF molecules can not penetrate into the SDS micelles, and that pure component NF and SDS micelles exist.

Summary

Three mixed surfactant systems were studied: (i) 6ED-LiFOS, (ii) 6ED-NF and (iii) SDS-NF.

In system (i), 6ED and LiFOS exhibit miscibility behavior similar to a mixed system consisting of two hydrocarbon surfactants, such as 6ED and SDS. Mixed micelles are formed over a wide range of concentrations.

In the case of system (ii), 6ED and NF are not miscible at concentrations below the CMC of both pure surfactants; above the both pure CMC values, the mixed micelles are formed.

On the other hand, in system (iii), SDS and NF are immiscible over the entire concentration range studied, resulting in the formation of the separate micelles.
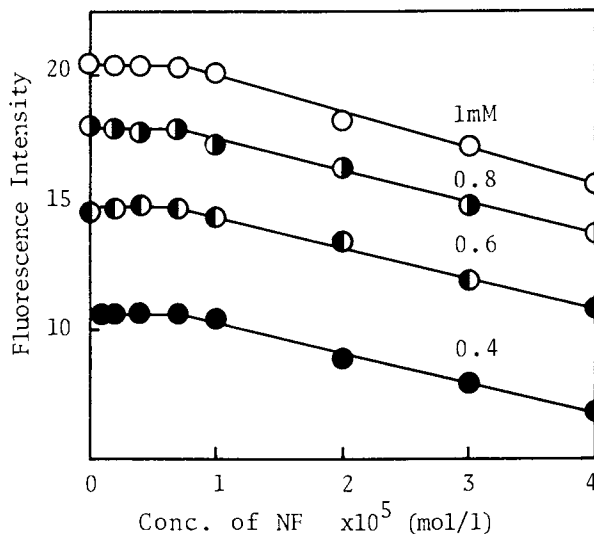
Figure 3.   The change in fluorescence intensity of ANS in
             6ED-NF mixed system as a function of NF concentration.
             The fixed 6ED concentrations are 1mM, 0.8mM, 0.6mM and
             0.4mM.
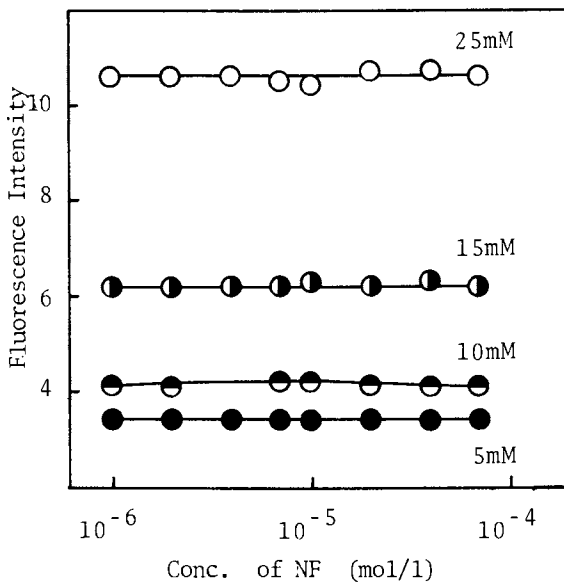
Figure 4.   The change in fluorescence intensity of ANS in SDS-NF
             mixed system as a function of NF concentration.   The
             fixed 6ED concentrations are 25mM, 15mM, 10mM and 5mM.

Acknowledgment

The authors wish to thank Neos Co. for supplying valuable samples.

Literature Cited
1.   Mukerjee, P. and Handa, T., J. Phys. Chem., 1981, 85, 2298.
2.   Funasaki, N. and Hada, S., Chem. Letters, 1979, 717.
3.   Mukerjee, P., JAOCS, 1982, 59, 573.
4.   Funasaki, N. and Hada, S., J. Phys. Chem., 1983, 87, 342.
5.   Mukerjee, P. and Yang, A.Y.S., ibid., 1976, 80, 1388.
6.   Carlfors, J. and Stilbs, P., ibid., 1984, 88, 4410.
7.   Meguro, K., Ueno, M., and Suzuki, T., Yukagaku, 1982, 31, 909.
8.   Suzuki, T., Esumi, K., and Meguro, K., J. Colloid Interface Sci., 1983, 93, 205.
9.   Funasaki, N., Hada, S., and Neya, S., Bull. Chem. Soc. Jpn., 1983, 56, 3839.
10. Haynes, D.H., and Staerk, H., J. Membrane Biol., 1974, 17, 313.
11. Haynes, D.H., ibid., 1974, 17, 341.
12. Birdi, K.S., Krag, T., and Klausen, J., J. Colloid Interface Sci., 1977, 62, 562.
13. Thomas, J.K., Chemical Review, 1980, 80, 283.
14. Lianos, P., and Zana, R., J. Colloid Interface Sci., 1981, 84, 100.

5

Solution Properties of Mixed Surfactant Systems

The Interaction Between Azo Oil Dyes and Mixed Surfactant Systems

Keizo Ogino and Masahiko Abe

Faculty of Science & Technology, Science University of Tokyo, 2641 Yamazaki, Noda, Chiba 278, Japan

Solution properties of anionic-nonionic mixed surfactant systems have been investigated with addition of azo oil dyes; 4-phenylazo-1-naphthylamine (4-NH$_2$) and 4-phenylazo-1-naphthol (4-OH). The interaction of 4-NH$_2$ with sodium dodecyl sulfate (SDS) was enhanced by the addition of alkyl poly(oxyethylene) ethers (C$_m$POE$_n$) surfactants which have a longer alkyl chain and/or fewer ethyleneoxide groups. The fading phenomena was obserbed when 4-OH was added into the mixed surfactant systems, and its rate of 4-OH accelerated by increasing the alkyl chain length or decreasing the number of ethyleneoxide groups in the C$_m$POE$_n$ molecule. The interactions of azo oil dyes with mixed surfactant systems would be larger for the system which is easy to form a mixed micelle than for the system which coexists two kinds of micelles.

Mixed surfactant systems are of importance from a fundamental and practical point of view. Therefore, many recent papers have reported on the micellar properties of mixed surfactant solutions (1-9). For example, Tokiwa et al. have measured the NMR spectra (4); Ingram has measured surface tension (5). Previously, we have reported the solution properties of anionic-nonionic surfactant mixed systems from the point of view of electrical (6,7) and surface tension measurements (8-10), and investigated the mixed micelle formation.

We have discussed the differences in the mixed micelle forming due to the different alkyl chain lengths (ACL) and/or polyoxy-ethylene chain lengths (PCL) in nonionic surfactants. We found that the mixed micelle would be formed more easily by a nonionic surfactant including long ACL (or shorter PCL) than by one having shorter ACL (or long PCL). We have also reported that the protonation of 4-phenylazo-1-naphthylamine (4-NH$_2$) was caused by

sodium dodecyl sulfate (SDS) micelles (11,12). We have, moreover, mentioned the effect of PCL and/or ACL in nonionic surfactant molecule on the tautomerism of 4-phenylazo-1-naphthol (4-OH)(13).
     In this paper, we report the solution properties of sodium dodecyl sulfate (SDS)-alkyl poly(oxyethylene) ether (C_mPOE_n) mixed systems with addition of azo oil dyes (4-NH_2, 4-OH). The 4-NH_2 dye interacts with anionic surfactants such as SDS (11,12), while 4-OH dye interacts with nonionic surfactants such as C_mPOE_n (13). However, 4-NH_2 is dependent on the molecular characteristics of the nonionic surfactant in the anionic-nonionic mixed surfactant systems, while in the case of 4-OH, the fading phenomena of the dye is observed in the solubilized solution. This fading rate is dependent on the molecular characteristics of nonionic surfactant as well as mixed micelle formation. We discuss the differences in solution properies of azo oil dyes in the different mixed surfac-tant systems.

Experimental

Materials

Anionic surfactant: Sodium dodecyl sulfate (SDS, $C_{12}H_{25}OSO_3Na$) was supplied by Nihon Surfactant Industries Co., Ltd Tokyo, Japan. It was extracted with ether and recrystallized from ethanol. The purity was ascertained by surface tension measurement. Nonionic surfactant: Alkyl poly(oxyethylene) ether (C_mPOE_n, $C_mH_{2m+1}O(CH_2CH_2O)_{20}H$, m=12, 14, 16, and 18; $C_{16}H_{33}O(CH_2CH_2O)_nH$, n=10, 20, 30, and 40) were supplied by Nihon Surfactant Industries Co., Ltd. These have a narrow molecular weight distribution. Azo oil dye: The synthesis and purification of 4-phenylazo-1-naphthylamine (4-NH_2), 4-phenylazo-1-naphthol (4-OH) were described in our previous paper (14). Water used in this experiment was twice distilled and was deionized by an ion-exchange instrument (NANO pure D-1791 of Barnstead Co., Ltd.); its resistivity was about 18.0 megohm·cm and its pH was 6.7.

Method

Preparation of surfactant solutions including oil dye.
I. For 4-NH_2 dye. First, into several 100 ml glass-stoppered Erlenmeyer flasks, 25 ml portions of a given concentration of pure surfactant solution were placed. Next a measured amount of 4-NH (5.0×10^{-5} mol/l) was added to each solution. The mixture were stirred ultrasonically for 5 min and then agitated with a shaker (Model SS-82D type of Tokyo Rikakikai Co., Ltd, Tokyo, Japan) for 24 hr and allowed to stand for 24 hr in a thermostat at 30°C in order to established a solubilization equilibrium. After the equilibrium had been established, these pure anionic surfacant solutions including 4-NH_2 were mixed with pure nonionic surfactants solutions involving one.
II. For 4-OH dye. Into several 100 ml flasks, 25 ml portions of a given concentration of anionic surfactant solution were placed, followed by addition of a given concentration of nonionic surfactant solution. The mixtures were stirred for 1 hr in a thermostat at 30°C in order to establish their equilibria, and then

a measured amount of 4-OH (5.0×10^{-5} mol/l) was added into the
mixed surfactant solution.

Determination of maximal absorption wavelength (λ_{max}) and optical
density of each solution
The measurement was the same as that described in the previous
paper (13), except that the spectrophotometer used was a model
MPS-2000 double beam type (Shimadzu Co., Tokyo, Japan) with a
quartz cell (10.0 mm in light pass length).

Results and Discussion

(1) Protonation equilibrium of 4-NH$_2$
Matsuoka (15) suggests that, when the proton goes to β-azo-nitrogen
atom, electric charge transfer occurs; as a result, a nitrogen atom
of amino group becomes positively charged (quinoidal form). The
protonation equilibrium occurred in solutions of anionic surfactant
like SDS which has a strongly anionic hydrophilic group (11,14).
On the other hand, this azo form was observed in other surfactant
micelle solutions such as sodium laurate (11) and nonionic
surfactants (16). The maximal absorption wavelength is at 535 nm
(quinoidal form) in the SDS solution, while at 450 nm (azo one) in
the C_mPOE_n soution.

(1·1) Effect of alkyl chain length in C_mPOE_n on the absorption
spectra. The relationship between the absorption spectra and the
mixed molar ratio of the SDS-$C_{12}POE_{20}$ surfactant system is shown in
Fig.1. The maximal absorption wavelength almost shifts to 450 nm
with increasing the molar ratio of $C_{12}POE_{20}$, and the absorption at
535 nm by the quinoidal form of 4-NH$_2$ does not appear. This seems
to be a result of the difference in the solubilizing power and the
value of the cmc of each pure surfactant. In the former, $C_{12}POE_{20}$
is about 15-times larger, and in the latter, C_mPOE_n is about 100-
times smaller. Therefore, at a given concentration, a solution of
C_mPOE_n has much more surfactant in the micellar phase than a
solution of SDS. These micelles of $C_{12}POE_{20}$ solubilized 4-NH$_2$ more
than did SDS micelles. Figure 2 represents the case of SDS-
$C_{18}POE_{20}$ mixed systems. The shift of the maximal absorption
wavelength is not remarkable like that in Fig.1. Even the molar
ratio of $C_{18}POE_{20}$ increases up to 0.5, the absorption spectra
corresponding to the quinoidal form of 4-NH$_2$ still remains.
     As the alkyl chain length of C_mPOE_{20} is increased, it seems
that the micelle becomes the more stable for the quinoidal form of
4-NH$_2$ and the absorption spectra corresponding to the quinoidal
form of 4-NH$_2$ is more pronounced at the same mixed molar ratio of
the surfactants.

(1·2) Effect of polyoxyethylene chain length in C_mPOE_n on the
absorption spectra. In the case of SDS-$C_{16}POE_{10}$ mixed surfactant
system, the maximal absorption wavelength almost shifts to 535 nm
except for the pure nonionic, and then the peak at 450 nm
disappear. For SDS-$C_{16}POE_{40}$ mixed system, the maximal absorption
wavelength almost shifts to 450 nm regardless of the molar ratio,
and the absorption at 535 nm is very weak. This is enhanced by the
difference in the solubilizing power for 4-NH$_2$ as was observed in
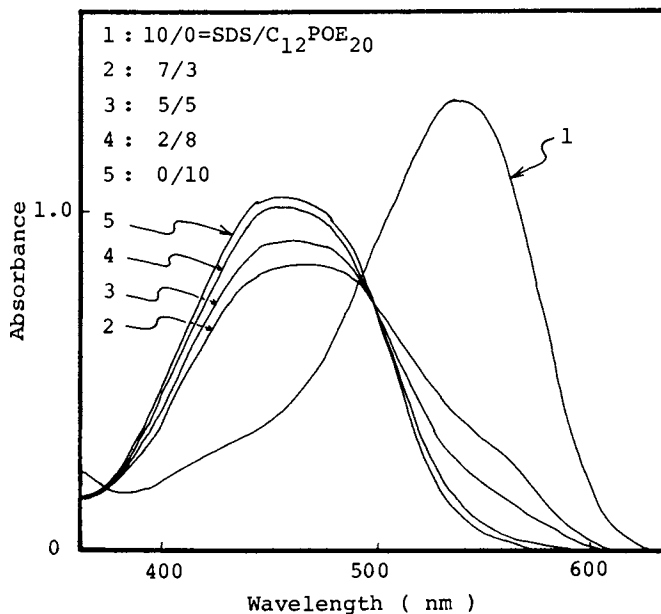
Fig.1   Variation of absorption spectra for 4-NH$_2$ (5.0 x 10^{-5} mol/l) with mixed molar ratio of SDS/C$_{12}$POE$_{20}$ at 30°C. Total concentration is 2.5 x 10^{-2} mol/l, above the cmc. Numbers by data curves represent mixed molar ratio.
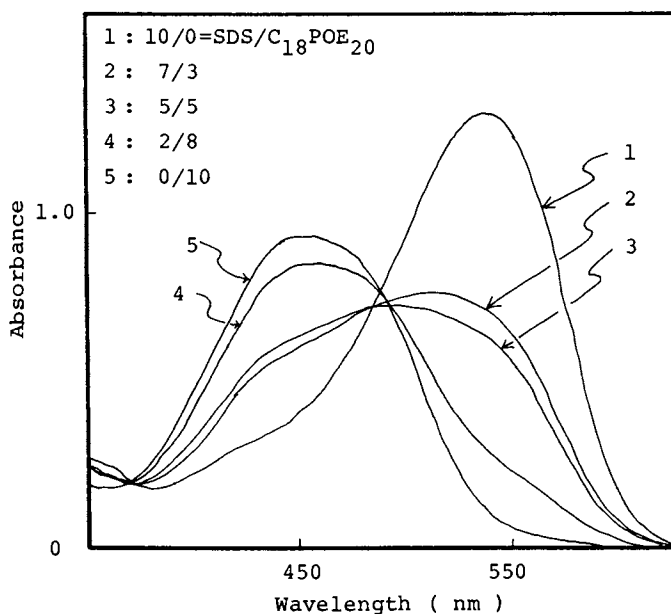
Fig.2   The change of maximal absorption with molar ratio of SDS/C$_{18}$POE$_{20}$ at 30°C.

the SDS-$C_{12}POE_{20}$ system. At the same mixed molar ratio of the surfactants, shorter the polyoxyethylene chain length, the more stable the micelle becomes for solubilization of the quinoidal form of 4-NH_2 and the absorption spectra corresponding to the quinoidal one is easily recognized. Especially in the case of the SDS-$C_{16}POE_{10}$ mixed surfactant system, the absorption at 535 nm increases remarkably. This seems to be due to the effect of the low HLB value of $C_{16}POE_{10}$.

(1·3) Examination of mixed micelle formation. We have studied the mixed micelle formation of polyoxyethylene carboxylate and C_mPOE_n systems by electric measurements (17,18) and surface tension measurements (8-10). We found that the mixed micelle was formed more easily by a nonionic surfactant including long ACL (or shorter PCL) than by one having shorter ACL (or long PCL). We have also obtained almost the same mentioned above for SDS-C_mPOE_n systems (19). The model of mixed micelle formation is showm in Fig.3 to summarize the coments above. When SDS and C_mPOE_n are mixed, mixed micelles form easier as the number of carbons in the alkyl chains increaed and the number of ethyleneoxide groups is decreased on the C_mPOE_n surfactant. This tendency of C_mPOE_n is accord with the trend of HLB values of C_mPOE_n. The lower the HLB value of C_mPOE_n, the greater interaction with SDS, and the quinoidal form of 4-NH_2 appears to be stablized in the mixed micelle. On the other hand, the fewer carbon atoms and/or the more ethyleneoxide groups C_mPOE_n has, the interaction between C_mPOE_n and SDS decrease, and they seem to form two type of micelles, one rich in ionic the other rich in nonionic. In this case, the azo form of 4-NH_2 is more stable due to the solubilizing power of C_mPOE_n.

(2) Tautomerism equilibrium of 4-OH
Mitsuishi et al. described (20) that 4-OH was in the hydrazo form in polar solvents, and azo form in nonpolar solvents. It was suggested that one hydrogen atom of the hydroxide group at the 4-position of the naphthalene ring transferred to the β-position of the azo group, and the tautomerism was established between hydrazo form of the keto type and the azo form of the enol type. In this study, we consider that the spectrum with a peak at the 480 nm corresponds to the former and that at the 415 nm to the latter in aqueous solutions of C_mPOE_n surfactant. The 4-OH goes into the azo form when it is solubilized in the carbon core of C_mPOE_n micelles. On the other hand, 4-OH becomes hydrazo form when solubilized in the polyoxyethylene chain. Figure 4 demonstrates the absorption spectra of 4-OH in pure SDS, pure $C_{16}POE_{20}$ and mixtures of these surfactants. As can be seen from Fig.4, the λ_{max} of 4-OH appears at 480 nm in the SDS solution, on the other hand, at 415 nm in the $C_{16}POE_{20}$ solution and a shoulder appears at 480 nm. Tautomerism of 4-OH is also observed in these mixed solution. Time dependence of optical density of 4-OH at two peaks are not observed in the single solutions.

(2·1) Fading phenomena of 4-OH. One special effect on 4-OH is the fading phenomena of the dye observed in the mixed surfactant systems. Time dependence of the absorption spectra of 4-OH in the mixed solution is shown in Fig.5. The absorbances at both 415 and
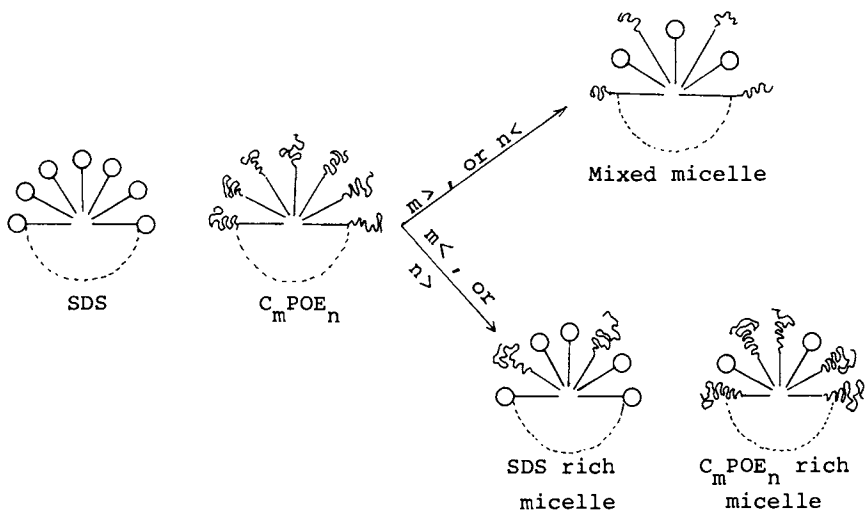
Fig.3 Micellization models for SDS/C_mPOE_n mixed surfactant systems.

Wavelength (nm)
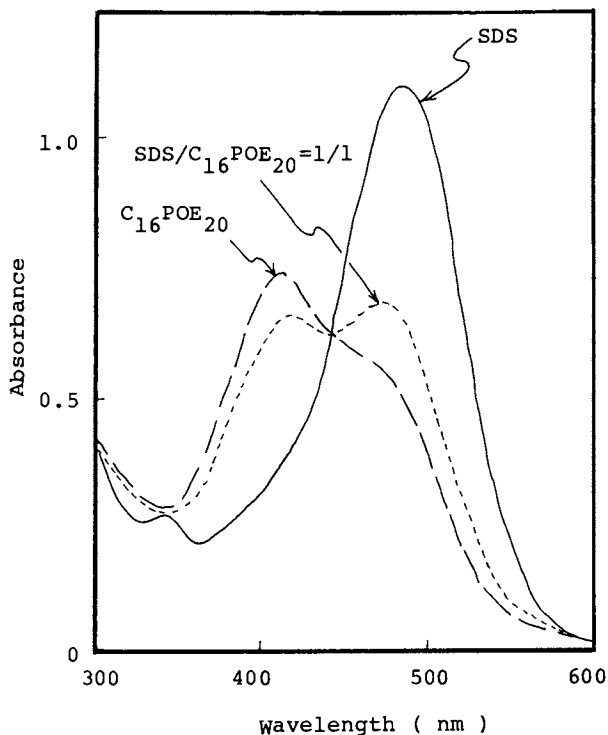
Fig.4 Absorption spectra of 4-OH in pure SDS, pure $C_{16}POE_{20}$, and mixtures of these surfactants solutions at 30°C.

480 nm decrease with time. This fading phenomena is also observed
for other anionic surfactants; for example, polyoxyethylene
carboxylate and sodium dodecylbenzene sulfonate. The change of the
absorbance at 480 nm is plotted against time in Fig.6. The
absorbance at 480 nm in each surfactant solution is independent of
time and is constant. In the mixed solution, the absorbance at 480
nm decreases with time, and fading phenomena of 4-OH is observed.
The absorbance becomes a minimum in the vicinity of molar ratio of
$SDS/C_{16}POE_{20}=1/1$. On the other hand, a fading effect like this is
not recognized in cationic-nonionic surfactant mixed systems.
Namely, the fading phenomena of 4-OH seems to arise from the system
which consists of anionic surfactant having strongly polar groups
and nonionic surfactant. It seems that the interaction between
hydrophilic groups of SDS and C_mPOE_n participate in fading
phenomena of 4-OH.

(2·2) Effect of alkyl chain length and oxyethylene groups in
C_mPOE_n on the fading rate. The effect of the number of carbon
atoms on the fading rate is shown in Fig.7. As can be seen from
Fig.7, for longer alkyl chain lengths, the fading rate accelerates
in the mixed surfactant systems. The opposite effect of ethylene-
oxide groups is shown in Fig.8. As the PCL decreases, the fading
rate accelerates in the mixed systems. From Figs.7 and 8, this
phenomena is dependent on the molecular characteristics of C_mPOE_n
added to the mixed surfactant systems. We found that, for nonionic
surfactant including long ACL (or shorter PCL), the mixed micelle
is formed more easily than others; for one having shorter ACL (or
long PCL), there are two kinds of micelles coexisting (one rich in
anionic surfactant and the other rich in nonionic surfactant)
(8,9,17-19). Therefore the fading phenomena of 4-OH in the
mixed surfactant systems appears to be related to the mixed micelle
formation of SDS and C_mPOE_n.

(2·3) Effect of oxygen on the fading rate. We must consider why
the fading phenomena of 4-OH occurs only in anionic-nonionic mixed
surfactant solutions. The mixed solution after bubbling O_2 gas
accelerates the fading rate, while that after bubbling N_2 gas
decelerates. Ball et al. (21) have reported the photofading of
4-OH in films of polymer substrates. They have described that
photofading of 4-OH is caused by oxidative attack on the ground
state hydrazo form by singlet oxygen. Griffith et al.(22) have
also stated that the photochemical oxidation of 4-arylazo-1-
naphthols are caused by the oxidation of singlet oxygen. Kousaka
et al.(23) have described that the solubility of oxygen increases
with increasing surfactant concentration because of the penetration
of it into micelles. However, this fading phenomena does not take
place in single(or pure) or mixed surfactant solutions
(cationic-nonionic). Merkel et al.(24) have declared that the
lifetime of singlet oxygen is approximately 10 times shorter in H_2O
than in D_2O. It can be speculated that, when the transition energy
of the oxygen is not exchanged to the internal energy of the water,
mainly to the vibrational energy of the water molecule, the singlet
oxygen lifetime makes long. The long lifetime of singlet oxygen
can make the fading rate of 4-OH faster.
      We have found that the fading rate becomes faster under the
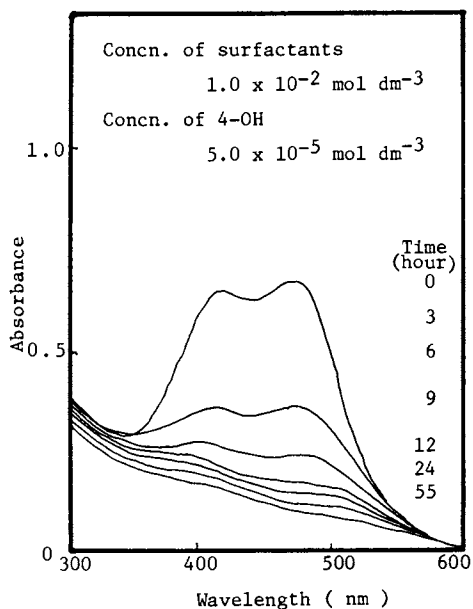
Fig.5   Time dependence of absorption spectra of 4-OH in SDS/$C_{16}POE_{20}$=1/1 mixed solution.   Numbers by curve represent time.
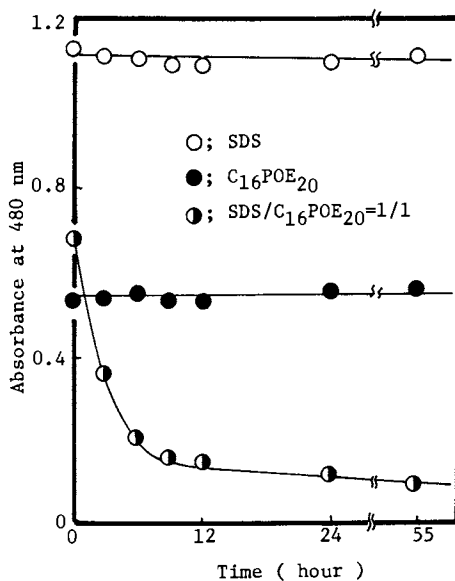
Fig.6   Time dependence of absorbance at 480 nm in SDS/$C_{16}POE_{20}$ mixed solution at 30°C.
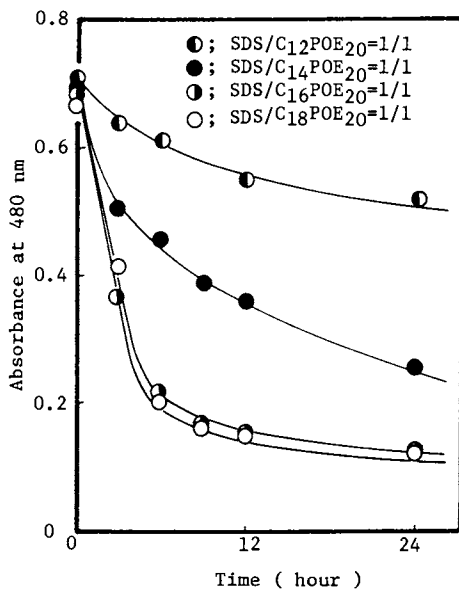
Fig.7   Effect of the number of atoms in $C_m POE_n$ on the fading
         rate of 4-OH at 30°C.
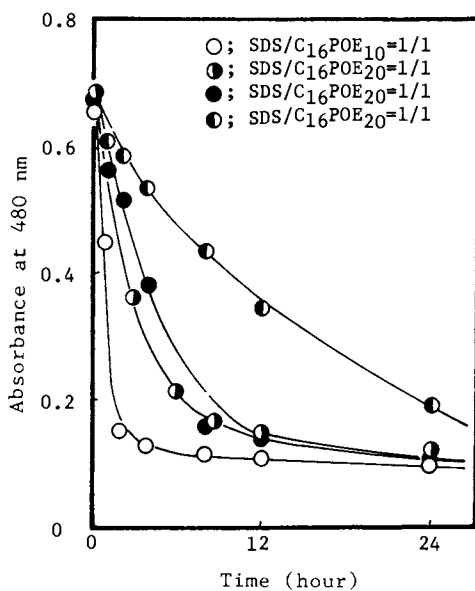
Fig.8   Effect of the number of ethyleneoxide groups in $C_m POE_n$
         on the fading rate at 30°C.

following conditions: (1) anionic surfactant having strongly polar group–nonionic surfactant systems; (2) nonionic surfactant including long alkyl chain length (or shorter PCL); (3) in the vicinity of molar ratio of 0.5.

The above suggestion is illustrated by the hydration model for SDS–C_mPOE_n mixed surfactant system shown in Fig.9. When– the mixed micelle of molar ratio of 0.5 is formed, the water molecule would be mechanically trapped in the parts between the oxygen atoms of hydrophilic group of SDS and ethyleneoxide in C_mPOE_n molecule to depress the vibrational motion. The structure of 4–OH solubilized into the palisade layer of micelles will be hydrazo form; the singlet oxygen attacks on the hydrazo form of 4–OH as mentioned above; the azo form of 4–OH should turn to the hydrazo form due to the tautomerism equilibrium; the absorbance at two peaks are getting to disappear. Thus, we would guess that the fading phenomena observed in this study is caused by the hydrophilic-hydrophilic interaction in anionic–nonionic mixed surfactant system.

Conclusion

The interactions between azo oil dye and mixed surfactant systems will be dependent on the difference in mixed surfactant micelle due to different molecular characteristic of nonionic surfactant.
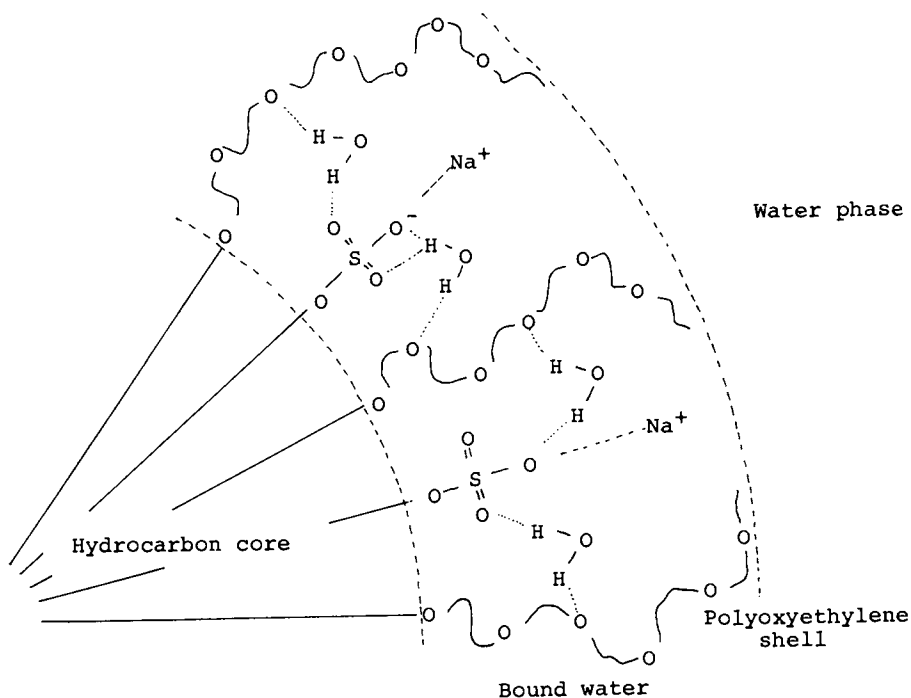
Fig.9   Schematic hydration model for SDS–C_mPOE_n mixed surfactant system.

Acknowledgment

Literature Cited

1. Meguro, K.; Akasu, H.; Ueno, M. J. Am. Oil Chem. Soc. 1976,
    53, 145.
2. Funasaki, K.; Hada, S. J. Phys. Chem. 1979, 83, 2471.
3. Hall, D. G.; Price, T. J. J. Chem. Soc., Faraday Trans. 1
    1984, 80, 1193.
4. Tokiwa, F.; Tsujii, K. J. Phys. Chem. 1971, 75, 3560.
5. Ingram, B. T. Colloid & Polym. Sci. 1980, 258, 191.
6. Ogino, K.; Tsubaki, N.; Abe, M. J. Colloid Interface Sci.
    1984, 98, 78.
7. Abe, M.; Tsubaki, N.; Ogino, K. Yukagaku 1983, 32, 672.
8. Abe, M.; Tsubaki, N.; Ogino, K. J. Colloid Interface Sci. in
    press.
9. Ogino, K.; Tsubaki, N.; Abe, M. J. Colloid Interface Sci. in
    press.
10. Ogino, K.; Abe, M.; Tsubaki, N. Yukagaku 1982, 31, 953.
11. Abe, M.; Ohsato, M.; Suzuki, N.; Ogino, K. Bull. Chem. Soc.
    Jpn. 1984, 57, 831.
12. Abe, M.; Ohsato, M.;Ogino, K. Colloid & Polym. Sci. 1984,
    262, 657.
13. Abe, M.; Ohsato, M.; Kawamura, T.; Ogino, K. J. Colloid
    Interface Sci. 1985, 104, 228.
14. Abe, M.; Suzuki, N.; Ogino, K. J. Colloid Interface Sci.
    1984, 99, 226.
15. Matsuoka, M. Shikizai Kyokai Shi 1980, 53, 724.
16. Unpublished data, this laboratory.
17. Ogino, K.; Tsubaki, N.; Abe, M. J. Colloid Interface Sci.
    1984, 98,78.
18. Abe, M.; Tsubaki, N.; Ogino, K. Colloid & Polym. Sci. 1984,
    262, 584.
19. Ogino, K.; Kakihara, T.; Abe, M. Proc. 38th Symposium on
    Coloid & Surface Chemistry (Japan) 1985, p.426.
20. Mitsuishi, M; Kamimura, R.; Ieda, M.; Shinohara, K.; Ishii, N.
    SEN-I GAKKAISHI 1976, 32, T-382.
21. Ball, P.; Nicholls, C. H. Dyes Pigm. 1984, 5, 437.
22. Griffith, J.; Hawkins, C. J. Chem. Soc., Perkin II 1977,
    747.
23. Kousaka, K.; Kise, H.; Seno, M. Yukagaku 1980, 26, 177.
24. Merkel, P. B.; Kears, D. R. J. Am. Chem. Soc. 1972, 94,
    7244.

Thermodynamics of the Mixed Micellar System Sodium Decanoate–2-Butoxyethanol in Water at 25 °C

Fumitaka Yamashita[1,2], Gérald Perron[1,3], Jacques E. Desnoyers[3,4], and Jan C. T. Kwak[2,4]

[1] Department of Chemistry, Université de Sherbrooke, Sherbrooke, Québec, Canada, J1K 2R1
[2] Department of Chemistry, Dalhousie University, Halifax, NS, Canada B3H 4J3
[3] Institut National de la Recherche Scientifique, C.P. 7500, Sainte-Foy, Québec, Canada G1V 4C7

Medium-chain alcohols such as 2-butoxyethanol (BE) exist as microaggregates in water which in many respects resemble micellar systems. Mixed micelles can be formed between such alcohols and surfactants. The thermodynamics of the system BE-sodium decanoate (Na-Dec)-water was studied through direct measurements of volumes (flow densimetry), enthalpies and heat capacities (flow microcalorimetry). Data are reported as transfer functions. The observed trends are analyzed with a recently published chemical equilibrium model (J. Solution Chem. 13,1,1984). By adjusting the distribution constant and the thermodynamic property of the solute in the mixed micelle, it is possible to fit nearly quantitatively the transfer of BE from water to aqueous NaDec. The model is not as successful for the transfert of NaDec from water to aqueous BE at low BE concentrations indicating self-association of NaDec induced by BE. The model can be used to evaluate the thermodynamic properties of both components of the mixed micelle.

Most of the studies on thermodynamics of mixed micellar systems are based on the variation of the critical micellar concentration (CMC) with the relative concentration of both components of the mixed micelles (1-4). Through this approach it is possible to obtain the free energies of formation of mixed micelles. However, at best, the sign and magnitude of the enthalpies and entropies can be obtained from the temperature dependences of the CMC. An investigation of the thermodynamic properties of transfer of one surfactant from water to a solution of another surfactant offers a promising alternative approach (5), and, recently, mathematical models have been developed to interpret such properties (6-9).

The thermodynamic functions of transfer can be defined in terms

---

[4] To whom correspondence should be addressed.

of apparent or partial molar quantities. For example,

$$\Delta Y_3 \ (1 \to 1 + 2) = Y_{3,\phi}(1 + 2) - Y_{3,\phi}(1) \tag{1}$$

where Y stands for any thermodynamic property, $Y_{3,\phi}$ is the apparent molar quantity of solute 3 in pure water, component 1, or in the solution of component 2.

If the concentration of solute 3 is sufficiently low, relative to its CMC, the transfer functions become identical for partial and apparent molar quantities and are said to approach the standard state.

The trends in the transfer functions, as the concentration of solute 2 is varied to cover its pre- and post-micellar region, can be interpreted in terms of three main factors if both solutes are hydrophobic (6,10).
1. In the pre-micellar region of both solutes, the interactions between the two types of monomers can be accounted for by a second virial coefficient.
2. If solute 2 is in the post-micellar region and solute 3 in its pre-micellar state, the solute 3 will distribute itself between water and the micelles of solute 2.
3. In forming a mixed micelle, solute 3 will shift the CMC of solute 2 to lower values, and this will be reflected in the apparent molar properties of solute 3 in the CMC region of solute 2.

This model was shown to account for the observed trends of enthalpies, volumes, compressibilities and heat capacities of many types of hydrophobic solutes (hydrocarbons, alcohols and surfactants) in micellar solutions and also for the observed trends for the transfer of hydrophobic solutes to some alcohol-water mixtures. This latter observation supports the view that some alcohol-water mixtures exist as microphases which in many respects resemble micellar systems (11-12).

Work is presently under way to extend the above model so as to extract from the experimental data the relevant parameters from a least-squares analysis (13). This model should be applicable to nonionic and ionic systems. In the latter case, an extra term is required to account for the shift in the CMC of solute 2 due to the salting-out of the monomers of 2 by solute 3 (7). The model in its present form can still be used to estimate the thermodynamic properties of solute 3 in the micelle of surfactant 2 by adjusting the parameters to get a good fit with the experimental data.

In such studies, it is preferable to use two surfactants with widely different CMC's so as to explore the possibility of coexistence of two types of mixed micelles, 2 in 3 and 3 in 2. In this respect, the system cetyltrimethylammonium bromide (CTAB)-2-butoxyethanol (BE)-water is being investigated (14). Unfortunately, with CTAB, the CMC is too low to allow thermodynamic measurements below the CMC. Still, this study shows unambiguously that BE dissolves in the CTAB micelles and also that CTAB can distribute itself in the BE microaggregates.

In the present study, the system sodium decanoate (NaDec)-BE-water will be reported. The advantage of this system is that it is possible to make measurements below the CMC of NaDec (0.12 mol kg^{-1}) while this CMC is still far from the effective CMC of BE ($\sim$ 1 mol kg^{-1}). Also, it is possible to prepare a silver/silver decanoate

specific ion electrode which allows the study of free energies. The present study will present enthalpies, volumes and heat capacities. Free energies will be reported elsewhere (15).

Experimental

Decanoic acid was purchased from Aldrich Chemicals, Gold Label, and from BDH, special pure grade. BE was obtained from Shefford Chemicals. It was distilled and kept over molecular sieves. The preparation of NaDec and its purification are the same as in previous studies (16). The purity of NaDec was checked by surface tension. A minimum in surface tension is observed which disappears when NaDec is prepared at a pH higher than 11. This suggests that the impurity in NaDec is most probably free decanoic acid. In consideration of the previous discussion (16), NaDec was prepared at a pH of 9.2 and used as such, since a trace of decanoic acid should have less effect on the thermodynamic properties than an excess of NaOH.

The techniques used to measure densities (17,18), heats of mixing (19) and heat capacities (18,20) have been described elsewhere.

All solutions were prepared by mass with deionized distilled water. All measurements were made at 25.00 ± 0.01°C.

Results and Discussion

The densities and volumetric heat capacities of the binary systems, which are required for the calculation of the transfer functions, were measured at the same time as those of the ternary systems. The derived apparent molar quantities of the binaries were in excellent agreement with those in the literature (11,16).

The enthalpies of dilution of BE were required to calculate the enthalpies of transfer (19). From these integral enthalpies of dilution ΔH_{ID} the relative apparent molar enthalpies $L_{2,\phi}$ were derived following the technique of Fortier et al (21). The values of ΔH_{ID} corresponding to the initial and final molalities are given in Table 1 along with the parametric equation for $L_{2,\phi}$.

The original densities, heat capacities per unit volume and enthalpies of mixing from which the various thermodynamic functions are calculated for the ternary systems are given elsewhere[1].

From these data it is possible to calculate the transfer functions of BE from water to a solution of NaDec. In general, for any transfer function defined in terms of apparent molar quantities,

$$\Delta Y_3(1 \rightarrow 1 + 2) = Y_{3,\phi}(1 + 2) - Y_{3,\phi}(1)$$

$$= \frac{Y(1 + 2 + 3) - Y(1 + 2)}{m_3} - \frac{Y(1 + 3) - Y(1)}{m_3}$$

$$= \frac{m_2}{m_3} \Delta Y_2(1 \rightarrow 1 + 3) \qquad (2)$$

---

[1]: Complete set of tabular data may be purchased from: The Depository of Unpublished Data, CISTI, National Research Council of Canada, Ottawa, Canada, K1A 0S2

where Y is the total property of the solution containing 1 kg of solvent or mixed solvent. In this relation m_3 is a constant low concentration relative to the CMC of 3 and m_2 is a variable concentration. Therefore, from the differences between the two volumes and heat capacities in Figure 1, the corresponding transfer functions of Be from water to aqueous NaDec are calculated and illustrated in Figure 2. The trends are similar to those measured directly for the transfer of BE from water to aqueous octylamine hydrobromide (10).

The apparent molar volumes and heat capacities, $V_{2,\phi}$ and $C_{p,2,\phi}$ of NaDec in water and in 0.05 mol kg^{-1} BE are shown in Figure 1. As expected from the formation of mixed micelles, BE shifts the CMC of NaDec to lower values.

Table I.   Enthalpies of Dilution of BE in Water at 25°C.

$\frac{m^i}{\text{mol kg}^{-1}}$	$\frac{m^f}{\text{mol kg}^{-1}}$	$\frac{-\Delta H_{ID}}{\text{J mol}^{-1}}$	$\frac{m^i}{\text{mol kg}^{-1}}$	$\frac{m^f}{\text{mol kg}^{-1}}$	$\frac{-\Delta H_{ID}}{\text{J mol}^{-1}}$
0.1008	0.04918	192.5	0.5673	0.2698	1158
0.1588	0.07716	293.6	0.7025	0.3301	1491
0.2091	0.1012	399.6	0.7542	0.3517	1702
0.2471	0.1194	474	0.8887	0.4086	2154
0.3065	0.1476	591	0.8887	0.4237	2128
0.3174	0.1527	610	1.0883	0.4948	3036
0.4093	0.1959	795	1.0883	0.5178	2957
0.5100	0.2408	1040	1.3925	0.7126	4115
0.5193	0.2443	1157	1.3925	0.6995	4168
0.5216	0.2367	1044	1.6516	0.7173	4800

$L_{2,\phi} = 3,400 \; m + 700 \; m^2$ for m < 1.7 mol kg^{-1}

The transfer of NaDec from water to BE solutions are shown for volumes and heat capacities in Figures 3 and 4 for two molalities of NaDec (0.05 and 0.10 mol kg^{-1}).

The functions of transfer can be simulated with the chemical equilibrium model of Roux et al. (6)

$$\Delta V_3(1 \rightarrow 1+2) = 2 \; \alpha \; \beta \; v_{23} \; m_2 + (m_2/m_3) \; \Delta V_2^M \; (\alpha_0 - \alpha) + (1-\beta) \; \Delta V_3^M \quad (3)$$

$$\Delta C_{p,3}(1 \rightarrow 1+2) = 2 \; \alpha \; \beta \; c_{23} \; m_2 + (m_2/m_3) \; \Delta C_{p,2}^M \; (\alpha_0 - \alpha)$$

$$+ (1-\beta) \; \Delta C_{p,3}^M + (m_2/m_3) \; \Delta H_2^M \; (\partial \alpha_0/\partial T - \partial \alpha/\partial T)$$

$$- \Delta H_3^M \; (\partial \beta/\partial T) \quad (4)$$

where α and β are the fractions of monomers of solute 2 and of solute 3 in water, α_0 is the value of α in the absence of solute 3, ΔY_1^M are the changes in the thermodynamic functions between the micellar state and water. The first term in equation 3 takes into account the pairwise interactions between the two monomeric solutes, the second term allows for the shift in CMC of solute 2 caused by the presence of solute 3 and the last term accounts for the distribution of solute 3 between water and the micelle of solute 2. The terms in $\partial \alpha/\partial T$ and $\partial \beta/\partial T$ are introduced in equation 4 since there is a shift in CMC caused both by the presence of solute 3 and by temperature. The fraction α and β are calculated from the micellization constant K_M and
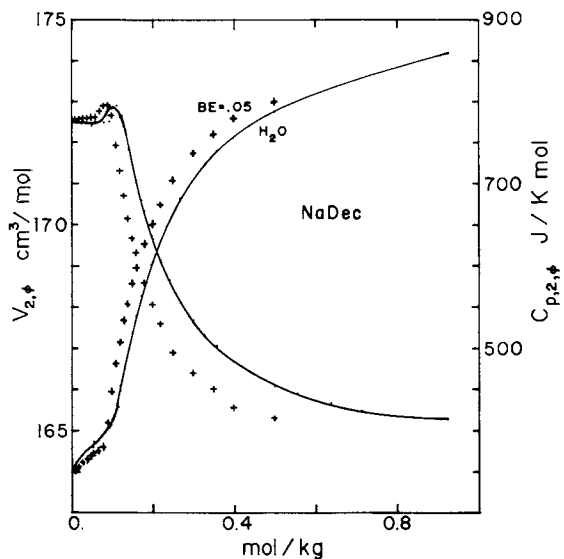
Figure 1: Apparent molar volumes and heat capacities of sodium deca noate in water (ref. 11) and in 0.05 mol kg^{-1} of 2-butoxy- ethanol at 25°C.
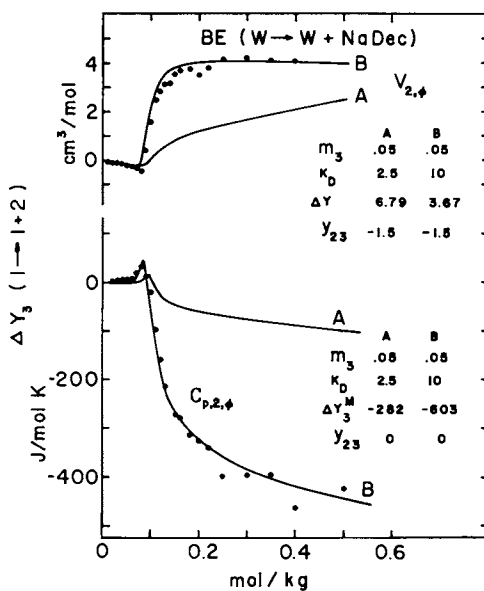
Figure 2: Volumes and heat capacities of transfer of 2-butoxyethanol from water to aqueous sodium decanoate at 25°C.
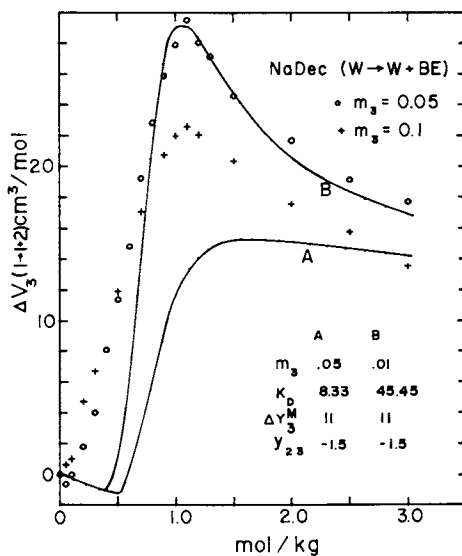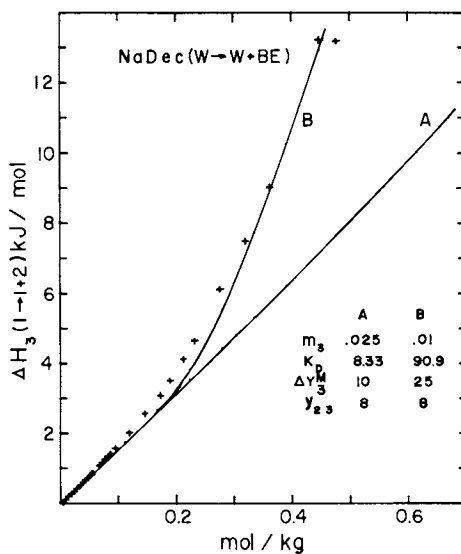
Figure 3: Volumes of transfer of sodium decanoate from water to
2-butoxyethanol solutions at 25°C. Simulations (curves A
and B) with a chemical equilibrium model.
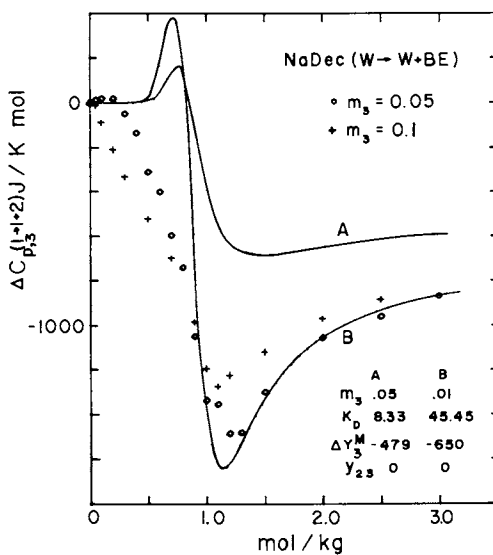
Figure 4: Heat capacities of transfer of sodium decanoate from water
to 2-butoxyethanol solutions at 25°C. Simulations (curves
A and B) with a chemical equilibrium model.

the distribution constant K_D. The constant K_D is delivred in such a way that it has the units of reciprocal molalities and represents the reciprocal effective solubility of solute 3 in the aqueous solution.

It is possible to estimate all the parameters of equations 3 and 4 from data on the binary systems. For example, data for solute 2 are derived from a mass-action model (22), while data for solute 3 can be estimated from the CMC of 3 (from which a distribution cons-tant and consequently β can be derived) and from the molar values of 3 in the pure liquid state or in the micellar form (6). The parame-ters, derived from the mass-action model using data from the litera-ture (16,23), are summarized in Table II. The curves A shown in Figures 2 to 4 are simulations with no adjustable parameters except v_{23} and c_{23}. These simulations, which essentially correspond to ideal mixing of the mixed micelles, generally underestimate the transfer functions. Better fits are obtained, at least at high m_2, if the parameters K_D and ΔY_3^M are adjusted. These new parameters are also given in Table III. It should be noted that if K_D is increased, it is sometimes necessary to decrease the value of m_3 in the simula-tions since K_D is related to the solubility of solute 3 in water and the model does not allow m_3 to be higher than this effective solubi-lity.

Table II. Parameters* from the Mass-Action Model for the Binary Sys-tem at 25°C

	Y_A^θ	A_Y	B_Y	$Y_A^{\theta ,}$	C_Y	m_I	n	Equil
NaDec								
$V_{2,\phi}$	164.010	1.867	4.6429	175.198	0.7085	0.12626	20	
$C_{p,2,\phi}$	771.834	28.99	−70.372	302.142	40.148	0.11901	20	104
$L_{2,\phi}$	0	1,975	13,510	10,000		0.11807	18.57	
BE								
$V_{2,\phi}$	122.826		−1.2353	129.622		1.1171	8.607	
$C_{p,2,\phi}$	553.014		1.9525	270.665		1.1201	14.306	83.23
$L_{2,\phi}$	0		4,100	7,847		1.1200	9	

* These parameters are defined in References 22 and 24.

Table III. Parameters for Simulations of Transfer Functions of NaDec from Water to BE Solutions at 25°C

Solute 3		m_3 mol/kg	Property	ΔY_3^M	K_D kg/mol	Y_{23}
NaDec	A	0.05	V	11.0 cm^3/mol	8.33	− 1.05
	B	0.01	V	11.0 cm^3/mol	45.45	− 1.05
	A	0.05	C_p	− 479 J/K mol	8.33	0
	B	0.01	C_p	− 650 J/K mol	45.45	0
	A	0.025	H	10 kJ/mol	8.33	8.0
	B	0.01	H	25 kJ/mol	90.9	8.0
BE	A	0.05	V	6.79 cm^3/mol	2.5	− 1.5
	B	0.05	V	3.67 cm^3/mol	10	− 1.5
	A	0.05	C_p	− 282 J/K mol	2.5	0
	B	0.05	C_p	− 603 J/K mol	10	0
	A	0.025	H	7.85 kJ/mol	2.5	8.0
	B	0.025	H	2 kJ/mol	23.26	8.0

The fits for the transfer of BE from water to aqueous NaDec are quite good over the whole m_2 range when the parameters y_{23}, K_D and ΔY_3^M are adjusted. This gives credibility to the model and shows that the assumptions and approximations are generally valid for this transfer system. The parameters K_D and ΔY_3^M are somewhat interdependent and must therefore be interpreted with care. Still, the much larger values of K_D that are needed to get a good fit and the magnitude of ΔY_3^M all suggest that the formations of a mixed micelle between BE and NaDec is quite a favorable event.

The transfers of NaDec from water to aqueous BE are more difficult to fit. The initial slopes y_{23} were taken identical to those of the converse transfer functions (in Figure 2) since this follows directly from the reciprocity theorem. The values of K_D and ΔY_3^M were then adjusted so as to get a good fit at high m_2 concentrations. The simulations cannot account for the data at low concentration of BE. The deviations are larger at 0.10 mol kg^{-1} NaDec. The origin of the difference is obvious once it is realized that the value of m_3 is not low compared to the CMC of NaDec (0.12 mol kg^{-1}). Since BE lowers the CMC of NaDec, there is some self-micellization of NaDec induced by BE occuring before the normal micellization or aggregation of BE. A single micellization process would have been observed only if $m_3 \ll$ CMC of NaDec. This phenomenon was also observed with other systems (5,14). As for the converse transfer functions K_D and ΔY_3^M are generally different from the predicted values for ideal mixing and in the direction of a favorable mixing. This again confirms the large affinity of BE and NaDec to form mixed micelles. Under the experimental conditions of Figures 3 and 4, micelles of NaDec containing small quantities of BE are produced initially but, as the concentration of BE is increased, the prefered mixed micelles are those of BE with small quantities of NaDec.

The enthalpies of transfer of BE (0.025 mol kg^{-1}) from water to NaDec solutions are shown in Figure 5. With no adjustable parameters curve A is predicted with the model of Roux et al (6). The relation is analogous to Equation 3. By adjusting K_D and ΔH_3^M a nearly quantitative fit can again be obtained as shown in curve B of Figure 5. The value of K_D used in this simulation is about twice as large as the one used for volumes and heat capacities. If K_M was fixed as the same value as that used for other properties the maximum in Figure 5 is then underestimated.

The enthalpies of transfer of NaDec from water to BE solutions are shown in Figure 6. Unfortunately, data at high BE concentration are not available since, at BE initial concentrations above 1 mol kg^{-1} complete mixing of the solutions could not be obtained in the flow calorimeters. The initial slopes of these enthalpies of transfer are experimentally the same as in Figure 5, as expected, and the parameter h_{23} could be fixed at the same value as for this converse system. The parameter K_D can also be fixed using the values for volumes and heat capacities. Curve A corresponds again to the ideal mixing situation and, as with other functions, largely underestimates the experimental trends. If K_D is taken as 45.45, the value needed to fit the high m_2 data for volumes and heat capacities, the experimental transfer function is again underestimated unless unrealistically large ΔH_3^M are used (> 80 kJ mol^{-1}). Even if K_D is taken as 90 (curve B), some deviation is still observed at about 0.2 mol kg^{-1}.
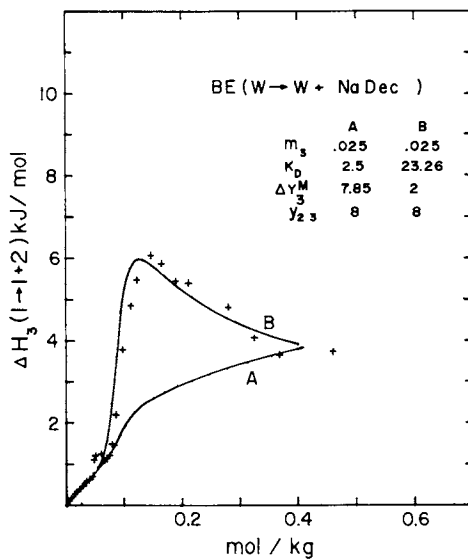
Figure 5: Enthalpies of transfer of 2-butoxyethanol from water to sodium decanoate solutions at 25°C. Simulations (curves A and B) with a chemical equilibrium model.

Figure 6: Enthalpies of transfer of sodium decanoate from water to 2-butoxyethanol solutions at 25°C. Simulations (curves A and B) with a chemical equilibrium model.

The $\Delta H_3{}^M$ are not reliable in these simulations since high m_2 data are not available. Still the lack of agreement between the predicted and experimental enthalpies of transfer in Figure 6 again supports self-association of NaDec induced by BE as with other functions. The deviation is not as pronounced as with volumes and heat capacities since m_3 was maintained at a lower value in the enthalpy experiments.

Conclusion

The chemical equilibrium model of Roux et al (6) is a powerful tool for the study of the thermodynamics of mixed micellar solutions. It can estimate the distribution constant of the surfactant 3 between water and micelles of the surfactant 2 and the thermodynamic properties of the surfactant 3 in the mixed micelles. For this it is necessary to obtain reliable data over a large concentration range of solute 2.

The present comparison between the experimental functions of transfer and the simulations show that NaDec will have a tendency for self-micellization in the presence of BE since the experimental concentration of NaDec is relatively close to its CMC. On the other hand, no such pre-aggregation of BE is observed when this solute at 0.05 mol kg^{-1} or lower is transfered to a solution of NaDec.

The magnitude and sign of the distribution constants and of the thermodynamic functions of the transfered solute to the mixed micelle, when compared with those predicted from the binary systems, indicate that the formation of a mixed micelle between BE and NaDec is a highly favorable event.

Acknowledgment

Literature Cited

1. Rubingh, D.N. in "Solution Chemistry of Surfactants", Vol. 1, Mittal, K.L. ed.; Plenum Press, New-York, 1979, p. 337.
2. Nishikido, N.; Moroi, Y.; Matuura, R. Bull. Chem. Soc. Jpn. 1975, 48, 1387.
3. Goto, A.; Sakura, R.; Endo, F. J. Colloid. Interface Sci. 1978, 67, 491.
4. Funasaki, N.; Hada, S. J. Phys. Chem. 1982, 86, 2504.
5. Perron, G.; DeLisi, R.; Davidson, I.; Généreux, S.; Desnoyers, J.E. J. Col. Interf. Sci. 1981, 79, 432.
6. Roux, A.H.; Hétu, D.; Perron, G.; Desnoyers, J.E. J. Solution Chem. 1984, 13, 1.
7. Treiner C. J. Coll. Interf. Sci. 1982, 90, 444.
8. Christian, S.D.; Tucker, E.E.; Lane, E.H. J. Coll. Interf. Sci. 1981, 84, 423.
9. DeLisi, R.; Liveri, V.T. Gazetta Chimica Italiana 1983, 113, 371.

10. Desnoyers, J.E.; Hêtu, D.; Perron, G. J. Solution Chem. 1983, 12, 427.
11. Roux, G.; Perron, G.; Desnoyers, J.E. J. Solution Chem. 1978, 7, 639.
12. Iwasaki, K.; Fujiyama, T. J. Phys. Chem. 1979, 83, 463.
13. Roux, A.H.; Hêtu, D.; Desnoyers, J.E. (in préparation).
14. Quirion, F.; Desnoyers, J.E. (in préparation).
15. Yamashita, F.; Kwak, J.C.T.; Perron, G.; Desnoyers, J.E. (in préparation).
16. DeLisi, R.; Perron, G.; Desnoyers, J.E. Can. J. Chem. 1980, 58, 959.
17. Picker, P.; Tremblay, E.; Jolicoeur, C. J. Solution Chem. 1974, 3, 377.
18. Avédikian, L.; Perron, G.; Desnoyers, J.E. J. Solution Chem. 1975, 4, 331.
19. Desnoyers, J.E.; Perron, G.; Avédikian, L.; Morel, J.P. J. Solution Chem. 1976, 5, 631.
20. Picker, P; Leduc, P.A.; Philip, P.; Desnoyers, J.E. J. Chem. Thermodynamics 1971, 3, 631.
21. Fortier, J.L.; Leduc, P.A.; Picker, P.; Desnoyers, J.E. J. Solution Chem. 1973, 5, 467.
22. Desnoyers, J.E.; Caron, G.; Delisi, R.; Roberts, D.; Roux, A.; Perron, G. J. Phys. Chem. 1983, 87, 1397.
23. Roux, G.; Perron, G.; Desnoyers, J.E. J. Solution Chem. 1978, 7, 639.
24. Caron, G.; Perron, G.; Lindheimer, M.; Desnoyers, J.E. J. Colloid Interf. Sci. 1985, 106, 324.

7

Characterization of Inverted Micelles of Calcium Alkarylsulfonates by Some Pyrene Fluorescence Probes

Tze-Chi Jao and Kenneth L. Kreuz

Texaco Research Center, Beacon, NY 12508

1-Pyrene carboxaldehyde and a series of pyrene carbox-
ylic acids were found useful as fluorescence probes in
describing the constitution of inverted micelles of
certain   calcium   alkarylsulfonates   in   hydrocarbon
media.   1-Pyrene carboxaldehyde is a convenient probe
for studying the particle sizes of micelles in the
region of 100A.   A series of graded probes, pyrene
carboxylic acids with varying alkyl chain length, have
been used to determine internal fluidity and micro-
polarity as a function of distance from the polar core
of these inverted micelles.   Pyrene excimer to monomer
fluorescence intensity ratio and fluorescene lifetime
provided the means of measurement of internal fluidity
and micropolarity, respectively.

The use of the fluorescence probe as a tool for characterizing
aggregate systems in non-polar media (e.g., "inverted micelles") has
become increasingly popular within the last decade among chemists
and biochemists (1-4).   Its utility has been demonstrated for
providing constitutional (e.g., micro-viscosity, -polarity, and -pH)
information on aggregates, and for demonstrating the dynamic nature
of these structures.   Such information has been applied toward an
improved understanding of the function of bio-membranes, and to a
better   utilization   of   surfactants   in   industrial   processes   and
products.
     Much remains to be learned, however, regarding the limits of
applicability of the fluorescence probe technique to aggregates in
non-polar media.   A number of obvious experiments are conspicuous by
their absence from the published literature.   For example, 1-pyrene
carboxaldehyde is a well known probe which has been used to measure
the microscopic polarity of sodium dodecyl sulfate micelles in
aqueous medium (5); there is, however, no account of its use in
non-polar media.

The present study demonstrates the utility of the above probe in describing the constitution of aggregates of certain alkarylsulfonates in hydrocarbon media. It also demonstrates the use of the probe technique in measuring the micropolarity of these same aggregates as a function of distance from the polar core. The microviscosity of inverted or normal micelles in the past has been estimated only as an average value of either the polar or non-polar regions (6).

It is worthy of note that the micellar systems dealt with in this study differ from conventional "inverted micelles" in that they contain solubilized inorganic species in their cores. It was of additional interest to observe the response of such systems to the fluorescence probe technique.

Experimental

Materials.   1-pyrene carboxaldehyde, 1-pyrene valeric acid (PVA), 1-pyrene nonanoic acid (PNA), and 1-pyrene hexadecanoic acid (PHA) were purchased from Molecular Probes, Inc. (Eugene, Oregon). Spectral grade n-hexane, n-heptane, n-octane and n-nonane were obtained either from Burdick and Jackson Laboratories, Inc. (Muskegan, Michigan) or from Pfaltz and Bauer, Inc. (Stamford, Connecticut). Two kinds of calcium alkarylsulfonates were used: sulfonate A contained basic Ca equivalent to one-half mole $Ca(OH)_2$ per mole of Ca alkarylsulfonate; sulfonate B contained 20 mole of a mixture of $CaCO_3$ and the above type of basic Ca. The average molecular weight of the parent sulfonic acid for both materials was 450. Both sulfonates were a mixture of 35% (w/w) synthetic sulfonate (containing over 90% di-dodecyl benzene sulfonate) and 65% (w/w) petroleum sulfonate (branched monoalkaryl sulfonate ca. C_{28-35}). These two sulfonates were the subject of a previous communication from this laboratory (7). Aerosol OT was purchased from Pfaltz and Bauer, Inc. Further purification was carried out by precipitation from methanol; the precipitate was then dried under vacuum at 40°C for several days.

All test solutions, except otherwise mentioned, were degassed by three freeze-pump-thaw cycles with a vacuum line operated under 10^{-3} torr pressure. Problems of background fluorescence originating from sulfonates themselves could be adequately minimized by proper choice of probe/sulfonate ratios. The excitation wavelength was set at 340 nm. Emission spectra were obtained in constant energy mode. The spectral resolution was 3 nm.

Instrumentation.   The steady-state fluorescence spectra were measured with Perkin-Elmer MPF-44B fluorescence spectrophotometer. The single-photon counting instrument for fluorescence lifetime measurements was assembled in-house from components obtained from EG&G ORTEC. A PRA-510B light pulser filled with N_2 gas was used as the excitation source. Instrument response function was obtained with DuPont Ludox scatter solution at the excitation wavelength.

Results

1-Pyrene Carboxaldehyde Probe Studies. Fluorescence spectra of 1-pyrene carboxaldehyde in nonane solutions of sulfonates A and B and in an octane solution of Aerosol OT are compared to the probe spectra in pure hydrocarbon media in Figure 1. Parts (a) and (b) are of sulfonates A and B systems, respectively; part (c) is of aerosol OT system. They were constructed at different gain settings and therefore the intensities shown for the individual system are not directly comparable. The fluorescence intensity of 1-pyrene carboxaldehyde in nonane alone is much weaker than in either the sulfonate A or sulfonate B solution. Aerosol OT containing solubilized H_2O does not enhance the fluorescence intensity of 1-pyrene carboxaldehyde as much as sulfonates A and B, but the band maximum is shifted as expected for this probe in a water-rich medium.

We measured the time-dependent anisotropy of 1-pyrene carboxaldehyde in sulfonate A and B systems. The results are shown in Figure 2. Relaxation times determined from the unconvoluted anisotropy decays for sulfonates A and B in heptane solution were found to be 7 ns and 28 ns, respectively.

In order to test further the applicability of 1-pyrene carboxaldehyde as a fluorescent probe, we applied Keh and Valeur's method (4) to determine average micellar sizes of sulfonate A and B micelles. This method is based on the assumption that the motion of a probe molecule is coupled to that of the micelle, and that the micellar hydrodynamic volumes are the same in two apolar solvents of different viscosities. For our purposes, time averaged anisotropies of these systems were measured in two n-alkanes: hexane and nonane. The fluorescence lifetime of 1-pyrene carboxaldehyde with the two sulfonates in both these solvents was found to be approximately 5 ns. The micellar sizes (diameter) calculated for sulfonates A and B were 53 ± 5A and 82 ± 10A, respectively. Since these micelles possesed solid polar cores, they were probably more tightly bound than typical inverted micelles such as those of aerosol OT. Hence, it was expected that the probe molecules would not perturb the micelles to an extent which would substantially affect the micellar sizes measured.

If one assumes for an extreme case that the core materials of sulfonates A and B are $Ca(OH)_2$ and $CaCO_3$ plus $Ca(OH)_2$, respectively, one can derive a limiting constitution for these micelles. If one further assumes that the densities of calcium hydroxide and calcium carbonate in the polar core are 2.2 g/cm^3 and 2.4 g/cm^3, respectively, and that the average density of both micelle types excluding the polar core is about 1 g/cm^3, one arrives at aggregation numbers, calculated from the micellar sizes determined, for these two sulfonate micelles to be nearly the same, approximately 50.

Lateral Mobility(Fluidity) of Sulfonate A and B Micelles. The ratio of excimer to monomer fluorescence intensity of pyrene had previously been used to measure the fluidity of biological membranes (8). The ease of excimer formation was correlated with the fluidity of the membrane. The same principle may be applied to the measurement of fluidity in inverted micelles. To this end, we used three pyrene carboxylic acid probes of varying chain length: PVA, PNA and
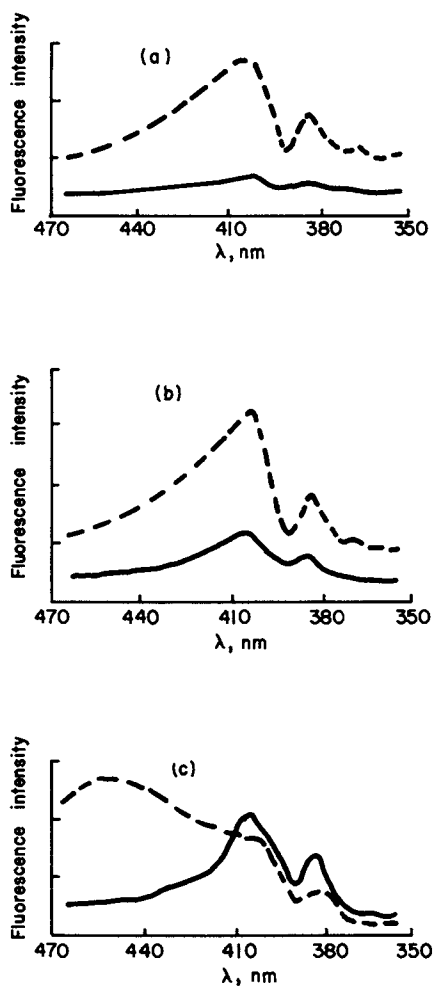
Figure 1. Fluorescence spectra of 1-pyrene carboxaldehyde $(2.5 \times 10^{-5} M)$ in: (a) ---- sulfonate A $(5.0 \times 10^{-4} M)$/ nonane solution, ——— heptane, (b) --- sulfonate B $(5.0 \times 10^{-4} M)$/ nonane solution, ——— heptane, (c) ---- 3% (w/w) AOT/1.5% (w/w) H_2O/Octane solution, ——— Octane. Excitation wavelength is 340 nm.
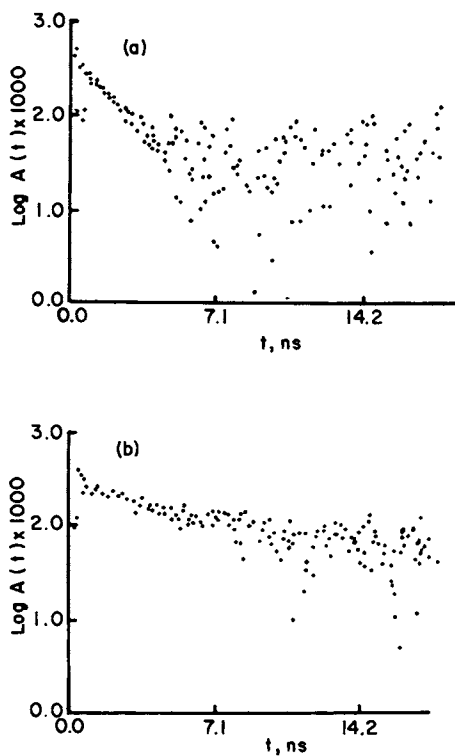
Figure 2. Unconvoluted anisotropy decays of 1-pyrene carbox-aldehyde in sulfonate micelles: (a) sulfonate A (5×10^{-4} M)/heptane (7 ns), (b) Sulfonate B (5×10^{-4} M)/heptane (28 ns). The cmc of sulfonate A is less than 10^{-6} M, while that of sulfonate B is "infinitely" dilute.

PHA. The relative location of each probe in the micelle had reason-
ably been established in our earlier report (7) by demonstrating the
anchoring of the carboxylate moiety in the polar core.

For this study, we maintained the pyrene probe concentrations
constant, while we varied sulfonate concentration. The measured
excimer to monomer ratios as a function of the molar ratio of probe
to sulfonate for sulfonates A and B are shown in Figure 3.

It can be seen that the excimer to monomer fluorescence inten-
sity ratios for the same molar ratio of probe to sulfonate are much
smaller in the sulfonate A system than in the sulfonate B system.
For both sulfonates A and B, the intensity ratio tends to increase
with the chain length of the carboxylic acid. The variation is
distinctly established for sulfonate B micelles, but less so for
sulfonate A micelles. The results indicate that the internal
fluidity of the micelles decreases from the edge of the polar core
to the continuous hydrocarbon medium; the gradient is steeper for
sulfonate B.

Polarity Variation in Sulfonate Micelles.   Other   workers   have
established a correlation between the fluorescence lifetime of
pyrene in solution and the polarity of the solvent medium (9).
Polar media quench the excited electronic state of pyrene and hence
shorten its fluorescence lifetime. We applied this principle to
measure the polarity variation within the micelles of sulfonates A
and B.

The fluorescence lifetimes of the three pyrene carboxylic acid
probes (PVA, PNA, PHA) were determined without convolution with
respect to the instrument response function, since the fluorescence
lifetimes of the pyrene probes (280 ns) are sufficiently long
compared with the pulse-width of the N_2 lamp profile (5 ns).
Background fluorescence from the aromatic moieties of the sulfonates
was found to be sufficiently strong to give the appearance of a
double exponential (see Figure 4). The shorter component largely
originated from the sulfonate itself. We analyzed the longer
lifetime component in order to calculate the fluorescence lifetime
for pyrene. The results are shown in Figure 5.

Fluorescence lifetimes of PVA, PNA and PHA in heptane alone
were found to vary slightly among themselves. Since it would not
affect our interpretation, no attempt was made to study the origin
of the discrepancy. It was concluded that the probe (PVA) that is
closest to the polar core of the micelle experiences the most polar
environment, since its fluorescence lifetime was found to be shorter
than those of PNA and PHA. The variation in polarity is seen to be
greater in the micelles of sulfonate A than those of sulfonate B.

Discussion

1-Pyrene Carboxaldehyde in Calcium Alkarylsulfonates. Our   work
shows that 1-pyrene carboxaldehyde as a fluorescent probe for the
sulfonate systems behaves very much the same as rhodamine B (1) and
anilinonaphthalene sulfonate (2), whose fluorescence intensities in
hydrocarbon media are enhanced in the presence of inverted micelles.
However, the intensity increase observed with AOT was considerably
less than that observed with the sulfonates. It is speculated that
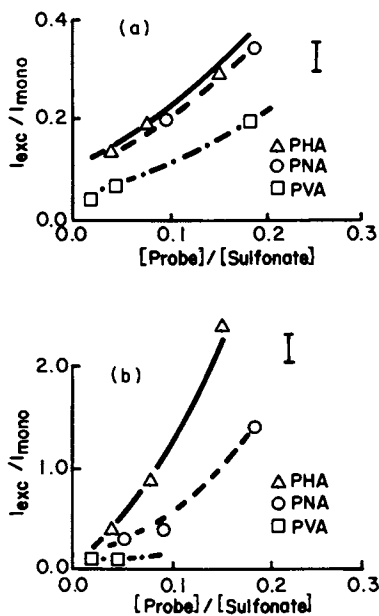
Figure 3. Plots of excimer (at 470 nm) to monomer (370 nm) intensity ratios as a function of probe/sulfonate molar ratio. (a) sulfonate A /heptane, (b) sulfonate B /heptane. The concentrations of PHA, PNA, and PVA are 1 x 10^{-5}M, 1 x 10^{-5}M, and 5 x 10^{-6}M, respectively.
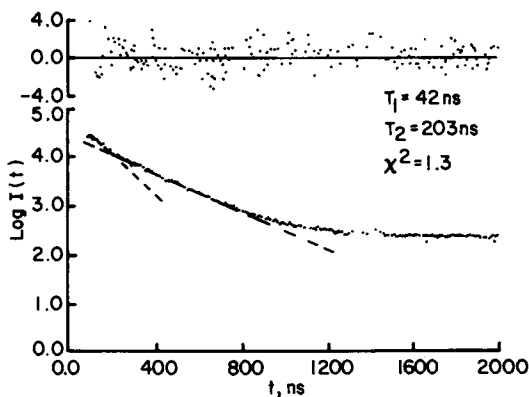
Figure 4. Fluorescence decay of PVA in the sulfonate A/heptane system. Wavelength of excitation is 340 nm and emission is collected at 390 nm.
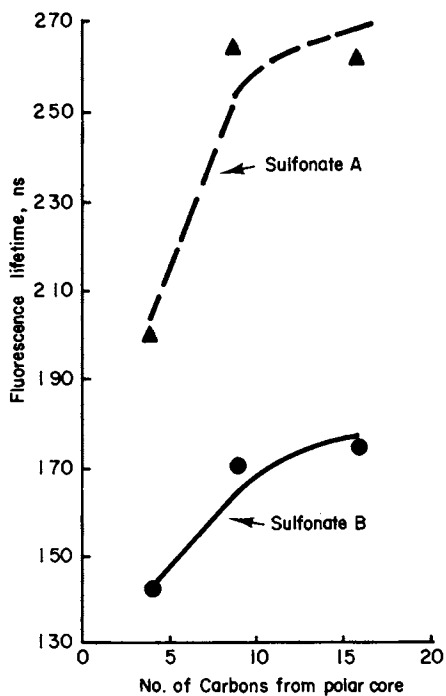
Figure 5. Plots of the fluorescence lifetime of pyrene as a function of distance from the polar core of the micelles of sulfonates A and B in heptane solutions.

in the case of sulfonate system, 1-pyrene carboxaldehyde could react with the basic species in the polar core, so that the probe could be firmly held by the micelle. Aerosol OT, of course, lacks such basic materials, and in contrast to the sulfonates is actually a water-in-oil microemulsion.

The internal rotational relaxation times of 1-pyrene carbox-aldehyde in sulfonate systems may offer some indication of the extent of probe binding to the inverted micelle. In the absence of any background fluorescence interference to the time-dependent anisotropy decay profile, the internal rotational relaxation time should correlate with the strength of binding with the polar material in the polar core. However, spectral interference from the aromatic moieties of sulfonates is substantial, so that the values of internal rotational relaxation time can only be used for quali-tative comparison.

Lateral Mobility in Alkarylsulfonate Micelles.   In order to make a valid comparison of fluidity between sulfonates A and B, the micellar sizes should be comparable. This condition is required so that equal population of pyrene moieties between the two sulfonate systems can be assumed. Alternatively, the requirements might be met if they have equal aggregation numbers. If the above-mentioned (See Section A under "Results") assumptions regarding polar core composition are reasonable, the condition for equal probe population between the two sulfonate micelles can still be reasonably approximated.

The lateral mobility experiments demonstrate that the micellar aggregate, excluding polar core, of sulfonate A is less fluid than that of sulfonate B. It would then follow that the sulfonate moieties are less densely packed on the polar core of sulfonate B.

Polarity Variation in Sulfonate Micelles.   Our   results   here suggest that a polarity gradient in the inverted micelles of sulfonates, excluding the polar core, does exist in a manner similar to the oxygen concentration gradient for the same sulfonates reported previously by us (7). Earlier, Wheeler and Thomas (10) established that the vibrational fine structure of bands II and III of a pyrene derivative probe can be used to measure the local polarity of a micro-environment in aggregates. We noted that bands II and III in the vibrational fine structure of PVA for both sulfonate systems has completely disappeared, while that of PHA is retained. The disappearance of bands II and III indicates that the probe has experienced a highly polar medium. Hence, the polarity gradient observed here is reasonably established despite the fact that background fluorescence interference from the aromatic moieties of sulfonates produced considerable uncertainty in the lifetime values measured.

The oxygen concentration gradient and polarity gradient seem to be related. It is likely that the oxygen concentration gradient is created by the existence of the polarity gradient. More work is needed to establish the relationship.

Conclusion

1-Pyrene carboxaldehyde has utility as a fluorescent probe in some inverted micellar systems containing solubilized inorganic species in the polar core. Its fluorescence lifetime is ca. 5 ns; thus it is an appropriate probe for measuring micellar sizes which are approximately 100A.
  Variation of lateral mobility (fluidity) and polarity gradient have been reasonably established in certain calcium alkarylsulfonate micelles using 1-pyrene carboxylic acid probes with varying alkyl chain lengths. The existence of a polarity gradient in an inverted micelle may be responsible for the creation of an oxygen concentration gradient.

Acknowledgment

Literature Cited

1. (a) Arkin, L., and Singleterry, C. R. (1948). J. Am. Chem. Soc. 70, 3965; (b) Arkin, L., and Singleterry, C. R. (1949). J. Colloid Sci. 4, 537-539; (c) Singleterry, C. R., and Arkin-Weinberger, L. (1951). J. Am. Chem. Soc. 73, 4574-4579.
2. (a) Wong, M., Thomas, J. K., and Gratzel, M. (1976). J. Am. Chem. Soc. 98, 2391-2397; (b) Thomas, J. K. (1984). The Chemistry of Excitation at Interfaces, ACS Monograph 181, ACS, Washington, D.C.
3. (a) Correll, G. D., Chester, III, R. N., Nome, F., and Fendler, J. H. (1978). J. Am. Chem. Soc. 100, 1254-1262; (b) Fendler, J. H. (1982). Membrane Mimetic Chemistry, Wiley, New York.
4. Keh, E., and Valeur, B. (1981). J. Colloid Interface Sci. 79, 465-478.
5. Kalyanasundaram, K., and Thomas, J. K. (1977) J. Phys. Chem. 81, 2176-2180.
6. Love, L. J. Cline, Harbata, J. G., and Dorsey, J. G. (1984). Anal. Chem. 56, 1133A-1148A.
7. Jao, T. C., and Kreuz, K. L. (1984). J. Colloid Interface Sci. 102, 308-310.
8. Galla, H.-J., and Luisetti, J. (1980). Biochim. Biophys. Acta 596, 108-117.
9. Morris, D. A. N., and Thomas, J. K. (1977). In Micellization, Solubilization, and Microemulsions (K. L. Mittal ed.) Plenum Press, New York, Vol. 2, pp. 913-926.
10. Wheeler, J., and Thomas, J. K. (1982). In Inorganic Reactions in Organized Media (S. L. Holt, ed.) American Chemical Society, Washington, D.C., ACS Symp. Ser. No. 177, pp. 97-111.

8

Nonideal Mixed Monolayer Model

Paul M. Holland

Miami Valley Laboratories, The Procter & Gamble Company, Cincinnati, OH 45247

A generalized nonideal mixed monolayer model
based on the pseudo-phase separation approach is
presented. This extends the model developed
earlier for mixed micelles (J. Phys. Chem. 1983
87, 1984) to the treatment of nonideal surfac-
tant mixtures at interfaces. The approach
explicity takes surface pressures and molecular
areas into account and results in a nonideal
analog of Butler's equation applicable to mi-
cellar solutions. Measured values of the
surface tension of nonideal mixed micellar
solutions are also reported and compared with
those predicted by the model.

In mixed surfactant systems, physical properties such as the
critical micelle concentration (cmc) and interfacial tensions are
often substantially lower than would be expected based on the
properties of the pure components. Such nonideal behavior is of
both theoretical interest and industrial importance. For example,
mixtures of different classes of surfactants often exhibit
synergism (1-5) and this behavior can be utilized in practical
applications (6).In addition, commercial surfactant
preparations usually contain mixtures of various species (e.g.
different isomers and chain lengths) and often include surface
active impurities which affect the critical micelle concentration
and other properties.
    An important motivation for understanding the behavior of mixed
micellar solutions is that equilibrium between the micelles and
monomers establishes the chemical potential of the different surfac-
tant species in bulk solution. In turn, these chemical potentials
provide the driving force for processes such as interfacial tension
lowering,contact angle changes and partitioning, and at equilibrium
exert a controlling influence on physical properties at the solution
interfaces of interest. Viewed from this perspective, the mixed
micellar problem represents the crucial first step toward developing

a generalized model for the behavior of nonideal mixed surfactant
systems.
     Pseudo-phase separation models for treating mixed micellization
have become increasingly useful since the early 1950's when they
were first developed for binary systems based on the assumption of
ideal mixing in the micelles (7,8). Further developments for
the ideal models have included explicit treatment of monomer concen-
trations and micellar compositions (9), mixed ionic systems with
different counterions (10-11) two phase systems (12) and multi-
component surfactant systems (12-14). The earliest attempts
to explicitly treat nonideal mixing in micelles (15-16) were some-
what cumbersome and have not been widely used. However, a much
more tractable approach is based on the regular solution approxi-
mation and was first applied by Rubingh (17) to a wide range of
nonideal mixtures. Although this thermodynamic model was specifi-
cally developed for nonionic surfactant mixtures, it was also found
to be useful in describing the behavior of mixtures containing
ionic surfactants. Many subsequent treatments of nonideal
surfactant mixtures have employed the regular solution approach in
one form or another. These include Ingram's extension of binary
nonionic approach to model surface tensions of binary surfactant
mixtures (18-19), Rosen and coworkers' detailed treatment of
synergism in binary systems (2-5), a model including treatment
of nonideal binary ionic surfactant mixtures by Kamrath and Franses
(20), treatment of binary anionic-nonionic mixtures by
Scamehorn et. al. (21) and a generalized model for nonideal
multicomponent micelles by Holland and Rubingh (14). Although
the underlying assumptions of the regular solution approximation
are known to fail in a number of these cases (22-24) and it has
been criticized on fundamental grounds (25,26), it does provide
the most tractable and useful way to treat nonideal mixed micellar
solutions in many situations.
     The purpose of this paper will be to develop a generalized
treatment extending the earlier mixed micelle model (14) to non-
ideal mixed surfactant monolayers in micellar systems. In this
work, a thermodynamic model for nonionic surfactant mixtures is
developed which can also be applied empirically to mixtures contain-
ing ionic surfactants. The form of the model is designed to allow
for future generalization to multiple components, other interfaces
and the treatment of contact angles. The use of the pseudo-phase
separation approach and regular solution approximation are dictated
by the requirement that the model be sufficiently tractable to be
applied in realistic situations of interest.

Theory

The pseudo-phase separation approach has been successfully applied
in developing a generalized nonideal multicomponent mixed micelle
model (see 14) and it is interesting to consider whether this
same approach can be used to develop a generalized treatment for
adsorbed nonideal mixed surfactant monolayers. The preferred form
for such a model is that it be suitable (at least in principle) for
treating multiple components and be extendable to other interfaces
and properties of interest such as contact angles. Earlier models
(5, 18, 27) based on the pseudo-phase separation approach and

regular solution approximation have a more limited range of appli-
cation and are restricted to binary systems due to their functional
dependence on surface tension ratios. The form of the model to be
presented here is directly based on physical parameters and meets
the criteria for generality stated above. Here, the part of the
model which describes the behavior of the mixed micelles provides a
basis for establishing the chemical potentials of the individual
surfactant species in bulk solution, and thereby the equilibrium
chemical potentials in adsorbed mixed monolayers at the various
interfaces with the solution.

Using this approach, a model can be developed by considering
the chemical potentials of the individual surfactant components.
Here, we consider only the region where the adsorbed monolayer is
"saturated" with surfactant (for example, at or above the cmc) and
where no "bulk-like" water is present at the interface. Under
these conditions the sum of the surface mole fractions of surfactant
is assumed to equal unity. This approach diverges from standard
treatments of adsorption at interfaces (see ref 28) in that the
solvent is not explicitly included in the treatment. While the
"residual" solvent at the interface can clearly effect the surface
free energy of the system, we now consider these effects to be
accounted for in the standard chemical potentials at the surface and
in the nonideal net interaction parameter in the mixed pseudo-phase.

With these considerations in mind, the chemical potential of
the ith free monomeric surfactant component in solution is given by

$$\mu_i = \mu_i^o + RT \ln C_i^m \tag{1}$$

where μ_i^o is a standard state chemical potential and C_i^m the
monomer concentration of the ith species (see list of symbols).
For pure micelles of the ith component, a similar expression

$$\mu_i^{Mo} = \mu_i^o + RT \ln C_i \tag{2}$$

results which depends on the cmc of the pure surfactant, C_i. The
chemical potential of the ith surfactant component in an adsorbed
monolayer of pure surfactant can be expressed as

$$\mu_i^s = \mu_i^{os} + \pi_i \omega_i \tag{3}$$

where μ_i^{os} is a standard state chemical potential and $\pi_i \omega_i$
a force field term. Conveniently, both the surface pressure and
the molar area ω_i can be obtained experimentally from interfacial
tension measurements (such as surface tensions at the air/solution
interface used to determine the cmc). Here, π_i is given by

$$\pi_i = \gamma_{H_2O} - \gamma_i \tag{4}$$

and the molar area by

$$\omega_i = -RT \frac{d \ln C_i^m}{d\gamma_i} \tag{5}$$

Above the critical micelle concentration (C_i) in a pure surfactant solution the chemical potential of the monomer is given by

$$\mu_i = \mu_i{}^o + RT \ln C_i \qquad (6)$$

and that of surfactant species in the adsorbed (pure) monolayer by

$$\mu_i{}^s = \mu_i{}^{os} + \pi_i{}^{max}\omega_i \qquad (7)$$

where $\pi_i{}^{max}$ is the limiting value of the surface pressure above the cmc.

At equilibrium $\mu_i = \mu_i{}^s$ and the equations 6 and 7 can be combined to yield

$$\frac{\mu_i{}^{os} - \mu_i{}^o}{RT} + \frac{\pi_i{}^{max}\omega_i}{RT} = \ln C_i \qquad (8)$$

where the term containing the chemical potentials is in the form of a bulk-surface distribution coefficient.

In mixed surfactant systems above the cmc the chemical potential of the ith component (in the mixed micelle) is given by

$$\mu_i{}^M = \mu_i{}^{Mo} + RT \ln f_i x_i \qquad (9)$$

where f_i and x_i are the activity coefficient and mole fraction in the micelle, respectively. Combining this with equations 1 and 2 at equilibrium yields the monomer concentration as given in the nonideal mixed micelle model (14)

$$C_i{}^m = x_i f_i C_i \qquad (10)$$

The chemical potential of the ith component in the monolayer

$$\mu_i{}^s = \mu_i{}^{os} + RT \ln f_i{}^s x_i{}^s + \pi\omega'_i \qquad (11)$$

now includes a term containing its activity coefficient in the mixed monolayer $(f_i{}^S)$ as well as its mole fraction. As in the case of mixed micelles, the binary activity coefficients based on the regular solution approximation take the form

$$f_1{}^s = \exp \beta^s (1-x_1{}^s)^2 \qquad (12)$$

$$f_2{}^s = \exp \beta^s (x_1{}^s)^2 \qquad (13)$$

where β^s is a dimensionless net interaction parameter. At equilibrium the chemical potentials are equal and equations 8 and 9 can be combined to yield

$$\frac{\mu_i{}^{os} - \mu_i{}^o}{RT} + \frac{\pi\omega'_i}{RT} = \ln\left(\frac{f_i x_i C_i}{f_i{}^s x_i{}^s}\right) \qquad (14)$$

where π is the total surface pressure. Combining equations 7 and 10 to eliminate their common term results in the generalized expression

$$\frac{f_i{}^s x_i{}^s}{f_i x_i} = e^{\dfrac{\pi_i{}^{max}\omega_i - \pi\omega'_i}{RT}} \qquad (15)$$

which directly relates the activity coefficients and mole fractions in the mixed micellar and monolayer psuedo-phases. Here, their ratio depends on the maximum surface pressures of the pure surfactants components, total surface pressure, and areas per molecule at the interface in the pure and mixed systems. This allows comparison between nonideal interactions in the micelle and monolayer as modeled by their respective interaction parameters.

Rearranging this expression gives the following nonideal analog of Butler's equation (29)

$$\pi\omega'_i = RT \ln\left(\frac{f_i x_i}{f_i{}^s x_i{}^s}\right) + \pi_i{}^{max}\omega_i \qquad (16)$$

Assuming the areas per molecule remain unchanged on mixing this can be further simplified to

$$\pi = \frac{RT}{\omega_i} \ln\left(\frac{f_i x_i}{f_i{}^s x_i{}^s}\right) + \pi_i{}^{max} \qquad (17)$$

This relationship will be the focal point for the discussion of results in the present paper. However, it should be recognized that for some systems of interest, the areas per molecule can change significantly on mixing. Explicit treatment of such changes of the molecular area on mixing can be directly incorporated into the model based on equation 16, but to do this in a fully generalized and self-consistent way will require additional modeling of the changes in molecular area as a function of the composition of the monolayer. This is beyond the scope of the present paper and is reserved for future discussion.

One interesting feature of the functional form derived here is the direct relationship of the activity coefficients and composition between the micellar and surface psuedo-phases. This allows a comparison of nonideal interactions in the micelle and monolayer as modeled by their respective net interaction parameters. In principle, this form may also allow extension to more complicated situations such as the treatment of contact angles in nonideal mixed surfactant systems. Here, the functional form derived above depends on differences in surface pressures and these may be directly obtained from experimentally measured parameters under the proper conditions (30).

Experimental Section

Measurements of surface tension versus concentration were carried
out using a tensionmeter with du Nouy ring. Critical micelle
concentrations obtained from this work were reported earlier
(14). The compounds used in this study were pure single specie
surfactants determined to be of greater than 98% purity by thin-
layer or gas chromatography. Surface tension plots for the single
components did not show evidence of surface-active impurities.
Measurements on the various binary mixtures of decyl methyl sulfox-
ide ($C_{10}MSO$), decyl dimethylphosphine oxide ($C_{10}PO$) and sodium
dodecyl sulfate (SDS) were carried out at $24^{\circ}C$ in 1 mM sodium
carbonate (pH 10). Various binary mixtures of dodecyl dimethyl-
amine oxide ($C_{12}AO$), tetraoxy-ethylene glycol monodecyl ether
($C_{10}E4$) and SDS measurements were studied at $23^{\circ}C$ in 0.5 mM
sodium carbonate (pH 9.8). The final binary mixture studied was
sodium decyl sulfate (SDeS) and decyl trimethyl ammonium bromide
($C_{10}TAB$) at $23^{\circ}C$ in 0.05 M NaBr.

Results and Discussion

Results for the various binary mixed surfactant systems are shown
in figures 1-7. Here, experimental results for the surface tension
at the cmc (points) for the mixtures are compared with calculated
results from the nonideal mixed monolayer model (solid line) and
results for the ideal model (dashed line). Calculations of the
surface tension are based on equation 17 with unit activity coeffi-
cients for the ideal case and activity coefficients determined
using the net interaction β (from the mixed micelle model) and β^{S}
(equations 12 and 13) in the nonideal case. In these calculations
the area per mole at the surface for each pure component, ω_i, is
obtained directly from the slope of the linear region in experimen-
tal surface tension data below the cmc (via equation 5) and the
maximum surface pressure, π_i^{max}, from the linear best fit of
zero slope above the cmc (with the intersection of these defining
the cmc). Also shown for comparison are the experimental mixed
critical micelle concentrations for each system together with
calculated results from the mixed micelle model (from reference
14).
     Results for the binary mixture of $C_{10}PO$ and SDS are shown in
figure 1, and good agreement with the nonideal model is seen for
both mixed cmc's and the surface tensions at the cmc. Here, the
surface tensions show the interesting feature of a sharp increase
in going from pure $C_{10}PO$, followed by a leveling off, and a
further sharp increase in going to pure SDS. This suggests that
nonideal interaction of the more surface active $C_{10}PO$ with SDS
may be causing a relative enhancement of SDS at the surface. In
figures 2 and 3, nonideal surface tension results for $C_{10}MSO$ and
SDS, and nearly ideal results for $C_{10}MSO$ and $C_{10}PO$ are indi-
cated, both showing good agreement with the model. Although the
results in figure 2 also seem to be quite close to those of the
ideal model, it should be pointed out that the calculated surface
tensions for the ideal case (dashed lines) are calculated at the
higher predicted cmc's for ideal mixing in the micelles.
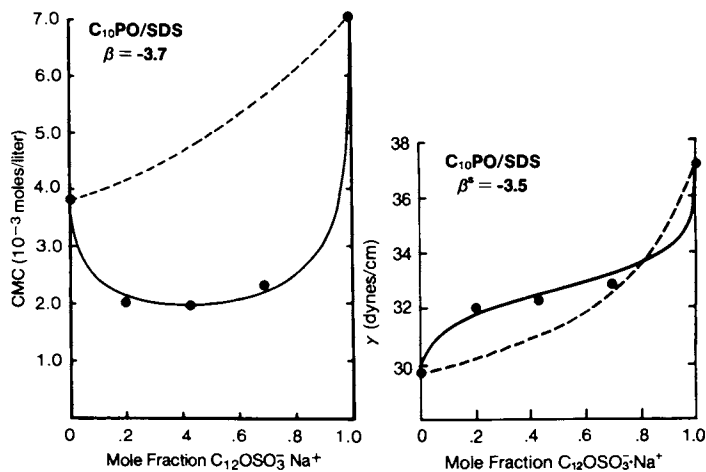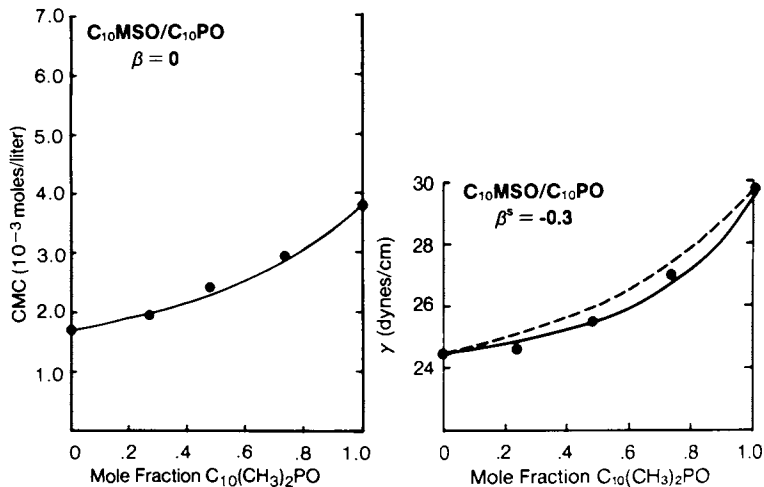
Figure 1. Mixed cmc's and surface tensions at the cmc for mix-
tures of $C_{10}PO$ and SDS in 1 mM Na_2CO_3 (at 24°C). The
plotted points are experimental results, the solid lines the
prediction of the nonideal model for β = -3.7 and β^S = -3.5
respectively, and the dashed lines the prediction for ideal
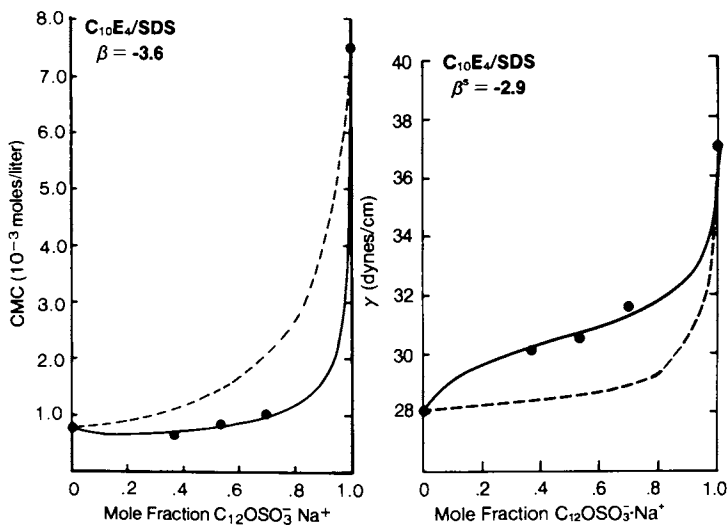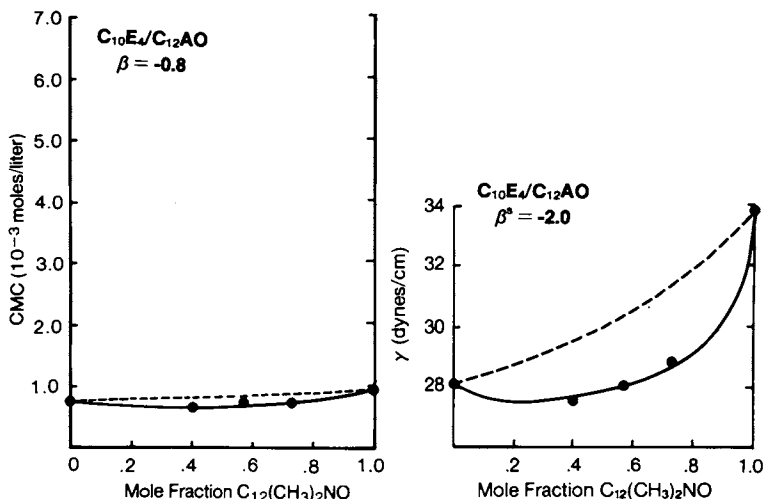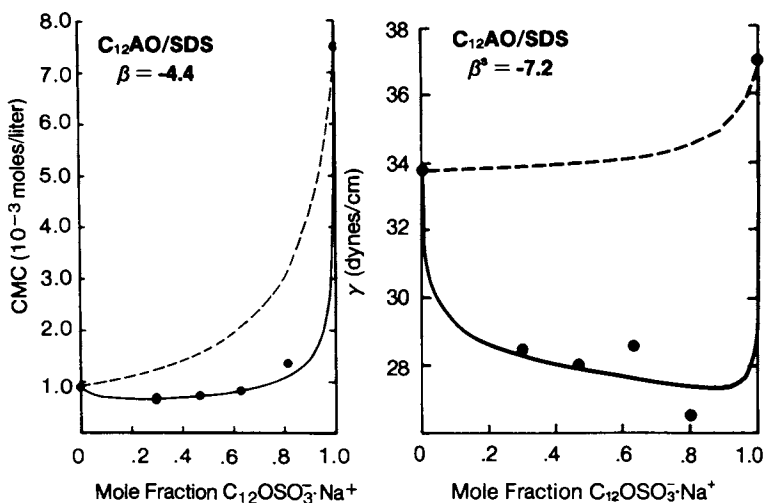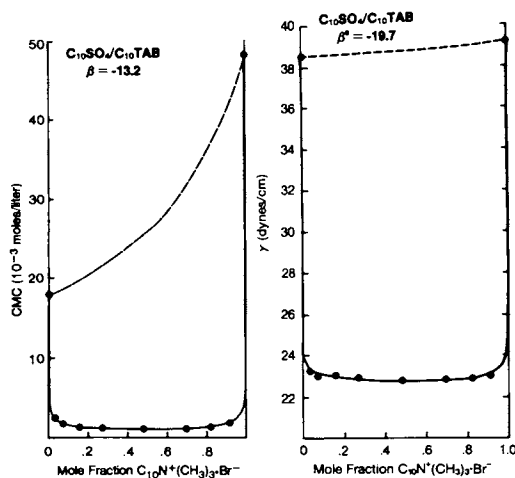mixing in the pseudo-phase.
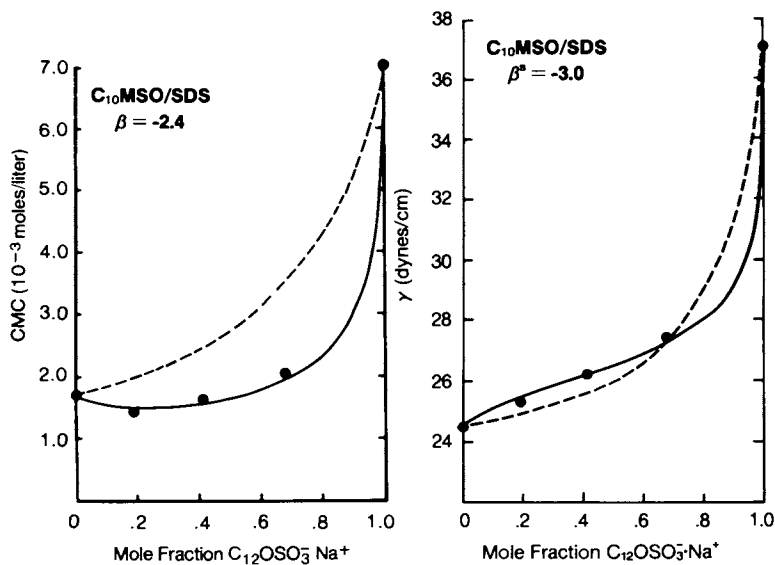
Figure 2. Mixed cmc's and surface tensions at the cmc for mix-
tures of $C_{10}MSO$ and SDS in 1 mM Na_2CO_3 (at 24°C). The
plotted points are experimental results, the solid lines the
prediction of the nonideal model for β = -2.4 and β^S = -3.0
respectively, and the dashed lines the prediction for nonideal
mixing in the pseudo-phase.

Good agreement with the model is seen in figure 4 for the binary mixture of $C_{10}E_4$ and SDS, with predicted nonideal surface tension behavior similar to that seen for $C_{10}PO$ and SDS in figure 1. The results for the mixture of $C_{10}E_4$ and $C_{12}AO$ are given in figure 5 and suggest possible synergism in the surface tension behavior for this system, which exhibits nearly ideal mixed cmc behavior. Clear evidence of such synergism is seen for the non-ideal mixture of $C_{12}AO$ and SDS in figure 6. Here, a substantially more negative net interaction parameter is calculated for the surface monolayer than for the micelles and significant surface tension lowering is observed.

The final binary mixture, which exhibits extreme deviations from ideality, is $C_{10}SO_4$ with $C_{10}TAB$. This mixed anionic-cationic system shows excellent agreement with the model over the full range of compositions, and large synergistic effects on both surface tensions and cmc. Here, the calculated net interaction parameter β^S for surface mixing (based on equation 17) is substantially more negative than the β value from mixed micellization. However, it should also be pointed out that the assumption that $\omega_i' = \omega_i$ would be expected to be substantially in error for this system. We find areas per mole in the mixed system to be in good agreement those of Corkill et. al. (31), which show the decyl-trimethylammonium decyl sulphate complex (1:1 molar mixture of these surfactants) to give an area of 58 Å^2 at the air-solution interface. This is about 70% of that for corresponding unmixed components under our conditions, indicating that a substantial change in molar area occurs on mixing. Explicitly incorporating this change in molar area into the calculation using equation 16 and an appropriate fractional adjustment to the area, results in excellent agreement for surface tensions that is virtually equivalent to the result in figure 7 but with β^S equal to -13.7. This suggests that the effects due to changes in the area per molecule on mixing (in binary systems) are empirically accounted for in the net interaction parameter for surface mixing.

Together, these results for binary surfactant mixtures demonstrate that a nonideal mixed monolayer model based on the pseudo-phase separation approach, some simplifying assumptions, and the regular solution approximation can be successfully applied to a considerable range of nonideal mixed surfactant systems. As in the cases of mixed micelles, it is interesting to note that mixtures containing ionic surfactants seem to be adequately treated even though the model neglects effects due to the binding of counter-ions. This implies that deviations due to such effects are either relatively small or can be empirically accounted for by use of the regular solution approximation. Calorimetric studies of excess heats of micellar mixing in anionic-nonionic systems show regular solution theory to fail, and suggest that the net interaction parameter of the micelle model be interpreted as an excess free energy parameter in such cases (22).

Adopting this viewpoint, the net interaction parameter for surface mixing in the present model may be seen as a useful way to account for changes in the surface free energy in nonideal mixed surfactant monolayers. Here, the parameter must not only account for the effects due to counterions, but for changes in molar surface

Figure 3. Mixed cmc's and surface tensions at the cmc for mixtures of C_{10}MSO and C_{10}PO in 1 mM Na_2CO_3 (at 24°C). The plotted points are experimental results, the solid lines the prediction of the nonideal model for $\beta = 0$ and $\beta^S = -0.3$ respectively, and the dashed lines the prediction for ideal mixing in the pseudo-phase.

Figure 4. Mixed cmc's and surface tensions at the cmc for mixtures of $C_{10}E_4$ and SDS in 0.5 mM Na_2CO_3 (at 23°C). The plotted points are experimental results, the solid lines the prediction of the nonideal model for $\beta = -3.6$ and $\beta^S = -2.9$ respectively, and the dashed lines the prediction for ideal mixing in the pseudo-phase.

Figure 5. Mixed cmc's and surface tensions at the cmc for mixtures of $C_{10}E_4$ and $C_{12}AO$ in 0.5 mM Na_2CO_3 (at 23°C). The plotted points are experimental results, the solid lines the prediction of the nonideal model for $\beta = -0.8$ and $\beta^S = -2.0$ respectively, and the dashed lines the prediction for ideal mixing in the pseudo-phase.

Figure 6. Mixed cmc's and surface tensions at the cmc for mixtures of $C_{12}AO$ and SDS in 0.5 mM Na_2CO_3 (at 23°C). The plotted points are experimental results, the solid lines the prediction of the nonideal model for $\beta = -4.4$ and $\beta^S = -7.2$ respectively, and the dashed lines the prediction for ideal mixing in the pseudo-phase.

Figure 7. Mixed cmc's and surface tensions at the cmc for mixtures of $C_{10}SO_4$ and $C_{10}TAB$ in 0.05 M NaBr (at 23°C. The plotted points are experimental results, the solid lines the prediction of the nonideal model for $\beta = -13.2$ and $\beta^S = -19.7$ respectively, and the dashed lines the prediction for ideal mixing in the pseudo-phase.

areas on mixing and for effects due to "residual" solvent at the interface. As suggested by the results for anionic-cationic systems (figure 7 and discussion), incorporating changes in molar surface areas due to mixing into the model may significantly effect the magnitude of the parameters used in the monolayer model and make them more comparible to those for the mixed micelles.

In conclusion, a generalized nonideal mixed monolayer model is presented which uses a single net interaction parameter to model nonideal interactions in binary micellar systems, and depends only on experimental information that is readily available from surface tension measurements used to obtain cmc's. The form of this simplified model is designed to allow for future generalization to multiple components, other interfaces and the treatment of contact angles.

Legend of Symbols

μ_i	chemical potential of monomeric surfactant i
μ_i^o	standard chemical potential of monomeric surfactant i
μ_i^s	chemical potential of i at surface
μ_i^{so}	standard chemical potential of i at surface
μ_i^M	chemical potential of i in mixed micelles
μ_i^{Mo}	chemical potential of i in pure micelles
c_i^m	monomer concentration of surfactant i
π_i	surface pressure of surfactant component i
π_i^{max}	surface pressure of surfactant component i above cmc in pure system
π	surface pressure in mixed system
ω_i	area per mole of surfactant i in pure system
ω_i'	area per mole of surfactant i in mixed system
γ_i	surface tension in presence of surfactant i (pure system)
γ_{H_2O}	surface tension of water
f_i^s	activity coefficient of surfactant i in mixed monolayer
f_i	activity coefficient of surfactant i in mixed micelles

x_i^s mole fraction of surfactant i in mixed monolayer

x_i mole fraction of surfactant i in mixed micelles

C_i cmc of pure surfactant i

α_i mole fraction of surfactant i in total mixed solute

C^* cmc of mixed system

β^s dimensionless net interaction parameter in mixed monolayer

β dimensionless net interaction parameter in mixed micelle

R   gas content

T   absolute temperature

Literature Cited

1. Lucassen-Reynders, E. H.; Lucassen, J.; Giles, D. J. Colloid Interface Sci. 1981., 81, 150.
2. Hua, X. Y.; Rosen, M. J. J. Colloid Interface Sci. 1982, 90, 176.
3. Rosen, M. J.; Hua, X. Y. J. AM. Oil Chemists Soc. 1982, 59, 582.
4. Rosen, M. J.: Zhu, B. Y. J. Colloid Interface Sci. 1984, 99, 427.
5. Zhu, B. Y.; Rosen, M. J. J. Colloid Interface Sci. 1984, 99, 435.
6. Rubingh, D. N.; Jones, T. Ind. Eng. Chem. Prod. Res. Dev. 1982, 21, 176.
7. Lange, H. Kolloid Z. 1953, 13, 96.
8. Shinoda, K. J. Phys. Chem. 1954, 58, 541.
9. Clint, J. J. Chem. Soc. 1975, 71, 1327.
10. Moroi, Y.; Motomura, K.; Matuura, R. J. Colloid Interface Sci. 1974, 46, 111.
11. Moroi, Y.; Nishikido N.; Matuura, R. J. Colloid Interface Sci. 1975, 50, 344.
12. Harusawa, F.; Tanaka, M. J. Phy. Chem. 1981, 85, 882.
13. Warr, G. G.; Griese, F.; Healy, T. W. J. Phys. Chem. 1983, 87, 1220.
14. Holland, P. M.; Rubingh, D. N. J. Phys. Chem. 1983, 87, 1984.
15. Moroi, Y.; Nishikido, N.; Saito, M.; Matuura, R. J. Colloid Interface Sci. 1975, 52, 356.
16. Nishikido, N. J. Colloid Interface Sci. 1977, 60, 242.
17. Rubingh, D. N., in "Solution Chemistry of Surfactants"; Vol. 1 Mittal, L., Ed.; Plenum Press: New York, 1979; p. 337.

18. Ingram, B. T. Colloid Polym. Sci. 1980, 25, 191.
19. Ingram, B. T.; Luckhurst, A. H. W., in "Surface Active Agents"; Soc. Chem. Ind.: London, 1979, p. 89.
20. Kamrath, R. F.; Franses, E. I. Ind. Eng. Chem. Fundam. 1983, 22, 230.
21. Scamehorn, J. F.; Schechter, R. S.; Wade, W. H. J. Disp. Sci. Tech. 1982, 3, 26.
22. Holland, P. M., ACS Symposium Series 1984, 253, 141.
23. Hey, M. J.; MacTaggart, J. W.; Rochester, C. H. J. Chem. Soc. Faraday Trans. 1 1985, 81, 207.
24. Holland, P. M., "Nonideal Mixed Micellar Solutions", Adv. Colloid Interface Sci. , in press.
25. Osborne-Lee, I. W.; Schechter, R. S.; Wade, W. H.; Barakat, Y., J. Colloid Interface Sci. 1985, 108, 60.
26. Hall, D. G.; Huddleston, R. W., Colloids Surfaces, 1985, 13, 209.
27. Rosen, M. J.; Hua, X. Y., J. Colloid Interface Sci. 1982, 86, 164.
28. Lucassen-Reynders, E. H. in "Anionic Surfactants;" Lucassen-Reynders, E. H., Ed.; Marcel Dekker: New York, 1981; p. 1.
29. Defay, R.; Prigogine, I.; Bellemans, A., "Surface Tension and Adsorption"; Longmans: London, 1966; p. 167.
30. Holland, P.M. Unpublished.
31. Corkill, J. M.; Goodman, J. F.; Ogden, C. P.; Tate, J. R., Proc. Royal Soc. 1963, A273, 84.

9

Monolayer Properties of Octadecyldimethylamine Oxide and Sodium Alkyl Sulfate

David L. Chang[1] and Henri L. Rosano

Department of Chemistry, City College, The City University of New York, New York, NY 10031

Monolayer properties of octadecyldimethylamine oxide alone and in combination wth sodium alkyl sulfate on aqueous substrate have been investigated. Nonionised amine oxide produces more expanded film than the ionised species; minimum film expansion and highest surface potential are obtained at half ionisation. Due to hydrogen ion competition, sodium octadecyl sulfate exhibits film expansion with increasing acidity of the substrate. Mixed films of these two compounds show marked contraction at all pH investigated. The sequence of film condensation of C_{18}amine oxide/$C_{18}SO_4Na$ association follows the order 1:1 (pH 10.9) < 1:1 (pH 2.2) < 2:1 (pH 5.5). C_{18}amine oxide/$C_{12}SO_4Na$ mixed monolayers still show film condensation at both pH 10.9 and pH 5.5, the former corresponds to an ion-dipole interaction, and the latter is an ion-ion interaction. Due to chain incompatibility, C_{18}amine oxide/$C_{12}SO_4Na$ form less tightly bound associations than C_{18}amine oxide/$C_{18}SO_4Na$. Correlation between surface and bulk properties of these two classes of compounds are discussed.

In a previous publication (1), results were presented on the micellar properties of binary mixtures of surfactant solutions consisting of alkyldimethylamine oxide (C_{12} to C_{18} alkyl chains) and sodium dodecyl sulfate. It was reported that upon mixing, striking alteration in physical properties was observed, most notably in the viscosity, surface tension, and bulk pH values. These changes were attributed to 1) formation of elongated structures, 2) protonation of amine oxide molecules, and 3) adsorption of hydronium ions on the mixed micelle surface. In addition, possible solubilisation of a less soluble 1:1 complex, form between the protonated amine oxide and the long chain sulfate was also considered.

[1] Current address: The Gillette Company, Gillette Park 6F-1, Boston, MA 02106.

In the present study, the monolayer technique is used to investigate the surface properties of octadecyldimethylamine oxide and sodium octadecyl sulfate, as single component films and in combination. The interpretation of the results provides a direct understanding of the mechanism of interaction between these two surface active agents.

Goddard and Kung (2) studied the surface characteristics of docosyldimethylamine oxide alone and in mixed films with nonadecylbenzene sulfonate. The amine oxide single component film showed large variations with the pH of the substrate, but the mixed films did not reveal evidence of pronounced interaction. However, these authors indicated that a differential thermal analysis study of the shorter chain homologs, dodecyldimethylamine oxide and sodium dodecylbenzene sulfonate, did show interaction between these components, in accord with results obtained from studies of aqueous solution containing similar materials (3). They suggested that the choice of more suitable spreading solvents, to effect more complete mixing of the components would enable the detecton of interaction between these two species.

Experimental

Octadecyldimethylamine oxide ($C_{18}DAO$) was a commercial sample from Onyx Chemical Company, Jersey City, N. J. (25% active). After evaporating the solvent in a rotary evaporator under reduced pressure, the crude product was recrystallised several times from ethyl acetate. The final product was dried and stored in vacuo over P_2O_5. Sodium octadecyl sulfate (SODS) was a sample prepared in this laboratory previously, and was recrystallised from ethanol before use. Sodium dodecyl sulfate (SDS) was obtained from Aldrich Chemical Company, and was of 98% purity. It was further purified by repeated crystallisation from ethanol followed by ether extraction. Benzene and methanol were gold-label reagent grade, purchased from Aldrich Chemical Company (Metuchen, N. J.).

The spreading solutions were prepared as follows: $C_{18}DAO$ was dissolved in 45/5, the SODS in 25/25, the SDS in 40/10, benzene/methanol mixture. The concentrations of these solutions were $1.157 \times 10^{-3}M$. For mixed monolayers, mixtures at different volume ratio were made from stock solutions prior to spreading. The aqueous substrates used were unbuffered, and the experiments were performed in the presence of atmospheric CO_2. Deionised-distilled water was used to prepare the substrate.

The experimental apparatus employed was described elsewhere (4). Briefly, surface pressures were determined continuously from surface tension measurements using a sand blasted platinum blade, suspended from a transducer-amplifier (Sandborn, model 311A). The transducer signal was fed to a X-Y recorder. Surface potential was measured with an electrometer (Keithly, model 610B) using an air electrode coated with ^{226}Ra and an Ag/AgCl electrode in the subsolution.

The surface of the subsolution was cleaned by first dusting it with Talc powder and then sweeping the surface by moving a Teflon slide from one side of the trough to the other. The Talc powder along with the impurities (if any) were then removed using

suction from an aspirator. This was done several times to make
sure no impurities remained on the surface. The monolayers were
spread evenly on the surface using an Agla microsyringe. A time
interval of three minutes was allowed for spreading solvent to
evaporate from the monolayers. Three to five monolayers of each
solution were made, and the results reported are the average sur-
face pressure for each area plotted.

Results

Single Component Systems. Surface pressure-area (π-A) and surface
potential-area (ΔV-A) isotherms of $C_{18}DAO$ on 0.01M NaCl subsolution
at various pH values are shown in Figure 1, (the NAOH/HCl was post-
added. At the highest pH investigated, viz., pH 10.9, the amine
oxide is in the nonionic form and gives rise to the most expanded
curve as well as a lower collapse pressure. Reduction in bulk pH
results in contractions of the film. At pH 2.2, protonated amine
oxide predominates and results in a less expanded curve. However,
the least expanded film is obtained at an intermediate bulk pH value,
viz., pH 5.5. The film is expected to be composed of both nonionic
and cationic forms of the amine oxide molecules at approximately a
1:1 mole ratio, as suggested by the acid-base titration behaviour of
its C_{14} homolog ($\underline{1}$). These results are in agreement with the mono-
layer properties of docosyldimethylamine oxide reported by Goddard
and Kung ($\underline{2}$); however in their case the amine oxide also shows a
phase transition from expanded to the condensed states, and that the
film condensation upon ionisation is more pronounced than in the
case of $C_{18}DAO$. The surface potentials of amine oxide films vary
strongly with the bulk pH of the substrate, and hence the cationic/
nonionic ratio of the constituent molecules in the film. With a
formal positive charge on the nitrogen in the cationic species, it
is expected that the cationic film has the highest potential. How-
ever, the mixed film of cationic and nonionic amine oxides exhibits
an even higher potential than the completely ionised film, while
the nonionic species (pH 10.9) shows the lowest potential. This
behaviour is also seen with the C_{22} homolog which show a maximum in
surface potential in the vicinity of pH 5.6 under identical experi-
mental conditions.
      In Figure 2 the π-A and ΔV-A plots for SODS on 0.01M NaCl sub-
solutions having different pH values are shown. In all cases,
phase transitions from liquid-expanded to liquid-condensed state
are evident ($\underline{5}$). Acidification of the subsolution increases the
transition pressure but the transition is less pronounced at the
lowest pH studied. This is also accompanied by an expansion of the
condensed part of the curve. Small negative surface potentials are
observed over most areas. The highest potential is obtained for
film spread on the pH 2.2 subsolution. For small areas, the sur-
face potential attains a positive value. This may be related to
reorientation of the dipole moments of the molecules which occur
once a threshold surface concentration is exceeded ($\underline{6}$). Mingins
and Pethica ($\underline{7}$) studied the monolayer properties of SODS on various
sodium chloride solutions (0.1, 0.01 and 0.001M) at 9.5°C, and they
showed that the monolayer is only stable on the more concentrated
salt solutions (0.1 and 0.01M). In this work, no noticeable
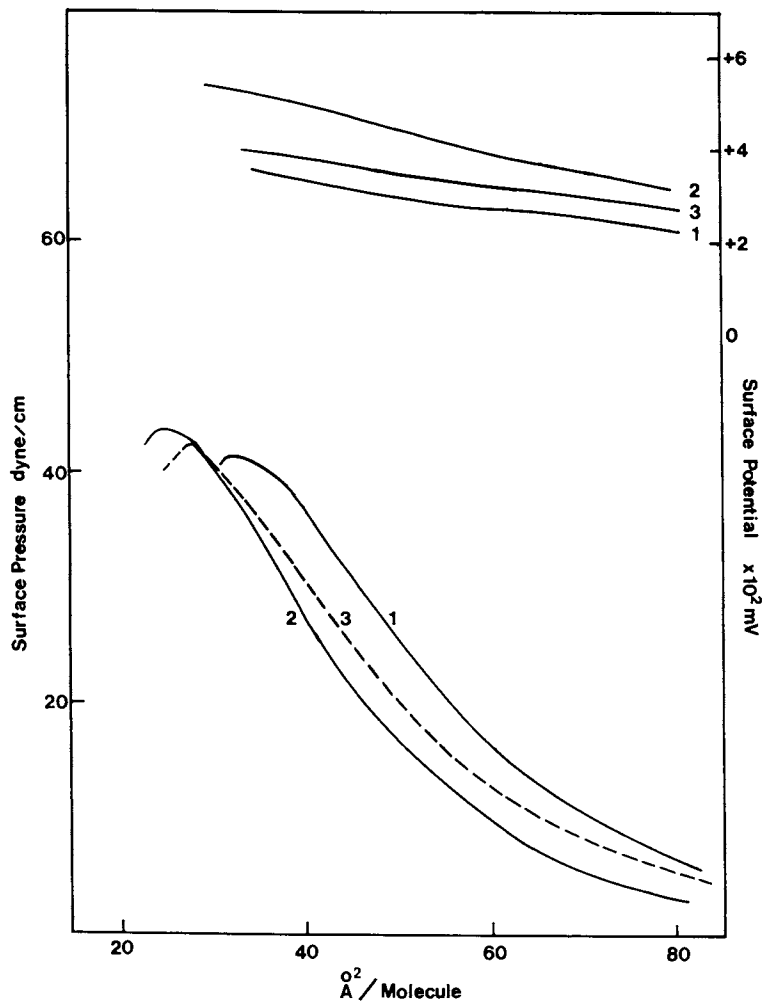
Figure 1. Effect of pH on π-A and ΔV-A isotherms of octadecyl-dimethylamine oxide (C_{18}DAO) at 25°C, 0.01M NaCl subsolutions (NaOH or HCl/NaCl). Substrate pH:1-10.9, 2-5.5, 3-2.2.
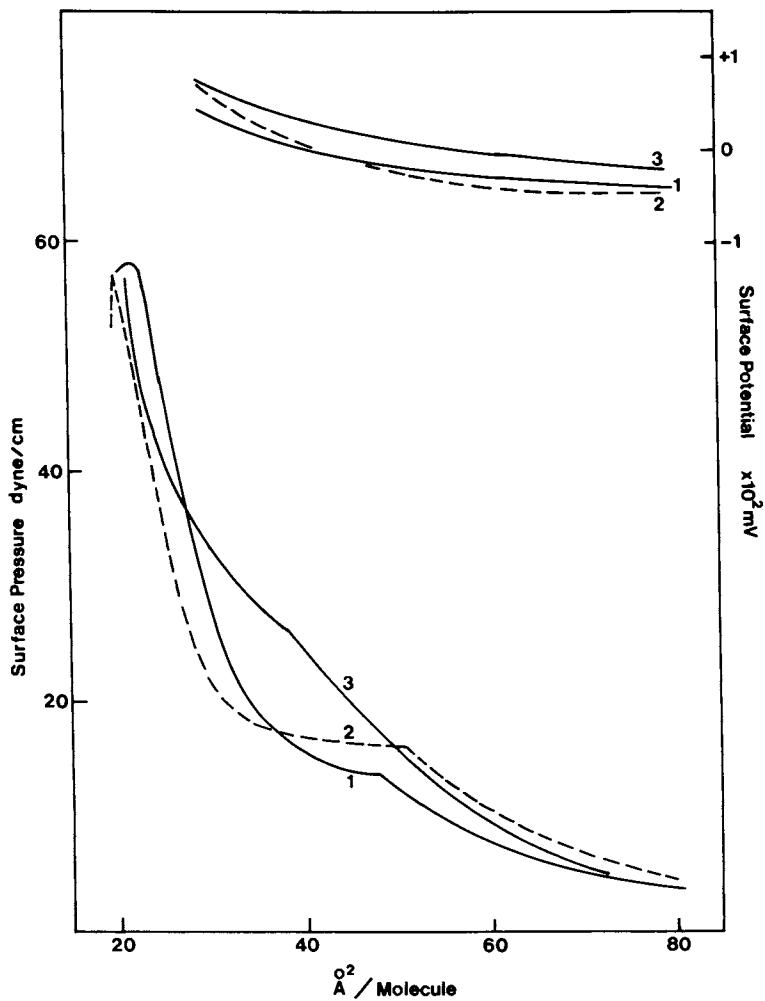
Figure 2. Effect of pH on π-A and ΔV-A isotherms of sodium octa-decyl sulfate (SODS) at 25°C, 0.01M NaCl subsolutions (NaOH or HCl/NaCl). Substrate pH: 1-10.9, 2-5.5, 3-2.2.

difference in both the π and ΔV results were observed from the
different experimental runs.

Mixed Component Systems. C_{18}DAO/SODS. These systems were examined
at three subsolution pH values, namely 10.9, 5.5, and 2.2 (0.01M
NaCl), and various compositions. The compression isotherms are
shown in Figuers 3-5, respectively, and for comparison, isotherm of
the C_{18}DAO is also plotted. At high pH value, interaction between
the two components is quite noticeable. Addition of SODS produces
a condensing effect on the film (with respect to C_{18}DAO film in all
cases, and in most cases with respect to SODS film). The phase
transition which is characteristic of the SODS curve, is still evi-
dent at all mixing ratios. Reduction in transition pressure is
observed for the mixed films with increasing SODS content up to the
equimolar mixture, which shows the lowest transition pressure,
thereafter the value increases when the amount of SODS in the film
becomes excess. In terms of the C_{18}DAO/SODS molar ratio, the 4:1
and 3:1 mixed films have higher collapse pressures than the C_{18}DAO
film, but lower than that of the SODS film. The 2:1 and 1:1 mix-
tures form solid films, and the isotherms become identical at high
pressure and small area, but the equimolar mixture shows the most
condensed film for large areas. Mixed films containing excess SODS
show the highest collapse pressures, suggesting these films are
quite stable. Surface potentials of the mixed films generally fall
between the values of those of the pure component films. However,
for small areas, mixtures containing excess amine oxide show an
even higher potential than the pure C_{18}DAO film, probably due to
closer packing of the molecules.
     Mixed monolayers on the pH 5.5 subsolution (Figure 4) show
pronounced condensation, indicating very strong interaction among
the components; these include both the cationic and nonionic forms
of amine oxide, as well as the long chain sulfate. The most con-
densed curve is observed for the 2:1 amine oxide/SODS mixture,
closely followed by the equimolar mixture, and at high pressures
the two isotherms become identical. Unlike the case at high pH
subsolution, no phase transition was detected in the present case.
Surface potentials of the mixed films fall between those of the
amine oxide and SODS at constant area. However, the 4:1 and 3:1
films have surface potential values that are slightly higher than
the pure amine oxide film at small areas.
     At the lowest pH value of the subsolution investigated, viz.,
pH 2.2, the amine oxide molecules are protonated, therefore large
interaction is expected with an anionic substance, such as the long
chain sulfate. Such an interaction is reflected in the monolayer
behaviour of the mixed film, as shown in Figure 5. The mixed films
are all more condensed than the pure component films, with the
equimolar mixture exhibiting the most condensed curve. Phase
transitions are still detected in some cases when the SODS content
is in excess, but with lower transition pressure than the SODS
single component film, and the transition pressure increases with
increasing amount of the anionic constituent. A well defined film
collapse is observed only when the amine oxide is in large excess
(4:1 and 3:1), all others become incompressible at high pressures.
The surface potentials are similar to those discussed previously.
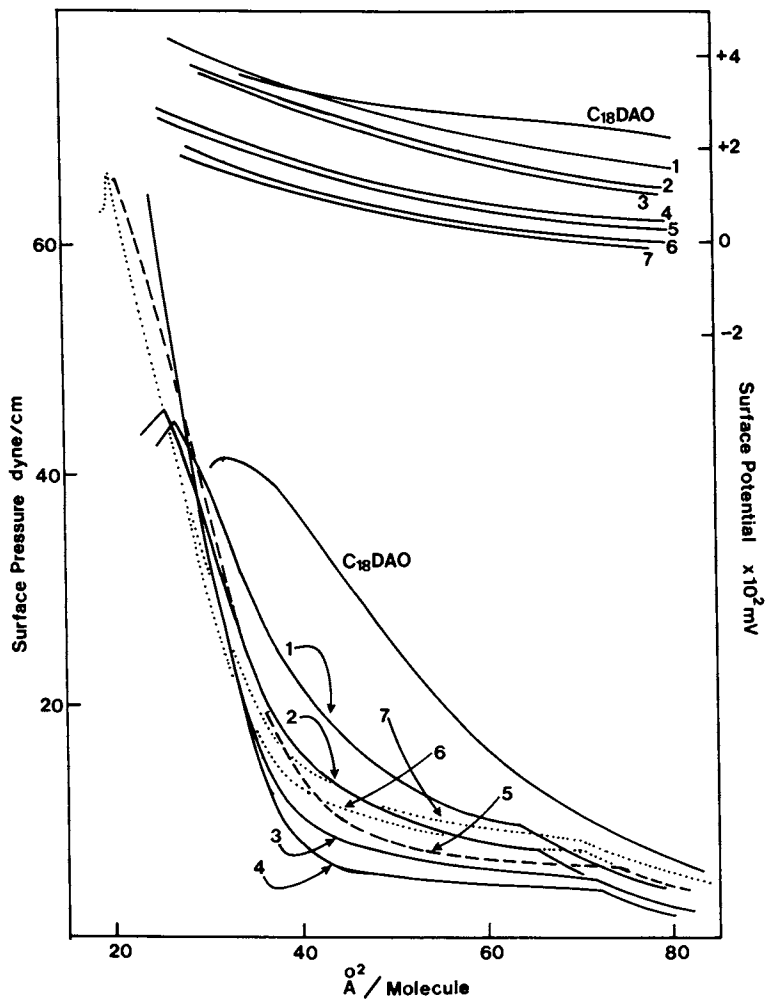
Figure 3. π–A and ΔV–A isotherms of mixed films of $C_{18}DAO$ and SODS on pH 10.9 (NaOH), 0.01M NaCl subsolution at 25°C. $C_{18}DAO$/SDS ratio: 1-4:1, 2-3:1, 4-1:1, 5-1:2, 6-1:3, 7-1:4.
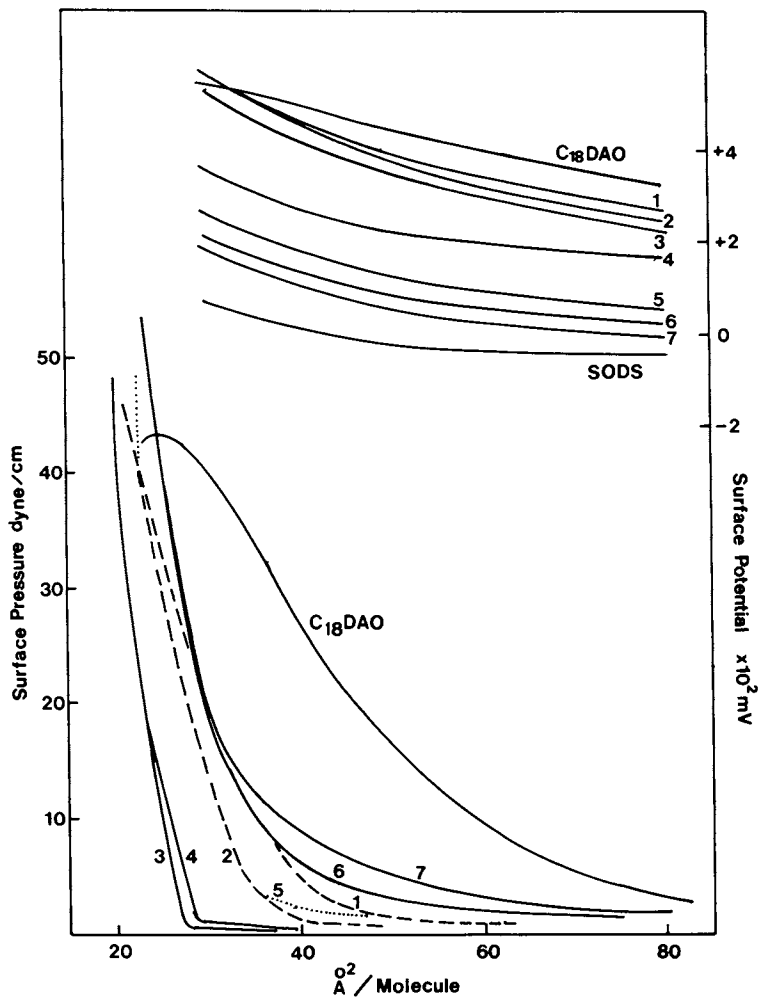
Figure 4.   π–A and ΔV–A isotherms of mixed films of C₁₈DAO and SODS on pH 5.5 (HCl), 0.01M NaCl subsolution at 25°C.   C₁₈DAO/SODS ratio: 1–4:1, 2–3:1, 3–2:1, 4–1:1, 5–1:2, 6–1:3, 7–1:4.
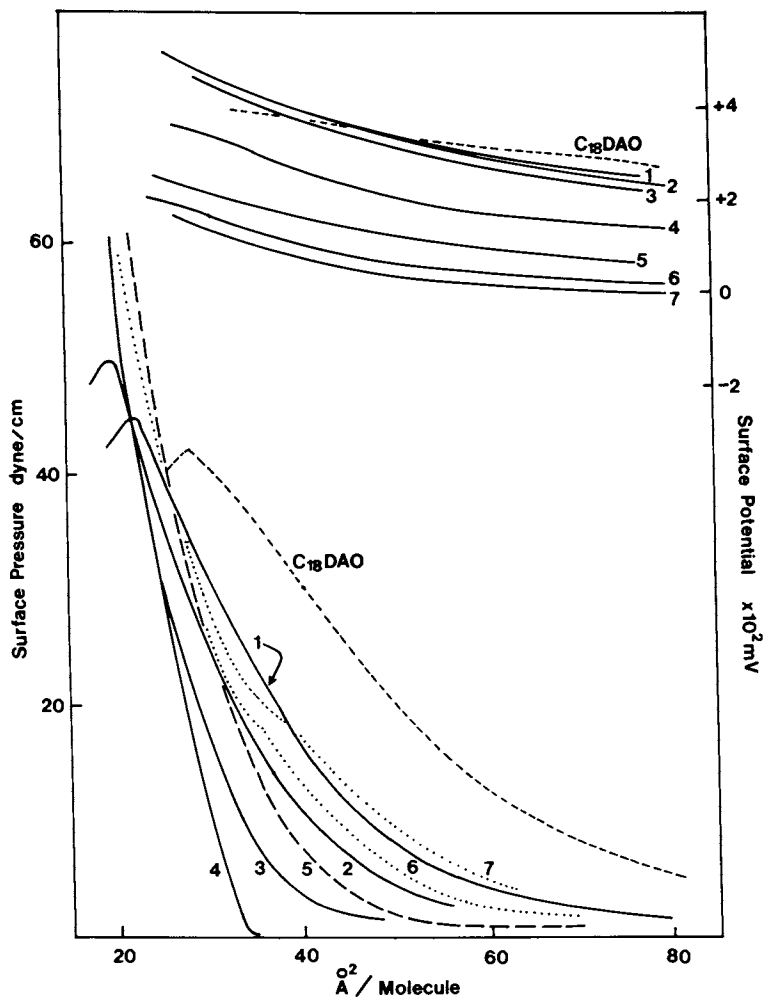
Figure 5. π–A and ΔV–A isotherms of mixed films of C_{18}DAO and SODS on pH 2.2 (HCl, 0.01M NaCl subsolution at 25°C. C_{18}DAO/SODS ratio: 1-4:1, 2-3:1, 3-2:1, 4-1:1, 5-1:2, 6-1:3, 7-1:4.

$C_{18}DAO/DSD$. Mixtures of $C_{18}DAO/SDS$ were spread on subsolutions of pH 10.9 (NaOH) and pH 5.5 (HCl), and 0.01M NaCl. Since SDS is highly soluble in water, and hence has a high desorption rate, compressions were made at a faster speed. The resulting curves were fitted such that the vertical portion of each curve corresponds to 20 $Å^2$/molecule, which approximates the limiting value of an alkyl chain, if the original curve showed a value smaller than that. Figures 6 and 7 show the fitted isotherms for pH 5.5 and pH 10.9, respectively. At low pH, it appears that the addition of SDS causes contraction of the film, and that transition in film type is evident for all mixtures. It also appears that the relative degree of film contraction increases with increasing amount of SDS in the mixed film. However, with excess SDS in the mixture, the apparent increase is probably caused by the desorption of SDS. At high pH, the mixed isotherms are similar to those obtained at low pH, except that the transition in film type is evident only when the amount of SDS is equal to or greater than the amount of amine oxide, and that there seems to be a more systematic increase in film contraction with increasing amount of SDS in the mixed film. Interaction between the two components is definite, since SDS alone did not reveal a reasonable compression pattern under the present experimental conditions.

Discussion

$C_{18}DAO$ Films. The unusual feature of alkyldimethylamine oxide is that the ionised form yields a less expanded film that the non-ionised species, contrary to the expectation that the presence of charged head groups should result in a more expanded film, due to electrical repulsion among the charges. This particular characteristic of amine oxide films has been attributed (2) to the ability of the hydroxy group in ionised amine oxide to hydrogen bond. This leads to a reduction in repulsive forces among the head groups, giving rise to the condensing effect upon ionisation. At an intermediate pH, viz., pH 5.5, the appearance of cationic species can cause the condensing effect by associating with the nonionic species, since the ionisable proton is capable of hydrogen bonding to the neighbouring oxygen thereby decreasing the average distance between adjacent head groups effectively. In the bulk solution, this effect manifests itself in an increase in the viscosity if the solution concentration is sufficiently high. From the acid-base titration studies of the C_{12} and C_{18} homologs (1), it was reported that the appearance of cationic species leads to a substantial increase in the solution viscosity, reaching a maximum value at half ionisation. This change in viscosity was explained in terms of reduction of repulsion, and the formation of elongated micelles.

The surface potential of the nonionised species is relatively high for a nonionic surfactant. This indicates that there is a strong dipole in the head group, which is the primary cause of expansion of the film. A mixture of cationic and nonionic species has an even higher surface potential value, this may be due to, at least in part, the closer packing of the molecular assembly in the film, consequent of the diminishing repulsion in the head group region.
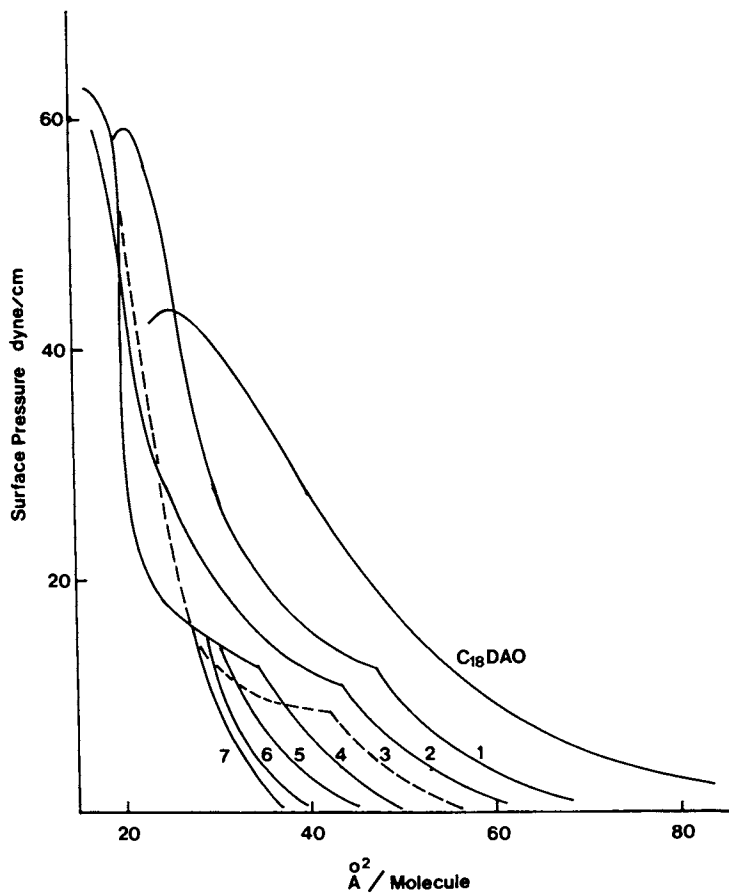
Figure 6.   π-A isotherms of mixed films of $C_{18}DAO$ and sodium dodecyl sulfate (SDS) on pH 5.5 (HCl), 0.01M NaCl subsolutions at 25°C. Each curve is fitted such that the high pressure region corresponds to $20Å^2$ if the experimental value preceded this number. $C_{18}DAO/SDS$ ratio: 1-4:1, 2-3:1, 3-2:1, 4-1:1, 5-1:2, 6-1:3, 7-1:4.
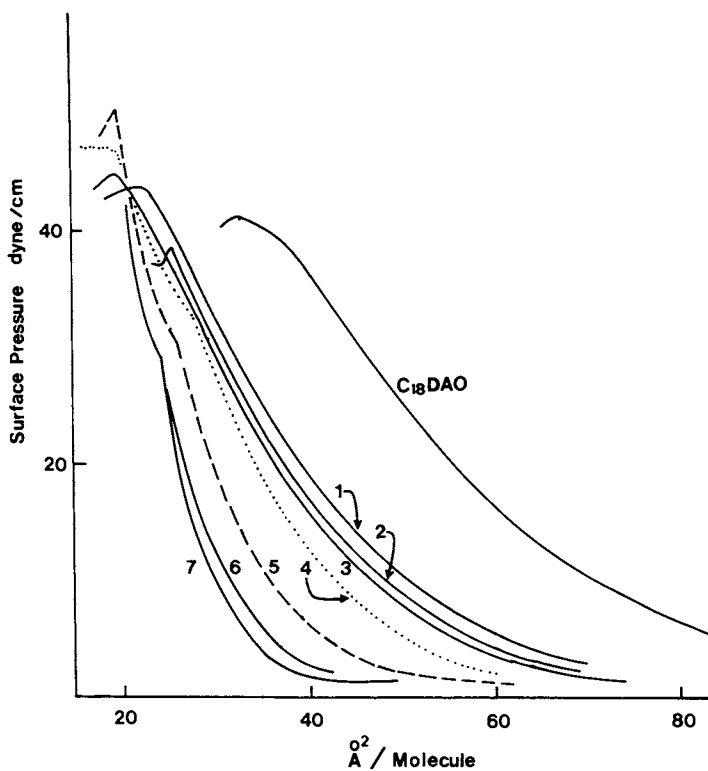
Figure 7.   π-A isotherms of mixed films of $C_{18}DAO$ and SDS on pH 10.9 (NaOH).   0.01M NaCl subsolution at 25°C.   Each curve is fitted such that the high pressure region corresponds to 20Å^2 if the experimental value precedes this number. $C_{18}DAO$/SDS ratio: 1-4:1, 2-3:1, 3-2:1, 4-1:1, 5-1:2, 6-1:3, 7-1:4.

It has been shown (8) that the cationic form of amine oxide is more soluble in water than the nonionised species, it has a higher CMC value. More importantly, a C-13 nmr study of this class of compound (8) indicated that the degree of penetration of water molecules into the micellar core increases with increasing cationic character of the micelle (up to three carbons of a fully ionised micelle), resulting in an upfield chemical shift of carbon atoms near the head group region with increasing degree of protonation of the micelle surface. The condensing effect on the monolayer upon ionisation can therefore be considered as a consequence of the increased solvation; the molecules penetrate into the bulk aqueous substrate. At an intermediate substrate pH, the protonated molecules are more soluble, therefore more are embedded in the subsolution, while the nonionised fraction remains higher in the surface in order to minimise paraffin-water interfacial area. Under these conditions, the monolayer can assume the least expanded configuration, due to possible "staggering" of the surfactant molecules, and this spatial arrangement is best seen at half ionisation. Further acidification of the aqueous substrate increases the fraction of molecules ionised, but the condensing effect due to increased solvation is offset by an increased electrical repulsion between neighbouring charged head groups, resulting in a slight expansion of the monolayer. This interpretation is most consistent with both the C-13 nmr and the monolayer results.

SODS Films. For an ionised monolayer, a relatively large surface potential is expected, negative in sign for a long chain sulfate monolayer. However, the present results show that the surface potential is small, indicating that the surface is probably not completely ionised, or that the counter ions, although dissociated, are within a very close vicinity to the plane of the negatively charged interface, as was suggested by the electromotive force determination of the apparant binding of counterions (Na^+ ions) on the sodium dodecyl sulfate micelle surface (9), and on sodium tetradecyl sulfate micelle surface from an electrochemical study (10).

The expansion of the film with increasing acidity of the substrate may be due to the competition of counterions at the interface. The swamping amount of H^+ ions in low pH subsolution competes with Na^+ ions at the negatively charged interface. Such competition has been shown to exist between H^+ ions and K^+ ions at the negatively charged micelle-solution interface (11). Studies on the counterion effects in sodium docosyl sulfate monolayers (6,12) have shown that the film expansion follows the sequence $Li^+ > Na^+ > K^+$. It follows that H^+ should give rise to the most expanded film.

Mixed Films. Isotherm data from two-component monolayers are frequently represented by plotting the mean molecular area as a function of film composition at constant surface pressure. A linear relationship is usually obtained when the two components are immiscible or when they form an ideal two-dimensional solution. For miscible components, deviations from ideality result in a nonlinearity in the plot. Positive deviations indicate an increase in the area occupied by either one or both components, probably due to

a more repulsive interaction in nature, whereas negative deviations
are indicative of condensation. Figure 8 represents such a plot
for the system $C_{18}DAO/SDS$ studied on the pH 5.5 subsolution.
Clearly these two components interact favourably so as to produce
condensation of relatively large magnitude. Mixtures studied at
pH 10.9 and pH 2.2 exhibit the same features. At least two factors
are involved in the process: 1) chain length compatibility and 2)
head group interaction. The former is responsible for the hydro-
phobic interaction between the chains: compatibile chains result
in maximum cohesive interactions between the alkyl groups while
incompatible chains have a disruptive effect on the packing of
molecules in the monolayer. Shibata et al. (13) have shown that
the most pronounced condensing effect is usually observed when the
two components have equal chain length, for a fixed total number of
carbon atoms. This compatibility is important in determining the
properties of mixed micellar solutions (1), and in the formation of
microemulsion systems (14-16).
     The second factor, namely the head group interaction, can also
influence the surface properties of mixed surfactant markedly. In
particular, anionic/cationic surfactant mixtures exhibit the
largest effect (17,18). In nonionic/anionic surfactant mixtures,
synergistic effects can still take place to a significant extent,
as revealed in Figure 3 (pH 10.9, nonionic amine oxide with
anionic long chain sulfate), since insertion of nonionic surfactant
molecules into an ionic surfactant molecular assembly minimises
electrostatic repulsion (19).
     Except in a very acidic medium in which the amine oxide mole-
cules are protonated by the excess protons already present in the
bulk solution, it is also possible that the strong interactions
between these two species is a reflexion of an induced acid-base
equilibrium shift of the amine oxide in the aqueous medium, brought
about by the addition of long chain sulfate. As is known from the
Gouy-Chapman theory (20,21), a diffuse layer of counter-cations
builds up and anion depletion is established near a negatively
charged surface. One additional consequence of this negative sur-
face potential is the accumulation of protons at the surface and
hence the surface pH is lower than the bulk value. The presence of
a long chain sulfate in an amine oxide molecular assembly can
therefore significantly modify the acid-base equilibrium state of
amine oxide; production of the protonated species is enhanced.
This interpretation is confirmed by the solution behaviour of
$C_{18}DAO/SDS$ mixtures. Solutions of these two components have been
shown to be turbid and birefringent, and the addition of SDS to
$C_{18}DAO$ results in the production of filament-like structures and an
increase in the bulk pH value, suggesting the formation of a new
species between protonated $C_{18}DAO$ and SDS, which is also respon-
sible for the surface tension lowering (1). The increase in bulk
pH value is then a consequence of the consumption of hydrogen ions
in the production of cationic amine oxide, and the protonated amine
oxide and the long chain sulfate precipitate out stoichiometrically.
     Mixtures of compatible chain systems, viz., $C_{12}DAO/SDS$ and
$C_{14}DAO/SDS$, lead to the formation of mixed micelles which is also
accompanied by an increase in the pH of the solution. However, the
increase in pH in these two cases may not be caused by the protona-
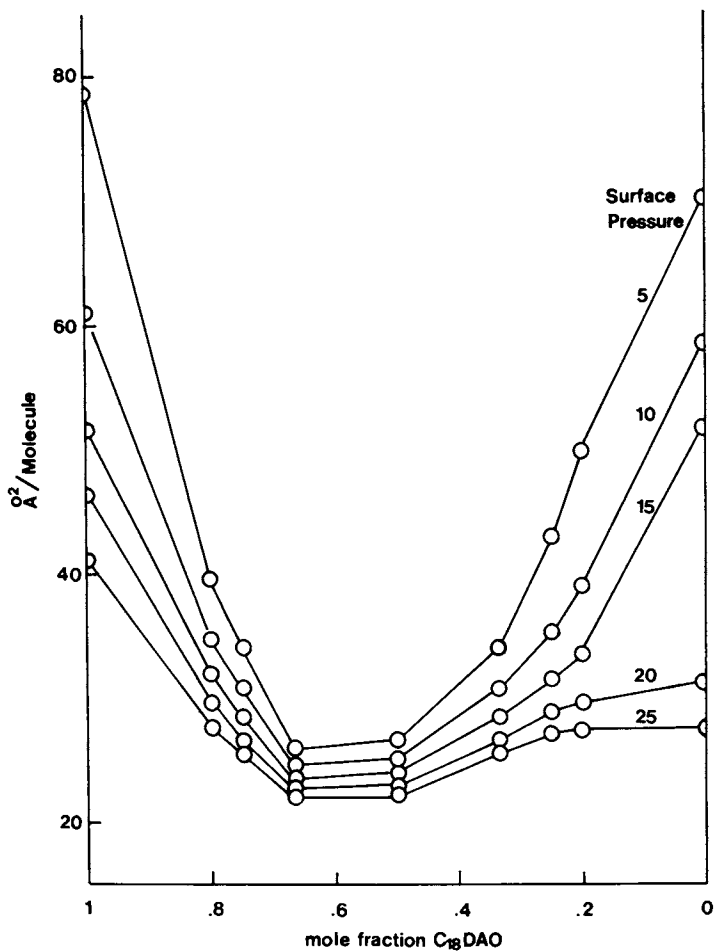
Figure 8. Mean molecular area vs. composition plots for $C_{18}DAO/SDS$ mixed films spread on 0.01M NaCl, pH 5.5 (HCl) subsolution at 25°C.

tion process. Protonation in its usual sense implies an actual
bond formation. If the amine oxide molecules are protonated, then
an ion-ion interaction with the sulfate will be reflected in the
bulk by the formation of an insoluble 1:1 double long chain salt;
the absence of precipitation would then be indicative of the ab-
sence of any substantial ion-ion interaction. In the cases of
C_{12}DAO/SDS and C_{14}DAO/SDS mixtures, since no precipitation occurs
for all mixing ratios investigated, the observed increase in bulk
pH is probably due to the adsorption of H_3O^+ ions on the micelle
surface, rather than actual protonation of amine oxide molecules,
only when there are sufficient protons available, such as with the
addition of an acid, will protonation of the amine oxide and the
formation of the double chain complex take place. This alternative
interpretation of the increased pH value has been considered pre-
viously. Therefore it is proposed that there are two different
mechanisms, both of which are needed in order to explain the inter-
actions between alkyldimethylamine oxide and alkyl sulfate satis-
factorily. When the alkyl chains match in length, paraffin-
paraffin interaction is maximised, the formation of mixed micelle
is favoured and is accompanied by the adsorption of hydronium ions
on the surface. When the alkyl chains do not match, head group
interaction predominates, and protonation of amine oxide is
favoured, resulting in the formation of a 1:1 insoluble complex.

Goddard and Kung (2) have investigated the mixed monolayer
properties of docosyldimethylaminde oxide and nonadecyl benzene
sulfonate under conditions identical to this study. The mean mole-
cular area versus composition plots show small positive deviations
from ideality, and the π-A curves of the mixed films are of similar
shape. This is probably due to the presence of benzene ring in the
chain; the bulky group has a negative steric effect on the packing
of the alkyl chains. Nevertheless, favourable interactions can
still be expected. Kolp et al. (3) have investigated the solution
behaviours of the shorter chain homologs, dodecyldimethylamine
oxide and dodecylbenzene sulfonate. They found that the protonated
amine oxide molecules and the long chain sulfonate precipitate
metathetically. Removal of the bulky group optimises the packing of
the chains, and can produce synergistic effects. Another study has
confirmed (22) that mixtures of dodecyldimethylamine oxide and
sodium dodecane sulfonate show very pronounced surface tension
lowering upon mixing, and that precipitation occurs only in dilute
solutions. Hence the expected but not detected interaction between
C_{22} amine oxide and nonadecyl benzene sulfonate is probably a
steric effect due to the presence of a bulky group in the mixed
molecular assembly.

Acknowledgments

Literature Cited

1.   Chang, D. L., and Rosano, H. L., In "Structure/Performance
     Relationships in Surfactants"; ACS SYMPOSIUM SERIES No. 253,
     American Chemical Society: Washington, D.C., 1984; p. 129-140.

2. Goddard, E. D., and Kung, H. C. J. Colloid Interface Sci.
    1973, 43, 511-520.
3. Kolp, D. G., Laughlin, R. G, Krause, F. P., and Zimmerer,
    R. E. J. Phys. Chem. 1963, 67, 51-55.
4. Christodoulou, A. P., and Rosano, H. L., In "Molecular Associ-
    ation in Biological and Related Systems"; ADVANCES IN
    CHEMISTRY SERIES No. 84, American Chemical Society: Washington,
    D.C., 1968 p. 210-234.
5. Corkill, J. M., Goodman, J. F., Harrold, S. P., and Tate,
    J. R. Trans. Faraday Soc. 1967, 63 247-256.
6. Hendrix, Y., and Mari, D. J. Colloid Interface Sci. 1980,
    78, 74-86.
7. Mingins, J., and Pethica, B. A. Trans. Faraday Soc. 1963, 59,
    1892-1905.
8. Chang, D. L., Rosano, H. L., and Woodward, A. E., accepted
    for pubication. J. Colloid Interface Sci.
9. Feinstein, M. E., and Rosano, H. L. J. Colloid Interface Sci.
    1967, 24, 73-79.
10. Hall, D. G., and Price, T. J. J. Chem. Soc. Faraday Trans. I
    1984, 80, 1193-1199.
11. Rosano, H. L., Christodoulou, A. P., and Feinstein, M. E.
    J. Colloid Interface Sci. 1969, 29, 335-344.
12. Goddard, E. D., Kao, O., and Kung, H. C. J. Colloid Inter-
    face Sci. 1968, 27, 616-624.
13. Shibata, O., Kaneshina, S., and Nakamura, M. J. Colloid
    Interface Sci. 1980, 77, 182-188.
14. Tadros, T. F. in Ref (1), p. 153.
15. Stilbs, P., Rapacki, K., and Lindman, B. J. Colloid Interface
    Sci. 1983, 95, 583-585.
16. Birdi, K. S. Colloid Polymer Sci. 1982, 260, 628-631.
17. Hua, X. Y., and Rosen, M. J. J. Colloid Interface Sci. 1982,
    92, 212-219.
18. Lucassen-Reynders, E. H., Lucassen, J., and Giles, D.
    J. Colloid Interface Sci. 1982, 81, 150-157.
19. Moroi, Y., Nishikido, N., Saito, M., and Matuura, R.
    J. Colloid Interface Sci. 1975, 52, 356-363.
20. Verwey, E. J. W., and Overbeek, J. Th. G. "Theory of the
    Stability of Lytropic Colloids", Elsevier, Amsterdam, 1948.
21. Davis, J. T., and Rideal, E. K. "Interfacial Phenomena",
    Academic Press, New York, 1961.
22. Rosen, M. J., Friedman, D., and Gross, M. J. Phys. Chem.
    1964, 11, 3219-3225.

The Penetration of Monolayers by Surfactants

D. M. Alexander, G. T. Barnes, M. A. McGregor, and K. Walker

Department of Chemistry, University of Queensland, Brisbane, Australia

When a surfactant is injected into the liquid beneath
an insoluble monolayer, surfactant molecules may
adsorb at the surface, penetrating between the
monolayer molecules. However it is difficult to
determine the extent of this penetration. In
principle, equilibrium penetration is described by the
Gibbs equation, but the practical application of this
equation is complicated by the need to evaluate the
dependence of the activity of monolayer substance on
surface pressure. There have been several approaches
to this problem. In this paper, previously published
surface pressure-area isotherms for cholesterol
monolayers on solutions of hexadecyl-trimethyl-
ammonium bromide have been analysed by three
different methods and the results compared. For this
system there is no significant difference between the
adsorption calculated by the equation of Pethica and
that from the procedure of Alexander and Barnes,
but analysis by the method of Motomura, et al. gives
results which differ considerably. These differences
indicate that an independent experimental measurement
of the adsorption should be capable of discriminating
between the Motomura method and the other two.

If a surfactant is injected into the liquid beneath an insoluble
monolayer, there are often marked changes in the properties of the
monolayer. These changes are usually attributable to the
penetration or adsorption of surfactant between the monolayer
molecules. Early experiments, beginning with Schulman and Hughes
(1), concentrated on the kinetics of penetration, and
interpretations ranged from the formation of stoichiometric
complexes between monolayer and surfactant (2-3) to simple space-
filling models (4). However in recent years there has been a
recognition (5) that equilibrium measurements are essential to a
proper understanding of the phenomena.

In such an equilibrium study the surfactant is injected beneath a monolayer (6), the surface is compressed in stages with equilibrium being established at each step, and the equilibrium surface pressure-area isotherm is established. In this way, isotherms for a range of surfactant concentrations are produced.

For interpreting these data, and as a first step towards formulating a model for monolayer penetration, it is clearly desirable to calculate the amount of surfactant that has penetrated the monolayer. This has proved to be a difficult theoretical problem, but in recent years some limited solutions and a general solution have been found. In this paper we examine data for the penetration of cholesterol monolayers by hexadecyl-trimethyl-ammonium bromide (CTAB) (7) and compare the penetration or adsorption values calculated from the different treatments.

Theory

In principle, the penetration or adsorption of surfactant, Γ_S is given by the Gibbs equation. For a non-ionic monolayer and an ionised surfactant (as in the system examined), this equation is:

$$d\Pi/RT = \Gamma_M d \ln \lambda_M + \Gamma_S d \ln \lambda_S + \Gamma_C d \ln \lambda_C \tag{1}$$

where subscripts M, S, C refer to monolayer molecules, surfactant ions and counter-ions respectively.

For the very dilute solutions usually encountered in penetration studies, it is reasonable to put

$$\lambda_S = m_S \tag{2}$$

and if there is no added electrolyte and no surface hydrolysis,

$$\lambda_C = \lambda_S = m_S \tag{3}$$

and

$$\Gamma_S = \Gamma_C \tag{4}$$

Also by definition,

$$\Gamma_M = 1/\hat{A}_M \tag{5}$$

Equation 1 then yields the expression:

$$\Gamma_S = \frac{1}{2RT}\left(1 - \frac{RT}{\hat{A}_M}\left(\frac{\partial \ln \lambda_M}{\partial \Pi}\right)_{A,n_M}\right)\left(\frac{\partial \Pi}{\partial \ln m_S}\right)_{A,n_M} \tag{6}$$

In the usual experimental situation all quantities on the right of this equation are known or measurable except for the dependence of λ_M on surface pressure. There have been several attempts to resolve this difficulty.

Pethica (5) put

$$RT(\partial \ln \lambda_M/\partial \Pi)_{A,n_M} = \bar{A}'_M \tag{7}$$

which he called the partial molar area of M, and assumed that for a chosen surface pressure,

$$\bar{A}'_M = \hat{A}^\bullet_M \tag{8}$$

the area per molecule of the pure M monolayer. His equation is, therefore,

$$\Gamma_S = \frac{1}{2RT}\left(\frac{\hat{A}_M - \hat{A}^\bullet_M}{\bar{A}_M}\right)\left(\frac{\partial \Pi}{\partial \ln m_S}\right)_{A,n_M} \tag{9}$$

and all quantities on the right can be determined.

Later, Alexander and Barnes (8) showed that the constant conditions of equation 7 are not those required for the partial molar area. This is given by:

$$\bar{A}_M = RT(\partial \ln \lambda_M/\partial \Pi)_{n^\sigma_M,n^\sigma_S} \tag{10}$$

As a consequence equation 9 can only be used in the region of saturation adsorption or in certain special circumstances.

They derived a general equation which, however, requires the use of several approximations if Γ_S is to be calculated from experimental data. In addition to the usual assumptions (equations 2-4), they put (after Pethica)

$$\bar{A}_M = \hat{A}^\bullet_M \tag{11}$$

and

$$n^\sigma_S \ll n^\sigma_M \tag{12}$$

and derived the equation:

$$\left(\frac{\partial \Pi}{\partial \ln m_S}\right)_{A,n^\sigma_M} = \frac{2RT}{\bar{A}_S}\left(1 - \frac{2RT\hat{A}_M(\partial \hat{A}^\bullet_M/\partial \Pi)_{n^\sigma_S,n^\sigma_M}}{(\hat{A}_M - \hat{A}^\bullet_M)\hat{A}^\bullet_M(\hat{A}_M - \hat{A}^\bullet_M + \bar{A}_S)}\right)^{-1} \tag{13}$$

This equation can be solved for $\bar{A}_S$ which in turn yields the adsorption:

$$\Gamma_S = (\hat{A}_M - \hat{A}^\bullet_M)/\hat{A}_M\bar{A}_S \tag{14}$$

It should be noted that in both of these approaches it is necessary to make an assumption about the partial molar area of monolayer (equation 8 or 11).

Finally, Motomura *et al.* (9) derived an expression which, with equations 3 and 4, becomes

$$\Gamma_S = \Gamma_S^O - (m_S/2RT\hat{A}_M) \int_{\hat{A}_M}^{\infty} (\partial\Delta\Pi/\partial m_S)_{T,P,A} d\hat{A}_M \qquad (15)$$

All quantities on the right can be determined and no assumption about the partial molar area of M is necessary.

Results

Numerical data are available from our earlier penetration work for a number of monolayer/surfactant systems. The simplest of these systems was selected for this initial analysis: the penetration of cholesterol monolayers by hexadecyl-trimethyl-ammonium bromide (CTAB) (7). Cholesterol monolayers at 298 K exhibit a single, highly incompressible, condensed phase with the transition to a gaseous phase occurring at a negligibly low surface pressure. CTAB does not appear to undergo surface hydrolysis (10) and the gaseous-to-expanded phase transition occurs at a low concentration (0.043 mmol kg^{-1}) and a low surface pressure (1.0 mN m^{-1}).

Adsorption values calculated for this system by the three procedures described above are shown in Figures 1-4.

The values calculated by the procedure of Alexander and Barnes (equations 13 and 14) are indistinguishable from those obtained from the Pethica equation (equation 9). In contrast, markedly different values were obtained by the Motomura analysis (equation 15).

All three methods rely on the accurate determination of the slopes of curves. This is a major source of error when there is some scatter in the data, as there is in this case. However, it is not sufficient to explain the differences between the Motomura analyses on the one hand and the adsorptions calculated by the other two methods.

Discussion

For this system, and over the experimental range studied, the adsorption values calculated by the Pethica equation are very similar to those obtained by the procedure of Alexander and Barnes. Unfortunately there are insufficient data to permit analysis in those regions where the two procedures might be expected to yield different results.

When the curves in Figure 1 are compared with the curve for the monolayer-free system ($\hat{A}_M = \infty$) major differences are apparent. At low surfactant concentrations the adsorptions in the presence of monolayer often exceed the values for the monolayer-free system. Part of this effect might be attributable to the scatter in the original experimental data, but even when the most favourable interpretation is taken, the effect is not removed entirely. Thus these calculations suggest that the monolayer can enhance the adsorption of surfactant.

This does not happen with the analysis by the Motomura method. Equation 15 shows that the integral term is used as a correction to the monolayer-free adsorption Γ_S^O. To give an enhancement, the
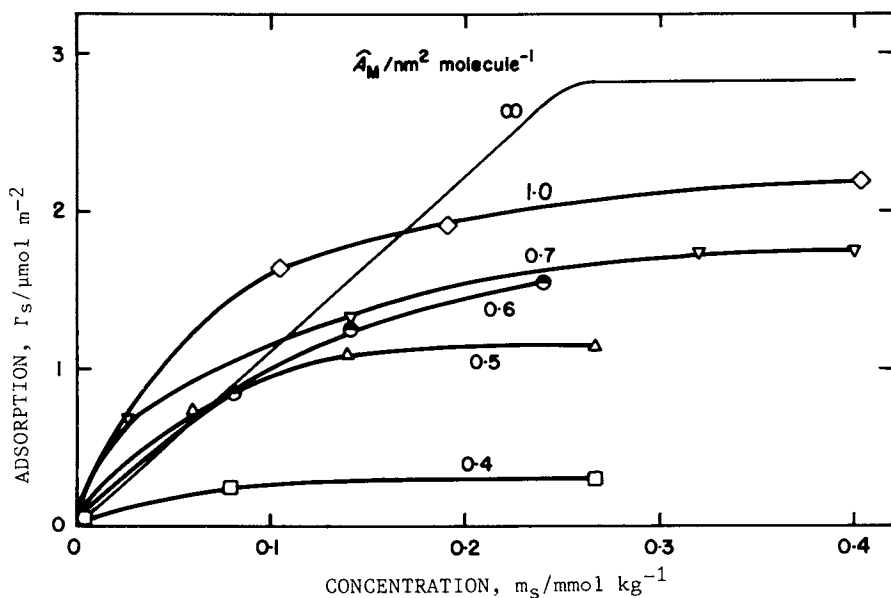
FIG. 1. Penetration of cholesterol monolayers by CTAB calculated by the equation of Pethica and the procedure of Alexander and Barnes.
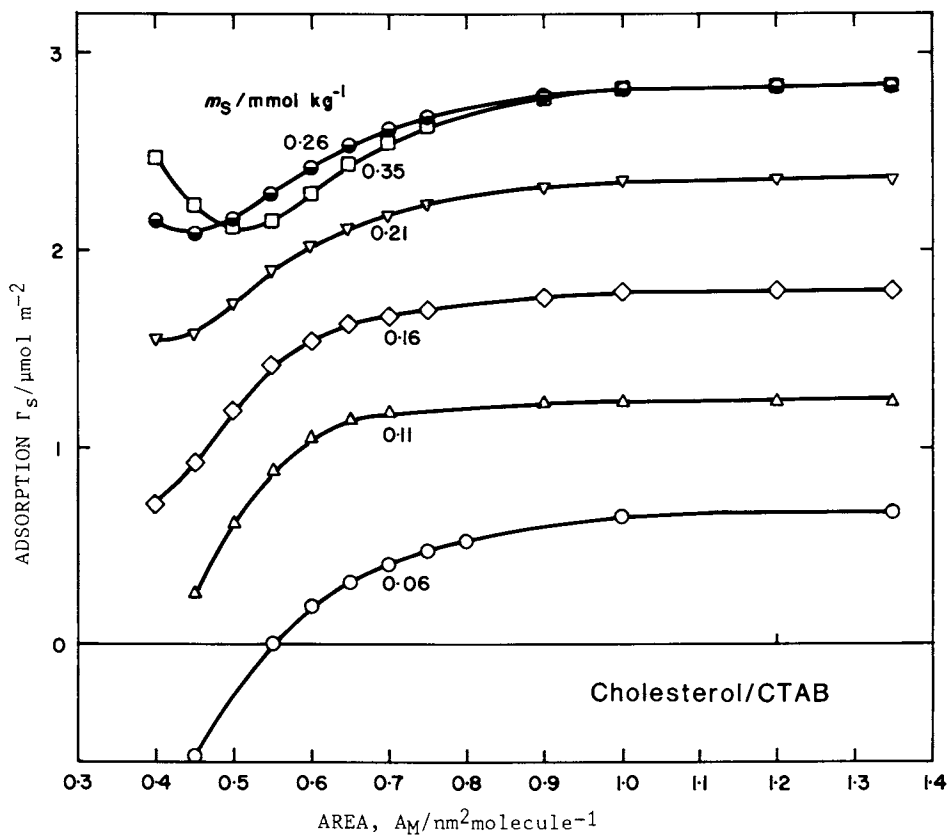
FIG. 2. Penetration of cholesterol monolayers by CTAB calculated by
the procedure of Motomura *et al.*
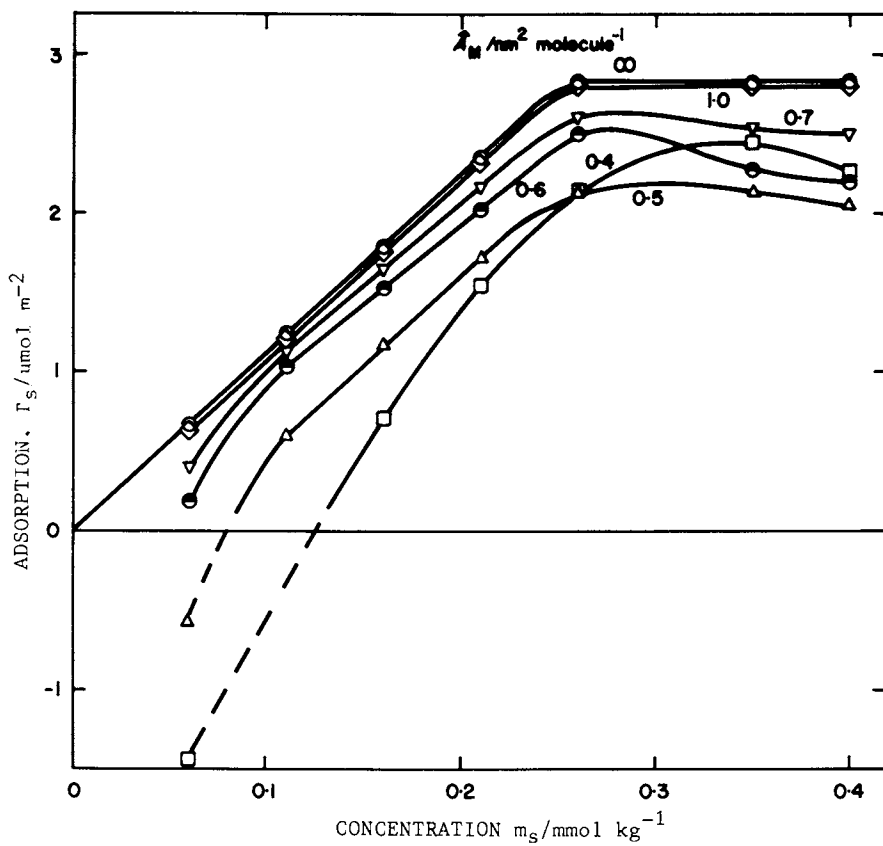
FIG. 3. Penetration of cholesterol monolayers by CTAB calculated by
the procedure of Motomura *et al.*
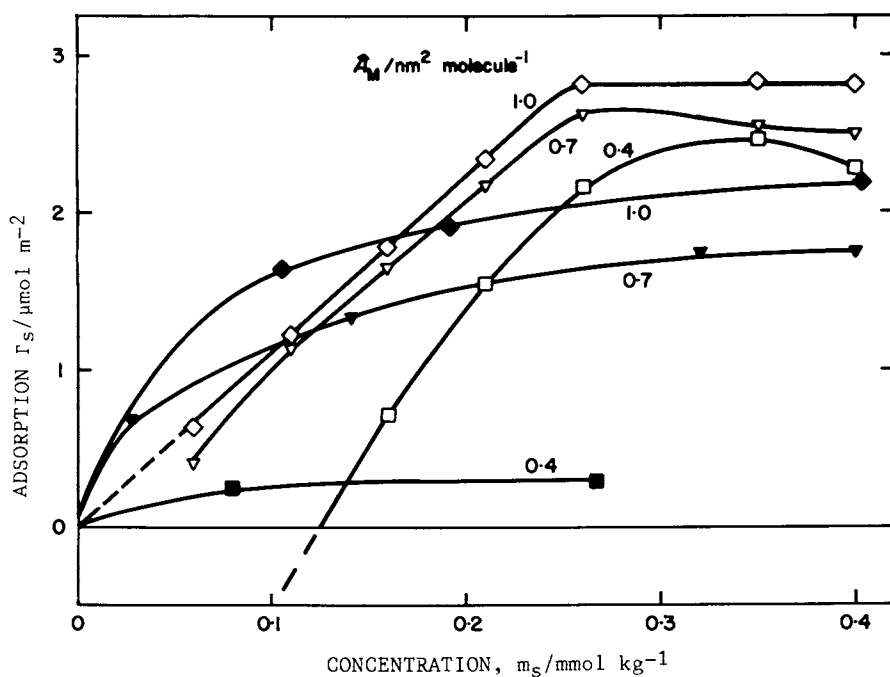
FIG. 4. Comparison of different procedures for calculating the
penetration of cholesterol monolayers by CTAB: closed points,
Pethica and Alexander and Barnes; open points, Motomura *et al.*

integral would have to be negative which would in turn require negative slopes $(\partial \Delta\Pi/\partial m_S)$. This system does give negative slopes, but only at low $\hat{A}_M$, and the integrals nevertheless remain positive.

At high surfactant concentrations the surface pressure – area curves tend towards the surface pressures of the pure surfactant $(\Delta\Pi \to 0)$. Thus the integrals in equation 15 appear to be zero for $\hat{A}_M > 1.4$ nm^2 molecule^{-1} and the adsorptions are then equal to the adsorptions for the monolayer-free system. In contrast, the Pethica equation at this area still imposes a significant correction factor on the adsorption: the slope $(\partial\Pi/\partial \ln m_S)$ for $\hat{A}_M = 1.4$ nm^2 molecule^{-1} equals that for the monolayer-free system but $(\hat{A}_M - \hat{A}_M^{\bullet})/ \hat{A}_M \cong 0.7$.

The Motomura analysis in Figure 2 shows the effects of monolayer compression. As expected, compression causes some ejection of surfactant, particularly at low surfactant concentrations. There even appears to be negative adsorption at 0.6 mmol kg^{-1}, but while this result is plausible in a qualitative sense, the depth from which surfactant would need to be excluded is unacceptably great.

Conclusions

The adsorption values calculated by the method of Motomura *et al.* differ appreciably from those calculated by the procedures of Pethica and of Alexander and Barnes. Discrimination between these theories should therefore be possible by measuring the adsorptions by an independent experimental method, such as through the use of radio-labelled surfactants (11–12).

The Motomura equation is apparently derived without extra-thermodynamic assumptions, but the other approaches, through the necessary approximations, are based on models for the system. Independent adsorption measurements could reveal any deficiencies in these models and suggest refinements.

Acknowledgments

Legend of Symbols

A = area

$\hat{A}_M$ = area per mole (or molecule) of M

$\hat{A}_M^{\bullet}$ = area per mole (or molecule) of M without surfactant present

$\bar{A}_i$ = partial molar area of i

m_S = molality of surfactant

n_i, n_i^{σ} = amount of i adsorbed

P = pressure

R =   gas constant

T =   temperature

γ =   surface tension

Γ_i =   adsorption of i

Γ_i^o =   adsorption of i without monolayer

λ_i =   absolute activity of i

Π =   surface pressure = $\gamma_{water} - \gamma_{film}$

$\Delta\Pi$ = $\Pi - \Pi_S^o$

Subscripts

M, monolayer molecules

S, surfactant ions

C, counter-ions

Literature Cited

1. Schulman, J.H.; Hughes, A.H. Biochem. J. 1935, 29, 1243.
2. Schulman, J.H.; Rideal, E.K. Proc. Roy. Soc. (London) B 1937, 122, 29.
3. Goddard, E.D.; Schulman, J.H. J.Colloid Sci. 1953, 8, 329.
4. Dervichian, D.G. In "Surface Phenomena in Chemistry and Biology"; J.F. Danielli; K.G.A. Pankhurst; A.C. Riddiford, Eds.; Pergamon: New York, 1958; p.80.
5. Pethica, B.A. Trans. Faraday Soc.1955, 51, 1402.
6. McGregor, M.A.; Barnes, G.T. J. Colloid Interface Sci. 1977, 60, 408.
7. McGregor, M.A.; Barnes, G.T. J. Pharm. Sci. 1978, 67, 1054.
8. Alexander, D.M.; Barnes, G.T. J. Chem. Soc. Faraday I 1980, 76, 118.
9. Motomura, K.; Hayami, Y.; Aratono, M.; Matuura, R. J.Colloid Interface Sci. 1982, 87, 333.
10. McGregor, M.A.; Barnes, G.T. J. Colloid Interface Sci. 1976, 54, 439.
11. Muramatsu, M. In "Surface and Colloid Science"; E. Matijevic, Ed.; Wiley: New York, 1973; Vol.6, p.101.
12. Hendrikx, Y.; Ter-Minassian-Saraga, L. J. Chim. Phys. 1970, 67, 1620.

RECEIVED February 3, 1986

11

Molecular Interaction and Synergism in Binary Mixtures of Surfactants

Milton J. Rosen

Department of Chemistry, Brooklyn College, The City University of New York, Brooklyn, NY 11210

Non-ideal solution theory is used to calculate the value of a parameter, β, that measures the interaction between two surfactants in mixed monolayer or mixed micelle formation. The value of this parameter, together with the values of relevant properties of the individual, pure surfactants, determines whether synergism will exist in a mixture of two surfactants in aqueous solution. The conditions for synergism in surface tension reduction efficiency, mixed micelle formation, and surface tension reduction effectiveness in aqueous solution have been derived mathematically together with the properties of the surfactant mixture at the point of maximum synergism. This treatment has been extended to liquid-liquid (aqueous solution/hydrocarbon) systems at low surfactant concentrations.) The effect of chemical structure and molecular environment on the value of β is demonstrated and discussed.

During the past few years, the determination of the interfacial properties of binary mixtures of surfactants has been an area in which there has been considerable activity on the part of a number of investigators, both in industry and in academia. The interest in this area stems from the fact that mixtures of two different types of surfactants often have interfacial properties that are better than those of the individual surfactants by themselves. For example, mixtures of two different surface-active components sometimes reduce the interfacial tension at the hydrocarbon/water interface to values far lower than that obtained with the individual surfactants, and certain mixtures of surfactants are better foaming agents than the individual components. For the purpose of this discussion we define synergism as existing in a system when a given property of the mixture can reach a more desirable value than that attainable by either surface-active component of the mixture by itself.

In my laboratory at Brooklyn College, we have been investigating molecular interactions and synergism in binary mixtures of surfactants for the past five years (1-6). The key to both investigations is the determination of the value of a parameter, β, that measures the nature and the extent of the interaction between the two surfactants. If the interaction between the two surfactants is attractive, β is negative; if the interaction is repulsive, then β is positive. The larger the value of β, the stronger the interaction, either attractive or repulsive, between the two surfactants. To date, β values, determined either in our laboratory or in the laboratory or in the laboratories of other investigators, have ranged from 0 to −30; 0 indicating no interaction and −30 an extremely strong interaction. The β values for mixtures of two given surfactants at a specified temperature varies, depending upon the particular interfacial phenomenon being investigated. For example, for mixtures of sodium n-octyl sulfate and n-octyl trimethylammonium bromide, the β value for mixed monolayer formation of 25°C at the aqueous solution/air interface is −14.2, while that for mixed micelle formation at 25°C in water is −10.2 (6).

The evaluation of the interaction parameters is based upon equations (1 and 2), derived by Rubingh (7) for mixed micelle formation from the thermodynamics of the system:

$$\alpha C_{12}^M = X^M f_1^M C_1^M \qquad (1)$$

$$(1-\alpha)\, C_{12}^M = (1-X^M)\, f_2^M C_2^M \qquad (2)$$

α = mole fraction of surfactant 1 in the total surfactant in the solution phase; C_1^M, C_2^M, C_{12}^M = critical micelle concentrations of individual surfactants 1 and 2 and their mixture, respectively, at a given value of α; X^M = mole fraction of surfactant 1 in the total surfactant in the mixed micelle; f_1^M, f_2^M = activity coefficients of individual surfactants 1 and 2, respectively, in the mixed micelle; and equations (3 and 4) for the activity coefficients, f_1^M and f_2^M,

$$f_1^M = \exp \beta^M (1-X^M)^2 \qquad (3)$$

$$f_2^M = \exp \beta^M (X^M)^2 \qquad (4)$$

using regular solution theory.

From equations (1-4), we obtain

$$\frac{(X^M)^2 \ln (\alpha C_{12}^M / X^M C_1^M)}{(1-X^M)^2 \ln [(1-\alpha) C_{12}^M / (1-X^M) C_2^M]} = 1 \qquad (5)$$

and $\quad \beta^M = \dfrac{\ln\ (\alpha C_{12}^M / X^M C_1^M)}{(1-X^M)^2}$ $\qquad\qquad$ (6)

Equation (5) is solved numerically for X^M, and substitution of X^M in equation (6) yields the value of β^M (the molecular inter-action parameter for mixed micelle formation in aqueous solution).

We have extended this treatment (equations 7 and 8) to mixed monolayer formation (1),

$$\alpha \overline{C}_{12} = X f_1 C_1^{\,\text{o}} \qquad\qquad (7)$$

$$(1-\alpha) C_{12} = (1-X)\ f_2 C_2^{\,\text{o}} \qquad\qquad (8)$$

X = mole fraction of surfactant 1 in the total surfactant in the mixed monolayer; $C_1^{\,\text{o}}$, $C_2^{\,\text{o}}$, C_{12} = solution phase molar concentrations of surfactants 1, 2, and their mixture, respectively, required to produce a given surface tension value;

$f_1 f_2$ = activity coefficients of individual surfactants 1 and 2, respectively, in the mixed monolayer;

using the non-ideal solution approximations (8) for the activity coefficients,

$$f_1 = \exp\ \beta^\sigma\ (1-X)^2 \qquad\qquad (9)$$

$$f_2 = \exp\ \beta^\sigma\ X^2 \qquad\qquad (10)$$

where β^σ is the molecular interaction parameter for mixed monolayer formations at the aqueous solution/air interface. Equation (7-10) yield

$$\dfrac{X^2 \ln\ (\alpha C_{12} / X C_1^{\,\text{o}})}{(1-X)^2\ \ln\ [(1-\alpha)\ C_{12}/(1-X) C_2^{\,\text{o}}]} \qquad\qquad (11)$$

$$\beta^M = \dfrac{\ln\ (\alpha C_{12} / X C_1^{\,\text{o}})}{(1-X)^2} \qquad\qquad (12)$$

analogous to equations (5) and (6), from which β^σ can be evaluated.

We have shown (1), not only that the single parameter, β^σ, can be used to predict surface tension values for any value of α,

as Rubingh did for critical micelle concentrations using β^M, but that the values of X, obtained by use of the equation for mixed monolayer formation, agree well with those calculated by an independent method from surface excess concentrations by use of the Gibbs adsorption equation.

The experimental determination of β^σ and β^M is shown in Figure 1. It involves determining the surface tension-log concentration curves for each of the pure components and for at least one mixture of them at a specific value of α. For calculating β^σ (the interaction parameter for mixed monolayer formation), c_1^o, c_2^o, and C_{12} are needed; for determing β^M (the interaction parameter for mixed micelle formation in aqueous solution), the critical micelle concentrations, C_1^M, C_2^M, and C_{12}^M, are required.

Synergism in surface tension reduction efficiency. The efficiency of surface tension reduction by a surfactant is defined (9) as the solution phase concentration required to produce a given surface tension (reduction). Synergism in this respect is present in a binary mixture of surfactants when a given surface tension (reduction) can be attained at a total mixed surfactant concentration lower than that required of either surfactant by itself. This is illustrated in Figure 2.

From equations (7) and (9), we obtain

$$\ln C_{12} - \ln C_1^o = \ln \alpha + \beta^\sigma (1-X)^2 \qquad (13)$$

The condition for synergism is: $C_{12} < C_1^o, C_2^o$

Thus $\ln X - \ln \alpha + \beta^\sigma (1-X)^2 < 0 \qquad (14)$

When synergism exists, a minimum will exist in the C_{12} vs. α curve, i.e., $dC_{12}/d\alpha = 0$

From the preceding, it can be shown (1) that when $dC_{12}/d\alpha = 0$, then $X = \alpha_*$, i.e., the mole fraction of each surfactant in the total surfactant in the total surfactant in the mixed monolayer equals its mole fraction in the solution phase at the point of maximum synergism. Substituting this into equations (7), (8), and (14), we obtain the conditions for synergism in this respect:

1. β^σ must be negative.

2. $\left| \ln C_1^o/C_2^o \right| < \left| \beta^\sigma \right|$

where C_1^o and C_2^o are the solution phase molar concentration of pure, individual surfactants 1 and 2, respectively, required to attain a given surface tension (reduction).

At the point of maximum synergism, the mole fraction α_*, of surfactant 1 in the solution phase equals its mole fraction in the mixed monolayer at the aqueous solution/air interface, and is given
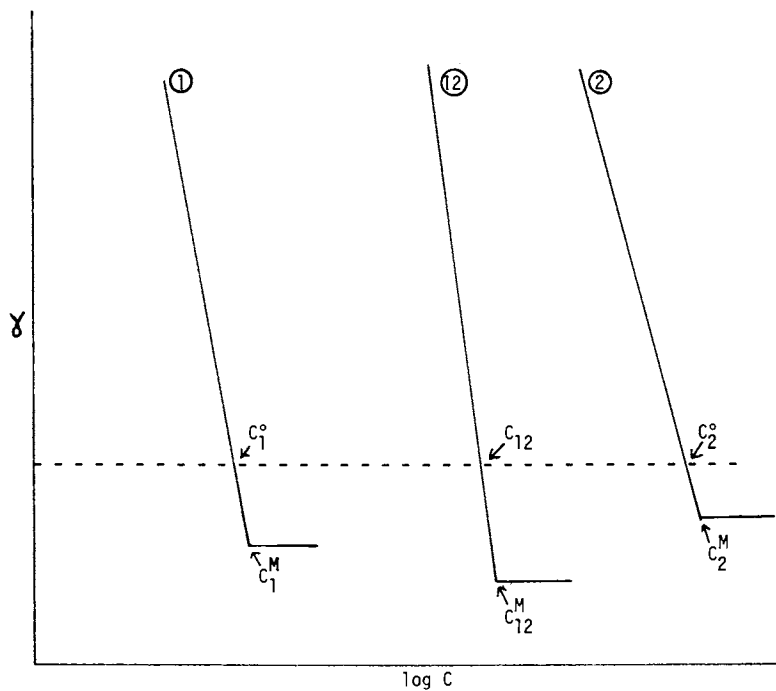
Figure 1. Experimental evaluation of β^σ or β^M. ① Pure surfactant 1; ② Pure surfactant 2; ⑫ Mixture of surfactants 1 and 2 at a given mole fraction, α, in solution.
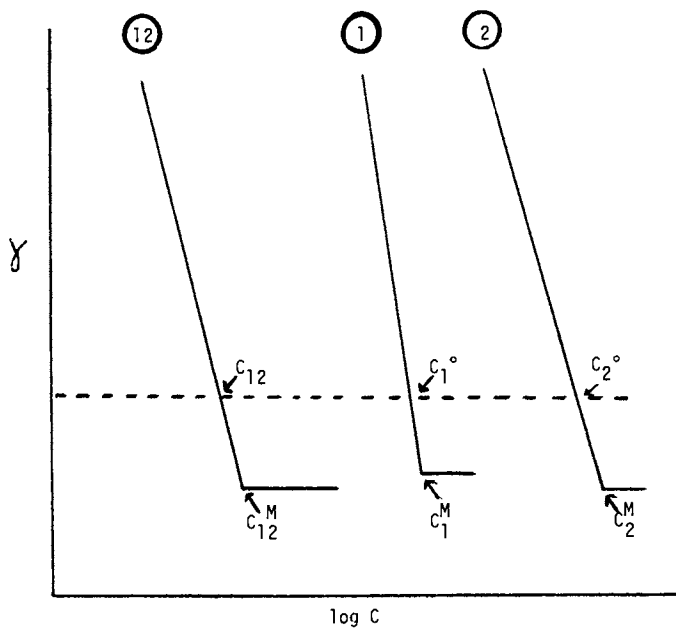
Figure 2. Synergism in surface tension reduction efficiency
$(C_{12} < C_1^o$ or $C_2^o)$ or in mixed micelle formation
$(C_{12}^M < C_1^M$ or $C_2^M)$ ① Pure surfactant 1;
② Pure surfactant 2; ⑫ Mixture of surfactants 1 and 2 at
a given mole fraction, α, in solution.

by the relationship:

$$\alpha_* = X = \frac{\ln (c_1^o/c_2^o) + \beta^\sigma}{2\beta^\sigma} \tag{15}$$

where X is the mole fraction of surfactant 1 in the mixed monolayer. The minimum mixed surfactant concentration in the solution phase, $C_{12,min}$, required to attain a given surface tension (reduction) is given by the expression:

$$C_{12,min} = C_1^o \exp\left[\beta^\sigma\left(\frac{\beta^\sigma - \ln c_1^o/c_2^o}{2\beta^\sigma}\right)^2\right] \tag{16}$$

Figure 3 shows the total surfactant concentration required to attain a given surface tension (reduction) as a function of α in a number of binary surfactant systems. It illustrates the requirement that $\left|\ln c_1^o/c_2^o\right|$ must be less than $\left|\beta^\sigma\right|$ for synergism in surface tension reduction efficiency to occur. Table I shows some data for a system showing synergism, together with values calculated for α_* and $C_{12,min}$, using equations (12) and (13).

Table I. Synergism in Surface Tension Reduction Efficiency[a]

System: $C_{12}H_{25}SO_4Na/C_{12}H_{25}(OC_2H_4)_8OH$ in 0.5 M NaCl

   $\beta = -3.2$; $\ln c_1^o/c_2^o = 1.7$; $\gamma = 36$ dyne cm^{-1}

α	X	C_{12}, mol dm^{-3}
0	0	5.0×10^{-5}
0.20	0.22	4.6×10^{-5}
0.40	0.30	4.9×10^{-5}
0.60	0.38	5.0×10^{-5}
0.80	0.47	6.5×10^{-5}

Calc: $\alpha_* = 0.23$; $C_{12,min} = 4.2 \times 10^{-5}$ mol dm^{-3}

[a]
    Adapted with permission from Ref. 3. Copyright 1982, American Oil Chemists' Society .

We have extended this treatment to the liquid-liquid interface and have determined the condition for synergism in _interfacial_ tension reduction efficiency. The interaction parameter, β_{LL}^σ, for mixed monolayer formation at the liquid-liquid interface is determined from plots of _interfacial_ tension vs. total surfactant concentration in the system at constant phase volume ratio and constant initial ratio of the two surfactants. The conditions for synergism
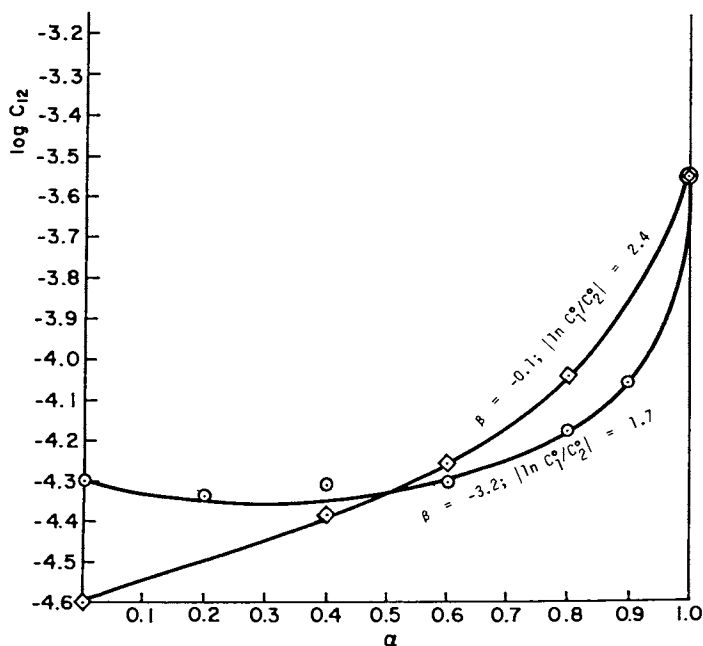
Figure 3. Synergism in surface tension reduction efficiency
for some binary surfactant mixtures.

◇ $C_{12}H_{25}SO_4Na/C_{14}H_{29}SO_4Na$ mixtures in 0.5 M NaCl at 25°C
($\gamma = 36$ mJm^{-2}), showing no synergism;

⊙ $C_{12}H_{25}$ $SO_4Na/C_{12}H_{25}(OC_2H_4)_8OH$ mixtures in 0.5 M NaCl at

25°C ($\gamma = 36$ mJm^{-2}), showing synergism.
Data from Lange, H. and K. H. Beck, Kolloid Z. Z. Polym. 251,
424 (1973). Adapted with permission from Ref. 3. Copyright 1982,
American Oil Chemists' Society .

in this respect, as derived by this treatment, are completely
analogous to those obtained for the liquid-air interface:

1) β_{LL}^{σ} must be negative

2) $\left| \beta_{LL}^{\sigma} \right| > \left| \ln \dfrac{C_{1,t}^{o}}{C_{2,t}^{o}} \right|$

where $C_{1,t}^{o}$ and $C_{2,t}^{o}$ are the total system concentrations of individual
surfactants 1 and 2, respectively, required to produce a given
interfacial tension in the two-phase systems containing only the
individual surfactants and all systems (containing individual sur-
factants and their mixtures) are compared at the same phase volume
ratio(10).

Under these conditions, the mole fraction, α_{*}, of surfactant 1
in the total surfactant in the system at the point of maximum
synergism equals the mole fraction at the interface and is given by
the expression:

$$\alpha_{*} = X = \frac{\ln \left(C_{1,t}^{o}/C_{2,t}^{o}\right) + \beta_{LL}^{\sigma}}{2\beta_{LL}^{\sigma}} \tag{17}$$

The minimum total concentration of mixed surfactant in the
system $C_{12,t}\text{min}$, to produce a given interfacial tension is given by
the expression:

$$C_{12,t,min} = C_{1,t}^{o} \exp \left[\beta_{LL}^{\sigma} \left(\frac{\beta_{LL}^{\sigma} - \ln C_{1,t}^{o}/C_{2,t}^{o}}{2\beta_{LL}^{\sigma}} \right)^{2} \right] \tag{18}$$

Synergism in mixed micelle formation. Synergism in this respect
is present when the critical micelle concentration of any mixture is
lower than that of either pure surfactant. This is illustrated in
Figure 2.

By mathematical treatment similar to that for synergism in
surface tension reduction efficiency, we have found that the condi-
tions for synergism in mixed micelle formation are:

1. β^{M} must be negative

2. $\left| \ln \left(C_{1}^{M}/C_{2}^{M}\right) \right| < \left| \beta^{M} \right|$

At the point of maximum synergism in mixed micelle formation,
the mole fraction, α_{*}^{M}, of the surfactant 1 in the solution phase
equals its mole fraction in the mixed micelle and is given by the
relationship:

$$\alpha_{*}^{M} = X^{M} = \frac{\ln \left(C_{1}^{M}/C_{2}^{M}\right) + \beta^{M}}{2\beta^{M}} \tag{19}$$

where X^{M} is the mole fraction of surfactant 1 in the mixed micelle.

The cmc at the point of maximum synergism, i.e., the minimum total mixed surfactant concentration in the solution phase required for mixed micelle formation, $C_{12, min}^M$, is given by the relationship:

$$C_{12, min}^M = C_1^M \exp \left[\beta^M \left(\frac{\beta^M - \ln C_1^M/C_2^M}{2\beta^M} \right)^2 \right] \tag{20}$$

Figure 4 shows data for some systems in which synergism does and does not occur. We see that when the absolute value of β^M is greater than the absolute value for $\left| \ln C_1^M/C_2^M \right|$, then synergism does occur; when it is not greater, synergism does not occur.

Table II lists some data for a system showing synergism in mixed micelle formation, together with values of α_*^M, and $C_{12, min}^M$, calculated using equations (19) and (20).

Table II. Synergism in Mixed Micelle Formation at 25°C [a]

System: $C_{12}H_{25}SO_4Na/C_8H_{17}(OC_2H_4)_4OH$

$\beta^M = -3.1$; $\ln (C_1^M/C_2^M) = 0.13$

α	x^M	C_{12}^M(=c.m.c.), mol dm^{-3}
0.05	0.21	4.8×10^{-3}
0.20	0.35	3.6×10^{-3}
0.50	0.49	3.5×10^{-3}
0.80	0.62	3.9×10^{-3}
0.90	0.70	4.5×10^{-3}

Calc: $\alpha_*^M = 0.48$; $C_{12, min}^M = 3.4 \times 10^{-3}$ mol dm^{-3}

[a] Adapted with permission from Ref. 3. Copyright 1982, American Oil Chemists' Society .

Here, also we have extended (10) our treatment of synergism to 2-phase liquid systems and have derived equations that are completely analogous to those obtained for solutions in contact with air, when the nonaqueous phase is a hydrocarbon. The interaction parameter, β_{LL}^M, is obtained from the breaks in the plots of interfacial tension vs. total surfactant concentration in the system, indicating the onset of micellization in the aqueous phase.

Synergism in surface tension reduction effectiveness. This exists when the mixture of surfactants of its cmc reaches a lower surface tension than that obtained at the cmc of either component of the mixture by itself. This is illustrated in Figure 5.
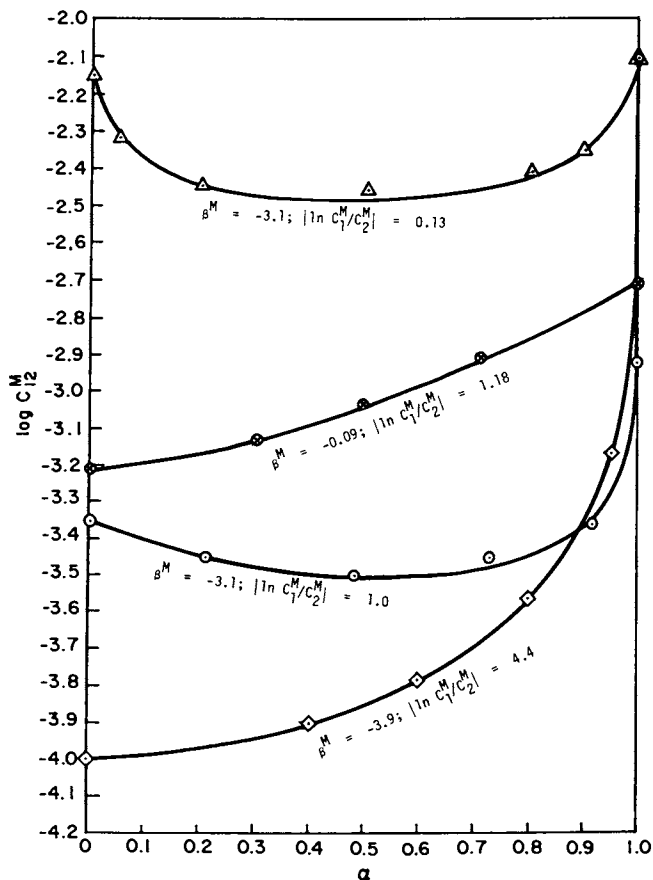
Figure 4.   Synergism in mixed micelle formation for some binary surfactant mixtures. ◇ $C_{12}H_{25}SO_4Na/C_{12}H_{25}(OC_2H_4)_8OH$ mixtures in water at $25°C$, showing no synergism;

△ $C_{12}H_{25}SO_4Na/C_8H_{17}(OC_2H_4)_7OH$ mixtures in water at $25°C$, showing synergism; data from Lange, H. and K. H. Beck, Kolloid Ζ. Z. Polym. 251, 424 (1973).

○ $(C_{12}H_{25}SO_4)_2 M/C_{12}H_{25}(OC_2H_4)_{49}OH$ (M = Zn^{++}, Mn^{++}, Cu^{++}, Mg^{++}) mixtures in water at $30°C$, showing synergism; data from Nishioka, N., J. Colloid Interface Sci. 60, 242 (1977).

⊗ $C_{10}H_{21}S(O)CH_3/C_{10}H_{21}(OC_2H_4)_3$ mixtures at $25°C$, showing no synergism; data from Ingram, B. T. and A.H.W. Luckhurst, in "Surface Active Agents" Soc. Chem. Ind., London, 1979, p.89. Adapted with permission from Ref. 3.   Copyright 1982, American Oil Chemists' Society .
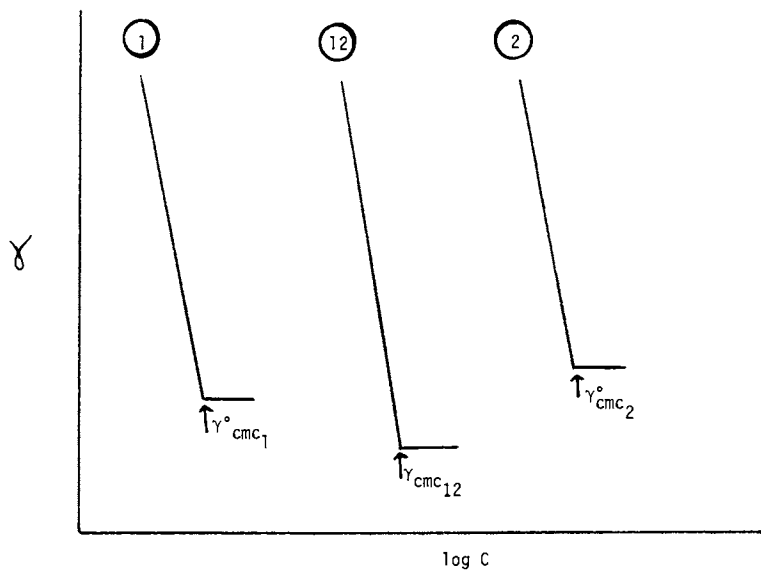
Figure 5. Synergism in surface tension reduction effectiveness. ($\gamma cmc_{12} < \gamma^{o}cmc_{1}$ or $\gamma^{o}cmc_{2}$). ① Pure surfactant 1; ② Pure surfactant 2; ⑫ Mixture of surfactants 1 and 2 at a given mole fraction, α, in solution.

The conditions for this to occur are (6):

1. β^{σ} must be negative

2. $\beta^{\sigma} - \beta^{M}$ must be negative

3. $|\beta^{\sigma} - \beta^{M}| > |(\gamma^{o}_{cmc1} - \gamma^{o}_{cmc2})/K|$

where γ^{o}_{cmc1}, γ^{o}_{cmc2} are the surface tensions of pure surfactants 1 and 2 by themselves in aqueous solution and K is the slope of the surface tension-natural log concentration curve of that surfactant having the larger surface tension value at its cmc.

Data on systems showing synergism in this respect indicate that for surfactants containing a single hydrophilic and a single hydrophic group, the point of maximum synergism is reached when

$$X = 0.5$$

that is, when there are approximately equal numbers of the two different surfactants at the interface.

With this assumption, at the point of maximum synergism in this respect,

$$\alpha^{*} = C^{M}_{1}/(C^{M}_{1} + C^{M}_{2}) \tag{21}$$

$$\gamma^{*}_{cmc} \text{ (the min.} \gamma \text{ of the system)} = \gamma^{o}_{cmc1(2)} - \frac{K_{1(2)}(\beta^{\sigma} - \beta^{M})}{4} \tag{22}$$

(this equation works best when γ^{o}_{cmc} is for the surfactant having the lower γ^{o}_{cmc} value).

cmc* (c.m.c. of the mixture at γ^{*}_{cmc}) $= \dfrac{C^{M}_{1} + C^{M}_{2}}{2} \exp{(\beta^{M}/4)}$ \hfill (23)

We have checked (6) these equations on 10 systems (Table III) for which data are available, and have found good agreement in all cases between theory and experimental results. Calculations show that synergism in this respect is very likely to occur if $|\beta^{\sigma} - \beta^{M}| = 2$ or more.

Extension of the treatment (10) to 2-phase liquid systems gives the analogous conditions for synergism in this respect:

1. $\beta^{\sigma}_{LL} < 0$

2. $\beta^{\sigma}_{LL} - \beta^{M}_{LL} < 0$

3. $|\beta^{\sigma}_{LL} \quad \beta^{M}_{LL}| > (\gamma^{o}_{cmc1,t} - \gamma^{o}_{cmc2,t})/K$

$\gamma^{o}_{cmc1,}$ and γ^{o}_{cmc2} are the interfacial tension values of surfactants 1 and 2, respectively, at the breaks in their plots of interfacial

Table III. Synergism in Surface Tension Reduction Effectiveness (6)

System	$\beta^\sigma - \beta^M$	$\dfrac{\gamma^\circ_{cmc_1} - \gamma^\circ_{cmc_2}}{K}$	Theory	Experiment
1) $C_{12}BMG - C_{12}SO_3Na$	-1.5	0.3	Yes	Yes
2) $C_{12}BMG - C_{12}NMe_3Br$	-0.11	0.38	No	No
3) $C_{12}BMG - C_{12}EO_8$	+0.31	-	No	No
4) $C_{12}Np - C_{10}SO_4Na$	-2.8	0.52	Yes	Yes
5) $C_{12}Np - C_{12}SO_4Na$	-1.6	0.36	Yes	Yes
6) $C_{12}Np - C_{14}SO_4Na$	0.0	-	No	No
7) $C_{12}NMe_2O - C_{12}SO_3K$	-5.1	0.19	Yes	Yes
8) $C_{12}SO_4Na - C_{12}NMe_3Br$	-2.3	0	Yes	Yes
9) $C_8SO_4Na - C_8NMe_3Br$	-4.0	0.24	Yes	Yes
10) $C_{12}HAA - LAS$	-3.2	0.76	Yes	Yes

tensions vs. $\ln C_t$, indicative of micelle formation. K is the slope of the interfacial tension – $\ln C_t$ for the individual surfactant having the larger interfacial tension at its cmc.

The Effect of Structural and Molecular Environmental Factors on β^σ and β^M

Since all these synergistic effects depend upon the values of β^σ and β^M, we have determined β^σ and β^M values for many binary systems with different hydrophilic and hydrophobic groups. It is instructive to see how the values are affected by the nature of the chemical structures of the two surfactants that are present in the systems and by the molecular environment surrounding them.

Table IV lists examples of systems showing strong interaction between the two surfactants ($|\beta^\sigma$ or $\beta^M| > 10$). These are anionic-cationic systems or those that can be converted to an anionic-cationic system by proton addition. Examples of the latter are the systems containing C_{12} dimethylamine oxide ($C_{12}NMe_2O$) or C_{12} ammoniopropionate $[C_{12}N^+H_2(CH_2)_2COO^-]$. These materials, in the presence of anionics, are converted to cationics by addition of a proton, even at neutral pH.

Table IV. Effect of Structural Factors on Values of β^σ and β^M

Mixture	Temp (°C)	β^σ	β^M
$C_8SO_4^-Na^+ - C_8N^+Me_3Br^-$	25	-14.2	-10.2
$C_{12}SO_4^-Na^+ - C_{12}N^+Me_3Br^-$	25	-27.8	-25.5
(both β^σ and β^M become more negative with increase in R)			
$C_{12}SO_4^-K^+ - C_{12}NMe_2O$	25	-21.6	-16.5
$C_{10}SO_4^-Na^+ - C_{12}N^+H_2(CH_2)_2COO^-$	30	-13.4	-10.6
$C_{12}SO_4^-Na^+ - C_{12}N^+H_2(CH_2)_2COO^-$	30	-15.7	-14.1
$C_{14}SO_4^-Na^+ - C_{12}N^+H_2(CH_2)_2COO^-$	30	-15.5	-15.5

($|\beta^\sigma|$ is max. at $R^1 = R^2$; $|\beta^M|$ increases with $R^1 + R^2$)

In general, the value of both β^σ and β^M become more negative as the chain lengths of the alkyl groups present are increased, indicating increased interaction of the two surfactants with this change. The value of β^M appears to increase somewhat more rapidly with this change than the value of β^σ, possibly the result of the closer packing of the chains below the curved surface of the micelle than at the planar air/water interface. Another difference between interactions in mixed monolayers and in mixed micelles is the maximum β^σ value shown when the lengths of the alkyl chains are

equal, which is not true for β^M values. The latter appears to increase monotonically with increase in the alkyl chain length of either of the two surfactants present in the system. This also may be due to the difference in packing of the chains in the planar monolayer and below the curved micellar surface.

Table V shows some systems with intermedicate strength interaction between the two surfactants ($|\beta^\sigma$ or $\beta^M|$ 3-10). The systems in the upper portion of the table are two different anionic-zwitterionic systems. The first system contains a zwitterionic (a betaine) capable of readily accepting a proton to become a cationic species; the second system contains a zwitterionic (a sulfobetaine) of similar structure that is much less capable of accepting a proton (The sulfonate ion is a much weaker base than the carboxylate ion.). The greater ability of the first system to accept a proton, with the resulting strong anionic-cationic interaction, gives it a significantly greater (negative) β^σ value than the second system, at similar pH. Note also the increase in the negative values of both β^σ and β^M, (increase in surfactant interaction) with decrease in pH, as would be expected for an interaction involving acceptance of a proton.

Table V.   Effect of Structural and Molecular Environmental Factors
           on Values of β^σ and β^M

Mixture	Temp (°C)	β^σ	β^M
$C_{12}SO_3^-Na^+$—$C_{12}N^+(B_z)(Me)CH_2COO^-$ (pH = 5.0)	25	-5.7	-5.0
$C_{12}SO_3^-Na^+$—$C_{12}N^+(B_z)(Me)CH_2COO^-$ (pH = 6.7)	25	-4.9	-4.4
(both $|\beta^\sigma|$ and $|\beta^M|$ decrease with increase in pH)			
$C_{12}SO_3^-Na^+$—$C_{10}N^+(B_z)(Me)C_2H_4SO_3^-$ (pH = 6.6)	25	-2.5	
$C_{12}SO_4^-Na^+$— $C_{12}(OE)_8OH$	25	-2.7	-4.1
$C_{12}SO_3^-Na^+$— $C_{12}(OE)_8OH$	25	1.5	-3.4
(RSO_4^- interaction > RSO_3^-)			

The two systems at the bottom of the table illustrate an effect that we do not yet fully understand: the significantly greater interaction of alkyl sulfates, compared to alkyl sulfonates, with POE nonionics. We have observed this in a number of systems, both in pure water and in the presence of electrolyte.

Table VI lists data on systems showing weak interactions ($|\beta^\sigma$ or $\beta^M| < 3$). Included are POE nonionic systems containing a

cationic, a zwitterionic, or a second POE nonionic as the second
surface-active component. In the cationic-POE nonionic systems,
the absolute values of both β^σ and β^M decrease with increasing
ionic strength of the aqueous phase, indicating that the interaction
between the two surfactants must be electrostatic in nature,
presumably between the ether oxygens of the polyoxethylene chain
and the positive charge of the pyridinium nitrogen.

Table VI.   Effect of Structural and Molecular Environmental
            Factors on Values of β^σ and β^M

Mixture	Temp (°C)	β^σ	β^M
$C_{12}Pyr^+Cl^-$—$C_{12}(OE)_8$ (H_2O)	25	−2.8	−2.7
$C_{12}Pyr^+Cl^-$—$C_{12}(OE)_8$ (0.1 M NaCl)	25	−2.2	−1.4
$C_{12}Pyr^+Cl^-$—$C_{12}(OE)_8$ (0.5 M NaCl)	25	−1.5	−1.0
(both $|\beta^\sigma|$ and $|\beta^M|$ decrease with increase in ionic strength)			
$C_{12}Pyr^+Cl^-$—$C_{12}(OE)_8$(0.1 M NaCl)	10	−2.5	---
$C_{12}Pyr^+Cl^-$—$C_{12}(OE)_8$(0.1 M NaCl)	40	−2.0	---
(decrease in $|\beta^\sigma|$ with temperature increase)			
$C_{12}N^+(B_z)(Me)CH_2COO^-$—$C_{12}(OE)_8$	25	−0.6	−0.9
$C_{12}(OE)_8$—$C_{12}(OE)_8$	25	−0.2	
(weak zwitterionic-nonionic or nonionic-nonionic interaction)			

     As might be expected, β^σ decreases with increase in tempera-
ture, in part because the area per molecule at the interface
increases as temperature increases, weakening the interaction
between adjacent molecules.
     Table VII shows some structural effects on POE nonionic-ionic
interactions. From the β^M values for the systems listed here, it
appears that interaction between an alkyl sulfate and a POE
increases with increase in the number of oxyethylene units in the
nonionic.
     Table VIII shows the effect of ionic strength on the inter-
action between ionics and POE nonionics. In the cationic-nonionic
systems, there is a monotonic decrease in the absolute value of β^σ,
i.e., a decrease in interaction between the two surfactants, with
increase in the ionic strength of the solution, indicating that
the nature of the interaction between the cationic and the non-
ionic is probably electrostatic (since increase in the ionic
strength of the solution decreases electrostatic interactions).

Table VII. Effect of Length of the POE Chain on β^M Value
at 25°C in Aqueous Solution[a]

Surfactant Pair	β^M
$C_{12}SO_4Na/C_8(EO)_4$	-3.1
$C_{12}SO_4Na/C_8(EO)_6$	-3.4
$C_{12}SO_4Na/C_8(EO)_{12}$	-4.1

[a]Calculated from data of Lange, H. and K. H. Beck, Kolloid
Z. Z. Polym. 251, 424 (1973).

Table VIII. Effect of Ionic Strength of Solution on $\beta(4)$
(Temp. = 25°C)

System	Medium	β
$C_{12}EO_8-C_{12}PyrCl$	H_2O	-2.8
$C_{12}EO_8-C_{12}PyrCl$	0.1 M T.I.S[a] (NaCl)	-2.2
$C_{12}EO_8-C_{12}PyrCl$	0.5 M T.I.S. (NaCl)	-1.5
$C_{12}EO_8-C_{12}SO_4Na$	H_2O	-2.7
$C_{12}EO_8-C_{12}SO_4Na$	0.1 M T.I.S. (NaCl)	-3.5
$C_{12}EO_8-C_{12}SO_4Na$	0.5 M T.I.S. (NaCl)	-3.1
$C_{12}EO_8-C_{12}SO_3Na$	H_2O	-1.5
$C_{12}EO_8-C_{12}SO_3Na$	0.1 M T.I.S. (NaCl)	-2.6
$C_{12}EO_8-C_{12}SO_3Na$	0.5 M T.I.S. (NaCl)	-2.0

[a]Total ionic strength

However, in the two anionic-nonionic systems, an increase in
the ionic strength of the solution produces first an increase, and
then a decrease, in the strength of the interaction between the two
surfactants. Our explanation for this initial increase (4) is that,
in the presence of anionic surfactant, there is complexing of the
Na^+ with the ether oxygens of the polyoxyethylene chain, in a
manner similar to their interaction with crown ethers.
       The extent of this complexing is small in pure water, since
the Na^+ concentration is very low. In 0.1 M NaCl, however, there
is a significant amount of complexing of the Na^+ with the poly-

oxyethylene chain. This complex formation gives the nonionic a small amount of cationic character, with the result that its interaction with the anionic increases. The decrease in the value of β^σ in 0.5 M NaCl is then the usual decrease in electrostatic interactions with increase in the ionic strength of the solution.

Our data, to date, show that molecular interaction between two surfactants, both in mixed monolayers at the aqueous solution/air interface and in mixed micelles in aqueous solution, increases in the order: POE nonionic-POE-nonionic < POE nonionic-betaine < betaine-cationic < POE nonionic-ionic (cationic, anionic) << betaine-anionic << cationic-anionic. The greatest probability of synergism exists, therefore, in cationic-anionic mixtures, followed by betaine-anionic mixtures. Synergism can exist in POE nonionic-ionic mixtures only if the surfactants involved have the proper structures.

Literature Cited

1. Rosen, M. J. and X. Y. Hua, J. Colloid Interface Sci. (1982) 86, 164.
2. Hua, X. Y. and M. J. Rosen, J. Colloid Interface Sci. (1982) 90, 212.
3. Rosen, M. J. and X. Y. Hua, J. Amer. Oil Chem. Soc. (1982), 59, 582.
4. Rosen, M. J. and F. Zhao, J. Colloid Interface Sci. (1983), 95, 443.
5. Rosen, M. J. and B. Y. Zhu, J. Colloid Interface Sci. (1984), 99, 427.
6. Zhu, B. Y. and M. J. Rosen, J. Colloid Interface Sci. (1984), 99, 435.
7. Rubingh, D. N., in "Solution Chemistry of Surfactants" (K. K. Mittal, Ed.), Vol. I, pp. 337-354, Plenum, New York, 1979.
8. Fried, V., Blukis, U. and Hameka, H. F., "Physical Chemistry", MacMillan, New York, 1977, pp. 224, 252.
9. Rosen, M. J., J. Amer. Oil Chem. Soc. (1974), 51, 461.

10. Rosen, M. J. and D. S. Murphy, submitted to J. Colloid Interface Sci.

Thermodynamic Study of the Surface Adsorption and Micelle Formation of Mixed Surfactants

Kinsi Motomura, Hidetsugu Matsukiyo, and Makoto Aratono

Department of Chemistry, Faculty of Science, Kyushu University 33, Fukuoka 812, Japan

The surface tension of the aqueous solution of dode-
cylammonium chloride (DAC) — decylammonium chloride
(DeAC) mixture was measured as a function of the total
molality m of surfactants and the mole fraction X of
DeAC in the total surfactant in the neighborhood of
the critical micelle concentration (CMC). By use of
the thermodynamic equations derived previously, the
mole fraction X^H in the mixed adsorbed film was evalu-
ated from the γ vs. X and m vs. X curves. Further,
the mole fraction X^M in the mixed micelle was evalu-
ated from the CMC vs. X curve. By comparing these
values at the CMC, it was concluded that the behavior
of DAC and DeAC molecules in the mixed micelle is
fairly similar to that in the mixed adsorbed film.

It was recently ascertained that the behavior of the adsorbed film
of two surfactants in equilibrium with their micelle can be ex-
plained by assuming both the surface region and the micelle particle
to be mixtures of the surfactants (1-6). Further, the application
of the regular solution theory to the mixtures was shown to be use-
ful to describe the nonideal behavior of ionic surfactants (4-6).
However, the above treatments are incomplete from the thermodynamic
viewpoint, because they do not consider the dissociation of surfac-
tants and ignore the presence of solvent (7). In addition, it is
impossible to suppose that the regular solution theory is applicable
to both the adsorbed film and the micelle of ionic surfactants
accompanied by the electrical double layer (8).
On the other hand, we showed that the composition of surfactant
in a mixed adsorbed film can be estimated thermodynamically from
experimental results without introducing such a supposition (9-11).
Further, the composition of a mixed micelle was calculated assuming
that the micelle behaves thermodynamically like a macroscopic bulk
phase whose thermodynamic quantities are given by the excess thermo-
dynamic quantities similar to those used for the adsorbed film (8).
Therefore, we can now compare the composition of surfactant in the
mixed adsorbed film with that in the mixed micelle at the critical
micelle concentration (CMC).

In this paper, dodecylammonium chloride (DAC) and decylammonium
chloride (DeAC) are chosen to reveal the fundamental behavior of
surfactants in the mixed adsorbed film and micelle. The surface
tension of their aqueous solution is measured as a function of their
concentrations in the neighborhood of the CMC and the comparison
between the mixed adsorbed film and the mixed micelle is made in
terms of the composition evaluated.

Experimental

Dodecylammonium chloride and decylammonium chloride were synthesized
and purified by the method described previously (9,12). Water was
distilled triply from alkaline permanganate. Surface tension was
measured by means of the drop volume technique, of which the de-
tailed procedure was described in the previous paper (13). The
measurements were carried out at 298.15 K under atmospheric pres-
sure; the surface tension values were reproducible to $\pm$ 0.05 mN m^{-1}.

Results and Discussion

Useful information regarding the adsorbed film and micelle in equi-
librium with the aqueous solution of surfactant mixture at constant
temperature and pressure is provided by adopting as the experimental
variables the total molality m of surfactants and the mole fraction
X of surfactant 2 in the total surfactant defined by

$$m = m_1 + m_2 \tag{1}$$

and

$$X = m_2/m \tag{2}$$

respectively (8-11). Here m_i is the molality of surfactant i.
     The surface tension γ of the aqueous solution of dodecylammo-
nium chloride — decylammonium chloride mixture was measured as a
function of m at a given value of the mole fraction X of DeAC at
298.15 K under atmospheric pressure. The results are shown in Fig-
ure 1. It is seen that the γ vs. m curves are similar in appear-
ance. This behavior is in harmony with that observed previously in
a low concentration range (9). Moreover, the formation of micelle
is found to cause the curves to break sharply at the CMC which in-
creases with X. It should be noted, however, that the γ vs. m curve
of a mixture has a very shallow minimum in the immediate vicinity of
the CMC.
     The variation of γ with X can be examined by consulting Figure
1. In Figure 2, the γ vs. X curves at constant m are drawn for the
solutions which contain only the monomers of surfactants. For com-
parison, the surface tension γ^{CMC} at the CMC are plotted against X
in the figure. It is seen that the curve deviates downward from the
straight line joining the γ values of pure DAC and DeAC. Further,
we are interested in examining how the total molality yielding a
given surface tension value varies with the composition. Figure 3
shows the m vs. X curve at constant γ obtained from Figure 1; in-
cluded in this figure for comparison is the CMC vs. X curve. Again
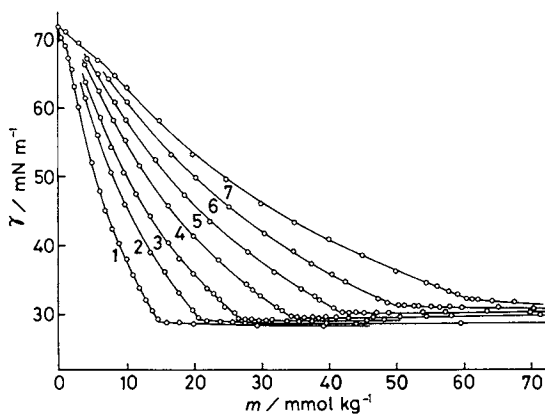
Figure 1. Surface tension vs. total molality curves at constant composition: 1, $X = 0$; 2, 0.500; 3, 0.700; 4, 0.833; 5, 0.915; 6, 0.965; 7, 1.
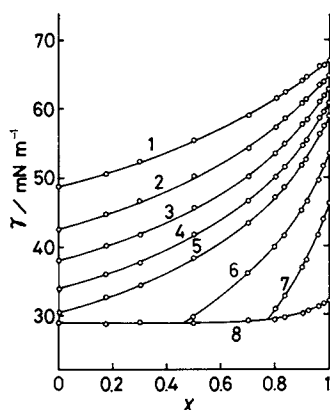
Figure 2. Surface tension vs. composition curves at constant total molality: 1, $m = 6$ mmol kg^{-1}; 2, 8 mmol kg^{-1}; 3, 10 mmol kg^{-1}; 4, 12 mmol kg^{-1}; 5, 14 mmol kg^{-1}; 6, 20 mmol kg^{-1}; 7, 30 mmol kg^{-1}; 8, γ^{CMC} vs. X.

the curve is observed to deviate from the straight line. Comparing
Figure 3 with Figure 2, we notice that the CMC vs. X curve is simi-
lar in shape to the m vs. X curve while the γ^{CMC} vs. X curve is
different from the γ vs. X curve. Taking into account that both the
m vs. X and γ vs. X curves are likewise related to the composition
of surfactant in the adsorbed film (9-11), this fact may suggest
that the γ^{CMC} vs. X and CMC vs. X curves afford different informa-
tion with regard to the micelle.

First, let us consider the surface density of surfactant. The
total surface excess number of moles per unit area Γ^H of surfactants
is evaluated by using the relation

$$\Gamma^H = - (m/2RT)(\partial\gamma/\partial m)_{T,p,X} \tag{3}$$

where T is temperature, p pressure, and R the gas constant (9).
Here the solution is assumed to be ideal. By applying Equation 3 to
the γ vs. m curves given in Figure 1, the values of Γ^H were calcu-
lated; they are plotted against m in Figure 4. It is seen that the
Γ^H value increases steeply with increasing m and approaches the
saturation value in the vicinity of the CMC. Furthermore, the Γ^H
vs. m curve changes its shape regularly. Therefore, it may be said
that the DAC and DeAC molecules are miscible with each other at the
surface and form a homogeneous adsorbed film.

The composition of surfactant in the mixed adsorbed film is
estimated by virtue of the relation

$$X^H = X - [(1 - X)X/RT\Gamma^H](\partial\gamma/\partial X)_{T,p,m} \tag{4}$$

where X^H is the mole fraction of DeAC in the adsorbed film defined
by the analog of Equation 2 (9,10). By applying this equation to
the γ vs. X curves given in Figure 2, the values of X^H were esti-
mated numerically. The values at $m = 6$, 10, and 14 mmol kg^{-1} are
illustrated in the form of the γ vs. X^H curve together with the
corresponding γ vs. X curve in Figure 5. It is important to note
that the composition in the adsorbed film is remarkably different
from that in the solution and enriched in the more surface-active
DAC though the DAC and DeAC molecules differ in the number of carbon
atoms only by two.

Similarly, the relation of X^H to X can be considered under the
condition that γ is constant. By use of the equation

$$X^H = X - [2(1 - X)X/m](\partial m/\partial X)_{T,p,\gamma} \tag{5}$$

derived previously (10), the m vs. X^H curve was obtained from the m
vs. X curve. In Figure 6, they are drawn at $\gamma = 60$, 50, and 40 mN
m^{-1}. It is observed again that the X^H value is significantly
smaller than the X value. Therefore, we may say that a slight dif-
ference in the surface activity of surfactant exerts a remarkable
effect on its adsorption behavior at concentrations near the CMC.
Moreover, such a diagram is found to be useful in studying the mis-
cibility of surfactants in the film state.

On the other hand, the mole fraction X^M of DeAC in the mixed
micelle, which is defined by the equation analogous to Equation 2,
can be estimated at the CMC by making use of the relation
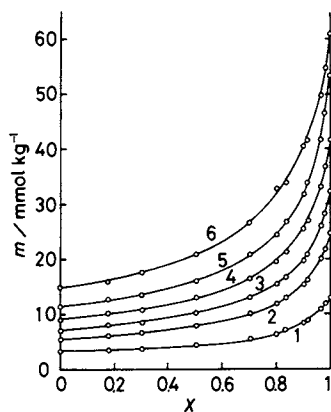
Figure 3. Total molality vs. composition curves at constant surface tension: 1, $\gamma = 60$ mN m^{-1}; 2, 50 mN m^{-1}; 3, 45 mN m^{-1}; 4, 40 mN m^{-1}; 5, 35 mN m^{-1}; 6, CMC vs. X.
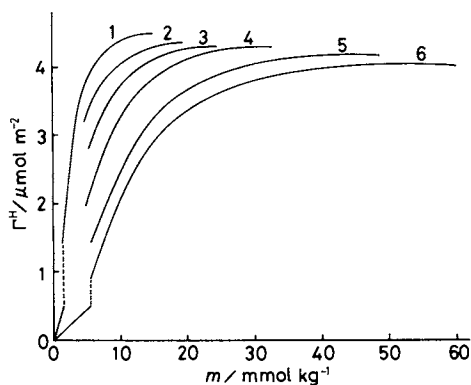
Figure 4. Total surface density vs. total molality curves at constant composition: 1, $X = 0$; 2, 0.500; 3, 0.700; 4, 0.833; 5, 0.965; 6, 1.
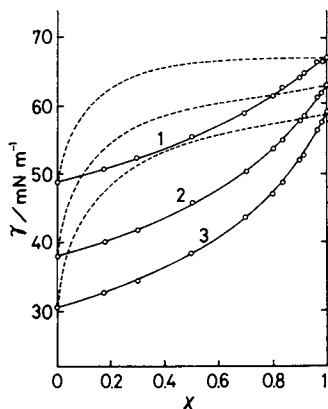
Figure 5. Surface tension vs. composition curves at constant total molality: X (———), X^H (-----): 1, m = 6 mmol kg^{-1}; 2, 10 mmol kg^{-1}; 3, 14 mmol kg^{-1}.
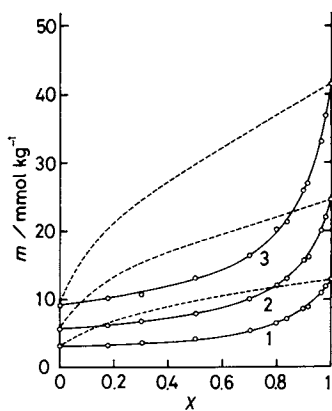
Figure 6. Total molality vs. composition curves at constant surface tension: X (———), X^H (-----): 1, γ = 60 mN m^{-1}; 2, 50 mN m^{-1}; 3, 40 mN m^{-1}.

$$X^{\text{M}} = X - [2(1 - X)X/\text{CMC}](\partial\text{CMC}/\partial X)_{T,p} \tag{6}$$

the solution being assumed to be ideal (8). Thus we can obtain the CMC vs. X^{M} curve from the CMC vs. X curve given in Figure 3. Both the curves are depicted in Figure 7. It should be noted that this figure is quite similar to that of the sodium tetradecyl sulfate — sodium dodecyl sulfate system (8,14). Comparing Figure 7 with Figure 6, we notice that there is a striking resemblance of shape between them. This fact suggests that the mixed micelle bears a similarity in the miscibility of surfactants to the mixed adsorbed film.

Now the relationship between X^{H} and X^{M} needs to be examined at the CMC. The mole fraction $X^{\text{H,CMC}}$ of DeAC in the adsorbed film at the CMC can be estimated by extrapolation of the X^{H} vs. m plot taken from Figure 6 to the CMC. However, it is instructive to derive the thermodynamic equation relating $X^{\text{H,CMC}}$ to X^{M}. As can be seen from Equations 3 and 4, the total differential of γ is expressed at constant T and p as

$$d\gamma = -(2RT\Gamma^{\text{H}}/m)\,dm - [RT\Gamma^{\text{H}}(X^{\text{H}} - X)/(1 - X)X]\,dX \tag{7}$$

Taking into account that m is assumed to be equal to CMC at the CMC and that Equation 6 yields

$$d\text{CMC} = -[\text{CMC}(X^{\text{M}} - X)/2(1 - X)X]\,dX \tag{8}$$

Equation 7 is rewritten at the CMC as

$$d\gamma^{\text{CMC}} = [RT\Gamma^{\text{H,CMC}}(X^{\text{M}} - X^{\text{H,CMC}})/(1 - X)X]\,dX \tag{9}$$

where $\Gamma^{\text{H,CMC}}$ is the total surface density of surfactants at the CMC. Accordingly, we can derive the relation

$$X^{\text{H,CMC}} = X^{\text{M}} - [(1 - X)X/RT\Gamma^{\text{H,CMC}}](\partial\gamma^{\text{CMC}}/\partial X)_{T,p} \tag{10}$$

Equation 10 states that the difference between $X^{\text{H,CMC}}$ and X^{M} are correlated to the slope of the γ^{CMC} vs. X curve. Inspecting Figure 8 where the γ^{CMC} vs. X curve taken from Figure 2 are illustrated together with the γ^{CMC} vs. X^{M} curve, therefore, $X^{\text{H,CMC}}$ may be supposed to have a value fairly close to X^{M}.

Evaluating the derivative of γ^{CMC} with respect to X and $\Gamma^{\text{H,CMC}}$ by extrapolation of the curve in Figure 4 to the CMC and then substituting them into Equation 10, the $X^{\text{H,CMC}}$ value was calculated as a function of X. For the purpose of comparison, the result is drawn in the form of the CMC vs. $X^{\text{H,CMC}}$ plot in Figure 7. The CMC vs. $X^{\text{H,CMC}}$ and CMC vs. X^{M} curves seem not to differ too greatly from each other when compared to the CMC vs. X curve. Therefore, we may conclude that the behavior of DAC and DeAC molecules in the mixed micelle is fairly similar to that in the mixed adsorbed film. This conclusion is consistent with the view, obtained in the previous papers (15,16), that the micelle resembles the adsorbed film closely in the thermodynamic behavior.

Finally, it is helpful in understanding the dependence of γ on m in the concentration range above the CMC to examine the difference between the γ^{CMC} vs. X^{M} and γ^{CMC} vs. X curves. From Figure 8, we can expect that the surface tension of the micellar solution of a
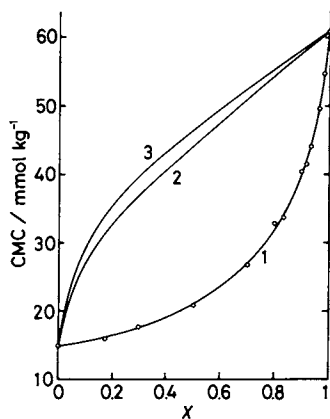
Figure 7. Critical micelle concentration vs. composition curves:
1, CMC vs. X; 2, CMC vs. X^M; 3, CMC vs. $X^{H,CMC}$.
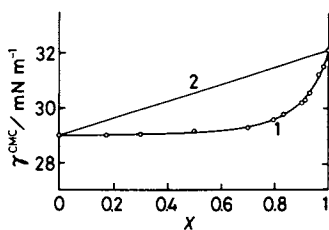
Figure 8. Surface tension at the CMC vs. composition curves: 1,
γ^{CMC} vs. X; 2, γ^{CMC} vs. X^M.

mixture increases slightly with increasing m if those of pure sur-
factants remain constant. Taking account of the fact that the γ vs.
m curves of pure DAC and DeAC shown in Figure 1 have small negative
slopes, the observation that the corresponding curve of their mix-
ture has a very shallow minimum followed by a indistinct maximum is
in accord with our expectation.

The above consideration has proved that surface tension mea-
surements are useful in elucidating the behavior of surfactants in
the mixed adsorbed film and micelle. The conclusion reached here
will be confirmed by measuring the variation of the surface tension
with temperature and then evaluating thermodynamic quantities. Fur-
ther information will be obtained from similar investigations made
for combinations of different types of surfactants.

Acknowledgments

Literature Cited

1. Lange, H.; Beck, K. H. Kolloid Z. u. Z. Polymere 1973, 251, 424.
2. Clint, J. H. J. C. S. Faraday I 1975, 71, 1327.
3. Rubingh, D. N. In "Solution Chemistry of Surfactants"; Mitall, K. L., Ed.; Plenum: New York, 1979; Vol. I, p. 337.
4. Ingram, B. T.; Luckhurst, A. H. W. In "Surface Active Agents"; SCI Symposium Proceeding, SCI: London, 1979, p. 89.
5. Hua, X. Y.; Rosen, M. J. J. Colloid Interface Sci. 1982, 90, 212.
6. Zhu, B. Y.; Rosen, M. J. J. Colloid Interface Sci. 1984, 99, 435.
7. Lucassen-Reynders, E. H. J. Colloid Interface Sci. 1982, 85, 178.
8. Motomura, K.; Yamanaka, M.; Aratono, M. Colloid & Polymer Sci. 1984, 262, 948.
9. Aratono, M.; Uryu, S.; Hayami, Y.; Motomura, K.; Matuura, R. J. Colloid Interface Sci. 1983, 93, 164.
10. Uryu, S.; Aratono, M.; Yamanaka, M.; Motomura, K.; Matuura, R. Bull. Chem. Soc. Jpn. 1983, 56, 3219.
11. Uryu, S.; Aratono, M.; Yamanaka, M.; Motomura, K.; Matuura, R. Bull. Chem. Soc. Jpn. 1984, 57, 967.
12. Aratono, M.; Yamanaka, M.; Matubayasi, N.; Motomura, K.; Matuura, R. J. Colloid Interface Sci. 1980, 74, 489.
13. Motomura, K.; Iwanaga, S.; Hayami, Y.; Uryu, S.; Matuura, R. J. Colloid Interface Sci. 1981, 80, 32.
14. Moroi, Y.; Nishikido, N.; Matuura, R. J. Colloid Interface Sci. 1975, 50, 344.
15. Motomura, K.; Iwanaga, S.; Yamanaka, M.; Aratono, M.; Matuura, R. J. Colloid Interface Sci. 1982, 86, 151.
16. Motomura, K. J. Colloid Interface Sci. 1984, 102, 303.

13

The Effect of Alkyl Alcohols on the Surface Adsorption and Micellization of Fluorocarbon and Hydrocarbon Surfactants

Bu-Yao Zhu, Guo-Xi Zhao, and Jun-Gang Cui

Laboratory of Colloid Chemistry, Department of Chemistry, Peking University, Beijing, People's Republic of China

Mixed aqueous solution of alkyl alcohol-
$C_7F_{15}COONa$ (I) and alkyl alcohol-$C_{10}H_{21}SO_4Na$
(II) were investigated by surface tension
analysis. The cmcs of mixtures of (I) and
(II) were mostly lower than those of the two
pure surfactants, but the reduction of cmc
in the systems with fluorocarbon surfactant
is less than that with hydrocarbon surfac-
tant, although the cmcs of the fluorocarbon
surfactant and the hydrocarbon surfactant
are nearly the same. The saturated surface
adsorptions of the mixtures are larger than
those of the pure surfactants, and the
average molecular areas of the mixtures are
smaller accordingly. All these facts,com-
bined with the results of molecular inter-
action parameter calculations, show that
alcohol could enhance the adsorption and
micellization of both anionic surfactants;
also, the mutual phobicity between fluoro-
carbon and hydrocarbon chains is revealed
in the alkyl alcohol-$C_7F_{15}COONa$ systems.

The addition of an alkyl alcohol to the aqueous solution
of an ionic surfactant greatly influences the surface ac-
tivity of the surfactant. The critical micelle concen-
tration (cmc) of the surfactant becomes lower in presence
of alkyl alcohol, and the surface tension of the aqueous
solution at cmc reaches a much lower value (1-4).
However, no systematic investigation of adsorption and
micellization of the alcohol-fluorocarbon (FC) surfactant
mixture has been made. Other studies have examined the
"mutual phobicity" between the hydrocarbon (HC) and FC
chain in the mixed system of FC and HC surfactants (5-10)
It is expected that "mutual phobicity" should be observed
in the alkyl alcohol-FC surfactant system.too. In this

paper, surface chemical properties of mixed aqueous solution of alkyl alcohol (ROH)-$C_7F_{15}COONa$ (C_7FNa) and ROH-$C_{10}H_{21}SO_4Na$ ($C_{10}SNa$) have been investigated (R = $n-C_5H_{11}$, $n-C_6H_{13}$, $n-C_7H_{15}$, $n-C_8H_{17}$). The effect of ROH on the surface adsorption and micellization of C_7FNa and $C_{10}Sna$ were compared.

Experimental

The alkyl alcohols are of chemically pure grade and redistilled, boiling point range: $n-C_5H_{11}OH$ (C_5OH), 137.3-138.0°C; $n-C_6H_{13}OH$ (C_6OH), 156.8-157.1°C; $n-C_7H_{15}OH$(C_7OH), 175.8-176.0°C; $n-C_8H_{17}OH$ (C_8OH), 194.2-194.8°C.
     C_7FNa and $C_{10}SNa$ are the same as used in the previous works (5). The water used for preparing solutions was obtained from distillation of the ion-exchange water pretreated with potassium permanganate. Surface tension of the water (30°C) was 71.4 mNm^{-1} (the literature value is 71.18 mNm^{-1} (11)).
     Surface tension (30°C) of the solution was determined by the drop-volume method (12). The density of the solution needed for calculating the surface tension was measured by a U-tube pycnometer.

Results and Discussions

Surface Activity. It is obvious from the γ-log C plots (Fig.1 and 2) that the addition of alkyl alcohol results in lowering both the surface tension and the cmc. In particular, it is worth noting that the surface tension of the mixed solution at cmc,γ_{cmc}, is significantly lower than the surface tension at the pure surfactant cmc. Cmc and γ_{cmc} of 1:1 (molar ratio) ROH-Surfactant mixed systems were shown in Table 1. γ_{cmc} of ROH-C_7FNa solution reaches

Table 1. γ_{cmc} and cmc of 1:1 ROH-Surfactant
           Mixture Solutions (with NaCl,
           Ionic Strength: 0.1m; at 30°C)

ROH-Surfactant	γ_{cmc} (mNm^{-1})	cmc (m)
C_5OH-C_7FNa	20.8	1.45 X 10^{-2}
C_6OH-C_7FNa	16.0	1.35 X 10^{-2}
C_7OH-C_7FNa	16.2	7.70 X 10^{-3}
C_8OH-C_7FNa	17.4	3.30 X 10^{-3}
Pure C_7FNa	24.4	1.48 X 10^{-2}
$C_5OH-C_{10}SNa$	33.5	1.48 X 10^{-2}
$C_6OH-C_{10}SNa$	28.0	1.37 X 10^{-2}
$C_7OH-C_{10}SNa$	23.0	7.76 X 10^{-3}
$C_8OH-C_{10}SNa$	22.4	3.10 X 10^{-3}
Pure $C_{10}SNa$	37.4	1.53 X 10^{-2}

a minimum value of $\sim$16 mNm^{-1} (ROH = C_6OH and C_7OH) whereas the γ_{cmc} of C_7FNa solution is $\sim$24 mNm^{-1}, and the lowest value of γ_{cmc} of ROH-C_{10}SNa solution is about 22-23 mNm^{-1} (ROH = C_7OH and C_8OH). All these facts show that the surface activity of FC surfactant can be greatly enhanced by the addition of alkyl alcohols, this could be of great practical significance, because we may obtain higher surface activity using a smaller amount of expensive FC surfactant.

Surface Adsorption.   From Fig.1 and Fig.2 we can calculate the total surface adsorption (Γ_t) of the ROH-surfactant mixture by applying the Gibbs adsorption equation(7). In the case of a mixed aqueous solution with a constant ionic strength, the equation is written as

$$-d\gamma/RT = \Gamma_{C_7F^-(or\ C_{10}S^-)}\ d\ \ln\ m_{C_7F^-(or\ C_{10}S^-)} + \Gamma_{ROH}\ d\ \ln\ m_{ROH} \qquad (1)$$

where γ is the surface tension of solution, $\Gamma_{C_7F^-(or\ C_{10}S^-)}$ and Γ_{ROH} are the surface adsorptions of $C_7F_{15}COO^-$ (or $C_{10}H_{21}SO_4^-$) and ROH, respectively; m_{C_7F} and m_{ROH} are the molal concentrations (m) of C_7F^- and ROH in the solutions, respectively. For the 1:1 mixed solutionn

$$-d\gamma/RT = (\Gamma_{C_7F^-(or\ C_{10}S^-)} + \Gamma_{ROH})d\ \ln\ m_{ROH} = \Gamma_t\ d\ \ln\ m_{ROH} \qquad (2)$$

The surface tension-concentration relationships of the surfactant solutions at constant m_{ROH} are shown in Fig.3 and Fig.4. Under this condition (m_{ROH} kept constant) equation becomes

$$-d\gamma/RT = \Gamma_{C_7F^-(or\ C_{10}S^-)}\ d\ \ln\ m_{C_7F^-(or\ C_{10}S^-)}$$

and $\Gamma_{C_7F^-}$(or $\Gamma_{C_{10}S^-}$) may be calculated. From the intercept

Table 2.   Surface Adsorption and Molecular Areas of 1:1 ROH (1)-Surfactant (2) Solutions (with NaCl, Ionic Strength: 0.1 m; at 30°C)

Solution	$C_{1\ or\ 2}$ $(10^{-3}m)$	γ (mNm^{-1})	Γ_t	$\Gamma_{C_7F^-\ or\ C_{10}S^-}$ $(10\ mol.cm)$	X $(\Gamma_{C_7F^-\ or\ C_{10}S^-}/\Gamma_t)$	A $(\mathring{A}^2)$
C_7FNa-C_5OH	4.79	30.6	3.96	3.13	0.79	41.9
C_7FNa-C_6OH	3.31	31.5	4.38	2.89	0.66	37.9
C_7FNa-C_7OH	2.00	33.3	5.19	2.70	0.52	32.0
C_7FNa-C_8OH	0.603	39.0	5.69	2.33	0.41	29.2
C_7FNa	4.01	35.0		3.41		48.7
C_{10}SNa-C_5OH	3.98	47.0	4.41	3.62	0.82	37.6
C_{10}SNa-C_6OH	3.98	42.0	5.08	2.90	0.57	32.6
C_{10}SNa-C_7OH	1.20	48.0	5.66	2.29	0.45	29.4
C_{10}SNa-C_8OH	0.631	45.0	6.10	1.77	0.29	27.2
C_{10}SNa	6.60	45.0		3.65		45.0

point I in Fig.3 and 4, $\Gamma_t = \Gamma_{C_7F^-(or\ C_{10}S^-)} + \Gamma_{ROH}$, we can then obtain Γ_{ROH} from Γ_t and Γ_{C_7F} (or $\Gamma_{C_{10}S^-}$).
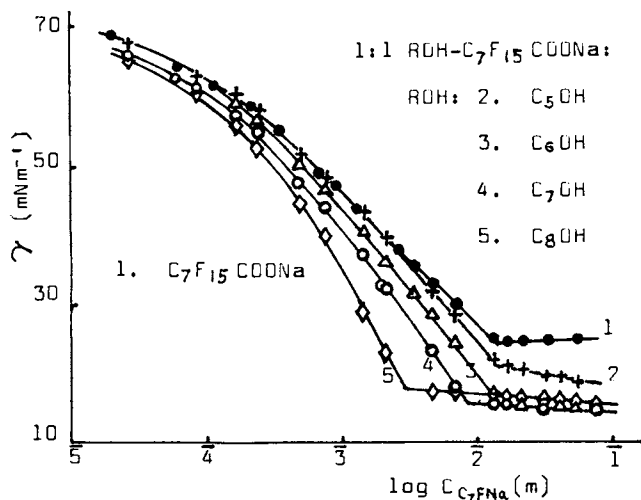
Figure 1.   Surface tension of aqueous solutions of
C_7FNa and 1:1 ROH-C_7FNa at 30°C (with NaCl, ionic
strength = 0.1 m).
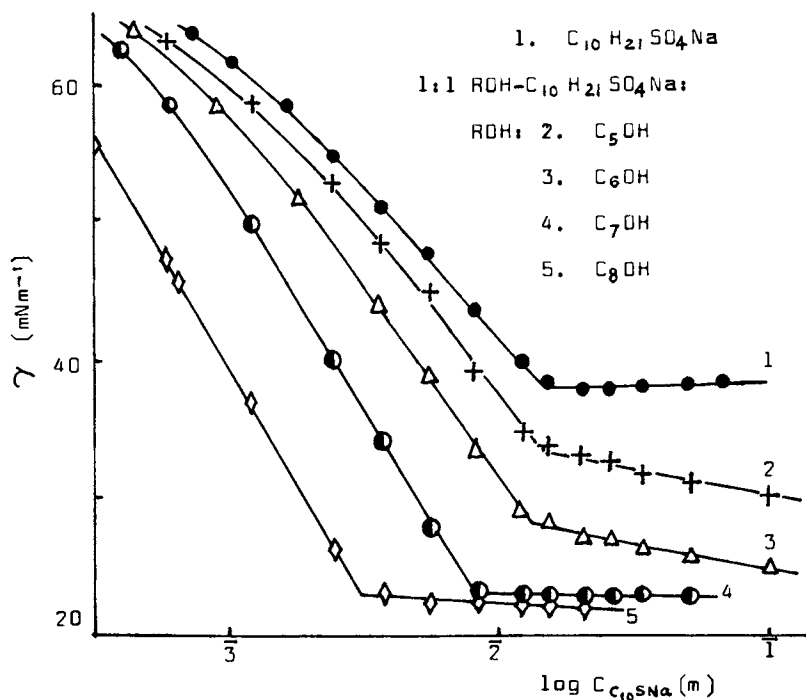
Figure 2.   Surface tension of aqueous solutions of
$C_{10}SNa$ and 1:1 ROH-$C_{10}SNa$ at 30°C (with NaCl, ionic
strength = 0.1 m).
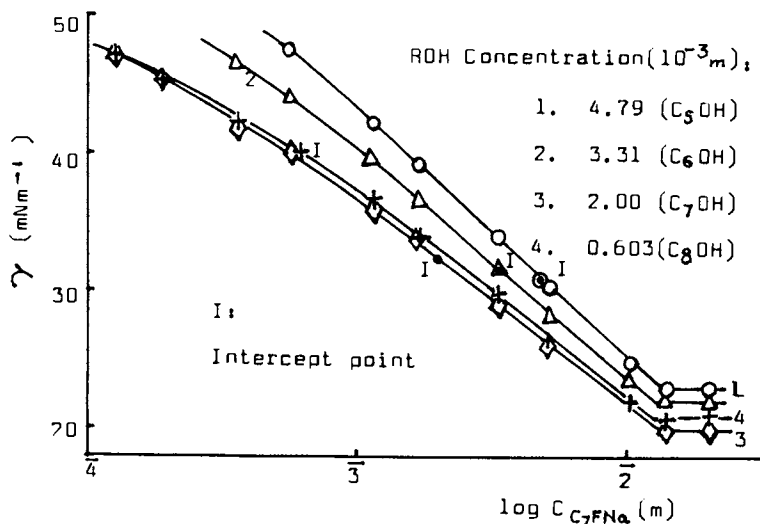
Figure 3. Surface tension of ROH-C$_7$FNa solutions at 30°C (with NaCl, ionic strength = 0.1 m; ROH concentration kept constant).
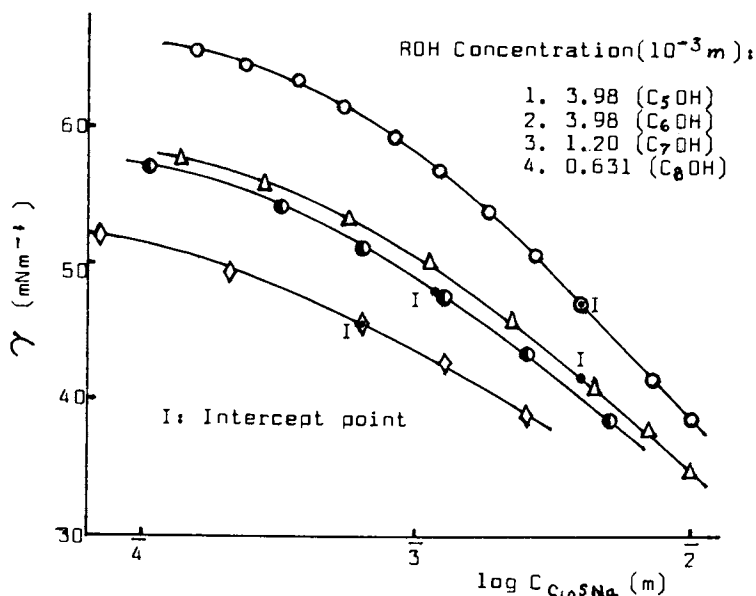
Figure 4. Surface tension of aqueous solutions of ROH-C$_{10}$SNa mixtures at 30°C (with NaCl, ionic strength = 0.1 m; ROH concentration kept constant).

The average molecular area (A) at the surface may be calculated by the following equation:

$$A = 1/\Gamma_t N_o \qquad (N_o = \text{Avogadro number})$$

The surface adsorption values are given in Table 2. The data show the strong effect of alcohol (especially those with longer hydrocarbon chains) on the surface adsorption of the surface active substances. The adsorption values given in the table are the saturation adsorption values. It is apparent that the adsorption of the ROH-surfactant mixture is much greater than that of pure surfactant, seemingly due to the penetration of the HC-chain of ROH into the C_7F^- (or $C_{10}S^-$) adsorption layer which has a loose packing of hydrophobic groups because of the repulsion between the surface active ions having the same charge and thus leaving enough room at the surface for ROH penetration. This results in the close-packing of the hydrophobic chains of ROH and the surfactant, leading to a very low surface tension of the aqueous solution.

We may calculate the surface adsorption of pure ROH (Γ^o_{ROH}) and pure surfactant ($\Gamma^o_{C_7F^-}$ and $\Gamma^o_{C_{10}S^-}$) corresponding to the 1:1 mixed solutions (the concentrations of surfactant and alcohol are equal). Table 3 shows the results. $\Gamma^o_{C_7F^-}$

Table 3.   Surface Adsorption of the pure Surfactant and ROH Solutions (with NaCl, ionic strength = 0.1 m; at 30°C)

C (10^{-3} m)	$\Gamma^o_{C_7F^-}$ (10^{-10} mol. cm^{-2})	Γ^o_{ROH}	C (10^{-3} m)	$\Gamma^o_{C_{10}S^-}$ (10^{-10} mol. cm^{-2})	Γ^o_{ROH}
4.79	3.41	2.13(C_5OH)	3.98	3.65	1.64(C_5OH)
3.31	3.41	3.24(C_6OH)	3.98	3.65	3.57(C_6OH)
2.00	3.28	4.76(C_7OH)	1.20	2.76	3.83(C_7OH)
0.603	3.17	4.83(C_8OH)	0.631	2.33	4.86(C_8OH)

and $\Gamma^o_{C_{10}S^-}$ were obtained from the γ-log C curves of the respective pure surfactant solutions in Fig.1 and 2, and Γ^o_{ROH}'s from Fig.5.

It is obvious from the data that the total surface adsorption of 1:1 mixed solution (Γ_t) is less than the sum of the surface adsorptions of pure surfactant and ROH solutions. Similarly, $\Gamma_{C_7F^-}$ (or $\Gamma_{C_{10}S^-}$) is less than $\Gamma^o_{C_7F^-}$ (or $\Gamma^o_{C_{10}S^-}$) and Γ_{ROH} less than Γ^o_{ROH}, too (e.g., for 1:1 C_7FNa-C_8OH system, $\Gamma_{C_7F^-}$ = 2.33x10^{-10} mol·cm^{-2} < $\Gamma^o_{C_7F^-}$ = 3.17x10^{-10} mol·cm^{-2} ; $\Gamma^o_{C_8OH}$ = 3.36x10^{-10} mol·cm^{-2} < $\Gamma^o_{C_8OH}$ = 5.03x10^{-10} mol·cm^{-2} ; and so forth for other systems). These results imply that although it is mainly the co-adsorption of ROH with ionic surfactant which enhances the total surface adsorption to attain a higher surface activity, there is also adsorption competition to some extent between ROH and ionic surfactant at the surface.
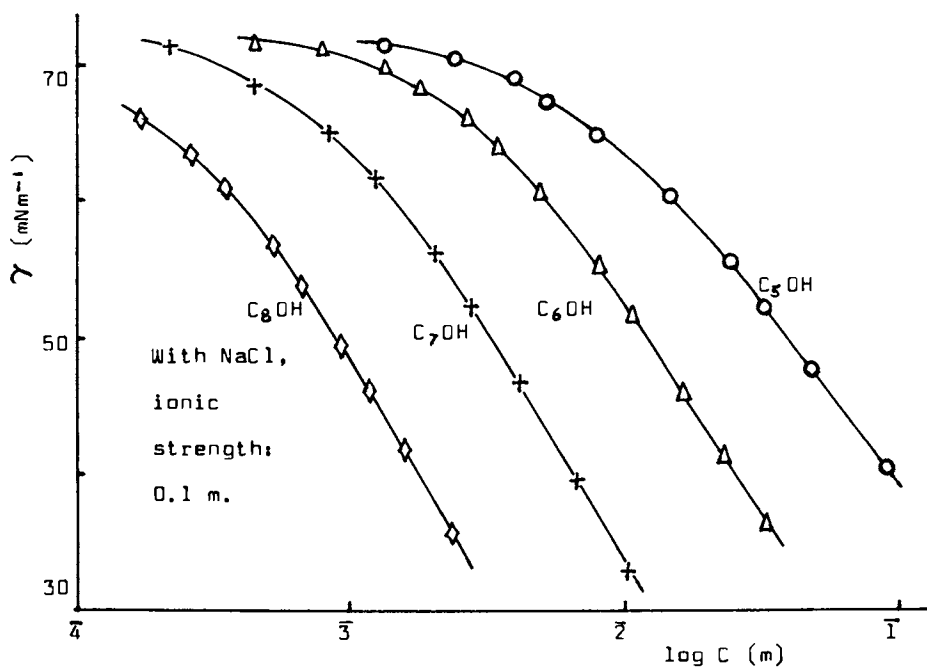
Figure 5. Surface tension of aqueous solutions of ROH at 30°C.

It is interesting to note that C_7FNa-ROH mixture packs more loosely than $C_{10}SNa$-ROH mixture in the saturated adsorption layer. Taking C_8OH-C_7FNa and C_8OH-$C_{10}SNa$ as the model system and the average molecular areas of C_8OH, C_7F^- and $C_{10}S^-$ to be 26.2 (from saturation adsorption value of C_8OH), 26 and 31 (both from molecular structure calculations) $\AA^2$, respectively. We can calculate the ideal average surface molecular area of C_8OH-C_7FNa mixture as $A_F = 26.2 X_{C_8OH} + 26 X_{C_7F^-} = 26.2 \times 0.59 + 26 \times 0.41 = 26.1 \AA^2$ and that of C_8OH-$C_{10}SNa$ mixture as $A_H = 26.2 X_{C_8OH} + 31 X_{C_0S} = 26.2 \times 0.71 + 31 \times 0.29 = 27.6 \AA^2$. Comparing with the real molecular area values (in Table 2) of 29.2 and 27.2, respectively, we can see that for the C_8OH-$C_{10}SNa$ system the calculated and the real molecular area values are nearly equal ($27.6 \approx 27.2$), but that for C_8OH-C_7FNa system the real molecular area value is larger than the calculated one ($29.2 > 26.1$). This seems to demonstrate the existence of "Mutual phobicity" between FC and HC chains in the adsorption layer of the C_8OH-C_7FNa mixture.

Molecular Interaction in the Surface Adsorption Layer. In order to elucidate the effect of alkyl alcohol on the surface adsorption of C_7FNa and $C_{10}SNa$, it is useful to calculate the surface molecular interaction parameters of the binary surface active mixtures (β_s) according to the equation at constant surface tension and constant ionic strength (13,14,10):

$$\beta_s = \ln (C_1/C_1^o X_{1S})/X_{2S}^2 = \ln (C_2/C_2^o X_{2S})/X_{1S}^2 \qquad (3)$$

where C_1^o and C_2^o are the solution concentrations of pure surface active substances 1 and 2, respectively; C_1 and C_2 are the concentrations of components 1 and 2 in the mixed solution and X_{1S} and X_{2S}, the surface mole fractions of 1 and 2, respectively.

The β_s-values of C_7FNa-ROH and $C_{10}SNa$-ROH systems are shown in Table 4, together with the relevant mole

Table 4. β_s-values and Surface Mole Fractions (X) of Surfactants in 1:1 Surfactant-ROH Systems

System	γ (mNm^{-1})	X	β_s	System	γ (mNm^{-1})	X	β_s
$C_{10}SNa$- C_8OH	40	0.31	-2.8	C_7FNa- C_8OH	40	0.47	-1.5
	50	0.33	-2.1		50	0.56	-0.9
	60	0.34	-1.3		60	0.69	-0.4
$C_{10}SNa$- C_7OH	40	0.44	-2.5	C_7FNa- C_7OH	40	0.65	-1.6
	50	0.48	-1.8		50	0.73	-1.3
	60	0.54	-1.1		60	0.80	-1.4
$C_{10}SNa$- C_6OH	40	0.59	-2.2	C_7FNa- C_6OH	40	0.79	-2.0
	50	0.65	-1 6		50	0.87	-1.4
	60	0.72	-1.4		60	0.96	-0.5

fractions of the surfactants. Table 4 shows that all the
β_s-values are negative, denoting the obvious surfactant-
ROH molecular interactions. It is also shown that the
negative β_s-values increase with the surface pressure of
the mixed solution for all systems. This may be reasona-
bly attributed to the stronger interactions between the
two components at the surface with a higher surface pres-
sure (concomitantly with a closer packing of the surface
adsorption molecules). It is interesting to compare the
data of the C_7FNa-ROH system with those of the $C_{10}SNa$-ROH
system. $|\beta_s|$-values of C_7FNa-ROH mixtures are always
smaller than $C_{10}SNa$-ROH, although C_7FNa is more surface
active than $C_{10}SNa$ (e.g., for C_7FNa-C_8OH and $C_{10}SNa$-C_8OH
systems, β_s-values are -1.47 and -2.75, respectively, at
$\gamma = 40$ mNm^{-1}). This clearly demonstrates the "Mutual
phobicity" between FC and HC chains in the mixed adsorp-
tion layer. It is also worth noting that the variation
of β_s-values for the series of alkyl alcohols for the
C_7FNa-ROH systems is entirely different from that in
$C_{10}SNa$-ROH systems. At a given surface tension, say,
40 mNm^{-1}, β_s-value of $C_{10}SNa$-ROH system varies in the
sequence: -2.00, -2.19, -2.47, -2.75 as ROH is C_5OH, C_6OH,
C_7OH, C_8OH ($|\beta_s|$-value increasing); but that of C_7FNa-ROH
systems varies in the sequence: -1.98, -1.56, -1.47 as
ROH is C_6OH, C_7OH and C_8OH (the β_s-value for C_7FNa-C_5OH
system can not be calculated because the γ-log C curve
of 1:1 mixture coincides with that of pure C_7FNa solution).
This result appears to be due to the "Mutual phobicity"
between FC and HC chains in the mixed surface layer. For
the $C_{10}SNa$-ROH system, the hydrophobic interactions bet-
ween HC chains of $C_{10}SNa$ and ROH increase with the chain
length of ROH, and the $|\beta_s|$-value for $C_{10}SNa$-C_8OH is the
greatest. In C_7FNa-ROH systems, however, the interaction
between FC and HC chains become weaker as the HC chain
length of ROH is increased, owing to the larger difference
between the solubility parameters of FC chain and a lon-
ger HC chain (16) (we may consider the surface layer as a
FC-HC mixture). For the C_7FNa-C_8OH system there would be
a stronger "Mutual phobicity" and a smaller $|\beta_s|$-value.

<u>Mixed Micelle Formation with Alkyl Alcohol</u>. From the
data in Table 1, it is obvious that the cmc values of both
C_7FNa and $C_{10}SNa$ are lowered. Is there any difference
between the effect of ROH on the micellization of C_7FNa
and $C_{10}SNa$ in the aqueous solutions? Taking ROH as a
solubilizate we may investigate the distribution of it
between the micelle and the aqueous solution.
    Assuming the phase separation model of micelles, ba-
sed on the thermodynamics of phase equilibrium and the
principle of diffuse electric double layer, the equation
for micelle formation is as follows (3,15):

$$\ln C_i = K_o (\ln \sigma^2 - \ln C_i^*) + A_2 \qquad (4)$$

where C_i is the cmc of surfactant i; C_i^*, the concentration

of the counterion of the surfactant; K_o, the constant concerning the degree of counterion binding to the micelle; σ, the surface charge density of the micelle and A_2, a constant of the system. For simplification, it is assumed that the surface charge density of the micelle does not change appreciably when the alcohol molecules are solubilized into the micelle. Then the equation for the micelle formation may be written as

$$\ln C_M = K_o (\ln \sigma^2 - \ln C_M^i) + \ln X_s + A_2 \qquad (5)$$

where C_M and C_M^i are the cmc and counterion concentration of the mixed solution, respectively; X_s is the mole fraction of surfactant in the micelle. In this work, the counterion concentrations of all solutions are made constant ($C_i^i = C_M^i = (Na^+) = 0.1$ m). Then combining equations (4) and (5) we have

$$\ln (C_M/C_i) = \ln X_s = \ln (1 - X_a) \qquad (6)$$

where X_a is the mole fraction of ROH in the micelle; then

$$X_a = 1 - (C_M/C_i) \qquad (7)$$

The mole fraction of ROH in the mixed solution ((Na^+) = 0.1 m) is

$$X_a^i = C_M/(55.5 + 0.1 + 2C_M) \qquad (8)$$

and the distribution coefficient (D) of ROH between the micellar and the aqueous solution phases is

$$D \cong X_a/X_a^i = (1/C_M - 1/C_i)(55.6 + 2C_M) \qquad (9)$$

In case of $C_M \ll 0.1$, equation (9) becomes

$$D \cong 55.6 (1/C_M - 1/C_i) \qquad (10)$$

and D can be conveniently evaluated.

Table 5 shows the evaluated distribution coefficients of the homologous alkyl alcohols. It is shown that the

Table 5. Distribution Coefficients of ROH between Micelles and Aqueous Solutions (at 30 C)

ROH \ Surfactant	C_5OH	C_6OH	C_7OH	C_8OH
C_7FNa	0.77x10 (0.020)*	3.67x10^2 (0.088)*	3.46x10^3 (0.48)*	1.31x10^4 (0.78)*
$C_{10}SNa$	1.83x10 (0.033)*	4.24x10^2 (0.11)*	3.53x10^3 (0.49)*	1.43x10^4 (0.80)*

* Mole fraction of ROH in the micelle, X_a.

distribution coefficient of an alcohol in the FC surfactant system is smaller than that in the HC surfactant system; i.e.,the alcohol is less solubilized in C_7FNa micelles than in $C_{10}SNa$ micelles. This is also evidenced by the smaller mole fraction of ROH (X_a) in the C_7FNa micelles. This is probably another example of the "Mutual phobicity" between FC and HC chains in the mixed C_7FNa-ROH system.

Conclusion

The addition of an alkyl alcohol, even a small amount (particularly an alcohol with a long chain), to a FC or a HC surfactant leads to a great enhancement of the surface activity of the surfactant—both cmc and γ_{cmc} are largely lowered. It is of practical significance in obtaining a FC and HC mixture having a much higher surface activity than the FC surfactant alone. Such a high surface activity of the mixture should be attributed to the great adsorption and hence the close-packing of hydrophobic chains in the adsorption layer, which results in a surface of sufficiently low energy, leading to the very low values of γ_{cmc}.
        The effect of alkyl alcohol on the surface adsorption and micellization of FC surfactant is noticeably different from HC surfactant. The molecular interactions between ROH and C_7FNa in the surface layer are shown to be weaker (Smaler $|\beta_s|$-value) as compared with ROH-$C_{10}SNa$ system. The cmc reduction degree of C_7FNa by ROH is less than that of $C_{10}SNa$. The distribution coefficients of ROH between the micelle and the aqueous solution have a smaller value in the ROH-C_7FNa system. All these facts show the existence of "Mutual phobicity" between FC and HC chains at the surface and in the micelles.

Literature Cited

1.   Brady, A. P.; Brown, A. G. in "Monomolecular Layers";
     Sobotka, H., Ed., Am.Assn.Adv.Sci., Washington, D.C.
     (1954), Chap. 3.
2.   Harkins, W. D. "Physical Chemistry of Surface Films";
     Reinhold, New York, 1954; Chap. 4.
3.   Shinoda, K. in "Colloidal Surfactants"; Academic Press,
     New York, 1963; Chap. 1.
4.   Zhao, G.-X. "Physical Chemistry of Surfactants";
     Peking University Publ., Beijing, 1984; Chap. 5.(Ch.)
5.   Zhu, B.-Y.; Zhao, G.-X. Acta Chimica Sinica, 1981, 39,
     493.(Ch.)
6.   Zhu, B.-Y.; Zhao, G.-X. Acta Chimica Sinica, 1982, 40,
     588.(Ch.)
7.   Zhao, G.-X.; Zhu, B.-Y.; Zhou, Y.-P.; Shi, L. "Acta
     Chimica Sinica", 1984, 42, 416.(Ch.)
8.   Mukerjee, P.; Mysels, K.J. in "Colloidal Dispersion
     and Micellar behavior", ACS Symp., 1975; p.239.
9.   Shinoda, K.; Nomura, T. J.Phys. Chem., 1980, 84, 365.
10. Zhao, G.-X.; Zhu, B.-Y., This Symposium.

11. "International Critical Tables", McGraw-Hill, New
     York, 1928; Vol.4, p.447.
12. Zhu, B.-Y.; Zhao, G.-X. Hua Xue Tong Bao, 1981(6), 341.
13. Rosen, M.J.; Hua, X.-Y. J.Colloid Interface Sci.,
     1982, 86, 164.
14. Rosen, M.J.; Zhu, B.-Y. J.Colloid Interface Sci.,
     1984, 99, 427.
15. Zhao, G.-X., "Physical Chemistry of Surfactants", (in
     Chinese), Peking Univ. Publ., Beijing, 1984; Chap. 4
     and 5.
16. Shinoda, K., "Principles of Solution and Solubility",
     Marcel Dekker, New York, 1978; Chap. 4.

14

Surface Adsorption and Micellization of the Mixed Solution of Fluorocarbon and Hydrocarbon Surfactants

Guo-Xi Zhao and Bu-Yao Zhu

Laboratory of Colloid Chemistry, Department of Chemistry, Peking University, Beijing, People's Republic of China

Various systems of fluorocarbon and hydro-
carbon surfactant mixtures were investiga-
ted. By considering the effect of counter-
ion on the interactions between the surface
active ions, the general equation for cal-
culating the interaction parameters in the
micelle (β_m) and at the surface (β_σ) have
been obtained and applied to the mixed sysb
tems. It is shown that: (1) the "mutual
phobicity" between FC- and HC-chains is
clearly illustrated by the positive β_σ-
values for the anionic-anionic and non-
ionic-nonionic surfactant mixtures, and by
the positive deviation of mixture cmc data
from ideal solution theory; (2) for the
cationic-anionic surfactant mixtures there
are significant synergism and very large
negative values of β_m and β_σ, indicating
the great molecular interactions between
them; (3) considerable interactions exist
in the ionic-nonionic FC- and HC-surfac-
tants system; (4) β_σ-value obviously increa-
ses with the surface pressure of the mixed
solutions (especially in the systems with
stronger interactions).

The fluorocarbon (FC) surfactants possess many salient
features which can not be found in the common hydrocarbon
(HC) surfactants. They are extremely surface active.
Dilute aqueous solution may have surface tension values
as low as ~ 15 mNm^{-1}. They are chemically stable and
resistant to heat. The FC-surfactant surface layer
formed on a solid renders the solid surface not only
hydrophobic but also leophobic. Recently more attention
was paid to the investigation of FC-surfactants and mix-
tures of FC- and HC-surfatants (1-9) partly because of

the practical importance of surfactant mixture with higher
surface activity but lower price than the FC-surfactant
itself, and partly because of the theoretical importance
of understanding the peculiarities of the interactions
between the CF- and CH-surfactants. These investigations
have shown that unlike the common HC-surfactant mixtures,
frequently the FC- and HC-surfactant mixtures cannot form
the entirely miscible micelles in the mixed solution, but
essentially the individual micelles of the single surfac-
tant. Some of the systems of FC- and HC-surfactants
exhibit extraordinary high interfacial and surface activi-
ty, hence such a mixed aqueous solution is capable of
spreading on an oil surface (9), and can be used as a
component in fire-extinguisher formulations. In order to
understand further the essential nature of the peculiari-
ties of the mixed FC- and HC-surfactants system, in this
investigation the surface adsorption and micelle forma-
tion of some mixed solutions of various type FC- and HC-
surfactants and the molecular interactions at the inter-
face and in micelles were studied.

Experimental

Perfluorooctanoic acid ($C_7F_{15}COOH$, C_7FH), sodium perfluo-
rooctanoate ($C_7F_{15}COONa$, C_7FNa), sodium decylsulfate
($C_{10}H_{21}SO_4Na$, $C_{10}SNa$), sodium dodecylsulfate ($C_{12}H_{25}SO_4Na$,
$C_{12}SNa$), octyltrimethylammonium bromide ($C_8H_{17}N(CH_3)_3 Br$,
C_8NBr), n-heptane, sodium chloride and sodium bromide are
all the same as used in the previous works (4-7). Triton
X-100: Rohm & Haas product ($t-C_8H_{17}-C_6H_4O(C_2H_4O)_{10}H$, TX-
100). "6203" ($C_{10}F_{19}O(C_2H_4O)_9H$): supplied by Shanghai
Institute of Organic Chemistry. Octylmethyl sulfoxide
($C_8H_{17}SOCH_3$, C_8SOC) and decylmethyl sulfoxide ($C_{10}H_{21}SOCH_3$,
$C_{10}SOC$): synthesized in our laboratory by the thioether-
oxidation method (with H_2O_2)(10), and purified by repeated
recrystallization from petroleum ether. The water used
was the distilled deionized water ($KMnO_4$-treated).
Surface tension and interfacial tension (n-heptane/H_2O)
were determined by the drop-volume method (11). The
density of solutions for calculating surface and interfa-
cial tension were measured with a U-tube pycnometer.

Theoretical background

The micellization of the surfactant in an aqueous solution
can be regarded as a phase separation process (4,12). At
equilibrium, the chemical potential of surfactant compo-
nent i, μ_i, is equal to that in the micelle (μ_{im}):

$$\mu_i = \mu_{im}$$

In the solution of a single surfactant

$$\mu_i^o + RT \ln a_i = \mu_{im}^o \tag{2}$$

In the solution of surfactant mixture

$$\mu_i^o + RT \ln a_i = \mu_{im}^o + RT \ln f_{im} X_{im} \tag{3}$$

where a_i is the activity of component i monomer in the solution; f_{im} and X_{im} are the activity coefficient and mole fraction of i in the micelle, respectively.

In general, the solution concentration of a surfactant at cmc (critical micelle concentration) is dilute enough to assume that molality equals activity; equations (2) and (3) become

$$\mu_i^o + RT \ln cmc_i^o = \mu_{im}^o \tag{4}$$

$$\mu_i^o + RT \ln cmc_i = \mu_{im}^o + RT \ln f_{im} X_{im} \tag{5}$$

in which cmc_i^o is the cmc of the pure surfactant i; cmc_i, the concentration of surfactant i monomer at cmc of the mixed solution.

For the ionic surfactants (1-1 type), we should take account of the electrically charged species and the possibility of doing electrical work. The micelle may be regarded as a charged pseudo-phase, and the chemical potential is replaced by the electrochemical potential (12). The effective electrical work in micelle formation is

$$N_o K_i e \psi = K_i RT (\ln (2000 \pi \sigma^2 / DRT) - \ln C_i') \tag{6}$$

in which N_o is the Avogardro number, K_i is a constant relating to degree of counterion binding to the micelle of surfactant i; e, the electronic charge; D, the dielectric constant; C_i', the counterion concentration; and σ is the surface charge density of the micelle. Then from Eqns. (4) and (5) we have

$$\ln cmc_i^o = A_o - K_i \ln C_i' \tag{7}$$

$$\ln (cmc_i / f_{im} X_{im}) = A_o - K_i \ln C_i^m \tag{8}$$

in which A_o is a constant ($= (\mu_{im}^{o'} - \mu_i^{o'})/RT + K_i \ln (2000 \pi \sigma^2 / DRT))$, C_i^m, the concentration of counterion in the mixed solution. Combining Eqns. (7) and (8), we have

$$f_{im} X_{im} = (cmc_i / cmc_i^o)(C_i^m / C_i')^{K_i} \tag{9}$$

For binary mixture systems, a simple f_{im} - X_{im} relationship may be obtained from solution theory:

$$\ln f_{1m} = \beta_m X_{2m}^2 \tag{10}$$

and $$\ln f_{2m} = \beta_m X_{1m}^2 \tag{10}$$

in which β_m is the molecular interaction parameter between two surfactants in the micelle. Combining these two relationships with Equation 9.,we obtain

$$\beta_m = \ln \left(\frac{cmc_1}{cmc_1^\circ X_{1m}}\left(\frac{C_1''}{C_1'}\right)^{K_1}\right) / X_{2m}^2 = \ln \left(\frac{cmc_2}{cmc_2^\circ X_{2m}}\left(\frac{C_2''}{C_2'}\right)^{K_2}\right) / X_{1m}^2$$

(11)

From the various concentration values and K_1, K_2 (in general, based on the theoretical and experimental results (12,14), K_i values for various 1-1 ionic surfactants are approximately ~ 0.6), equation (10) can be solved iteratively for X_{1m} and X_{2m}, and β_m is obtained simultaneously.

In the case where excess inorganic salt is added or the counterion concentration is held constant, i.e. $C_i' = C_i''$, then equation (10) becomes

$$\beta_m = \ln \left(cmc_1 / cmc_1^\circ X_{1m}\right) / X_{2m}^2 = \ln \left(cmc_2 / cmc_2^\circ X_{2m}\right) / X_{1m}^2$$

(12)

This equation is applied to the nonionic surfactant system as well.

In the case of surface adsorption, at constant surface tension of solutions, an equation of the same form as equation 12 is obtained for the binary surfactant mixture system (15,16):

$$\beta_\sigma = \ln \left(C_1 / C_1^\circ X_{1\sigma}\right) / X_{2\sigma}^2 = \ln \left(C_2 / C_2^\circ X_{2\sigma}\right) / X_{1\sigma}^2$$

(13)

in which β_σ is the molecular interaction parameter in the surface layer; C_1 and C_2 are the concentration of surfactant 1 and 2 in the mixed solutions, respectively; C_1° and C_2° are the concentrations of single surfactant 1 and 2, respectively; $X_{1\sigma}$ and $X_{2\sigma}$ the surface mole fractions of surfactant 1 and 2 respectively. Equation (13) can be applied only to systems with excess salt or constant counterion concentration. This equation is also applicable to nonionic surfactant systems.

In the case where no excess salt is added to the binary ionic surfactants system, assuming that the nature of the diffuse electrical double layer of the surface is similar to that of the micelle, the following equation can be obtained

$$\beta_\sigma = \ln \left(\frac{C_1}{C_1^\circ X_{1\sigma}}\left(\frac{C_1''}{C_1'}\right)^{K_1'}\right) / X_{2\sigma}^2 = \ln \left(\frac{C_2}{C_2^\circ X_{2\sigma}}\left(\frac{C_2''}{C_2'}\right)^{K_2'}\right) / X_{1\sigma}^2$$

(14)

in which K_1' and K_2' are constants relevant to the counterion binding of the fixed "Stern layer" (similar to the counterion binding constant of the micelle). As a first approximation, we may assume $K_i' \doteq K_i = 0.6$, then β_σ and $X_{i\sigma}$ can be calculated.

Results and Discussions

$C_7FNa-C_{10}SNa$ and $C_7FNa-C_{12}SNa$ systems.

These are the mixed anionic-anionic surfactants systems. The surface tension (interfacial tension) - concentration relationships are shown in Fig. 1 to 3. There are surfactant compositions at which uniform or homogeneous mixed micelle do not exist in these two systems due to the "mutual phobicity" between FC- and HC-chains of the surfactants (4,7) Therefore the molecular interaction parameter, β_m, of the two surfactants in micelles can not be calculated from the surface tension curves because this cmc has no longer the physical meaning of mixture cmc. However, we can obtain the β_σ values from the surface tension curves by means of equation 13. Table 1 and 2 show the results.

The β_σ-values are all positive, which is to say, the activity coefficient of the surfactants in the surface phase are greater than 1, clearly indicating the "mutual phobicity" between FC- and HC-chains of the surfactants. However, the positive values of β_σ are considerably small, showing a rather weak mutual-phobic interaction.

For the surface adsorption of binary mixed solution at a constant ionic strength, the Gibbs equation is (6)

$$-d\gamma/RT = \Gamma_1 d \ln C_1 + \Gamma_2 d \ln C_2 \qquad (15)$$

where Γ_1 and Γ_2 are the surface adsorptions of surface active ion 1 and 2, respectively; C_1 and C_2 the molal concentrations of 1 and 2, respectively. At a constant molal ratio (i.e., C_1/C_2 = constant), we have

$$-d\gamma/RT = (\Gamma_1 + \Gamma_2) \, d \ln C_{1(or\ 2)} \qquad (16)$$

When the concentration of component 1 is kept constant,

$$\Gamma_2 = (-1/RT)(d\gamma/d \ln C_2)_{C_1} \qquad (17)$$

The surface mole fractions can be defined as

$$X'_{1\sigma} = \Gamma_1/\Gamma_t \qquad (18_a)$$

$$X'_{2\sigma} = (\Gamma_t - \Gamma_1) / \Gamma_t = \Gamma_2 / \Gamma_t \qquad (18_b)$$

Hence the surface adsorption of surfactant 1 and 2, and their surface mole fractions can be obtained from the surface (interfacial) tension-concentration relationships (Fig.1 and fig.2) by applying the Gibbs adsorption equation.

The calculated data of $X'_{2\sigma}$ are also shown in table 1, which is essentially the same as $X_{2\sigma}$ obtained from calculation (equation 13). The fact that $X_{2\sigma}$ is nearly equal to $X'_{2\sigma}$ indicates the reasonableness and usefulness of the theory of molecular interactions.

It is worth noting that at air/water surface the surface mole fraction $X_{2\sigma}$ ($C_{10}SNa$) is much less than the
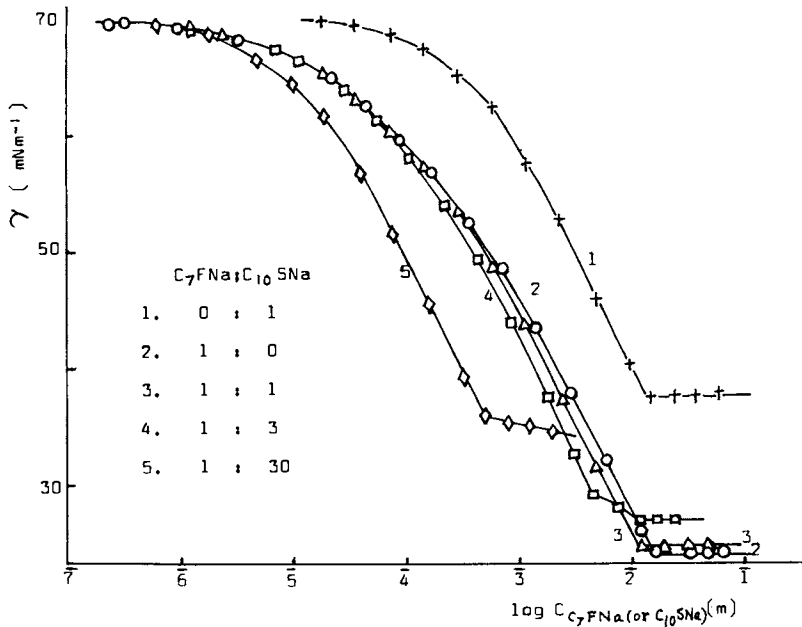
Figure 1. Surface tension of aqueous solutions of $C_7FNa-C_{10}SNa$ system at 30°C with NaCl, ionic strength = 0.1 m; C = C_{C_7FNa}, except curve 1).
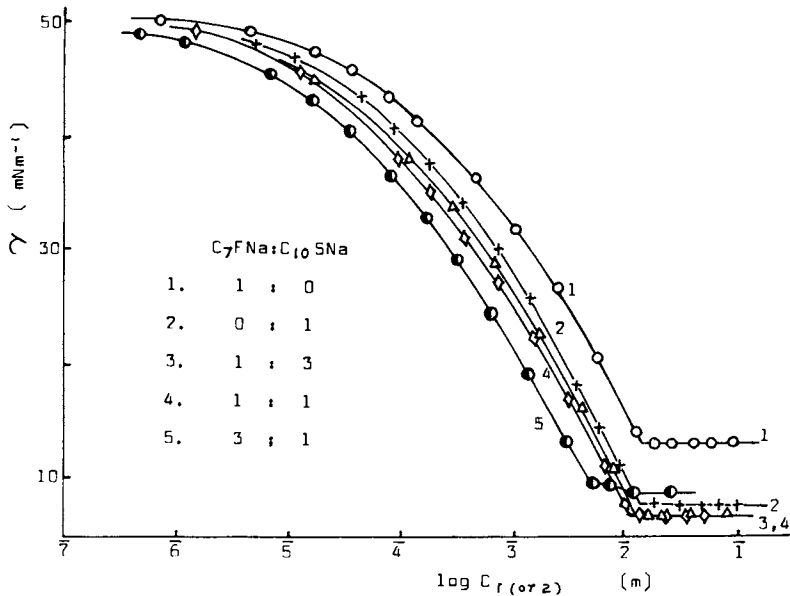
Figure 2. Interfacial tension of n-heptane/aqueous solutions of $C_7FNa-C_{10}SNa$ mixtures at 30°C (with NaCl, ionic strength = 0.1 m; C = $C_{C_{10}SNa}$, except curve 1).

Table 1. β_σ-values of C_7FNa-$C_{10}SNa$ System
(with NaCl, ionic strength = 0.1 m, 30°C)

C_7FNa:$C_{10}SNa$ (1) (2)	C_1 (10^{-3} m)	X_2 Eqn(13)	X'_2 Eqn(18b)	β_σ	γ (mNm^{-1})
air/water surface ($C^\circ_1 = 1.94\times10^{-3}$m; $C^\circ_2 = 8.81\times10^{-3}$m)					
1 : 1	1.75	0.11	0.07	+0.79	41.5
1 : 3	1.32	0.37	0.39	+0.51	41.5
1 : 10	0.641	0.71	0.60	+0.28	41.5
n-heptane/water interface($C^\circ_1 = 5.96\times10^{-3}$m; $C^\circ_2 = 2.88\times10^{-3}$m)					
3 : 1	3.57	0.41	0.43	+0.05	20.3
1 : 1	2.08	0.70	0.70	+0.33	20.3
1 : 3	0.82	0.87	0.85	+0.06	20.3

Table 2 β_σ-values of 1:1 C_7FNa-$C_{12}SNa$ System
(with NaCl, ionic strength = 0.1 m, 30°C)

C_1(C_7FNa) (10^{-5}m)	C°_1(C_7FNa) (10^{-5}m)	C°_2($C_{12}SNa$) (10^{-5}m)	X_1 (C_7FNa)	β_σ	γ (mNm^{-1})
6.49	14.7	8.03	0.24	+1.0	60.0
26.9	85.1	28.1	0.05	+2.0	50.0
78.9	317	82.1	0.04	+2.0	40.0

Table 3. β_σ-values of "6203"(1)-TX100(2) System (25°C)

γ(mNm^{-1})	C°_1 (10^{-6} m)	C (10^{-5} m)	C (10^{-5}m)	C (10^{-5}m)	$X_{2\sigma}$	β_σ
1:1 system :						
30	24.0	25.1	15.8	15.8	0.48	+1.0
40	7.24	8.91	4.90	4.90	0.41	+0.8
50	2.24	3.09	1.58	1.58	0.37	+0.8
1:3 system:						
30	24.0	25.1	6.46	19.4	0.76	+0.23
40	7.24	8.91	2.34	7.03	0.77	+0.56
50	2.24	3.09	0.832	2.5	0.77	+0.83

Table 4 β_σ-values of C_8NBr(1)-C_7FNa(2) System
(with NaBr, ionic strength = 0.1 m, 30°C)

(1) : (2)	C_1* (10^{-5}m)	$X_{1\sigma}$ Eqn (13)	$X_{1\sigma}$ Eqn (18a)	β_σ	γ (mNm^{-1})
1 : 100	19.5	0.14	0.21	-11.5	52.7
1 : 10	9.80	0.24	0.29	-13.5	"
1 : 1	3.72	0.33	0.30	-15.0	"
10 : 1	2.40	0.39	0.39	-13.3	"
100 : 1	1.02	0.46	0.44	-12.9	"
1 : 1	2.30	0.30	0.27	-12.0	60.0

* At γ = 52.7 mNm^{-1} , C°_1 = 0.100 m, C°_2 = 2.82$\times10^{-4}$ m;
At γ = 60.0 mNm^{-1} , C°_1 = 2.88$\times10^{-2}$m, C^a_2 = 9.70$\times10^{-5}$ m.

bulk mole fraction, whereas at n-C_7H_{16}/water interface the reverse is the case; e.g., with the 1:1 solution bulk mole fraction of C_{10}SNa is 0.5, and X_2 is 0.11 at the surface , 0.7 at the interface. There is preferential adsorption of C_{10}SNa at the interface although C_{10}SNa is less surface active than C_7FNa. This may be due to the "mutual phobicity" between FC-chain of C_7FNa and CH-chain of n-C_7H_{16} of the oil phase, thus C_{10}SNa adsorbs preferentially at the interface.

"6203"-TX100 (nonionic-nonionic) system. From Fig.4 some β_σ and X_σ values are evaluated and shown in Table 3. (again the β_m value can not be calculated because no miscible mixed micelle is formed). Two break points in the curves of 1:1 and 1:3 "6203"-TX100 mixed solutions are noted. This implies there would be two cmcs and hence two kinds of micelle may be present in the mixed solutions (4,5). The two cmc values of the 1:1 solution are 5.14x 10^{-4} m ("6203") and 2.75x10^{-4} m (TX100); the 1:3 solution, 5.01x10^{-4} m ("6203") and2.61x10^{-4}(TX100). It is noted that the values of 5.14x10^{-4} m and 5.01x10^{-4} m are close to the cmc of pure "6203" (4.78x10^{-4} m) and 2.75x10^{-4} m and 2.61x 10^{-4} m, close to the cmc of pure TX100 (2.57x10^{-4} m) —— an obvious evidence of the existence of two kinds of micelle in a mixed solution (4,7).

The β_σ in Table 3 are all small positive values. It once again clearly shows the mutual phobic interaction between FC- and HC-chains of the surfactants.

C_8NBr-C_7FNa (cationic-anionic) system. The common catー ionic-anionic mixture of HC surfactants is highly surface active (17), showing the strong interactions between the two oppositely charged surface active ions. Similar results have been observed in the case of C_8NBr-C_7FNa system. The γ-log C plot in Fig.5 illustrates such an interaction. We can see that the 1:1 C_8NBr-C_7FNa mixture is much more surface active than C_8NBr or C_7FNa. The cmc value of surfactants mixture is much more smaller than that of C_8NBr or C_7FNa, and the γ_{cmc} of the mixed solution is very low ($\sim$15 mNm-ı). The mixtures with various molal ratios other than 1:1 are also very surface active (6). We may calculate the surface adsorptions and surface mole fractions of C_8N^+ and C_7F^- from surface tension-concentration relationships by applying the Gibbs equations (equations (16), (17) and (18)). The β_σ and $X_{i\sigma}$ values are calculated by equation 13 from the surface tension-concentration relationships. Some results are shown in Table 4.

The results show that: (1) β_σ values are negative and rather large, indicating the strong molecular interactions due to the strong coulombic attraction between the two surface active ions with opposite charges; (2) the surface mole fractions ($X_{i\sigma}$) calculated by equation(13)are in accord with those obtained from Gibbs adsorption equation, showing the reasonableness of the application of the solution theory to the adsorption layer; (3) at constant
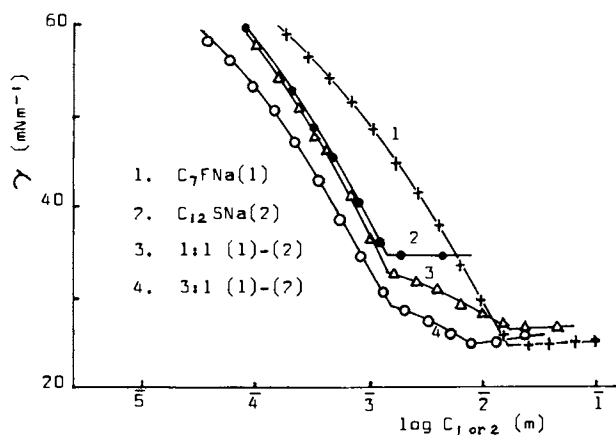
Figure 3. Surface tension of aqueous solutions of
$C_7FNa-C_{12}SNa$ system at 30°C (with NaCl, ionic strength
= 0.1 m; $C = C_{C_{12}SNa}$, except curve 1).
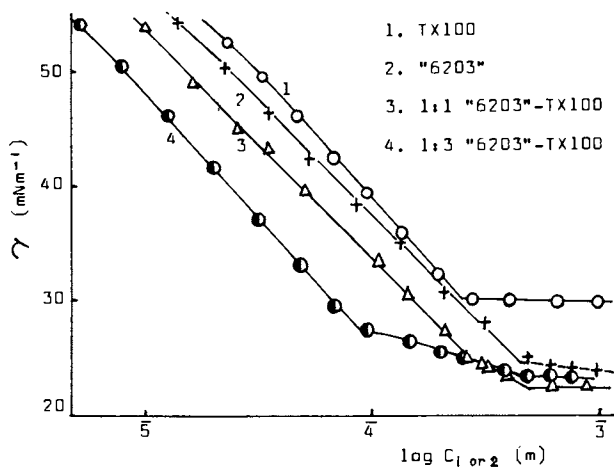
Figure 4. Surface tension of aqueous solutions of
"6203", TX100 and their mixtures at 25°C.

Table 5. β_σ-values of 1:1 $C_8NBr(1)$-$C_8SNa(2)$ System (with NaBr, ionic strength = 0.1 m, 25°C)

C_1°	C_2°	$C_1 = C_2$	γ	$X_{1\sigma}$		β_σ
(	10^{-3} m	)	(mNm^{-1})	Eqn (13)	Eqn (18)	
air/water surface						
100	40.1	0.841	52.7	0.47	0.48	-14.5
28.2	16.3	0.447	60.0	0.48	0.49	-12.7
4.35	2.75	0.178	68.0	0.48	0.49	- 9.1
n-heptane/water interface						
100	22.9	0.832	25.2	0.45	0.50	-13.3
2.82	1.05	0.105	42.0	0.42	—	- 8.3
0.631	0.178	0.040	46.0	0.42	—	- 5.5

Table 6. β_σ-values of $C_8NBr(1)$-$C_8SNa(2)$ System with various Molal Ratios (with NaBr, ionic strength = 0.1 m, 25°C)

molal ratio (1) : (2)	C^* (10^{-5}m)	γ (mNm^{-1})	$X_{1\sigma}$		β_σ
			Eqn(13)	Eqn(18)	
air/water surface					
1 : 1	84.1	52.7	0.47	0.48	-14.5
1 : 10	28.8	"	0.40	0.45	-13.5
1 : 100	6.7	"	0.32	0.34	-13.5
n-heptane/water interface					
1 : 1	83.2	25.2	0.45	0.50	-13.3
1 : 10	25.2	"	0.37	0.45	-12.6
1 : 40	12.0	"	0.32	0.34	-11.9

* At γ = 52.7, C_1° = 1.00×10^{-1} m, C_2° = 4.01×10^{-2} m;
At γ = 25.2, C_1° = 1.00×10^{-1} m, C_2° = 2.29×10^{-2} m.

Table 7. Surface Properties of 1:1 $C_8SOC(1)$-$C_7FNa(2)$ System (with NaBr, ionic strength = 0.1 m, 25°C)

γ(mNm)	C_1°(10^{-3}m)	C_2°(10^{-3}m)	$C_1 = C_2$(10^{-3}m)	$X_{2\sigma}$	β_σ
17	54.9	47.4	5.01	0.51	-6.51
30	18.6	10.5	1.78	0.54	-5.46
40	8.24	3.26	0.754	0.57	-4.74
50	3.40	0.902	0.293	0.61	-4.14

* Value obtained by extrapolation of the linear portion of γ-log C curve below γ_{cmc}.

Table 8. β_σ and Surface Mole Fraction of 1:1 $C_8SOC(1)$-$C_7FNa(2)$ System (without added salt, 25°C)

γ (mNm^{-1})	C_1°	C_2°	$C_1 = C_2$	β_σ	$X_{2\sigma}$	$X'_{2\sigma}$
	(	10^{-3} m	)	Eqn (20)	Eqn(20)	Eqn(22)
30	19.5	28.2	4.41	-5.86	0.41	0.38
45	5.37	10.0	1.59	-4.88	0.39	0.38
60	1.14	2.23	0.384	-4.58	0.37	0.38

surface tension, β_σ change little irrespective of the dif-
ferent molal ratio of the two surfactants; (4) β_σ values
(absolute) increase with the surface pressure (i.e., de-
crease as the surface tension increases).

   This is also obviously shown in the case of common
HC cationic-anionic surfactants system, $C_8NBr-C_8H_{17}SO_4Na$
(C_8SNa) (17). The results in Table 5 and 6 are fully in
line with the above mentioned four points.

   In these systems with the salt (NaBr) concentration
of 0.1m, β_m cannot be obtained because the cmcs of C_8NBr
and C_8SNa are both greater than 0.1m (they are 0.26 and
0.14 m, respectively).

$\underline{C_8SOC-C_7FNa}$ (nonionic-anionic) system. In order to avoid
the complex structure and function of polyoxyethylene
group in a common nonionic surfactant (e.g. TX100), we use
octylmethyl sulfoxide as a partner in the pair system to
study the molecular interactions. The surface tension of
the surfactants solutions (with and without adding salt)
are shown in fig.6 and 7. The surface properties of 1:1
C_8SOC-C_7FNa system with adding salt (from Fig.6) are
shown in Table 7.

   The rather great value of β_σ shows the strong molecu-
lar interaction between the two components' polar groups
since the two hydrophobic chains would be mutual-phobic.
β_m value calculated by equation(17)also shows this point:
$\beta_m = -3.2$ ($X_{2m} = 0.53$).

   For this system without added salt, the equation for
calculating β_m and β_σ should be as follows (from equation
(11) and equation(14))

$$\beta_m = \ln(cmc_1/cmc_1^\circ X_{1m}) \ / \ X_{2m}^2$$

$$= \ln((cmc_2/cmc_2^\circ)^{1+K_2}/X_{2m}) \ / \ X_{1m}^2 \qquad (19)$$

$$\beta_\sigma = \ln(C_1/C_1^\circ X_{1\sigma}) \ / \ X_{2\sigma}^2$$

$$= \ln((C_2/C_2^\circ)^{1+K_2'}/X_{2\sigma}) \ / \ X_{1\sigma}^2 \qquad (20)$$

From Fig.7 the calculated β_σ -values of 1:1 C_8SOC-C_7FNa
solution at different surface tension are shown in Table 8
together with the $X_{2\sigma}'$ obtained from the adsorption data
by the Gibbs theorem. For the 1:1 mixed solution, assum-
ing ideal (as the solution is dilute), then

$$-d\gamma/RT = \Gamma_{C_8SOC} d\ln C_{C_8SOC} + \Gamma_{C_7F}^- d\ln C_{C_7F}^- + \Gamma_{Na}^+ d\ln C_{Na}^+$$

$$= (\Gamma_{C_8SOC} + \Gamma_{C_7F}^- + \Gamma_{Na}^+) \ d\ln C$$

$$= \Gamma'' d\ln C \qquad (21)$$

where C is the molal concentration of C_8SOC or C_7FNa in
1:1 mixed solution, $\Gamma'' = \Gamma_{C_8SOC} + 2\Gamma_{C_7F}^-$ (as $\Gamma_{C_7F}^- = \Gamma_{Na}^+$).

The surface mole fraction of C_8SOC then is expressed as
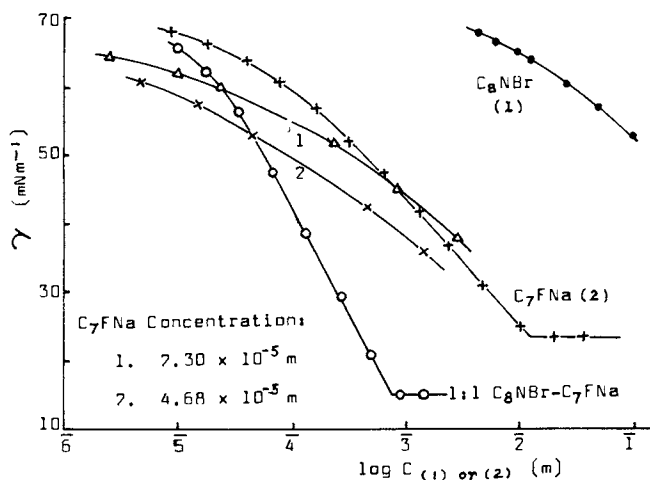
Figure 5.   Surface tension of aqueous solutions of
C_8NBr-C_7FNa system at 30°C (with NaBr, ionic strength
= 0.1 m; C = C_{C_8NBr} , except curve 2).
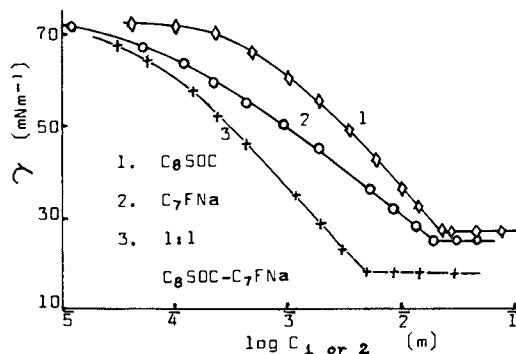
Figure 6.   Surface tension of aqueous solutions of
C_8SOC, C_7FNa and 1:1 mixture at 25°C (with NaCl, ionic
strength = 0.1 m).
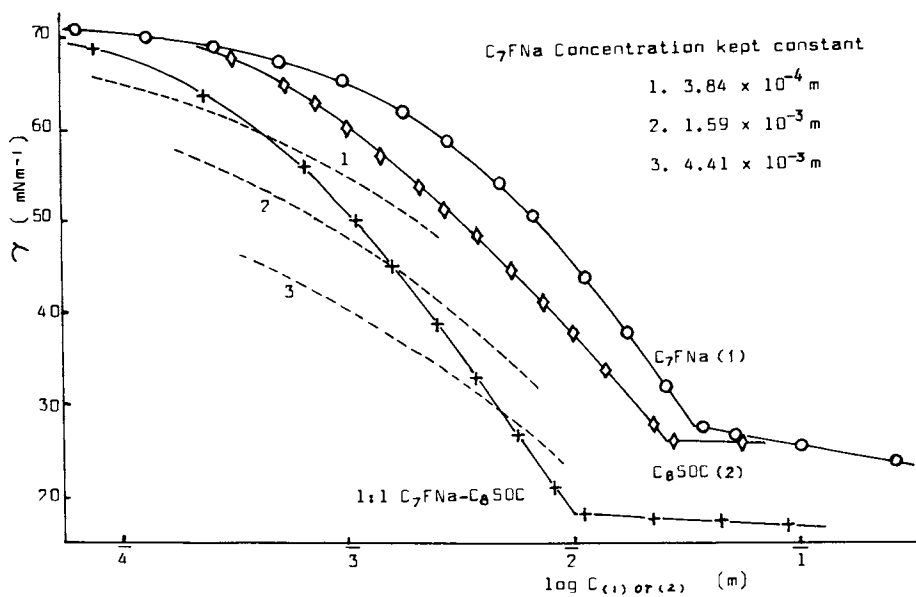
Figure 7. Surface tension of aqueous solutions of
C_7FNa, C_8SOC and their 1:1 mixture at 25°C.

$$X'_{2\sigma} = \Gamma_{C_8SOC} / (\Gamma_{C_7F^-} + \Gamma_{C_8SOC}) \qquad (22)$$

It is shown that $X_{2\sigma} \approx X'_{2\sigma}$, indicating equation (20) is obviously more appropriate to the nonionic-ionic systems with and without added salt. If equation 13 is applied here, at $\gamma = 30$, 45 and 60 mNm^{-1}, $X_{2\sigma}$ values would be 0.47 0.44 and 0.43, respectively, which are quite different from $X'_{2\sigma}$ values, showing further the appropriateness of equation (20) (or equation (14)) for the system without added salt.

From equation (19), we can calculate β_m (≈ -3.1) and X_m ($X_{C_7F^-} \approx 0.41$) The considerably strong molecular interaction between C_8SOC and C_7FNa may be probably attributed to the strong polarity of $>S=0$ group which would gain a proton in the aqueous solution to become slightly positively charged (i.e. $C_8SOC + H^+ \rightleftharpoons C_8S^+(OH)C$) and thus a stronger interaction takes place between C_8SOC and C_7F^- due to the coulombic attraction. This is evidenced by the fact that pH of the aqueous solution of C_8SOC becomes higher than water and the $|\beta|$ value for $C_8SOC-C_{10}H_{21}N(CH_3)_3Br$ system is much smaller than that of C_8SOC-C_7FNa or $C_8SOC-C_{10}SNa$ system

It is seen that in the 1:1 C_8SOC-C_7FNa system, as in the other above-mentioned system, $|\beta_\sigma|$ value decreases with the increasing γ-value.

$C_{10}SOC$ has a similar effect in the mixed systems (18).

Conclusion

The nature of surface adsorption and micelle formation of various mixed FC- and HC-surfactants systems can be conveniently and well investigated by the non-ideal solution theory semi-empirically applied in the surface layer and micelles. The weak "mutual phobic" interaction between FC- and HC-chains has been clearly revealed in the anionic-anionic and nonionic-nonionic systems as indicated by the positive β_σ-values. β_m-value cannot be obtained because of the absence of entirely miscible micelle due to "mutual phobicity".

In the systems with considerable molecular interactions between the two surfactant components, such as C_8NBr-C_7FNa (cationic-anionic) and C_8SOC-C_7FNa (nonionic-anionic) systems, the "mutual phobic interaction" can be concealed entirely and there are large negative β_σ and β_m values for these systems.

The results show that for a mixed solution, β_σ varies with the surface tension of solution. This is reasonable because the denseness of surface molecular packing is not the same at different γ ; the lower the γ, the denser the packing and the greater the molecular interaction. This is most obvious in system of large negative β_σ-values and less obvious or even vague in the case of weak interactions (such as in $C_7FNa-C_{10}SNa$ system).

For calculating β and X_i of the binary system con-

taining ionic surfactant without added salt, the general
equations with the counterion binding constant (K_l) term
(equations (11) an (14)) should be used instead of the equa-
tions (Eqns. (12),(13)) ever proposed(Eqns. (12),(13) are the
special cases of Eqns. (11),(14)).

It is evident that the non-ideal solution theory of
surface adsorption and micellization is a convenient and
useful tool for obtaining the surface and the micelle
compositions and for studing the molecular interaction in
the binary surfactant system.

Literature cited

1.   Ueno, M., Shioya,K., Nakamura, T., Meguro, K., in
      "Colloid and Interface Science"; Kerker, M, Ed.;
      Academic Press: New York, 1977; Vol. 2, p.411.
2.   Smith, I., Ottewill, R., in "Surface Active Agents";
      SCI Symp. Proc., London, 1979; p. 77.
3.   Funasaki, N., Hada, S. J.Phys. Chem., 1980, 84, 736.
4.   Zhu, B.-Y., Zhao, G.-X. Acta Chimica Sinica, 1981,
      39, 493.
5.   Zhu, B.-Y., Zhao, G.-X. Acta Chimica Sinica, 1982,
      40, 588.
6.   Zhu, B.-Y., Zhao, G.-X. Acta Chimica Sinica, 1983,
      41, 801.
7.   Zhao, G.-X., Zhu, B.-Y., Zhou, Y.-P., Shi, L. Acta
      Chimica Sinica, 1984, 42, 416.
8.   Shinoda, K., Nomura, T. J. Phys. Chem., 1980,84,365.
9.   Zhao, G.-X., Zhu, B.-Y. Colloid & Polymer Sci.,
      1983, 261, 89.
10.   Buscall, R., Ottewill, R., in "Monolayers", Goddard,
      E.D., Ed.; Adv. Chem. Ser., ACS: Washington, D.C.,
      1975, p. 83.
11.   Zhu, B.-Y., Zhao, G.-X. Hua Xue Tong Bao, 1981(6),
      341.
12.   Shinoda, K. "Colloidal Surfactants"; Academic: New
      York, 1963, Chap. 1.
13.   Shinoda, K. in "Proc. 4th INtern. Congr. Surface
      Active Substances, Overbeek, J.Th.G.,Ed.; Gordon &
      Breach Sci. Publ.: London & Paris, 1967, Vol.2,p.527.
14.   Lin, I.J., Somasundaran, P. J. Colloid Interface
      Sci., 1971, 39, 731.
15.   Rosen, M.J., Hua, X.-Y. J. Colloid Interface Sci.,
      1982, 86, 164.
16.   Ingram, B.-T. Colloid & Polymer Sci., 1980,258,191.
17.   Zhao, G.-X., Cheng, Y.-Z., Ou, J.-G., Tien, B.-S.,
      Huang, Z.-M. Acta Chimica Sinica, 1980, 38, 409.
18.   Zhu, D.-M., Zhao, G.-X., unpublished result.

15

Adsorption of a Mixture of Anionic Surfactants on Alumina

Bruce L. Roberts, John F. Scamehorn, and Jeffrey H. Harwell[1]

School of Chemical Engineering and Materials Science, University of Oklahoma, Norman, OK 73019

The adsorption of sodium decylsulfate and sodium dodecylsulfate and well defined mixtures thereof was measured on alumina. The thermodynamics of mixing upon formation of the bilayered surface aggregates (admicelles) was studied as well as that associated with mixed micelle formation for the system. Ideal solution theory was obeyed upon formation of mixed micelles, but positive deviation from ideal solution theory was found at all mixture compositions upon mixed admicelle formation. The mixed micelles are ideal because the hydrophobic groups of different length are in approximately the same environment in the spherical hydrophobic core of the mixed micelle as they are in the pure component micelles. In the planar core of the admicelle, however, the methylene groups nearest the hydrophilic group on the longer hydrocarbon chain surfactant are not exposed to as hydrophobic an environment as in the pure component admicelle, resulting in a reduced tendency for the mixed admicelle to form, compared to an ideal solution.

The adsorption of surfactant mixtures on metal oxide surfaces (e.g., minerals) from aqueous solutions is an important process in such applications as enhanced oil recovery and detergency. Since surfactants used in real-world applications are almost always mixtures, interactions between different adsorbed surfactant

[1] To whom correspondence should be addressed.

species, as well as surfactant-surface interactions, must be studied to provide a comprehensive understanding of these systems.

The adsorption of single-component anionic surfactants on metal oxide surfaces has been studied extensively (1-10). The surface of the adsorbent can be viewed as being composed of patches, each patch having a characteristic energy of adsorption (or formally, a characteristic standard state chemical potential change upon adsorption of surfactant on that patch). At low surfactant concentrations, the surfactants are adsorbing as individual, unassociated molecules on each patch on the surface. At a certain specific concentration, the surfactants form a surface aggregate on the most energetic patch on the surface. The adsorption on this patch increases sharply when this occurs. As the surfactant concentration is increased further, successively less energetic patches have a surfactant aggregate formed on them. On a substrate like alumina, the distribution of patch energies is nearly continuous, so that the adsorption isotherm is essentially continuous.

Surface aggregates formed by ionic surfactant adsorption on oppositely charge surfaces have been shown to be bilayered structures (1) and are called admicelles(2) in this paper, though they are sometimes referred to as hemimicelles. The concentration at which admicelles first form on the most energetic surface patch is called the Critical Admicellar Concentration (CAC) in analogy to the Critical Micelle Concentration (CMC), where micelles are first formed. Again, in much of the literature, the CAC is referred to as the Hemimicellar Concentration (HMC).

At concentrations below the CAC, there is no significant interaction between adsorbed surfactant molecules. Therefore, the adsorption in this region obeys Henry's law and is proportional to concentration. This region of the adsorption isotherm is known as the Henry's law region. At the CAC, the adsorption vs. concentration isotherm exhibits a sharp increase in slope as successive patches on the surface become filled with admicelles. Adsorption may continue to increase with increasing surfactant concentration until complete bilayer coverage occurs over the entire surface. However, often the CMC is reached before this occurs. The activity or chemical potential of the surfactant varies little at concentrations above the CMC. Therefore, for single component surfactants, the adsorption changes slowly with surfactant concentration above the CMC. The resulting characteristic isotherm shape for a single-component surfactant adsorption is illustrated in Figure 1 for the two pure surfactants shown.

The thermodynamics of formation of admicelles composed of two or more surfactants is the focus of this
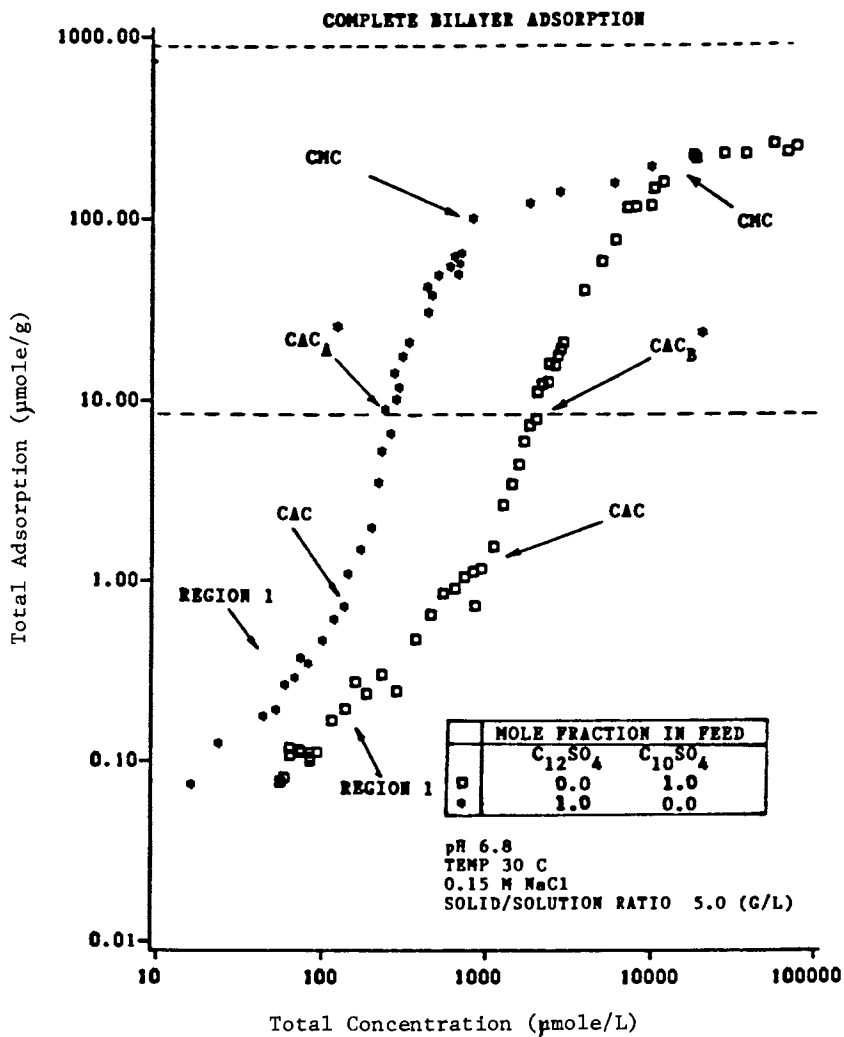
Figure 1. Effect of alkyl chain length on adsorption of alkyl sulfates on alumina.

study.   Other mixed aggregates formed by surfactants have
been studied,   such   as   mixed   micelles   (11-13),   mixed
monolayers (13,14),   mixed microemulsions (15-17),   mixed
liquid crystals (17),   and   mixed   coacervate   above   the
cloud   point   (18),   to   name   a   few.   However,   mixed
admicelles have received little attention,   despite their
commercial and theoretical interest.
     Scamehorn   et.   al.   (19)   reported   the   adsorption
isotherms for a binary mixture of anionic surfactants.   A
formal adsorption model developed for   single   surfactant
systems   (1) was extended to this binary system and shown
to accurately describe   the   mixed   adsorption   isotherms
(19).   That   theoretically   based   model was very complex
and   is   probably   not   feasible   to   extend   beyond   two
surfactant components.
     Scamehorn   et.   al.   (20)   also   presented a simple,
semi-empirical method based on ideal solution theory   and
the   concept   of   reduced adsorption isotherms to predict
the mixed adsorption isotherm and admicellar   composition
from   the   pure   component   isotherms.   In this work,   we
present a   more   general   theory,   based   only   on   ideal
solution   theory,   and present detailed mixed system data
for a binary mixed surfactant system (two   members   of   a
homologous   series)   and   use it to test this model.   The
thermodynamics of admicelle formation is also compared to
that of micelle formation for this same system.

Experimental

Materials.   The sodium n-decylsulfate ($C_{10}SO_4$) from Kodak
and the sodium n-dodecylsulfate ($C_{12}SO_4$) from Fisher were
purified   by   recrystallization   from   water   and   from
methanol, followed by drying under a vacuum.   The alumina
used   was   Aluminum   Oxide C (Degussa Inc.),   a primarily
gamma alumina, with a surface area of 100 m^2/g.   The NaCl
was Fisher reagent grade and the water was distilled   and
deionized.

Methods.   Adsorption   isotherms were run at constant feed
molar ratio of $C_{10}SO_4/C_{12}SO_4$.   The feed solutions   had   a
pH of 4.25 and a NaCl concentration of 0.15 M.   Ten ml of
feed   solution   was added to 0.5 g alumina in a screw top
centrifuge tube and centrifuged at 700 RPM for 45 minutes
at room temperature.   The tube was then placed in a water
bath at 30°C for four days,   the liquid decanted from the
mineral and analyzed.   The surfactant concentrations were
analyzed   using   high   performance   liquid chromatography
with a   conductivity   detector.   The   solution   pH   after
equilibration   was   determined   using pH electrodes.   The
equilibrium pH increased to 6.8   at   equilibrium   because
the PZC of alumina is approximately 9.

Theory

For   the   type   of   surfactants   studied   here,   at

concentrations significantly higher than the CAC, almost
all adsorbed surfactant on the surface is in the form of
admicelles; i.e., the patches with Henry's Law adsorption
contribute an insignificant amount of adsorbed surfactant
to the total. Consider a pure surfactant adsorption
isotherm at a surfactant concentration above the CAC. At
a specific total surfactant adsorption level, certain
specific patches on the surface contain admicelles, with
the rest of the surface patches containing only sparse
coverage of surfactant. For the other pure surfactant
component and for any surfactant mixture at that same
adsorption level, it is assumed that the same patches
(and only these patches) contain admicelles as for the
first pure surfactant. Taking this physical view of the
surface, it is convenient to model the total surfactant
concentration required to cause admicelles to form on
those surface patches corresponding to a specific total
adsorption level. Since total adsorption is a monotonic
function of total surfactant concentration for a specific
surfactant composition, predicting concentration as a
function of adsorption yields the same result as the more
traditional prediction of adsorption as a function of
concentration. If the composition of the adsorbate were
known, the adsorption of each individual surfactant
component could also be predicted in surfactant mixtures.
Equations to predict these quantities for mixture
adsorption, based on ideal mixing in the admicelle, will
be presented here.

 Consider the pure surfactant adsorption isotherms
shown in Figure 1. At concentrations between the CAC and
the CMC, there is a unique concentration level
corresponding to each adsorption level for each pure
component. Since this concentration corresponds to
formation of admicelles on specific patchs on the
surface, for component i, we call the concentration
CAC_i*; the variable CAC (no superscript) will be reserved
to refer to the concentration which corresponds to
admicelle formation on the most energetic patch on the
surface. We will only consider binary mixtures of
surfactants, so the subscript i can refer to either
component A or B. For a surfactant mixture, the total
surfactant concentration required to reach a specified
adsorption level is defined as CAC_M*.

 The mixed admicelle is very analogous to mixed
micelles, the thermodynamics of formation of which has
been widely studied. If the surfactant mixing in the
micelle can be described by ideal solution theory, the
Critical Micelle Concentration (CMC) or minimum
concentration at which micelles first form can be
described by (21):

$$CMC_M = CMC_A CMC_B / (y_A CMC_B + y_B CMC_A) \qquad (1)$$

where CMC_M is the mixture CMC, and CMC_A or CMC_B are the
CMC values for pure component A or B, and y_A or y_B are

the surfactant-only based mole fractions of component A
or B in the monomer in solution. The composition of the
micelles in equilibrium with the monomer, according to
ideal solution theory, can be described by ([11]):

$$x_A = y_A CMC_M / CMC_A \qquad \qquad (2)$$

$$x_B = y_B CMC_M / CMC_B \qquad \qquad (3)$$

$$y_A + y_B = 1 \qquad \qquad (4)$$

$$x_A + x_B = 1 \qquad \qquad (5)$$

where x_A or x_B are the surfactant-only based mole
fractions of component A or B in the mixed micelle.
Equations 1-5 provide *a priori* prediction of mixed CMC
values and composition of micelles.
    At a specific adsorption level, we can view the
surfactant monomers as being in equilibrium with
admicelles on specific surface patches, just as the
monomer is in equilibrium with the micelles at a
monomeric concentration of the CMC. Therefore, CAC* is
analogous for admicelles to the CMC for micelle
formation. If mixing between surfactant components is
ideal in the admicelle, at a specific adsorption level,
in analogy to Equations 1-3:

$$CAC_M^* = CAC_A^* CAC_B^* / (y_A CAC_B^* + y_B CAC_A^*) \qquad (6)$$

$$z_A = y_A CAC_M^* / CAC_A^* \qquad \qquad (7)$$

$$z_B = y_B CAC_M^* / CAC_B^* \qquad \qquad (8)$$

$$z_A + z_B = 1 \qquad \qquad (9)$$

where z_A or z_B are the surfactant-only based mole
fractions of component A or B in the mixed admicelle.
Once CAC_A^* and CAC_B^* are defined for any adsorption level
from the pure surfactant adsorption isotherms, Equations
6-9 can be used to predict the total adsorption and
admicelle composition for any mixture composition and
concentration in solution (at concentrations between the
CAC and the CMC for that mixture). From this, the
individual surfactant component adsorption levels can
also be calculated, all on an *a priori* basis.
    A previously proposed theory to describe mixed
adsorption in these systems ([20]) depended not only on
ideal solution theory, but also on the corresponding
states theory to apply to surfactant mixtures. In that
model, it was assumed that the adsorption isotherms for
the pure components coincided when plotted against a
reduced concentration. This occurs when the ratio
CAC_B^* / CAC_A^* is the same at any adsorption level. When
true, this simplifies the prediction of mixed adsorption
isotherms somewhat, but that model is really a special
case of the model presented here.

Results and Discussion

Mixed   Micelles.   The CMC values for the two pure
surfactants and well defined mixtures thereof are shown
in Figure 2.   The experiments were run at a high added
salt   level   (swamping   electrolyte)   so   the counterion
contributed by the dissolved surfactant is negligible.
Predicted mixture CMC values for ideal mixing from
Equation   1   are also shown.   Ideal solution theory
describes mixed micelle formation very well, as is
usually the case for similarly structured surfactant
mixtures (12,19,21-24).

Mixed Admicelles.   The total surfactant adsorption of the
two pure surfactants and mixtures thereof on alumina are
shown   in Figure 3.   The mixtures are at constant
surfactant ratio in the feed or initial solution, but not
necessarily in the final equilibrium solution.   The
concentration   on   the   abscissa is the equilibrium
concentration.   The individual surfactant   adsorption
isotherms for the pure surfactants and in the mixtures
are shown in Figures 4 and 5.   The experiments were run
at the same swamping electrolyte concentration as were
the CMC data.
    The   predicted   adsorption   isotherms   from   ideal
solution theory (Equations 6-9) are also shown in Figures
3-5.   Since it is difficult to see degree of fit on a
log-log plot, the ability to describe the data is better
illustrated in Figures 6-9, where the $CAC_M{}^*$ is plotted
for several adsorption levels as a function of monomer
composition along with predictions from Equation 6.
    From   Figures   3 and 6-9,   the predicted total
adsorptions for surfactant mixtures are higher than
observed values.   Therefore, the mixed admicelles showed
positive deviation from ideality at all compositions.
This remarkable behavior has not been observed before
because data of the accuracy and range reported here has
not (to our knowledge) previously been reported.
Observation of the expected ideal behavior for the CMC
data indicate that this is probably not due to a
peculiarity of the surfactants used.
    The explanation for this effect lies in the steric
constraints of the two-dimensional admicelle.   In the
admicelle, the thickness of the hydrophobic portion of
the admicelle is probably dictated by the length of the
longest alkyl chain present (i.e., the dodecyl chain).
In the mixed admicelle, the decyl chain is almost
completely surrounded by other alkyl chains and so is
exposed to approximately the same environment as in a
pure $C_{10}SO_4$ admicelle.   However, the two additional
methylene groups on the dodecyl chain are not in as
hydrophobic an environment as in the pure $C_{12}SO_4$
admicelle, since neighboring decyl chains cannot interact
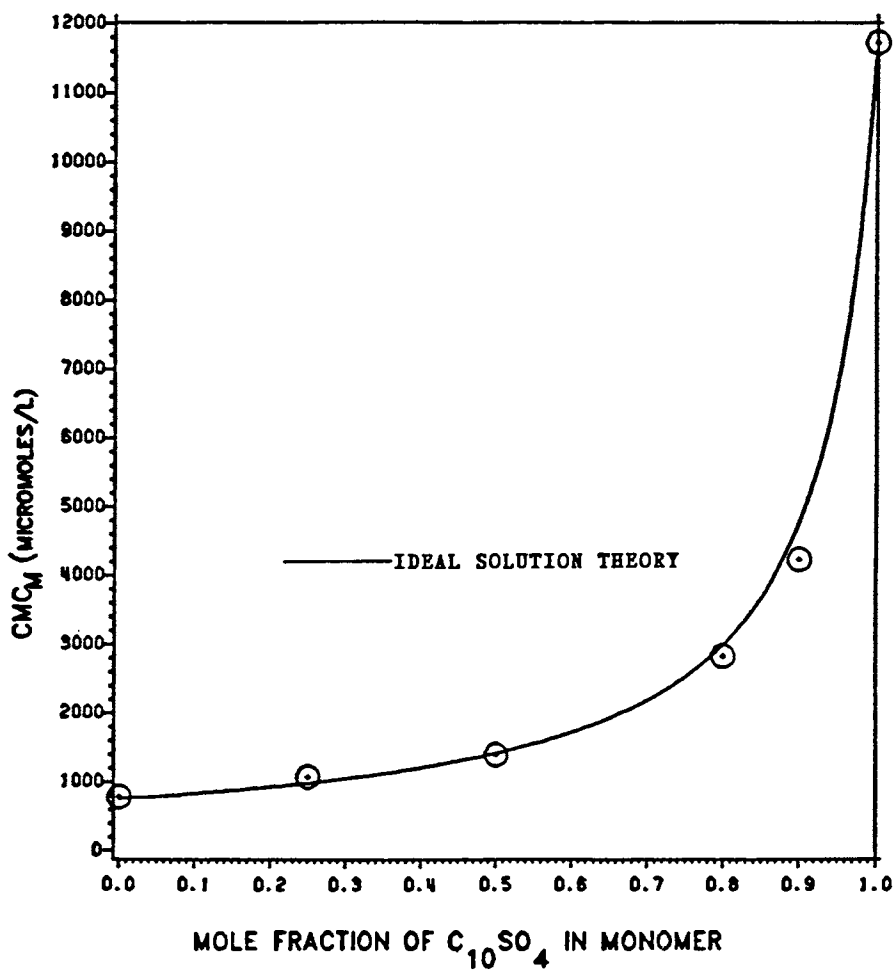
Figure 2. Mixture CMC values for $C_{10}SO_4/C_{12}SO_4$ System.
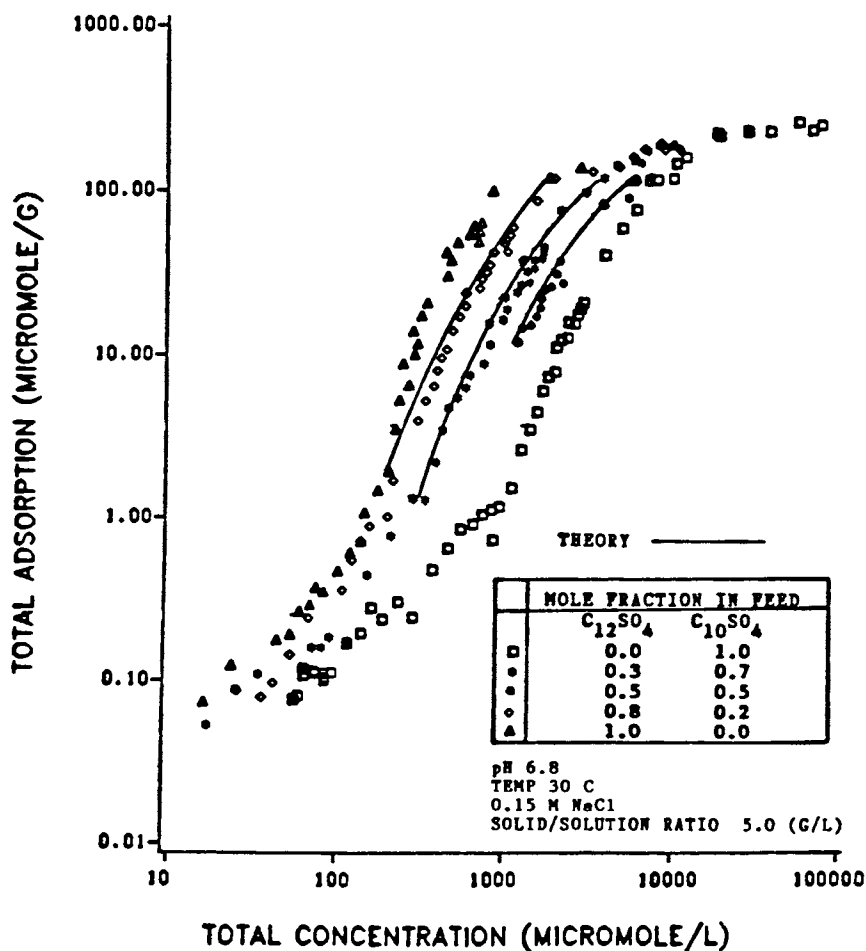
Figure 3.   Effect of surfactant concentration on total adsorption of $C_{10}SO_4/C_{12}SO_4$ mixtures on alumina.
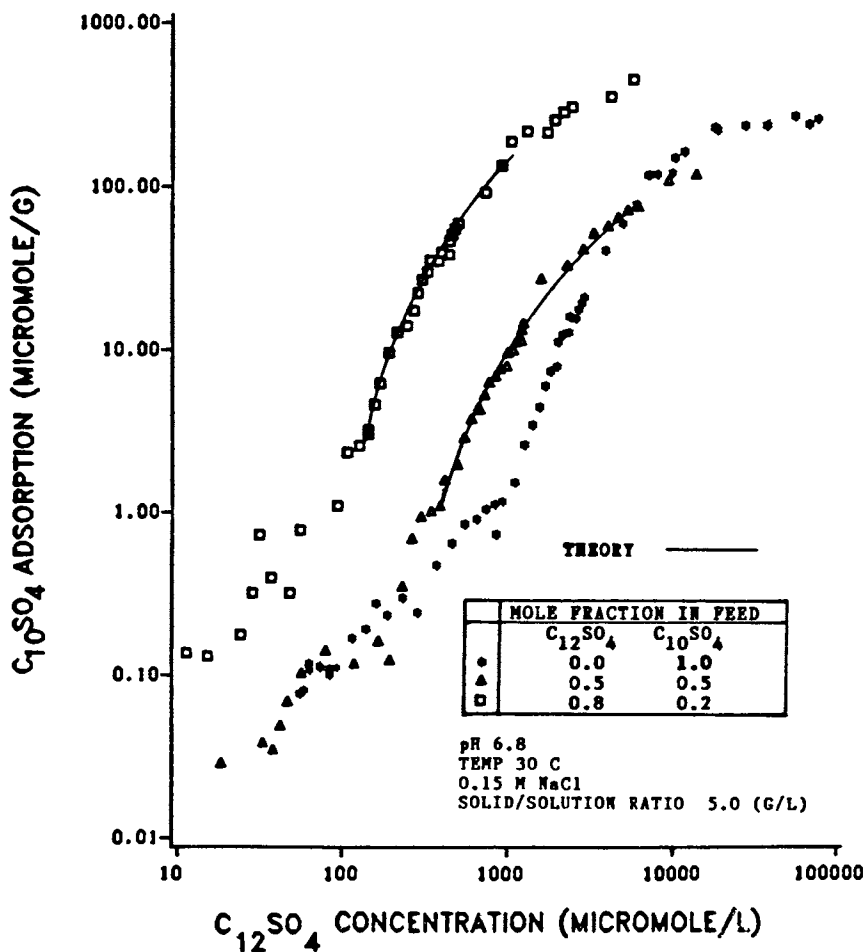
Figure 4. Effect of $C_{10}SO_4$ concentration on $C_{10}SO_4$ adsorption on alumina in a mixture with $C_{12}SO_4$.
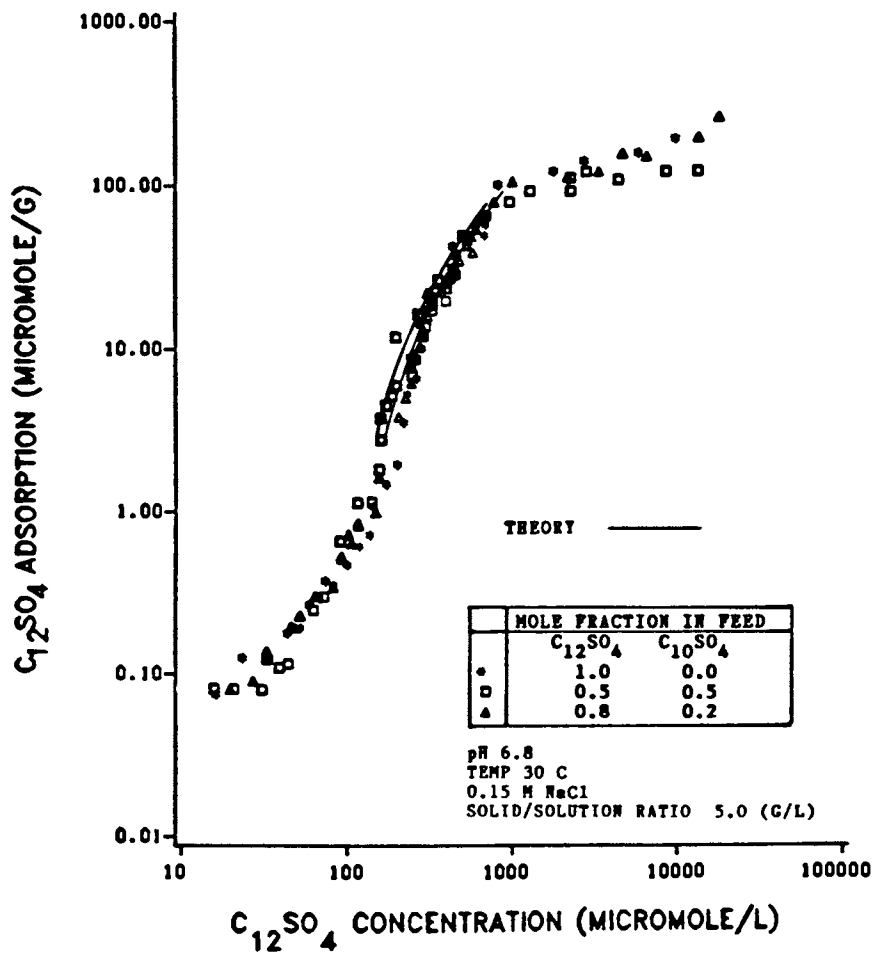
Figure 5. Effect of $C_{12}SO_4$ concentration on $C_{12}SO_4$ adsorption on alumina in a mixture with $C_{10}SO_4$.
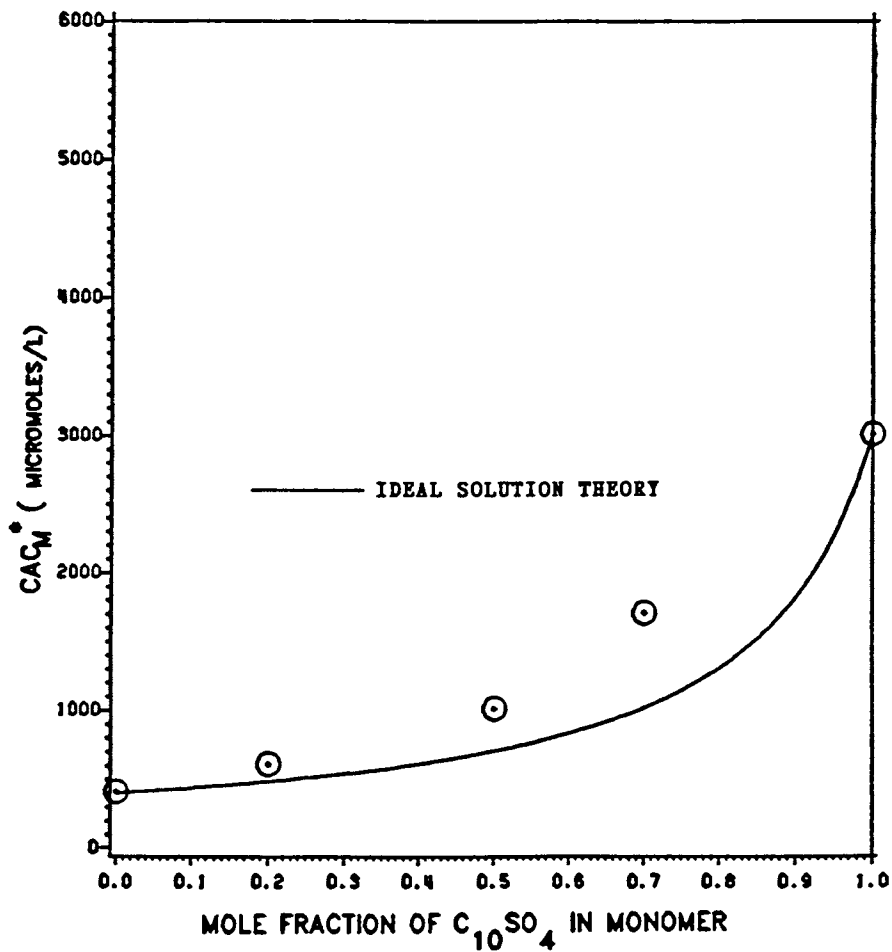
Figure 6. CAC_M^* for $C_{10}SO_4/C_{12}SO_4$ system at a total adsorption level of 20 micromole/g.
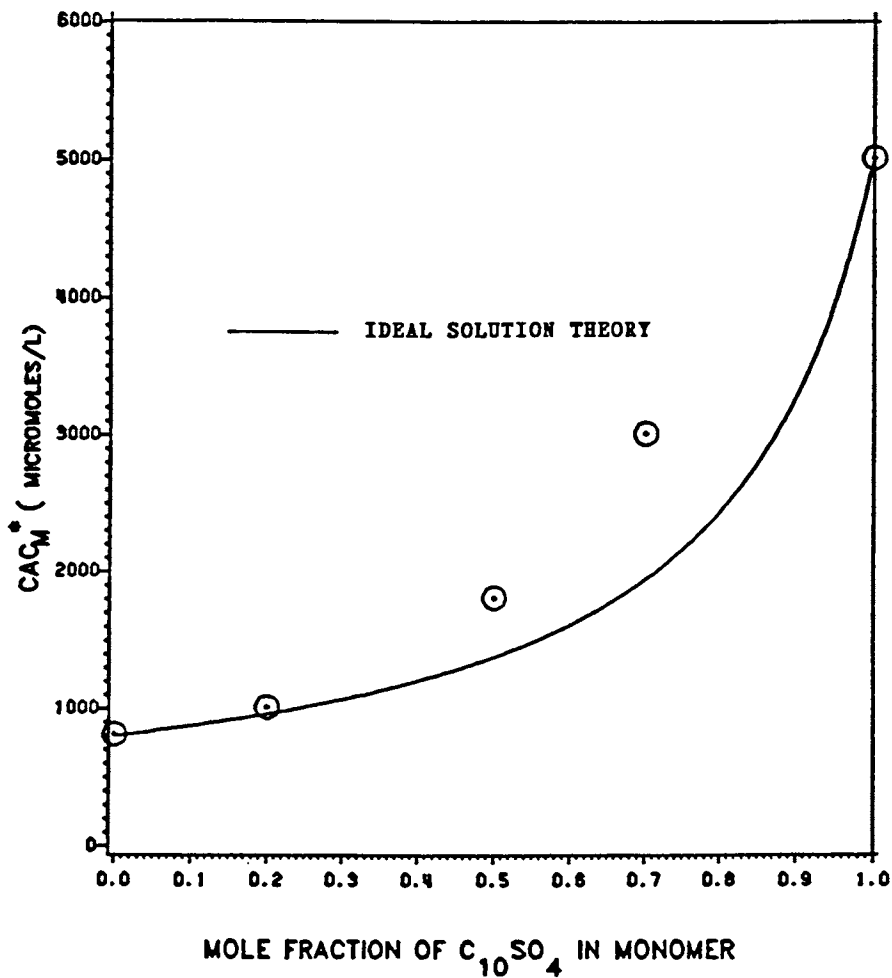
Figure 7.   CACₘ* for C₁₀SO₄/C₁₂SO₄ system at a total
adsorption level of 60 micromole/g.
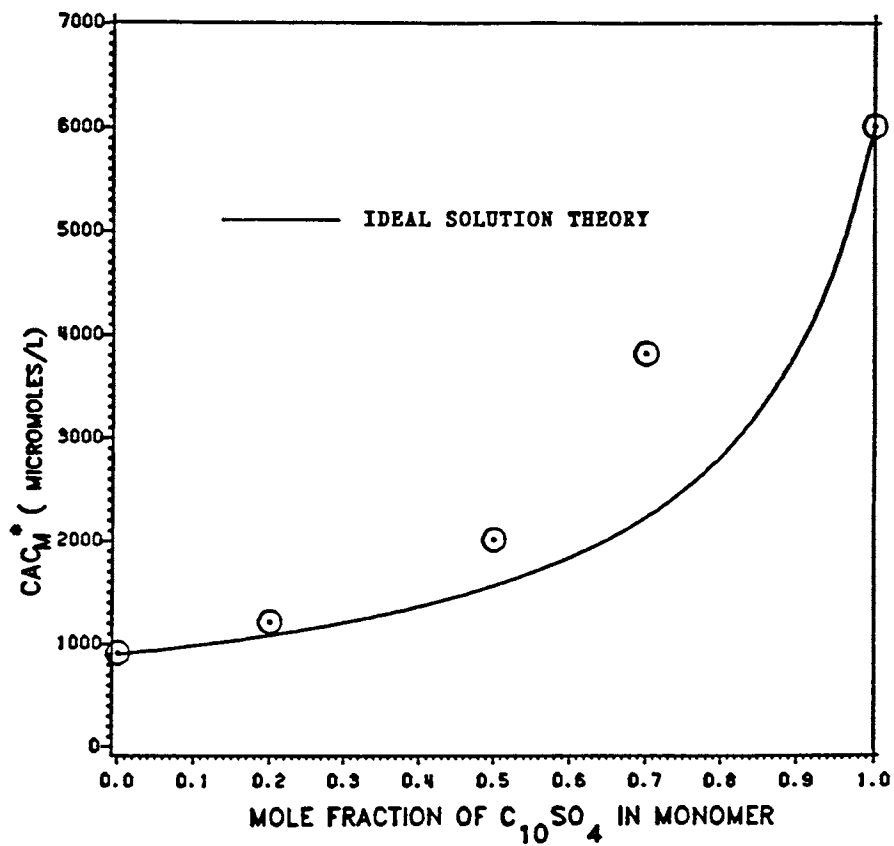
Figure 8. CAC_M^* for $C_{10}SO_4/C_{12}SO_4$ system at a total adsorption level of 80 micromole/g.

with these methylenes as can neighboring dodecyl chains. The two methylene groups in the dodecyl chain in the different environment are those nearest the hydrophilic group. From Figures 4 and 5, ideal solution theory predicts the $C_{10}SO_4$ adsorption in the mixed micelle very accurately, but predicts higher adsorption levels than those observed for $C_{12}SO_4$, consistent with this explanation. Therefore, the less favorable environment in the mixed admicelle for the dodecyl chain results in a higher free energy of mixed admicelle formation and positive deviation from ideal solution theory (i.e., the mixed admicelle forms with more difficulty than predicted by ideal solution theory).

These results are consistent with those of Rosen and Zhao (25), who found that in a monolayer, binary mixtures of surfactants interact most strongly when their alkyl chains contain the same number of carbon atoms.

This effect does not occur with the mixed micelles, where the spherical geometry of the hydrophobic core permits intimate contact between hydrocarbon chains of different lengths, so that the environment for hydrophobic groups is similar in the pure micelles as in the mixed micelles. As a result, ideal solution theory is obeyed.

Large negative deviations from ideality are well known when mixed micelles are formed between ionic and nonionic surfactants (11-13,21,24). Negative deviations from ideality have been reported for mixed ionic/nonionic admicelle formation (26), although the degree of nonideality was not quantified. Since this work has pointed out the similarities and differences between mixed micelles and admicelles, the study of these systems should elucidate this relationship even further and will be the subject of future publications.

Acknowledgments

Literature Cited

1. Scamehorn, J.F.; Schechter, R.S.; Wade, W.H. J. Colloid Interface Sci. 1982, 85, 463.
2. Harwell, J.H.; Hoskins, J.C.; Schechter, R.S.; Wade, W.H. Langmuir 1985, 1, 251.
3. Somasundaran, P.; Fuerstenau, D.W. J. Phys. Chem. 1964, 70, 90.
4. Wakamatsu, T.; Fuerstenau, D.W. Advan. Chem. Ser. 1968, 79, 161.
5. Dick, S.G.; Fuerstenau, D.W. J. Colloid Interface Sci. 1971, 37, 595.

6. Somasundaran, P.; Fuerstenau, D.W. Trans. Soc. Mining Eng. AIME 1972, 252, 275.

7. Fuerstenau, D.W.; Wakamatsu, T. Faraday Discuss. Chem. Soc. 1976, 59, 157.

8. Rosen, M.J.; Nakamura, Y. J. Phys. Chem. 1977, 81, 873.

9. Cases, J.M.; Goujon, G.; Smani, S. AICHE Symp. Ser. 1975, 71, 100.

10. Goujon, G.; Cases, J.M.; Mutaftschiev, B. J. Colloid Interface Sci. 1976, 56, 587.

11. Scamehorn, J.F.; Schechter, R.S.; Wade, W.H. J. Dispersion Sci. Technol. 1982, 3, 261.

12. Holland, P.M.; Rubingh, D.N. J. Phys. Chem. 1983, 87, 1984.

13. Rosen, M.J.; Hua, X.Y. J. Am. Oil Chem. Soc. 1982, 59, 582.

14. Zhu, B.Y.; Rosen, M.J. J. Colloid Interface Sci. 1984, 99, 435.

15. Haque, O.; Scamehorn, J.F., J. Dispersion Sci. Technol., In Press.

16. Graciaa, A.; Lachaise, J.; Bourrel, M.; Osborne-Lee, I.; Schechter, R.S.; Wade, W.H., SPE 13030, Presented at the 59th Annual Technical Conference and Exhibition of SPE, Houston, September, 1984.

17. Puig, J.E.; Franses, E.I.; Miller, W.G. J. Colloid Interface Sci. 1982, 89, 441.

18. Yoesting, O.; Scamehorn, J.F., Colloid Polym. Sci., In Press.

19. Scamehorn, J.F.; Schechter, R.S.; Wade, W.H. J. Colloid Interface Sci. 1982, 85, 479.

20. Scamehorn, J.F.; Schechter, R.S.; Wade, W.H. J. Am. Oil Chem. Soc. 1983, 60, 1345.

21. Lange, H.; Beck, K.H. Kolloid Z. Z. Polym. 1973, 251, 424.

22. Shinoda, K. In "Colloidal Surfactants"; Shinoda, K.; Tamamushi, T.; Nakagawa, T.; Isemura, T., Eds.; Academic Press: New York, 1963; Chapter 1.

23. Nishikido, N.; Moroi, Y.; Matuura, R. Bull. Chem. Soc. Jpn. 1975, 48, 1387.

24. Funasaki, N.; Hada, S. J. Phys. Chem. 1982, 86, 2504.

25. Rosen, M.J.; Zhao, F. J. Colloid Interface Sci. 1983, 95, 443.

26. Scamehorn, J.F.; Schechter, R.S.; Wade, W.H. J. Colloid Interface Sci. 1982, 85, 494.

16

Adsorption, Electrokinetic, and Flotation Properties of Minerals above the Critical Micelle Concentration

Bohuslav Dobiás

Department of Surface Chemistry and Flotation, Institute of Physical and Macromolecular Chemistry, University of Regensburg, 8400 Regensburg, Federal Republic of Germany

The problem of mineral flotability above the CMC with respect to the appearance of adsorption maxima has not yet been systematically studied. The aim of this paper was to correlate the adsorption maxima and the flotability of minerals with the kind of potential determining ions.

The flotation of minerals is based on different attachment forces of hydrophobized and hydrophilic mineral particles to a gas bubble. Hydrophobized mineral particles adher to gas bubbles and are carried to the surface of the mineral dispersion where they form a froth layer. A mineral is hydrophobized by the adsorption of a suitable surfactant on the surface of the mineral component to be flotated. The hydrophobicity of a mineral particle depends on the degree of occupation of its surface by surfactant molecules and their polar-apolar orientation in the adsorption layer. In a number of papers the relationship was analyzed between the adsorption density of the surfactant at the mineral-water interface and the flotability. However, most interpretations of adsorption and flotation measurements concern surfactant concentrations under their CMC.

A few papers have been published recently on the problem of surfactant adsorption maxima on solids in the region of the CMC (1-5). Scamehorn et al. (1,2) and Trogus et al. (3) explained the origin of these maxima by various ratios of the surfactant solution to the solid, in connection with isomeric impurity of the surfactant. Ananthapadmanabhan and Somasundaran (4) examined critically the presence of such maxima from the viewpoint of various proposed adsorption mechanisms. They have shown that a mechanism including micellar exclusion, mixed micelle formation and properties of solids, such as the pore size, cannot explain satisfac-

torily the reported results for the adsorption maxima
and hysteresis. According to these authors, the main
reason for the maxima is redissolution of surfactant-
multivalent ion precipitates above the CMC, and the
bulk precipitation upon dilution. The solubilization of
the reaction products between surfactants and multiva-
lent inorganic cations, or of weakly dissociated sur-
factant molecules at $c_{eq} >$ CMC was proposed also by
Dobiáš (5), as a possible explanation of maxima on ad-
sorption isotherms. The main reason for the occurrence
of these maxima is, according to Dobiáš and Strnad (6),
the formation of a new phase, micelle. This new phase
competes with the monomer for adsorption sites on the
mineral surface during the extraction of the letter
from the bulk phase. In other words, the presence of
micelles prevents the formation of an adsorption layer
an the mineral interface, obviously because the monomer
is thermodynamically more stable in a three dimensional
micelle than in an associated two-dimensional layer on
the mineral interface.

The problem of mineral flotability above the CMC
with respect to the appearance of adsorption maxima
has not yet been systematically studied. The aim of
this paper is to correlate the adsorption maxima and
the flotability of minerals with the kind of potential
determining ions(PDI).

Experimental

The adsorption density of surfactants was determined by
calculating the difference in the surfactant concentra-
tion before and after the adsorption of a mineral, as
described earlier (5).

The measurements with Na-dodecylbenzene sulfonate
were performed at pH 5.6 + 0.2 whereas those with ce-
tylpyridinium chloride at pH 6.0 + 0.2. The pH values
were not adjusted.

The minerals used in the experiments were of natu-
ral origin, in a crystalline form, and were > 99 % pure.
Specific surface of the minerals and their source were
the same as given in (5).

Solution solid ratios (l/g) were greater than 0.5.
The mineral flotability was calculated from kine-
tic data in a modified Hallimond tube (7). All measure-
ments were performed at 25.0 + 0.2 °C.

Results and Discussion

The adsorption isotherms of various surfactants were
measured on minerals with a different character of
PDIs. The course of the isotherms on minerals, with
H^+ and OH^- on one hand and those with latice ions as
PDIs on the other hand, is similar, with a maximum in
a region close to the CMC. Some characteristic adsorp-

tion isotherms are shown in figure 1 and 2. The plateau
on these isotherms characterizes filling the first ad-
sorption layer that should show the maximum hydropho-
bicity and therefore the optimal flotability. The value
of the zeta potential reaches in many cases its maximum
at the CMC, too (5).

The adsorption isotherms were discussed extensive-
ly in the previous paper (5). The surface area that the
adsorbed surfactant molecules occupy at the range of pla-
teau ($\theta \cong 1$) is different because it depends on the
chemical composition of the mineral and its clevage
plane.

The adsorption densities (Γ) on minerals (C$\leq$ CMC)
of the salt type are in some cases higher because of
precipitation of the ionic surfactant with multivalent
cations in the bulk phase. Measurements were carried
out to determine the fraction of the precipitated sur-
factant by divalent cations Ca^{2+} and Ba^{2+} leading to a
decrease in its equilibirum concentration. They showed
a shift of the adsorption maximum towards lower values
of Γ , even after a correction of the adsorption den-
sity due to the precipitation. On the other hand, a di-
rect co-adsorption of the precipitated surfactant on a
mineral surface cannot be excluded.

The decrease of the adsorption density over the
CMC as a consequence of the solubilization of the pre-
cipitated surfactant leads to an increase of its equi-
librium concentration (5). According to the structure
of the adsorption layer of a surfactant, the flotabi-
lity should correlate with the surface coverage of sur-
factant molecules. On the basis of this assumption, the
optimum flotability of the mineral should be reached
in the region of the first plateau on the adsorption
isotherm, (Fig. 1,2) whereas a minimum should be expec-
ted in the region of the maximum Γ value. The examples
with quartz (H^+ and OH^- as PDIs) and barite and fluori-
te (lattice ions as PDIs) in Figs. 3 - 5 show a good
agreement with this hypothesis on the structure of the
adsorption layer. For the sake of clarity in these fi-
gures, only the arrows show the concentration of the
surfactant at which a plateau is formed on the appro-
priate isotherm ($\theta \cong 1$, from Figs. 1,2) and the CMC.
A correlation of the values for C_Γ ($\theta \cong 1$) shows
that a maximum flotability is reached in the region of
these plateaus with a relatively good accuracy for the
shortest flotation time.

A decrease in flotability is characterized by an
increase in polarity of the adsorption layer of both
surfactants due to the formation of a second adsorp-
tion layer with polar groups of the surfactant orien-
tated toward the bulk phase, up to the CMC. The ana-
lysis of the flotation measurements was carried out on
the basis of kinetic data for the shortest constant
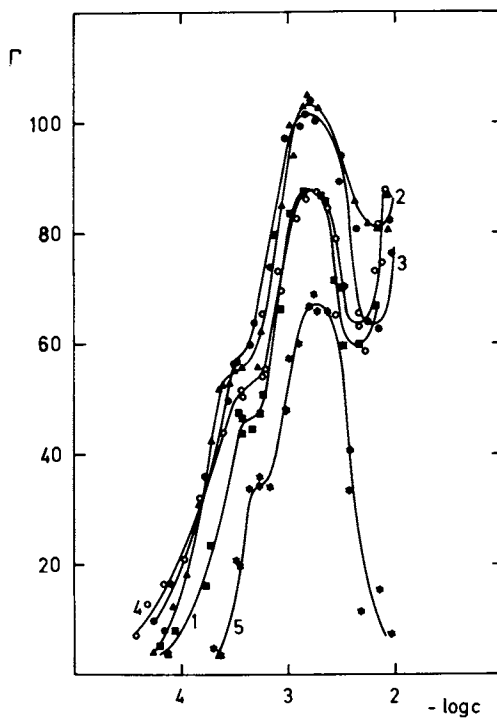
Figure 1. Adsorption isotherms of Na-dodecylbenzene-sulfonate on MgF_2(1), CaF_2(2), SrF_2(3), BaF_2(4- Γ /15) and barite (5)
$\Gamma .10^{-13}$ - number of molecules adsorbed per cm²
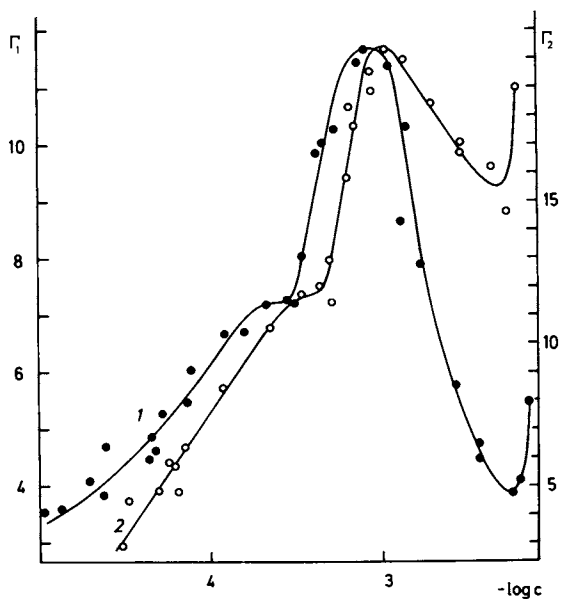
Figure 2. Adsorption isotherms of cetyl-
pyridinium chloride on TiO_2 $(1 -\Gamma_2)$ and SiO_2
$(2 -\Gamma_1)$
Γ_1, Γ_2 -number of molecules adsorbed per cm^2
$(\Gamma \cdot 10^{-13})$.
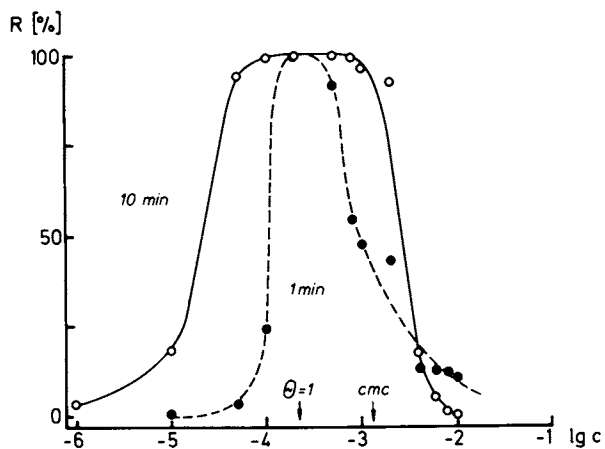
Figure 3. Flotation recovery $\underline{R}$ (in %) of fluorite as
dependent on the concentration $\underline{c}$ (in mol/L) of Na-do-
decylbenzenesulfonate.
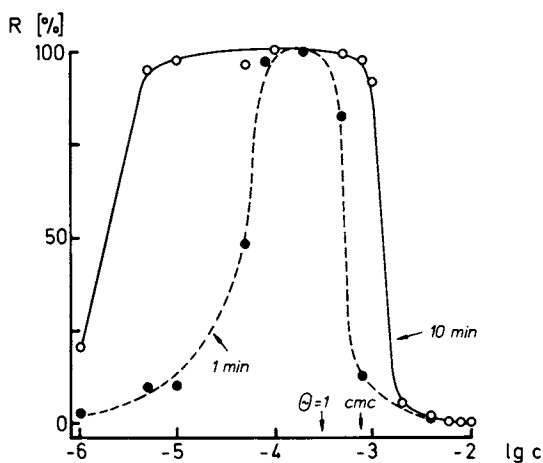
Figure 4. Flotation recovery R (in %) of quartz as dependent on the concentration c (in mol/L) of cetyl-pyridinium chloride.
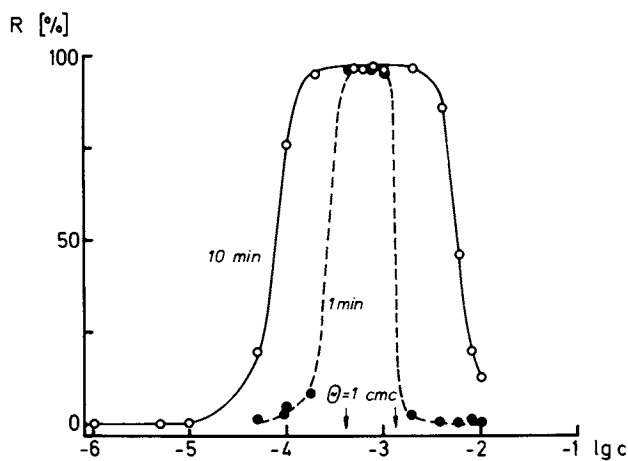
Figure 5. Flotation recovery R (in %) of barite as dependent on the concentration c (in mol/L) of Na-do decylbenzenesulfonate.

time. In this case the flotability is maximal at only
one concentration of the surfactant (8). For a constant
flotation time of 10 min, the maximum flotability can-
not be determined reliably.

Scamehorn et al (1,2) have studied the influence
of adsorption of isomerically pure surfactants and their
mixtures on the occurrence of adsorption maxima. We
have investigated, therefore, the flotability of barite
in solutions of pure Na-alkylsulfates (C_{10}, C_{12}, and
C_{14},) and their mixtures above the CMC. The decrease
in flotability begins at a concentration corresponding
to the adsorption density $\theta \cong 1$, and reaches a minimum
at the surfactant concentration $\gtrless$ CMC (Fig. 6). Similar-
ly as in Figs. 3 and 4, only arrows for $\theta \cong 1$ and CMC,
resp., were used. The minimum flotability of barite in
the mixtures of pure surfactants C_{10} + C_{12} and C_{10} +
C_{14} is also reached in the region of concentration $\gtrless$
CMC (Fig. 7,8). No adsorption isotherms were determined
for the flotation experiments shown since we gathered
from the data published by Scamehorn et al (2), who
studied the change of the adsorption density as a func-
tion of the composition of binary isomer mixtures of
Na-alkylbenzene sulfonates on alumina and kaolinite.
The location of flotation maxima depends on the ratio
of the isomers used.
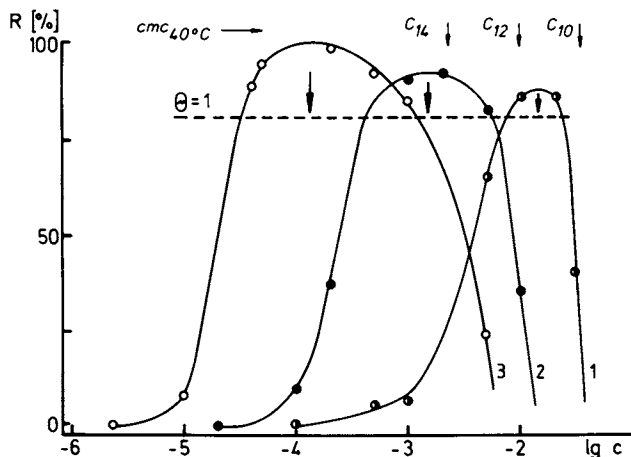
Figure 6. Flotation recovery R (in %) of barite as
dependent on the concentration c (in mol/L) of C_{10}
C_{12} and C_{14} alkylsulfate-Na (1-3).
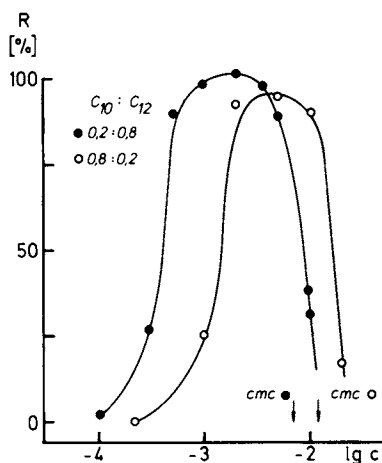
Figure 7. Flotation recovery $\underline{R}$ (in %) of barite as dependent on the concentration $\underline{c}$ (in mol/L) of C_{10}-C_{12} alkylsulfate-Na mixtures.
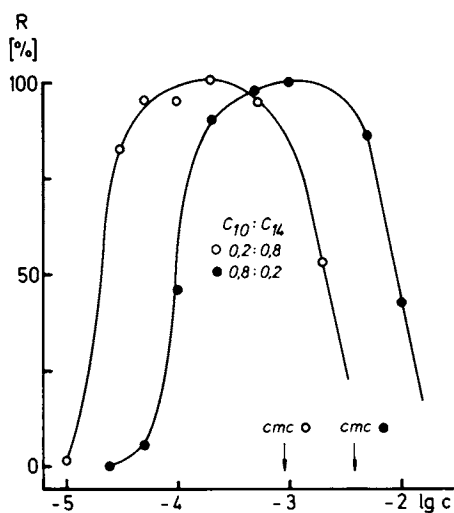
Figure 8. Flotation recovery $\underline{R}$ (in %) of barite as dependent on the concentration $\underline{c}$ (in mol/L) of C_{10}-C_{14}-alkylsulfate-Na mixtures.

Conclusions

1. At concentration > CMC, mineral flotability rapidly
decreases regardless of the character of PDIs. This de-
crease in flotability is in a good agreement with the
occurrence of adsorption maxima and gives evidence of
the change in the character and structure of the ad-
sorption layer.
2. The appeareance of maxima on the adsorption isotherms
and decrease in flotability can be explained by the hy-
pothesis that in the presence of micelles no adsorption
layer of the surfactant can be formed, the character
of which corresponds to the equilibrium state only with
monomers (sufficiently hydrophobic adsorption layer).
Due to a heterogeneity of forces acting at the surfac-
tant ion mineral interface it can be assumed that at
concentrations ⋝ CMC some of the molecules will be bound
much more firmly in a three-dimensional micelle than in
a two-dimensional adsorption layer.

Acknowledgment

Literature Cited

1.   Scamehorn, J.F.; Schechter, R.S.; Wade, W.H.; J.
     Coll. Interface Sci. 1982, 85, 463.
2.   Scamehorn, J.F.; Schechter, R.S.; Wade, W.H.; J.
     Coll. Interface Sci. 1982, 85, 479.
3.   Trogus, F.J.; Schechter, R.S.; Wade, W.H.; J. Coll.
     Interface Sci. 1979, 70, 293.
4.   Ananthapadmanabhan, K.P.; Somasundaran, P.; Coll-
     oids and Surfaces 1983, 77, 105.
5.   Dobias, B.; Colloid & Polymer Sci. 1977, 255, 682;
     ibid 1978, 256, 465.
6.   Dobias, B.; Strnad, J.; 8th Scandinavian Symposium
     on Surface Chemistry, Lund 4. - 6. June 1984.
7.   Dobias, B.; Trans. Instn. Min. Metall. Sect.C,
     Mineral Process Extr. Metall. 1983, 92, C 164.
8.   Dobias, B.; Bergakademie 1964, 16, 624.

Competitive Adsorption of an Anionic and a Nonionic Surfactant on Polystyrene Latex

B. Kronberg, M. Lindström[1], and P. Stenius

Institute for Surface Chemistry, Box 5607, S-114 86 Stockholm, Sweden

The simultaneous adsorption of two surfactants, sodium dodecyl sulfate (SDS) and nonylphenol deca(oxyethylene glycol) monoether (NP-EO$_{10}$), on polystyrene latex has been determined. The competitive adsorption of surfactant mixtures at different compositions is conveniently compared at the same total surface pressure. The basic assumption is that the pressures are equal at the onset of micellization in the mixed surfactant solutions. The results show that the surface composition differs greatly from the solution composition, viz. NP-EO$_{10}$ adsorbs in excess both in the mixed micelles and on the latex surface. Using regular solution theory of liquid mixtures it is shown that the dominating driving force in adsorption stems from the energetically unfavorable interaction between the water and the hydrocarbon part of the surfactant, i.e. it is akin to the driving force of micellization. Moreover, it is shown that this driving force also is the dominating factor determining the surface composition of surfactant mixtures. The competitive adsorption or surface composition can therefore be calculated from the cmc's of the single surfactants.

Mixed surfactant systems are frequently used in practice. For example, latexes are often prepared in the presence of an anionic surfactant. Later, a nonionic surfactant may be added in order to enhance the colloidal stability of the system.

In recent papers (1-2), we have shown how the thermodynamics of adsorption of nonionic surfactants on latex surfaces can be described in terms of a few simple parameters that may be used to predict the relative strength of adsorption of surfactants with different hydrophilic/hydrophobic balance on surfaces of different polarity.

We have shown that the main driving force of adsorption of surfactants in monolayers on latex surfaces is the (cooperative) inter-

[1]Current address: Kenobel AB, Box 11536, S-100 61 Stockholm, Sweden.

action between the hydrophobic groups of the surfactant molecules on
the surface. The direct interaction between the surface and the hydro-
phobic group of the surfactant does play a role in determining the
relative strengths of adsorption on different surfaces; however, at
least in the case of latex surfaces, this direct replacement of
solvent/surface interactions by surfactant/surface interactions cor-
responds to only 20% or less of the total free energy of adsorption.
The remainder of the adsorption free energy is due to the replacement
of unfavorable contacts between water and the hydrophobic group of
the surfactants with hydrophobic group-hydrophobic group contacts and
water-water contacts.

     These results indicate that it should be possible to make rough
predictions of competitive adsorption of different surfactants on
latex surfaces without any detailed knowledge about the properties of
the surface. The major difference in adsorption strength should be
due to differences in the hydrophilic/hydrophobic balance of the sur-
factants, i.e. to differences in their solution properties.

     In this paper we apply basic solution thermodynamics to both the
adsorption of single surfactants and the competitive adsorption of
two surfactants on a latex surface. The surfactant system chosen in
this model study is sodium dodecyl sulfate (SDS) and nonylphenol deca
(oxyethylene glycol) monoether (NP-EO$_{10}$). These two surfactants have
very different cmc's, i.e. the balance between their hydrophobic and
hydrophilic properties are very different while both are still highly
soluble in water.

Experimental

Materials. The polystyrene latex, with a mean diameter of 0.42 μm,
was synthesized by emulsifier-free emulsion polymerization. Potassium
persulfate was used as initiator and the surface charge that stabi-
lizes the latex particles thus originates from sulfate radicals. The
synthesis was carried out at the Department of Polymer Technology at
Åbo Akademi, Finland.

     Since the latex is slightly polydisperse the specific surface
area of the latex cannot be calculated with sufficient accuracy. We
will therefore present the adsorption results per unit mass of the
latex. Note, that we are in this work only concerned with the surfac-
tant composition on the surface and not the absolute value of the
amount of adsorbed surfactant per unit area.

     Conductometric titration of the surface groups gave a surface
charge density of strong acid (-SO$_4^-$) of 0.56 C/g and of weak acid
(-COO$^-$) of 0.23 C/g. Preceding the conductometric titration the latex
was cleaned by serum replacement with doubly distilled water and
5 · 10^{-4}M HCl as described in ref. (3).

     The nonionic surfactant, nonylphenol deca(oxyethylene glycol)
monoether, NP-EO$_{10}$, supplied by Berol Kemi AB, Stenungsund, Sweden,
was of technical grade and used without further purification. The
main impurity is free polyethylene oxide. Analysis of the sample gave
a polyethylene oxide content of ≈ 3% (4). Note, that polyethylene
oxide adsorbs on polystyrene latexes (5), but a monolayer is reached
at solution concentrations that are ≈ 10 times the concentration re-
quired to obtain a monolayer coverage with NP-EO$_{10}$. The free poly-
ethylene oxide, therefore, is expected to have negligible influence
on the adsorption measurements.

The anionic surfactant, sodium dodecylsulfate, SDS, was obtained
from Merck, Darmstadt, Federal Republic of Germany. It has a stated
purity of 99.99% and was used without further purification. Surface
tension measurements gave no minimum in the surface tension at the
critical micelle concentration, indicating that the sample did not
contain highly surface active impurities.

The water was doubly distilled and had a conductivity less than
1 µS/cm.

Methods. The adsorption was determined by adding a surfactant mixture
of known composition to the emulsifier-free latex. The solid/solution
ratio was held constant at 0.17 w/w. In this way a series of adsorp-
tion measurements was performed with increasing total surfactant con-
centration. Note that, while the ratio of the two surfactants in such
a series is constant in the whole system, it is not necessarily
constant on the surface or in the solution because of the preferential
adsorption of one of the surfactants.

After equilibrium, at 25 $\pm$ 0.1°C, for $\approx$ 24 h the serum was
collected for surfactant analysis by filtering the latex through a
0.22 µm Millipore filter.

Analysis of NP-EO$_{10}$ was made by UV-spectroscopy at 275 nm where
the phenyl ring gives a strong absorption. The accuracy in the deter-
mination of the adsorption of NP-EO$_{10}$ is about $\pm$ 0.5 mg/g. The total
surfactant concentration was determined by measuring the refractive
index increment on a Jena differential refractometer. These measure-
ments give the total surfactant adsorption with an accuracy of about
$\pm$ 3 mg/g. The SDS concentration was obtained from the difference
(total surfactant - amount of NP-EO$_{10}$), and hence is definitely not
known to an accuracy better than $\pm$ 3 mg/g.

The critical micelle concentrations (cmc) of the mixed surfactant
systems were determined by measuring the surface tension as a function
of total surfactant concentration on a du Noüy ring balance at 25°C.

Thermodynamic Background

Adsorption on the Latex Surface. The following thermodynamic treat-
ment is based on arguments similar to those given by Rubingh in his
treatment of micellization of mixed surfactants (6). The adsorbed
layer is considered to be a mixture of the two surfactants in the same
way as Rubingh has treated mixed micelles, but an additional term is
included in the free energy of the surface phases to account for the
interfacial free energy. As in Rubingh's treatment we do not explic-
itly take into account the fact that one of the surfactants is ionic,
i.e. the effect of counterions is implicitly included in the activity
coefficient of the ionic surfactant. As will be evident from the ex-
perimental results this can be justified in terms of the strong
shielding of ionic interactions in the mixed adsorbed layer. This has
also been found to be the case for mixed micelles (6).

Thus, the treatment includes some very crude simplifications.
Our aim, however, is to find a model that is as simple as possible
and yet makes it possible to estimate adsorption from surfactant
mixtures within experimental error in the type of systems investigated
by us, i.e. adsorption at coverages approaching monolayers on essen-
tially hydrophobic surfaces, the surfactants adsorbing with their

hydrocarbon moiety directed towards the surface. The adsorption on
hydrophilic surfaces, involving interactions between the polar end
group and the surface, has been treated extensively by e.g. Scamehorn
et al (8).

The chemical potential, μ_i, of component i in the bulk solution
is given by

$$\mu_i = \mu_i^o + kT \ln a_i \tag{1}$$

with i = 1, 2 or w for the two surfactants and water, respectively.
μ_i^o is the chemical potential in the standard state and a_i is the
activity.

The chemical potential of component i in the surface phase in
equilibrium with the bulk solution is given by

$$\mu_i = \mu_i^{os} + kT \ln a_i^s - A_i \gamma \tag{2}$$

where A_i is the area per molecule in the surface phase and γ is the
surface, or interfacial, tension.

Adsorption of a Single Surfactant. We denote a quantity valid for
surfactant i at its critical micelle concentration (cmc) in a solu-
tion of only surfactant i in water by the superscript c(i). Thus, the
chemical potential of the surfactant at the cmc in the equilibrium
solution or in the surface phase at the onset of micellization in the
solution is given by

$$\mu_i^{c(i)} = \mu_i^o + kT \ln a_i^{c(i)} \tag{3}$$

$$\mu_i^{c(i)} = \mu_i^{os} + kT \ln a_i^{s,c(i)} - A_i \gamma^{c(i)} \tag{4}$$

where $\gamma^{c(i)}$ denotes the surface, or interfacial, tension at the cmc
of surfactant i in the solution.

Choosing the pure component standard state, we obtain the
following expression for the interfacial tension by combination of
Equations 1-4.

$$\frac{A_i \gamma}{kT} = \frac{A_i \gamma^{c(i)}}{kT} + \ln \frac{a_i^s}{a_i} - \ln \frac{a_i^{s,c(i)}}{a_i^{c(i)}} \tag{5}$$

For the adsorption of water on the latex surface, Equations 1
and 2 give

$$\frac{A_w \gamma}{kT} = \frac{A_w \gamma_w^o}{kT} + \ln \frac{a_w^s}{a_w} \tag{6}$$

where

$$A_w \gamma_w^o = \mu_w^{os} - \mu_w^o \tag{7}$$

and γ_w^o is the interfacial tension between the pure water and the

solid. Finally, assuming $A_i = A_w = A$ and eliminating γ between Equations 5 and 6 we find the following expression for the surface composition:

$$\ln \frac{a_i^s/a_i^{s,c(i)}}{a_w^s} = \ln \frac{a_i}{a_i^{c(i)}} + \frac{A}{kT} (\gamma_w^o - \gamma^{c(i)}) \tag{8}$$

where we have put $a_w = 1$ for these dilute surfactant solutions.

Adsorption of Two Surfactants. We now denote a quantity valid at the onset of micellization in the equilibrium mixed surfactant solution by the superscript c. Thus, the chemical potential of surfactant i in the mixed solution or in the mixed surface phase at the onset of micellization is given by

$$\mu_i^c = \mu_i^o + kT \ln a_i^c \tag{9}$$

$$\mu_i^c = \mu_i^{os} + kT \ln a_i^{s,c} - A_i \gamma^c \tag{10}$$

where γ^c denotes the interfacial tension at the cmc of the equilibrium solution.

We now assume that the area per molecule in the mixed layer at the cmc and in the layers of single surfactants at their cmc is equal, i.e. $A_1 = A_2 = A$. Combination of Equations 3 and 4 with Equations 9 and 10 then gives the following expression for the interfacial tension:

$$\frac{A}{kT} \gamma^c = \frac{A}{kT} \gamma^{c(i)} + \ln \frac{a_i^{s,c}}{a_i^c} - \ln \frac{a_i^{s,c(i)}}{a_i^{c(i)}} \tag{11}$$

Using Equation 11 for both surfactants and eliminating γ we obtain

$$\ln \frac{a_1^{s,c}}{a_2^{s,c}} = \frac{A}{kT} (\gamma^{c(2)} - \gamma^{c(1)}) + \ln \frac{a_1^c/a_1^{c(1)}}{a_2^c/a_2^{c(2)}} + \ln \frac{a_1^{s,c(1)}}{a_2^{s,c(2)}} \tag{12}$$

It can be shown that since the aqueous solution is very dilute the ratio between the solution activities $(a_i^c/a_i^{c(i)})$ of the surfactants can be replaced by the corresponding concentration ratio $c_i^c/c_i^{c(i)}$. In the surface phase we introduce the activity coefficients of the surfactants, i.e.

$$a_1^s = x_1^s f_1^s; \quad a_2^s = x_2^s f_2^s \tag{13}$$

By analogy with the treatment of mixed micelles, we now assume that the free energy of mixing of the surface phase can be calculated using the standard regular solution expression for the activity coefficients in a binary mixture:

$$\ln f_1^s = (1 - x_1^s)^2 \chi_{12} \tag{14}$$

$$\ln f_2^s = (x_1^s)^2 \chi_{12} \tag{15}$$

where χ_{12} is the interaction parameter for the interaction between the two surfactants. By using these equations we introduce the assumptions that there is no water in the adsorbed layer at the cmc, i.e. $a_1^{s,c(1)} = 1$, that the molar volumes of the two surfactants are equal and that the effects of the counterions of the ionic surfactant are included in the interaction parameter. These assumptions are very crude, but we note that they have been used with some success in the description of the formation of mixed micelles (6).

The composition of the surfactant mixture in the equilibrium solution is described by the quantity

$$\alpha = \frac{c_1}{c_1 + c_2} \tag{16}$$

i.e., α is the fraction of the total surfactant concentration in the equilibrium solution that is due to surfactant 1. Combination of Equations 12-16 gives

$$\ln \frac{\alpha}{1-\alpha} = \ln \frac{x_1^{s,c}}{1-x_1^{s,c}} + \chi_{12}(1-2x_1^{s,c}) + \ln \frac{c_1^{c(1)}}{c_2^{c(2)}} + \frac{A}{kT}(\gamma^{c(1)} - \gamma^{c(2)}) \tag{17}$$

where $c_1^{c(1)}$ and $c_2^{c(2)}$ are the cmc's of two single surfactants, respectively.

Finally, assuming $\gamma^{c(1)} = \gamma^{c(2)}$ and ideal mixing of the two surfactants in the surface phase, i.e. $\chi_{12} = 0$, Equation 17 reduces to the following expression for the composition in the surface:

$$x_1^{s,c} = \frac{\alpha c_2^{c(2)}}{\alpha c_2^{c(2)} + (1-\alpha)c_1^{c(1)}} \tag{18}$$

Thus, a rough estimate of the surface composition, at solution concentrations around the cmc of the surfactant mixture, should be possible provided that the cmc's of the single surfactants are known.

Free Energy of Adsorption. a) System with only one surfactant. Experimentally, it is found that the adsorption of the single surfactants is well described by an equation of the form

$$Kx_i = \frac{x_i^s}{1 - x_i^s} \tag{19}$$

Assuming that the activities in the bulk and in the surface phases

can be replaced by the mole fractions (i.e. ideal behaviour) and that $a_i^{s,c(i)} = 1$, Equation 8 becomes:

$$\ln \frac{x_i^s}{1-x_i^s} - \ln x_i = - \ln x_i^{c(i)} + \frac{A}{kT}(\gamma_w^o - \gamma^{c(i)}) = \ln K \qquad (20)$$

In identifying $-RT \ln K$ with the standard molar free energy of adsorption we find that this energy can be split up into two terms, i.e.

$$\Delta \mu_{ads}^o = - RT \ln K = RT \ln x_i^{c(i)} - N_A A (\gamma_w^o - \gamma^{c(i)}) \qquad (21)$$

where N_A is the Avogadro number.
$RT \ln x_i^{c(i)}$ is the free energy of micellization and is independent of the interaction with the surface; it is determined by the hydrophobic interactions between hydrocarbon chains and the repulsion between end groups.
$- N_A(\gamma_w^o - \gamma^{c(i)})$ represents the molar free energy of replacing direct surface/water contacts by surface/surfactant contacts. The surfactants adsorb with their hydrocarbon tail directed towards a hydrophobic surface and hence we expect this term to be independent of the surfactant type and to cause a decrease in the free energy of adsorption.

b) Adsorption of two surfactants. We may now discuss Equation 17 in the same way as above for one surfactant. It reveals that there are three factors determining the distribution of the surfactants between the solution and the surface phase. The first factor is represented by the last term in Equation 17. It involves the change in the interaction with the surface when one surfactant is replaced by the other. It can be rewritten as

$$\frac{A}{kT}(\gamma^{c(1)} - \gamma^{c(2)}) = \frac{A}{kT}(\gamma_w^o - \gamma^{c(2)}) - \frac{A}{kT}(\gamma_w^o - \gamma^{c(1)}) \qquad (22)$$

This represents the difference in the second adsorption free energy term in Equation 21, i.e. the two terms on the right hand side each represent the change in free energy when a water-surface molecular contact is replaced with a surfactant-surface molecular contact. It is very reasonable to assume that, at close packing, both surfactants adsorb with only their hydrocarbon moieties (or part of these moieties) in direct contact with the surface. Hence, the two surfactants interact with the latex surface with the same strength and the last term in Equation 17 is equal to zero.
The second factor, represented by the second term from the right in Equation 17 involves the cmc's of the two single surfactants. It depends on the solution properties, or the relative balance between the hydrophobic and hydrophilic properties of the surfactants at this temperature. This term reflects the relative gain in the free energy when the hydrocarbon part of the surfactants is transferred from the aqueous solution to a hydrocarbon environment (either the micelle interior or the surface layer). The reason for this free energy gain is that the surfactant molecules are oriented at the

surface in such a way that the hydrocarbon moieties are directed to-
wards the latex surface and the hydrophilic part directed towards the
aqueous solution. This results in the well-known free energy gain due
to the cooperative effect of replacing hydrocarbon-water contacts
with hydrocarbon-hydrocarbon and water-water contacts.

The third factor determining the distribution of surfactant
between the solution and the surface phase is represented by the
third term from the right in Equation 17. It involves the interaction
between the two surfactant species, i.e. χ_{12}. Analysis of the cmc of
mixed surfactant systems (6-7) reveals that there is normally a net
attraction when anionic and nonionic surfactants are mixed. This
corresponds to a negative χ_{12}. The suggested explanation is that the
nonionic surfactant shields the lateral repulsion between the anionic
surfactant molecules at the surface, thus causing decrease in repul-
sion. According to Equation 17 this term causes deviations from ideal-
ity which are symmetric about the point $x_1^{s,c} = x_2^{s,c} = 0.5$.

Critical Micelle Concentration. In order to demonstrate the analogy
between our treatment of mixed adsorption and earlier treatments of
mixed micellization, we will briefly review the thermodynamics of
mixed micelles. The thermodynamics of formation of ideal mixed mi-
celles by two surfactants has been treated by Lange and Beck (9) and
Cling (10). Rubingh (6) extended the treatment to account for inter-
actions between the surfactants, essentially by writing the cmc in
the mixed surfactant solution as,

$$c^c = x_1^m \, f_1^m \, c_1^{c(1)} + x_2^m \, f_2^m \, c_2^{c(2)} \qquad\qquad (23)$$

where x_i^m and f_i^m are the mole fraction and activity coefficient of
surfactant i in the mixed micelle. Only micelles at the cmc are con-
sidered here. Thus, for the sake of simplicity, we have omitted
the superscript c on x_i^m and f_i^m.

As for the close packed surface layer it is assumed that the
micelles do not contain any water, i.e. $x_1^m + x_2^m = 1$. Assuming ideal
mixing of the two surfactant types in the mixed micelle, i.e. $f_1^m =
f_2^m = 1$, Equation 23 shows that the cmc is the arithmetic mean of the
two single surfactant cmc's with the surfactant composition in the
micelle as the variable.

The relation between c^c and the total surfactant composition, α,
is

$$\frac{1}{c^c} = \frac{\alpha}{f_1^m \, c_1^{c(1)}} + \frac{1-\alpha}{f_2^m \, c_2^{c(2)}} \qquad\qquad (24)$$

Introducing the regular solution expression for the activity coeffi-
cients (Equations 14 and 15 with superscript s replaced by m) into
Equation 24 Rubingh found the following useful relations:

$$\frac{(x_1^m)^2 \ln\left(\frac{c^c \alpha}{c_1^{c(1)} x_1^m}\right)}{(1-x_1^m)^2 \ln\left(\frac{c^c (1-\alpha)}{c_2^{c(2)} (1-x_1^m)}\right)} = 1 \qquad (25)$$

and

$$\chi_{12} = \frac{1}{(1-x_1^m)^2} \ln\left(\frac{c^c \alpha}{c_1^{c(1)} x_1^m}\right) \qquad (26)$$

Equation 25 can be solved iteratively for the micelle composition, x_1^m, and hence χ_{12} can be calculated from Equation 26.
Since

$$\alpha c^c = x_1^m f_1^m c_1^{c(1)} \qquad (27a)$$

and

$$(1-\alpha)c^c = (1-x_1^m)f_2^m c_2^{c(2)} \qquad (27b)$$

we find the following relation between the surfactant composition in the micelles, x_1^m, and in the solution, α, by using Equations 27, 14 and 15 where superscript s is replaced by m:

$$\ln\left(\frac{\alpha}{1-\alpha}\right) = \ln\left(\frac{x_1^m}{1-x_1^m}\right) + \chi_{12}(1-2x_1^m) + \ln\left(\frac{c_1^{c(1)}}{c_2^{c(2)}}\right) \qquad (28)$$

Equation 28 differs formally from Equation 17 only in that the term involving the interaction with the surface is missing in Equation 28. Thus, there are two factors determining the distribution of the sur- factants between the solution and the micelles. The first involves the cmc's of the two single surfactants and the second factor involves the interaction between the two surfactants in the micelle. In the ideal case, i.e. where $\chi_{12} = 0$, the surfactant composition in the micelle is related to the solution composition, at the onset of micelle forma- tion, through

$$x_1^m = \frac{\alpha c_2^{c(2)}}{\alpha c_2^{c(2)} + (1-\alpha)c_1^{c(1)}} \qquad (29)$$

which is identical to Equation 18 for the surfactant composition on the surface. This identity appears because in Equation 18 it is assumed that both surfactants adsorb with their hydrocarbon part directed towards the surface.

Results and Discussion

Critical Micelle Concentration. Figure 1 shows the cmc as a function
of the surfactant composition, α, defined as,

$$\alpha = \frac{c_{NP-EO_{10}}}{c_{NP-EO_{10}} + c_{SDS}} \tag{30}$$

according to Equation 16. As expected, the cmc decreases dramatically
when small amounts of $NP-EO_{10}$ are added to the anionic surfactant,
SDS. This is expected because of the shielding of electrostatic re-
pulsion between the SDS molecules in the micelle ([7]). The solid curve
in Figure 1 is calculated from Equation 24, i.e. under the assumption
that the two surfactants mix ideally in the micelle ($\chi_{12} = 0$).
    Assuming ideal mixing, the surfactant composition in the micelles
can be calculated from Equation 29, or alternatively from the experi-
mentally determined cmc of the surfactant mixture, c^c, using Equation
23,

$$x_1^m = \frac{c^c - c_2^{c(2)}}{c_1^{c(1)} - c_2^{c(2)}} \tag{31}$$

The results are presented in Figure 2 where the surfactant composi-
tion in the micelles is plotted as a function of the total surfactant
composition at the critical micelle concentration of the mixture. The
figure reveals a strong enrichment of $NP-EO_{10}$ in the micelles.
    In order to check how the introduction of the surfactant-surfac-
tant interaction affects the calculated cmc and the surfactant com-
position in the micelles, we used Equations 25 and 26 to obtain an
average value of χ_{12} , which was found to be -1.6. The dashed lines
in Figures 1 and 2 show that introducing a non-zero value of χ_{12} does
not affect the calculated cmc or the surfactant composition in the
micelles very much. This is because the dominating term in Equation
28 involves the difference in the cmc of the two surfactants. Thus,
to obtain an assessment of the importance of surfactant-surfactant
interaction in the mixed micelles, one should choose surfactants with
their cmc's close to each other.

Adsorption on Polystyrene Latex. Figure 3 shows the adsorption iso-
therms of the two single surfactants, $NP-EO_{10}$ and SDS, on the poly-
styrene latex surface. Both isotherms reach a limiting value when the
cmc is approached. The lines drawn in the figure are calculated from
the fitting Equation 19. The adsorption free energies, as obtained
from Equation 21, are shown in Table I. The table also shows the two
contributions to $\Delta\mu_{ads}^o$ according to Equation 21, where the first con-
tribution is obtained from the cmc's and the second from the differ-
ence between the two terms in Equation 21.
    The table reveals that the adsorption free energy is dominated
by the cmc term. Thus, the dominating driving force of adsorption is
of the same origin as for the micellization, i.e. it depends on the
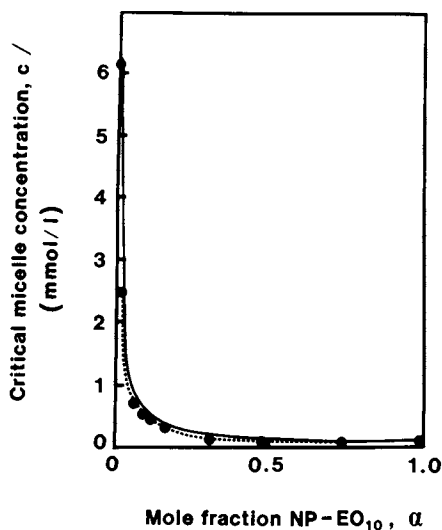
Figure 1. The critical micelle concentration, c^c, as a function of the surfactant composition, α. The curves are calculated from Equations 24, 14, and 15 with $\chi = 0$ (ideal case, solid line) and $\chi = -1.6$ (dashed line).
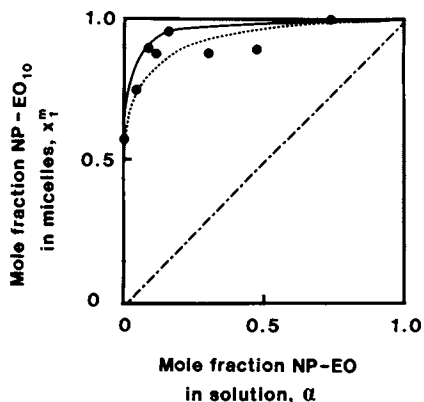
Figure 2. The calculated surfactant composition in the micelles, x_1^m, as a function of the surfactant composition in the bulk solution, α. The curves are calculated from Equation 28 with $\chi = 0$ (ideal case, solid line) and $\chi = -1.6$ (dashed line). The experimental points are calculated from Equation 31.

Table I. The Two Contributions to the Adsorption Free Energy
          of a Single Surfactant, According to Equation 21

$\Delta\mu^o_{ads}$ (kJ/mole)	$RT\ln(x_i^{c(i)})$ (kJ/mole)	$-(N_A A(\gamma_w^o - \gamma^{c(i)})$ (kJ/mole)
NP-EO$_{10}$ $\quad$ -38.2	-33.8	-4.4
SDS $\quad$ -28.0	-22.6	-5.4

solution properties of the surfactant. This is the reason we can use
the critical micelle concentrations to predict the competitive ad-
sorption between two surfactants (see below). We also note that the
$N_A A(\gamma_w^o - \gamma^{c(i)})$ term is almost identical for the two surfactants. This
is expected since both surfactants adsorb with their hydrocarbon part
directed towards the polystyrene surface. Thus, for both surfactants,
this term represents the free energy difference when polystyrene-
water contacts are replaced by polystyrene-hydrocarbon contacts.

Figure 4 shows an example of the adsorbed amount of NP-EO$_{10}$ and
SDS from a surfactant mixture as a function of the total surfactant
concentration. The figure shows that the adsorbed amount reaches a
limiting value, which is close to the cmc of the solution mixture. In
this example the initial NP-EO$_{10}$/SDS ratio is 30/70 (w/w), i.e. the
SDS is present in excess. The figure reveals, however, that NP-EO$_{10}$
is present in excess on the surface, i.e. a strong competitive adsorp-
tion is taking place.

It is important to realize that the graph presented in Figure 4
is not strictly an adsorption isotherm. The reason being that the
surfactant composition changes along the concentration axis, due to
the preferential adsorption of NP-EO$_{10}$. Therefore, at low total sur-
factant concentrations, the solution is depleted of NP-EO$_{10}$ and hence
$\alpha \approx 0$. The development of the surfactant composition in the solution
as a function of the total concentration is shown in Figure 5. In this
figure the cmc curve, from Figure 1, has been inserted. The crossing
point of the two curves gives the composition and concentration at
which micelles appear in the system. We are thus able to obtain the
surfactant composition on the surface (Figure 4) at the onset of
micellization and, at the same time, the surfactant composition in
the bulk solution from Figure 5. Thus, we use the total surfactant
concentration at the onset of micellization as a reference. In this
way we compare the competitive adsorption, at different surface com-
positions, but at the same surface pressure.

Table II presents the experimental data, obtained from using bulk
solutions of different NP-EO$_{10}$/SDS ratios. Figure 6 shows the surfac-
tant composition on the polystyrene latex surface as a function of the
surfactant composition in the bulk solution at concentrations corre-
sponding to the onset of micellization. If the surfactant composition
on the surface were the same as that in the bulk solution, the experi-
mental points would fall on the dashed line in the figure. Thus, the
figure reveals a strong preferential adsorption of NP-EO$_{10}$ on the
surface. For example, a solution with a NP-EO$_{10}$/SDS ratio equal to
10/90 is in equilibrium with a surface where the ratio is $\approx$ 90/10.
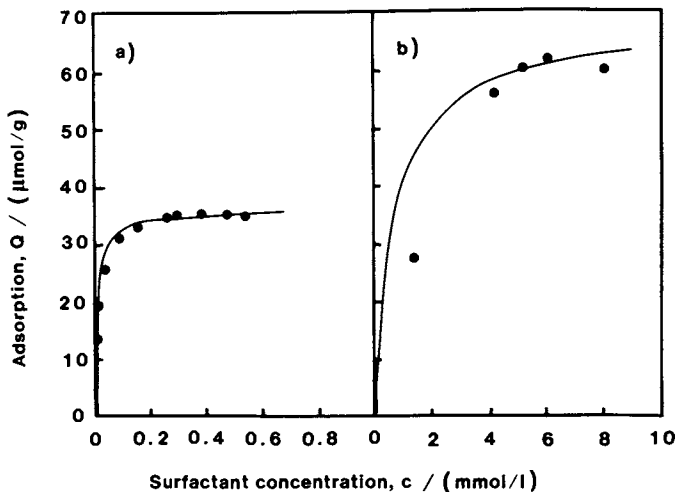
Figure 3. Adsorption of NP-EO$_{10}$ (a) and SDS (b) on polystyrene latex. The lines are isotherms calculated by fitting of Equation 19.
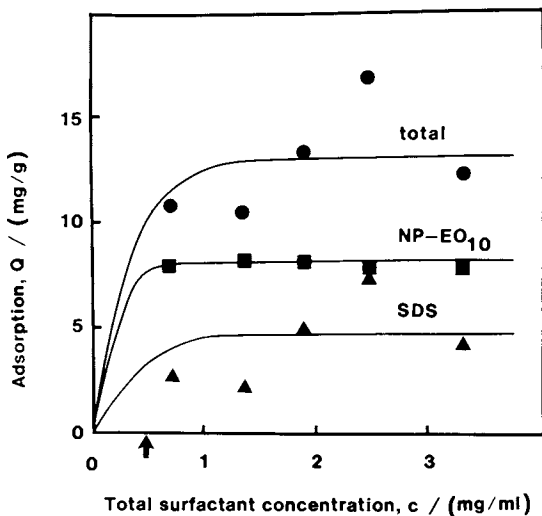
Figure 4. Adsorption of a 30/70 mixture of NP-EO$_{10}$ and SDS on polystyrene latex. The lines are drawn to make the best fit considering the inaccuracy in the determination of the total surfactant concentration. The arrow indicates the cmc of the surfactant mixture.
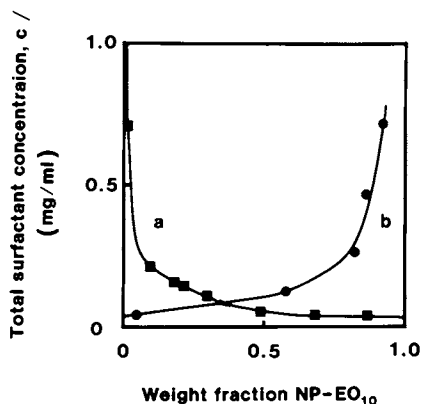
Figure 5. Dependence of the surfactant composition in the bulk solu-
tion on the total surfactant concentration, a) cmc curve and b) in
the presence of latex. The crossing of the curves gives the solution
composition and concentration at close packing of the surfactants on
the PS surface.
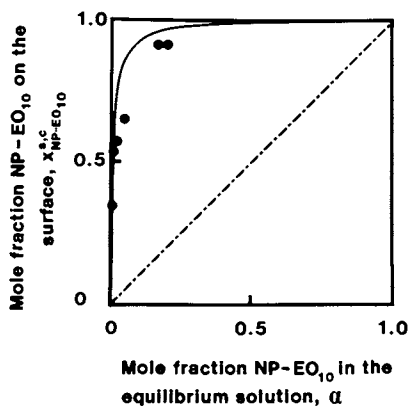
Figure 6. The surfactant composition on the PS surface, $x^{s,c}_{NP-EO_{10}}$,
as a function of the surfactant composition in the bulk solution, α.
The points are obtained at the cmc of the solution, i.e. with close
packing of the surfactants on the surface. The solid curve is calcu-
lated from Equation 18.

Table II. Adsorption Data for the Adsorption of NP-EO$_{10}$ and SDS
on PS latex

Mole-% NP-EO$_{10}$ of total surfactant content	Adsorbed amount, Q, at the onset of micellization (mole/g)		$x^{s,c}$ NP-EO$_{10}$	c^c (mg/ml)	$\alpha^{solution}$ NP-EO$_{10}$
	$Q_{NP-EO_{10}}$	Q_{SDS}			
0	0	61.4	0	1.78	0
4.6	11.3	21.8	0.34	1.0	0.007
10.0	14.9	12.9	0.54	0.8	0.009
16.1	17.6	13.6	0.56	0.4	0.022
30.3	25.2	13.6	0.65	0.3	0.046
49.0	29.7	2.8	0.92	0.1	0.16
71.9	26.8	2.8	0.91	0.08	0.20
100	32.8	0	1.00	0.05	1.00

In particular, we would like to point out two conclusions of practical importance. Firstly, a surface analysis of the serum (bulk solution) cannot give direct information on either the surfactant composition on the latex surface or in the total system. This is an important conclusion since such analyses are frequently carried out in industrial laboratories. Secondly, Figure 6 shows that if NP-EO$_{10}$ is added to a system stabilized with SDS, the latter will desorb. In practice, this causes foaming problems. Such problems can be predicted, as is shown below.

The solid line in Figure 6 is calculated from Equation 18, i.e. under the assumption that $\chi_{12} = 0$ and $\gamma^{c(1)} = \gamma^{c(2)}$ in Equation 17. The agreement with the experimental results indicates that these two assumptions are reasonably valid. Thus, it is possible to predict the competitive adsorption of two surfactants knowing only the cmc's of the single surfactants. For the adsorption of the single surfactants we noted that the cooperative effect of replacing hydrocarbon-water contacts with hydrocarbon-hydrocarbon and water-water contacts constitutes a major part of the free energy of adsorption. Since the cmc is a reflection of this effect, it is therefore not surprising that one can predict the competitive adsorption on hydrophobic surfaces knowing only the cmc's of the single surfactants. This effect also predicts that the more hydrophobic surfactant should be preferentially adsorbed on the latex surface as is found in Figure 6.

We have also calculated the competitive adsorption with the introduction of a non-zero value of the surfactant-surfactant interaction parameter, i.e. $\chi_{12} = 1.6$. As in the calculated composition in the mixed micelles we find that the calculated surfactant composition on the latex surface is rather insensitive to the value of χ_{12}. The reason is, as in the calculation of the cmc of the surfactant mixture, that the large contribution from the difference in the cmc's of the single surfactants outweighs this interaction contribution.

Thus, there is a simple way to predict the surfactant composition on a hydrophobic surface for a mixed surfactant system. The

only information needed is the critical micelle concentrations of the single surfactants. The two most important assumptions in such a prediction are (i) a water-free surfactant monolayer on the latex surface is formed at the onset of micelle formation and (ii) the mixed surfactant monolayer forms an ideal mixture. The prediction is not very sensitive to the validity of the latter assumption.

The reason for the success of such a simple model is that the dominating force in determining the surfactant composition on the surface originates from the free energy gain of replacing hydrocarbon-water contacts with hydrocarbon-hydrocarbon and water-water contacts when a surfactant molecule is adsorbed into the surfactant monolayer.

Literature Cited

1. Kronberg, B. J. Colloid Interface Sci. 1983, 96, 55.
2. Kronberg, B.; Stenius, P. J. Colloid Interface Sci. 1984, 102, 410.
3. Ahmed, S. M.; El-Aasser, M. S.; Pauli, G. H.; Poehlein, G. W.; Vanderhoff, J. W. J. Colloid Interface Sci. 1980, 73, 388.
4. Kronberg, B.; Käll, L.; Stenius, P. J. Dispersion Sci. 1981, 2, 215.
5. Kato, T.; Nakamura, K.; Kawaguchi, M.; Takahashi, A. Polymer J. 1981, 13, 1037.
6. Rubingh, D. N. In "Solution Chemistry of Surfactants; Mittal, K. L. Ed.; Plenum: New York, 1979; Vol. 1, p. 337.
7. Schick, M. J.; Manning, D. J. J. Am. Chem. Soc. 1966, 43, 133.
8. Scamehorn, J. F.; Schechter, R. S.; Wade, W. H. J. Colloid Interface Sci. 1982, 85, 463, 479, 494.
9. Lange, H.; Beck, K. H. Kolloid Z.-Z. Polym. 1973, 251, 424.
10. Clint, J. J. Chem. Soc. 1975, 71, 1327.

18

Self-Emulsification of Vegetable Oil–Nonionic Surfactant Mixtures

A Proposed Mechanism of Action

Mark G. Wakerly[1], Colin W. Pouton[1], Brian J. Meakin[1], and Frank S. Morton[2]

[1] School of Pharmacy and Pharmacology, University of Bath, United Kingdom
[2] R.P. Scherer Ltd., Blagrove, Swindon, United Kingdom

Binary mixtures of some commerical nonionic surfactants
and vegetable oils have been screened for their ability
to emulsify under conditions of gentle agitation. Such
mixtures may have potential use as pharmaceutical drug
delivery systems. The system Tagat TO, an ethoxylated
glycerol tri-oleate and Miglyol 812, a medium chain
triglyceride, has been studied in detail for its
ability to form stable, submicron-droplet oil-in-water
emulsions. Ternary phase studies have revealed a
specific region of lamellar liquid crystal dispersed in
the isotropic phase of solubilised water. The
occurrence of this dispersion phase correlates with
good self-emulsifying performance from the binary
mixture. The observed self-emulsification is
considered to be a result of aqueous penetration into
the liquid crystal aided by mechanical dispersion of
the resulting emulsion.

Soft gelatin capsules containing oily solutions of drugs, such as
sedatives, vitamins and steroidal hormones, are used as oral dosage
forms for medicinal products. Such drug delivery systems can have
therapeutic advantages over tablets or powder-filled hard gelatin
capsules; in particular the slow drug dissolution step often
encountered with lipophilic drugs can be avoided (1,2). This can
lead to better control of drug absorption from the gastro-intestinal
tract and hence improvement in the effectiveness of the medicinal
product (3-5). If the lipophilic drug is presented in an oil-in-
water emulsion further enhancement of bioavailability can be achieved
(6). However water-containing vehicles cannot be filled into soft
gelatin capsules due to the hydrophilic nature of the gelatin shell
which absorbs water thus dehydrating and eventually disrupting the
emulsion structure (7). Consequently we are studying surfactant-oil
solutions which exhibit the phenomenon of self-emulsification as a
method of achieving emulsions in the gastro-intestinal tract which
are derived from soft gelatin encapsulated formulations.

Self-emulsification is the formation of an emulsion from oil and water by weak mechanical shear forces. In vivo such levels of agitation would be provided by the digestive motility of the stomach and intestine ($\underline{8}$). Reiss has calculated that the free energy of oil-water mixing will be negative if the interfacial tension is less than 10^{-3} Nm^{-1}, and at about 10^{-7} Nm^{-1} emulsion droplets of diameter approximately 0.3 μm will form ($\underline{11}$). Such systems are described as being spontaneously-emulsifying ($\underline{9,10}$). Systems which have interfacial tensions of the order of 10^{-5} Nm^{-1} will emulsify readily although not spontaneously and are classified as self-emulsifying. For both self- and spontaneous emulsification the presence of added surface active materials is normally required ($\underline{12}$). The rationale behind this study necessitated the use of materials with potentially acceptable toxicity characteristics when ingested orally. The choice of surfactant was therefore restricted to the ethoxylated nonionic type which are likely to have acceptable toxicity profiles ($\underline{13}$) and oils were derived from vegetable sources.

Experimental

Materials. All materials were used as received from the suppliers. Nonylphenol ethoxylates (Synperonics) were obtained from Cargo Fleet Chemical Company Ltd, England. Alcohol ethoxylates (Marlipals) were obtained from Huls (UK) Ltd. Fatty acid ethoxylates (Leeks) were obtained from Leek Chemicals Ltd, England. Tween 85 was obtained from Atlas Chemical Industries (UK) Ltd. Tagat TO was supplied by Th. Goldschmidt AG, Germany. Vegetable oils were Miglyol 812 supplied by Dynamit Nobel (UK) Ltd and Arachis oil supplied by Evans Medical Ltd, England. All water was single distilled using all glass apparatus.

Methods. Initially a range of different nonionic surfactant-oil mixtures containing 30% w/w surfactant were screened for their ability to self-emulsify in water at 25 and 37°C. Gentle agitation was provided by a glass stirrer as described by Pouton ($\underline{14}$). The efficiency of self-emulsification was assessed subjectively on a scale of 1 to 5 (bad to excellent) by visual observation.

Emulsion preparation under controlled conditions. Those systems which appeared to emulsify efficiently were studied further by particle size analysis of the emulsions formed by self-emulsification under agitation conditions considered to be a reasonable simulation of the in vivo situation ($\underline{8}$). Mixtures containing between 5 and 70% w/w surfactant were examined over the temperature range 25 to 50°C. A concentration of 0.04% v/v of binary lipophilic mixture was achieved by the following method. 10 μl of self-emulsifiable mixture was delivered from an Agla micrometer syringe into 25 ml of distilled water in a 30 ml Pyrex glass tube fitted with a ground glass stopper. All materials were pre-equilibrated to the appropriate temperature. The tubes were immersed in a thermostatted shaking waterbath ($\pm$ 0.1°C) and rocked horizontally through 2.5 cm at a rate of 40 oscillations per minute for 10 minutes unless otherwise stated. The concentration of the resulting emulsions was such that droplet size determinations could be performed without dilution.

Analysis of Mean Emulsion Droplet Diameter (MEDD). Two techniques were used to measure the MEDD of the self-emulsified systems. Low angle laser light diffraction (Malvern model 3600E with small volume stirred cell) was used for emulsions with droplet distributions above 1 μm. The majority of determinations were carried out over the range 1-120 μm. Samples were analysed immediately after preparation. Quasi-elastic light scattering (QELS, Malvern model 4600 photon correlation spectrometer) was used for investigations of submicron dispersions and measurements were made 24 hours after preparation. The MEDD of such submicron emulsion systems has been shown to be unaltered by storage for 7 days (14). For both techniques three separate emulsion samples were examined. Each sample was determined in triplicate by laser diffraction and in quintriplicate by QELS. MEDD values are expressed as mean values of all data $\pm$ standard error.

Equilibrium Phase Behaviour. Phase studies were performed using approximately 10 g samples of oil-surfactant mixture diluted sequentially by the weighed addition of water. The initial binary mixture contained 5-70% w/w surfactant at 5% intervals. Phase boundaries were determined to $\pm$ 0.5% water. The ternary mixtures in Pyrex glass tubes fitted with PTFE lined caps were equilibrated to the required temperature (20-65 $\pm$ 0.1°C) for 2 hours and then thoroughly mixed for 5 minutes using a Fisons orbital whirlimixer. The tubes were then returned to the waterbath and left undisturbed for 48 hours before identification of the phase type using a crossed polarised viewer and an optical microscope.

Results and Discussion

Qualitative data obtained by visual assessment of self-emulsification at 25 or 37°C (Table I) show that the unsaturated ester-type surfactants exhibit better self-emulsifying behaviour than the equivalent saturated ether types with both oils. These data also show the phenomenon is not directly related to the hydrophile-lipophile balance (HLB) of the surfactant. The ester type surfactants probably show better behaviour due to mobility of the liquid-like oleate chains in these surfactant molecules. However , of the materials screened , the Tagat TO-Miglyol 812 and Tween 85-Miglyol 812 mixtures showed the best behaviour and the former was chosen as a model commercial system for more detailed study. The oil, Miglyol 812 is a fractionated triglyceride containing mainly caprylic (C_8, 50-65%) and capric (C_{10}, 45-30%) saturated carboxylic acid residues.
Tagat TO is an ethoxylated (25 moles per molecule) triglyceride of commercial oleic acid (65% oleic with the remainder mainly myristic C_{14}, palmitic C_{16}, stearic C_{18} and linoleic C_{18}:2 double bonds). The surfactant has a negligible bulk water solubility (15); however , the ethylene oxide condensation reaction used to manufacture the surfactant results in a distribution of polyoxyethylene residues. This means some of the constituents of the mixture will be sufficiently hydrophilic to be water soluble.

Table I. Qualitative Screening of Surfactant-Oil Mixtures for Self-Emulsifying Behaviour at 25 and 37°C. (S) Denotes Suspended
Material in Binary Mixture.

Surfactant	HLB	Self-emulsifying Behaviour			
		Miglyol 812		Arachis Oil	
		25°C	37°C	25°C	37°C
Ethers					
Nonylphenol (5) Ethoxylate	10.5	1	1	-	-
Nonylphenol (6) Ethoxylate	10.9	2	1	-	-
Nonylphenol (8) Ethoxylate	12.3	2	2	-	-
Nonylphenol (9) Ethoxylate	12.8	3	2	-	-
Nonylphenol (10) Ethoxylate	13.3	3	2	-	-
Stearyl (5) Ethoxylate	9.7	1	1	2	1
Stearyl (10) Ethoxylate	12.9	1(S)	1(S)	1	1
Dodecyl (9) Ethoxylate	14.2	1	1	1	1
Esters					
Polyoxyethylene (6.8) mono-oleate	10.1	1	1	1	1
Polyoxyethylene (13.6) di-oleate	10.2	2	1	1	1
Polyoxyethylene (9.1) mono-oleate	11.3	3(S)	2(S)	2	2
Polyoxyethylene (13.6) mono-oleate	13.3	2(S)	2(S)	1	1
Polyoxyethylene(25)sorbitan tri-oleate	11.0	5	5	4	4
Polyoxyethylene(25)glycerol tri-oleate	11.3	5	5	3	4

MEDD Analysis. The particle size-surfactant concentration profiles obtained by laser diffraction analysis of the self-emulsified Tagat TO-Miglyol 812 mixtures are shown in Figure 1. At a self-emulsification temperature of 30°C the profile shows three regions. Between 5 and 15% surfactant there is little change in measured MEDD with increasing surfactant concentration. Values obtained for MEDD in this region were however misleading due to the gross instability of these lower surfactant concentration emulsions. The creaming rate of droplets greater than approximately 100 μm was so rapid that although particle size determination was carried out immediately after formation, these large droplets were excluded from detection and consequent MEDD evaluation. Microscopical examination of these crude emulsions showed that oil droplets in excess of 500 μm were present. A reduction in the measured MEDD on repeated analysis also confirmed the instability of these samples. Increasing the surfactant concentration from 15 to 30% resulted in emulsions of improved stability (region 2). Replicate analysis of these samples gave reproducible results but excessive creaming still occurred on overnight storage. The reduction in the MEDD in this second region probably resulted from increased interfacial stabilisation by the water soluble surface active components as the surfactant concentration was raised.

Above 30% surfactant the MEDD apparently reached a minimum value of 1-2 μm. This third region was a function of the lower detection limit of the apparatus. Table II shows that the proportion of emulsion droplets below 3 and 1 μm increased as the surfactant concentration increased. The data emphasize the marked reduction in emulsion droplet size which occurred above 30% w/w surfactant.
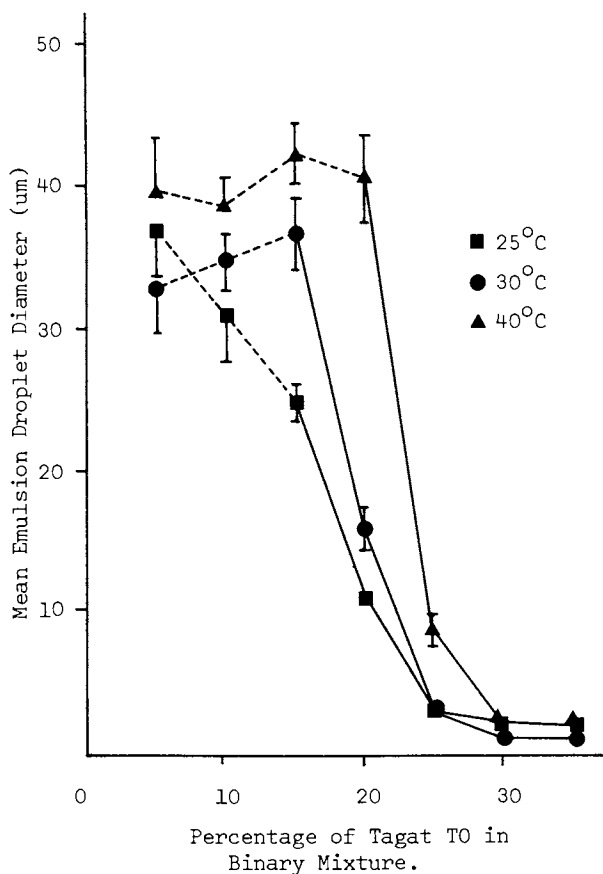
Figure 1. Effect of Binary Mixture Surfactant Concentration and
Self-Emulsification Temperature on Emulsion Droplet Size for the
Miglyol 812-Tagat TO System as Determined by Laser Diffraction.
Bars Represent Standard Errors.

Table II. Proportion of Emulsion Droplets below 3 and 1 μm as a Function of Increasing Surfactant Concentration of the Binary Mixture Tagat TO - Miglyol 812 as Measured by Laser Diffraction at a Self-Emulsification Temperature of 30°C.

Percentage Surfactant in Binary Mixture (w/w)	Percentage by Weight of Emulsion Droplets below size	
	3 μm	1 μm
5	6	0.1
10	6	0.4
15	5	0.3
20	12	3
25	48	8
30	95	39
35	99	50
40	99	61

At the self-emulsification temperature of 40°C (Figure 1) a similar profile was obtained and again three distinct regions were identified, however MEDD were larger at all surfactant concentrations. This is attributable to a reduction in the degree of hydrogen bonding of the oxyethylene groups with water (16). This in turn reduces the effective HLB of the surfactant and results in weaker interface stabilisation, and hence larger emulsion droplets form (17). Reducing the self-emulsification temperature to 25°C had the opposite effect on the effective HLB of the surfactant resulting in improved emulsion stability and hence smaller MEDD. However, the instability of larger droplets still affected the measured MEDD at the lower surfactant concentrations.

The results obtained from QELS examination of emulsions formed from binary mixtures containing 35% or more Tagat TO are shown in figures 2 and 3. Figure 2 indicates that the MEDD-surfactant concentration profiles are of a similar character for all self-emulsification temperatures studied (25-50°C) exhibiting a minimum MEDD at about 50-55% Tagat TO. Self-emulsification at 30°C yielded emulsions with the lowest MEDDs ; the minimum MEDD being approximately 100 nm at 52.5% surfactant in the binary mixture. At this temperature all binary mixtures containing 35-52.5% Tagat TO exhibited good, rapid self-emulsification. The time required to attain droplet size equilibrium at 30°C was less than 10 seconds at 35% surfactant increasing to about 120 seconds at 52.5% surfactant. Above this concentration self-emulsification characteristics deteriorated. Equilibrium times increased markedly , reaching about 20 minutes at 70% surfactant. This was accompanied by an increase in MEDD and a doubling of the polydispersity. Figure 2 also shows that better reproducibility of the formed emulsion in terms of MEDD occurred prior to and in the region of the minimum. At 30°C, MEDD values obtained with 40-55% surfactant had a relative standard deviation of about ± 2%; at 60% Tagat TO this figure increases to about ± 4%. Reproducible control of particle size is an important feature in the potential of self-emulsifying mixtures for oral drug delivery.
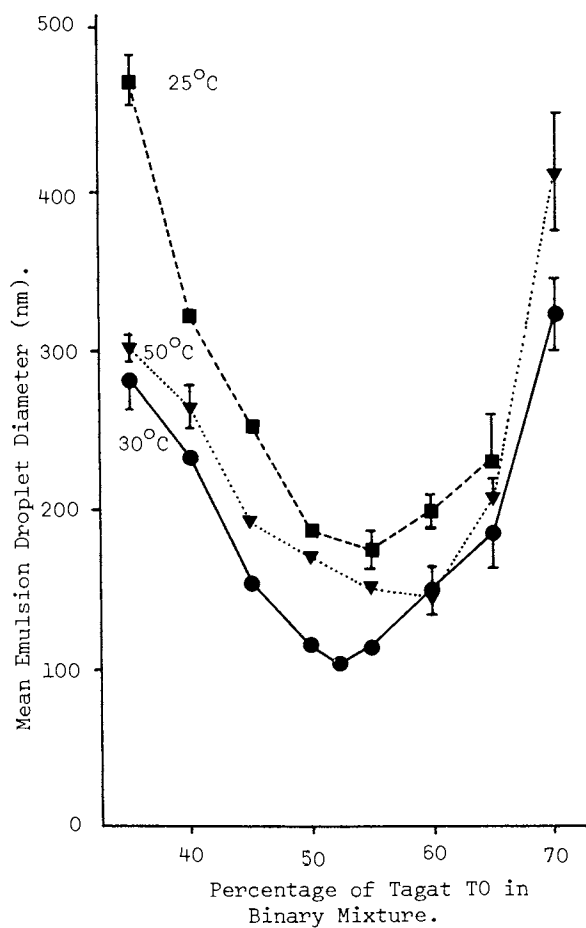
Figure 2.   Effect of Binary Mixture Surfactant Concentration and
Self-Emulsification Temperature on Emulsion Droplet Size for the
Miglyol 812-Tagat TO System as Determined by QELS.
Bars Represent Standard Errors.
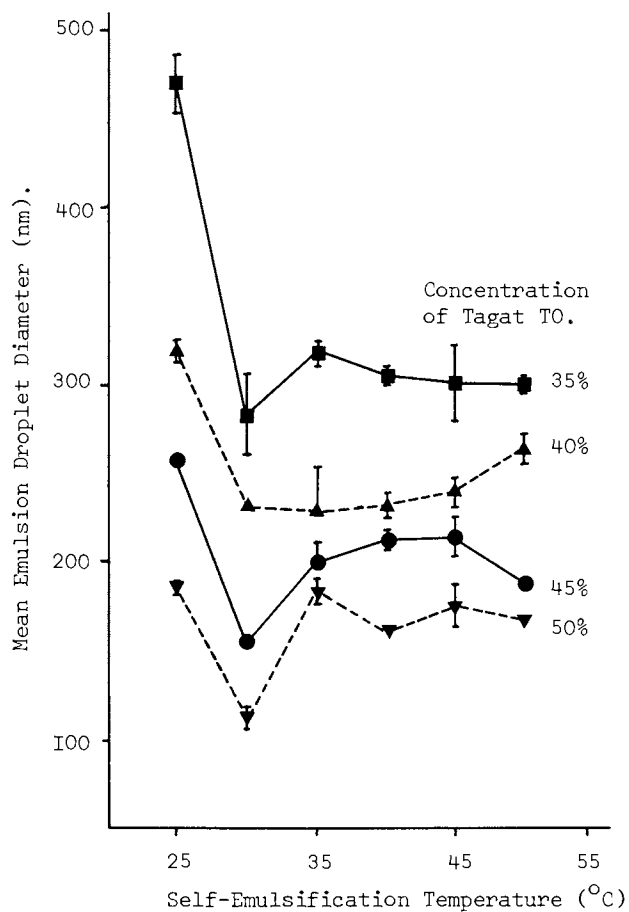
Figure 3. Effect of Self-Emulsification Temperature on Emulsion Droplet Size for the Miglyol 812-Tagat TO System as Determined by QELS. Bars Represent Standard Errors.

Figure 3 illustrates the effect of temperature over the range 25-50°C on the MEDD of the rapidly self-emulsifying systems (<2 minutes). These mixtures exhibited good self-emulsifying behaviour in terms of yielding submicron particles. All surfactant concentrations showed a decrease in MEDD between 25 and 30°C followed by a smaller increase and then little observable change. Qualitatively the effect of temperature was independant of the surfactant concentration, but quantitatively the MEDD decreased with increase in surfactant concentration between 35 and 50% over the whole temperature range considered. These studies show that in terms of minimum particle size and therefore potential ability to penetrate between the micro-villi of the gastro-intestinal mucosa thus presenting drug to the absorption site, the Tagat TO - Miglyol 812 system is optimised at 30°C. For use in vivo it would obviously be preferable to have an optimum temperature of 37°C and this could perhaps be achieved by using a slightly more hydrophilic surfactant (16). However this does not preclude the use of this system in vivo, since particles in the 200 nm region are achievable at 37°C.

Phase Behaviour. The differences in the self-emulsifying behaviour of Tagat TO - Miglyol 812 binary mixtures can, in part, be explained from considerations of their phase behaviour. Figures 4a-4d show the representative equilibrium phase diagrams obtained when binary mixtures containing 10,25,30 and 40% surfactant were sequentially diluted with water. The phase notation used is based on that of Mitchell et al (18).

For lower surfactant concentrations containing between 10-25% in the binary Tagat TO - Miglyol 812 mixture , Figures 4a and 4b show that a similar sequence of phases are formed on addition of water.

The L_2 phase always present at the right hand axis is an oil continuous phase of solubilised water. On crossing the phase boundary a two phase region, $L_1 + L_2$, is observed. Further dilution forms gel (G) or liquid crystalline (LC) phases, depending on the surfactant concentration and temperature. At higher water contents , two phase regions ($L_1 + L_2$) again form. These disperse systems extend across the phase diagrams to the water-rich side of the axis. If this equilibrium phase behaviour is applied to the dynamic process which occurs during self-emulsification, initially aqueous penetration into the oily phase will result in hydration of the oxyethylene part of the surfactant molecules. When the saturation limit of solubilised water is met, two phase systems form in all cases. It is likely that rapid dilution of these dispersions results in the crude emulsions observed in the corresponding studies of MEDD.

During the studies of phase behaviour two types of liquid crystalline phases were identified. LC material was viscous and exhibited intense "white" birefingence. LC_A material was apparently homogeneous but of low viscosity and exhibited "multi-coloured" birefringence. The liquid crystalline phases observed in the equilibrium studies of surfactant concentrations up to 25% are unlikely to take part in the self-emulsification process due to the presence of two-phase regions between L_2 and liquid crystalline phases; however , LC_A material may account for the improved stability of emulsions formed by 25% surfactant systems (Table II). Figure 4c indicates that by increasing the surfactant concentration to 30% the

Percentage w/w Water Content of Mixtures on Dilution.
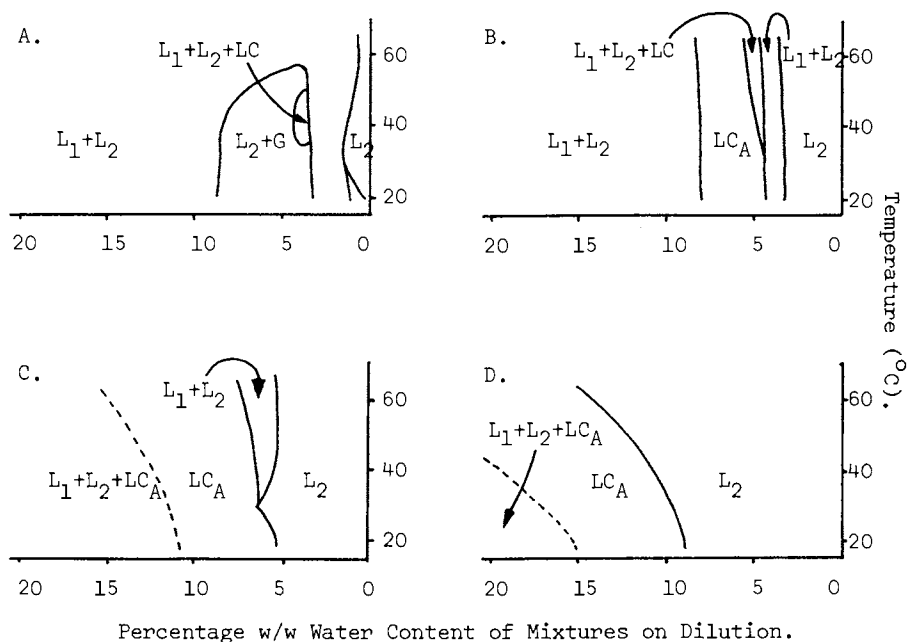
Figure 4. Equilibrium Phase Behaviour of Tagat TO-Miglyol 812 Mixtures on Dilution with Water. A. 10% Tagat TO. B. 25% Tagat TO C. 30% Tagat TO. D. 40% Tagat TO.

equilibrium phase behaviour changed and direct contact between LC_A and L_2 phases occured below $30^{\circ}C$. From the self-emulsifying studies this correlates with the formation of good quality products below $30^{\circ}C$ and impaired emulsifying performance at higher temperatures. The direct contact of these two phases would therefore appear to be most important in the self-emulsifying process. Further increases in surfactant concentration (Figure 4d) resulted in phase behaviour dominated by the LC_A phase in contact with the L_2 phase. These systems produced high quality emulsions containing submicron droplets.

The LC_A material formed by dilution of binary mixtures containing 35 to 50% surfactant was apparently a single phase exhibiting multi-coloured birefingence, the intensity of which increased with surfactant concentration. Above 55% surfactant in the binary mixture , partial separation into L_2 and liquid crystalline (LC_A type) phases occurred during the 48 hour period necessary to establish equilibrium, the degree of separation being enhanced with increasing surfactant up to 70% in the binary mixture. This was accompanied by an apparent change in the birefingence of the material as observed by colour loss to 'white', and an increase in density and hence a reduction in the molecular spacing of the crystal lattice. These observations indicate that the "LC_A phase" was in fact a dispersion of liquid crystals in isotropic L_2 phase. Over the range 35 to 50% surfactant similarities in refractive indices and densities of the L_2 and LC_A materials made separation difficult. However high speed centrifugation at controlled temperature has enabled partial separation of these dispersion phases. Comparison of the microscopical textures of LC_A material with those of Rosevear ([20]) suggests the LC_A liquid crystal material was lamellar, however the small amount present was not detectable by X-ray diffraction.

The concept of interfacial mesophases promoting spontaneous emulsification ([21,22]) can be applied to the Tagat TO - Miglyol 812 system, where stable liquid crystalline dispersion phases are adequate to premote the process of self-emulsification. The stability of the resulting emulsion systems can also be accounted for by liquid crystalline interface stabilisation ([23,24]). Phase separation of LC_A material as observed above 55% surfactant, in conjuction with the increased viscosities of such systems , will inhibit the dynamics of the self-emulsification process and hence the quality of self-emulsified systems declines when the surfactant concentration is increased above 55%.

<u>Mechanism of Self Emulsification.</u> For the binary mixtures containing between 35 and 55% Tagat TO in Miglyol 812 which form miscible L_2 + LC (LC_A) phases the following mechanism of self-emulsification can be proposed. Addition of the binary mixture to water results in interface formation between the oil and aqueous-continuous phases. As illustrated in Figure 5a, solubilisation of water with the oily phase results from aqueous penetration through the interface. This will occur until the solubilisation limit is reached close to the interface. Further aqueous penetration (Figure 5b) will result in the formation of the dispersed lamellar liquid crystal phase (LC_A) represented by the parallel lines. This material has a loosely associated lamellar lattice structure. As the aqueous penetration
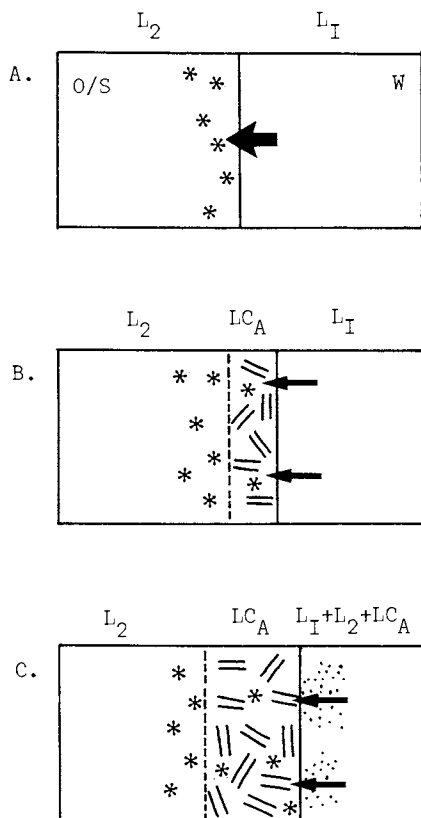
Figure 5. Schematic Representation of the Proposed Self-
Emulsification Mechanism. A. Water Penetration. B. Formation of
Liquid Crystal. C. Disruption and Emulsification.

proceeds , eventually virtually all material close to the interface will be liquid crystalline, the actual amount depending on the surfactant concentration in the binary mixture. Once formed , rapid penetration of water into the aqueous cores (Figure 5c) aided by the

gentle agitation of the self-emulsification process causes interface disruption and droplet formation.
The high stability of these self-emulsified systems to coalesence is considered to be due to a liquid crystalline interface surrounding the oil droplets.

Conclusions

The self-emulsifying behaviour of a binary nonionic surfactant vegetable oil mixture has been shown to be dependant on both temperature and surfactant concentration. The quality of the resulting emulsions as assessed by particle size analysis showed that manipulation of these parameters can result in emulsion formulations of controlled droplet size and hence surface area. Such considerations are important when the partition of lipophilic drugs into aqueous phases and drug release rates are considered.
     The commercial mixture of Tagat TO - Miglyol 812 exhibits optimum self-emulsifying behaviour at 30°C. Modification of the surfactant to produce a more hydrophilic molecule of similar structure is currently under investigation in an effort to achieve optimum behaviour at 37°C. The occurrence of good self-emulsification has been related to the direct contact between lamellar liquid crystalline dispersion phase and isotropic oil continuous phase. However the density and thus molecular packing of this crystalline material also affects the self-emulsifying behaviour.
     It is considered that penetration of water into this liquid crystalline dispersion in association with gentle agitation results in the observed self-emulsification.

Literature Cited

1. Russel, P.; Ojaka, K.; Manninen, V.; Sothman,A.
    Brit. J. Clin. Pharmacol. 1977, 4, 235.
2. Gibaldi, M. "Biopharmaceutics and Clinical Pharmacokinetics";
    3rd Edn.; Lea and Febiger: Philadelphia, 1984; Chap. 4,5,8.
3. Yamahira, Y.; Noguchi, T.; Noguchi, T.; Takenaka, H.; Maeda, T.
    Chem. Pharm. Bull. 1979, 27(5), 1190.
4. Fuccella, M. Eur. J. Clin. Pharm. 1977, 12, 383.
5. Palin, K.; Wilson, C. G.; Davis, S. S.; Philips, A. J.
    J. Pharm. Pharmacol. 1982, 34, 707.
6. Kakemi, K.; Sezaki, H.; Muronishi, S.; Ogata, H.; Giga, K.
    Chem. Pharm. Bull. 1972, 20(4), 715.
7. Ansel, H. C. "Introduction to Pharmaceutical Dosage Forms.";
    Lea and Febiger: Philadelphia, 1976; p. 189.
8. McClintic, J. R. "Physiology of the Human Body"; 2nd Edn.;
    John Wiley and Sons: New York, 1978; pp. 426-9.
9. Davies, J. T.; Haydon, D. A. In "Proc. 2nd Int. Cong. Surf.
    Active"; Butterworths: London, 1957; pp. 417-25.

10. Benton, W. J.; Miller, C. A.; Fort Jr., T. J. Disp. Sci. Technol. 1982, 3(1), 1.
11. Reiss, H. J. Coll. Interface Sci. 1975, 53(1), 61.
12. Becher, P. "Emulsions Theory and Practice"; 2nd Edn.; Reinhold: New York, 1966; pp 293-7.
13. Attwood, D.; Florence, A. T. In "Surfactant Systems, Their Chemistry, Pharmacy and Biology."; Chapman and Hall: London, 1983; Chap. 10.
14. Pouton, C. W. Ph.D. Thesis, University of London, London, 1982.
15. Th. Goldschmidt AG. Manufacturers Data, 1985.
16. Shinoda, K.; Hironubu, K. In "Encyclopedia of Emulsion Technology."; Becher, P.,Ed.; Decker: New York, 1983; Vol.I, Chap. 5.
17. Shinoda, K.; Saito, H. J. Coll. Interface Sci. 1969, 30(2), 258.
18. Saito, H.; Shinoda, K. J. Coll. Interface Sci. 1970, 32(4), 647.
19. Mitchell, D. J.; Tiddy, G. J. T.; Waring, L.; Bostock, T.; McDonald, P. J. Chem. Soc. Faraday Trans., 1 1983, 79, 975.
20. Rosevear, F. B. J. Am. Oil Chem. Soc. 1954, 31, 628.
21. Kislalioglu, S.; Friberg, S. In "Theory and Practice of Emulsion Technology"; Smith, A. L., Ed.; Academic: London, 1976; Chap. 15.
22. Raterman, K. T.; Shaeiwitz, J. A. J. Coll. Interface Sci. 1984, 98(2), 394.
23. Friberg, S.; Mandell, L. J. Am. Oil Chem. Soc. 1970, 47, 149.
24. Graciaa, A.; Bakakat, Y.; Schecter, R. S.; Wade, W. H.; Yiu, S. J. Coll. Interface Sci. 1982, 89(1), 217.

19

The Mesophase Formation

During a Dissolution of Cholesterol Monohydrate in Glycochenodeoxycholate–Glycoursodeoxycholate–Lecithin Solutions and Calcium Carbonate Solubility in Their Solutions

M. Ueno, H. Asano, and T. Okai

Department of Applied Chemistry, Faculty of Science, University of Tokyo, Tokyo, Japan

Solubility of calcium carbonate was measured in mixed solutions of glycochenodeoxycholate, glycoursodeoxycholate and lecithin in the presence of cholesterol monohydrate disk in the ranges of pH from 7.5 to 9.0 .
When mesophase, that is, liquid crystal, consisting of three components of bile salt, lecithin and cholesterol was produced, deposition of calcium salts of bile acids was observed on the cholesterol disk surface. The relation between mesophase formation and calcification will be elucidated in this paper.

Glycochenodeoxycholate and glycoursodeoxycholate are known to reduce the cholesterol saturation in bile and to induce the dissolution of cholesterol gallstones in humans.[1,2,3]
In most cases, Glycoursodeoxycholate has been used as the treatment of choice because it is effective at a lower dose and is free from side effects such as diarrhea. Figure 1 shows the structure for glycochenodeoxycholate and glyco-ursodeoxycholate, abrreviated as GCDC and GUDC, respectively.
In general, GUDC is known to produce a mesophase during dissolution of cholesterol(CHL) in the presence of lecithin(EL) in vitro, and then increases the dissolution rate of CHL by the mesophase formation.[4,5] However, the effect is less than that of GCDC in vivo.
Igimi et al[3] have predicted that the precipitation of GUDC could occur during treatment with GUDC. Bateson et al[6] have reported that 122 patients with cholesterol gall stones which can not take the picture even by Roentgen were treated with chenodeoxycholic acid(CDCA) and 56 patients were treated with ursodeoxycholic acid(UDCA) for six months or more. Six of the 56 patients treated with UDCA developed calcification, but none of the patients treated with CDCA showed any evidence of calcification on the surface of the

gallstones. This suggests that the dosage of UDCA is responsible for the calcification on the surface of the gallstones in a gallbladder and prevents further dissolution of the stones.[7]

This phenomenon would probably be associated with the mesophase formation, and so we will elucidate the mechanism of the relation between mesophase formation and calcification. This can be done by measuring the solubility of calcium carbonate added to varying aqueous mixtures of NaGCDC-NaGUDC-Lecithin in the range of pH from 7.5 to 9.0 in vitro, and by observing the surface of the cholesterol monohydrate fragments and disks dipped in the systems.

EXPERIMENTALS
MATERIALS: Sodium Glycochenodeoxycholate(NaGCDC) and Sodium Glycoursodeoxycholate(NaGUDC) were supplied from Tokyo Tanabe Seiyaku. These have been confirmed to have the purity above 99.99% by elemental analyses. Highly pure Lecithin was obtained from Asahi Kasei Kogyo. Calcium carbonate was prepared from highly pure calcium chloride (Kanto Kagaku) and highly pure sodium carbonate(Kanto Kagaku). Cholesterol monohydrate(CHLM) was prepared by recrystallization of cholesterol anhydrate in 100ml of 95% alcohol solution with 5% water. Five grams of cholesterol anhydrate was dissolved into 100ml alcohol including five grams of water kept at temperature of 60 C. After the solution being permitted to stand for 48 hours at room temperature in dark place, CHLM crystal produced in it was filtrated and was dried for 24 hours in water-bath kept 37°C and stored in desiccator filled with N_2 gas including water vapour.

PROCEDURES
32 mM egg lecithin was dissolved in mixed solutions with total NaGCDC and NaGUDC concentrations of 100 mM having six different ratios; NaGCDC/NaGUDC are 100/0, 80/20, 60/40, 40/60, 20/80, and 0/100, respectively. The pH of each solution were adjusted with Tris buffer and then 6.4 mM cholesterol monohydrate(CHLM) and excess calcium carbonate were added to the solutions. After N_2 gas had been sealed in the glass bottles containing the samples, these bottles were incubated in an agitated water-bath at 37°C. After 24 hours and 48 hours, the samples were filtered using a millipore filter(diameter 1.0 um and 0.22 um) and the amount of calcium and the amount of calcium ion dissolved in the solutions was measured by an atomic and flame absorption spectrometer(HITACHI-170-50 A type) at 422.8 nm. In addition, under the same conditions, the samples containing the CHLM disk(diameter 1.3 cm) were incubated for 6 months at 37°C in the agitated water-bath. after 6 months, the amount of calcium ion dissolved in each solution was measured and the presence or absence of liquid crystals was checked using polarized microscopy, Olympus B-3 type. X-ray photographs were taken, by using Softex 3 type, to confirm the deposition of calcium salt on the disk surfaces.

RESULTS AND DISCUSSION

Müller et al [8] have reported that in bile salt solutions in the presence of EL, if the EL concentration is less than half of that of the bile salts, the mixed micelle shape becomes spherical, but, otherwise, the shape is a disk as shown in Figure 2. All solutions used here include 32 mM lecithin and 100 mM total bile salts, therefore the micelle shape in all systems here must be spherical. Edward et al [9] have reported that bile ions bind to calcium ions and result in two types of salts ; one is an acid salt as cationic monomer and the other is neutral bile salt dimer as shown in Figuer 3. The same authors have shown that free monomers can be fixed on the surface of the mixed bile salt micelles, while neutral dimers are solubilized into the mixed micelles.

Figure 4 shows the calcium solubility in the mixed systems of NaGCDC-NaGUDC as a function of pH without CHLM and EL. The solubility decrases with increasing pH. This suggests that bile salt monomers form dimers as pH is increased and finally precipitate as neutral calcium salts. The systems with different mixture ratios showed almost the same values at a constant pH except the single system of NaGCDC.

Figure 5 shows the calcium salt solubility in the mixed systems of NaGCDC-NaGUDC-EL as a function of pH. The solubility exhibited a convex curve with a maximum at pH 8.0. This suggests that the dissolution of calcium salt differs from the system without EL as shown in Figure 4.

In general, choline groups in lecithin molecules have a positive charge in the low pH range. Therefore the positive charge of EL incorporated in the bile salt micelles prevents the fixation of the positively charged calucium-bile salt monomer on the micelle surface but allows incorporation of the dimer into the mixed micelles. As pH increaces, EL in the mixed micelles becomes negatively charged so that it is easy to deposit the monomers on the micelle surface, however calcium solubility decreases with increasing pH, because the monomers form dimers in the range of higher pH.

Figure 6 shows the calcium salt solubility in the mixed systems of NaGCDC-NaGUDC-EL-CHLM as a function of pH. The solubility exhibits a maximum at pH 7.5 and decreases gradually with increasing pH. Although this system has higher solubility than that of the system without EL in Figure 4, it does show a similarity. As CHL molecules are incorporated among the bile salt and EL molecules in the micelles by solubilization, the electrical repulsive force toward the positively charged monomer decreases. Therefore the solubilities of monomers and dimers may increase more than those of the systems without EL and CHL in Figure 4.

Figure 7 shows the calcium salt solubility in the mixed

Conformation of NaGUDC
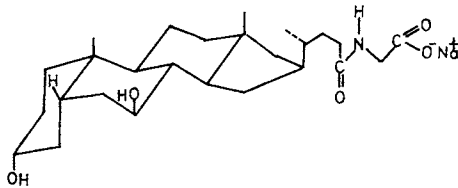
Conformation of NaGCDC
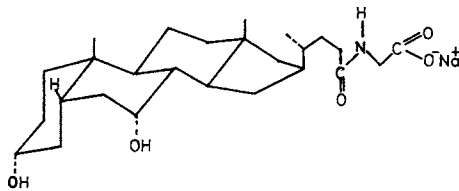
Figure 1   Conformation of NaGUDC and NaGCDC
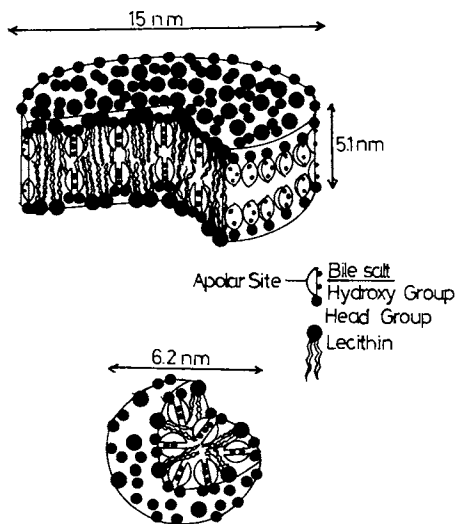
Figure 2   The mixed micelles consisting of Bile salts and
           Lecithin. Disk; Excess Lecithin. Sphere; Excess
           Bile salts.

Formation of FREE(non-micellar)ACID SALT
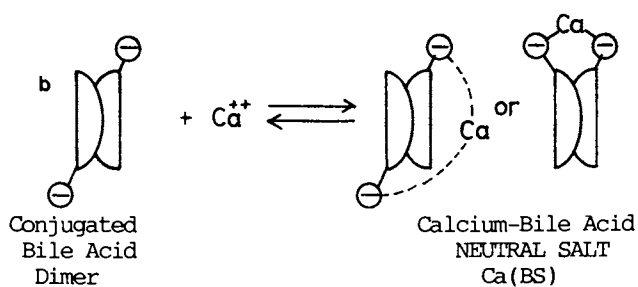
Figure 3   The formation of free acid salt and free neutral
           salt. (a) Calcium-Bile salt monomer, (b) Calcium-
           Bile salts dimer.
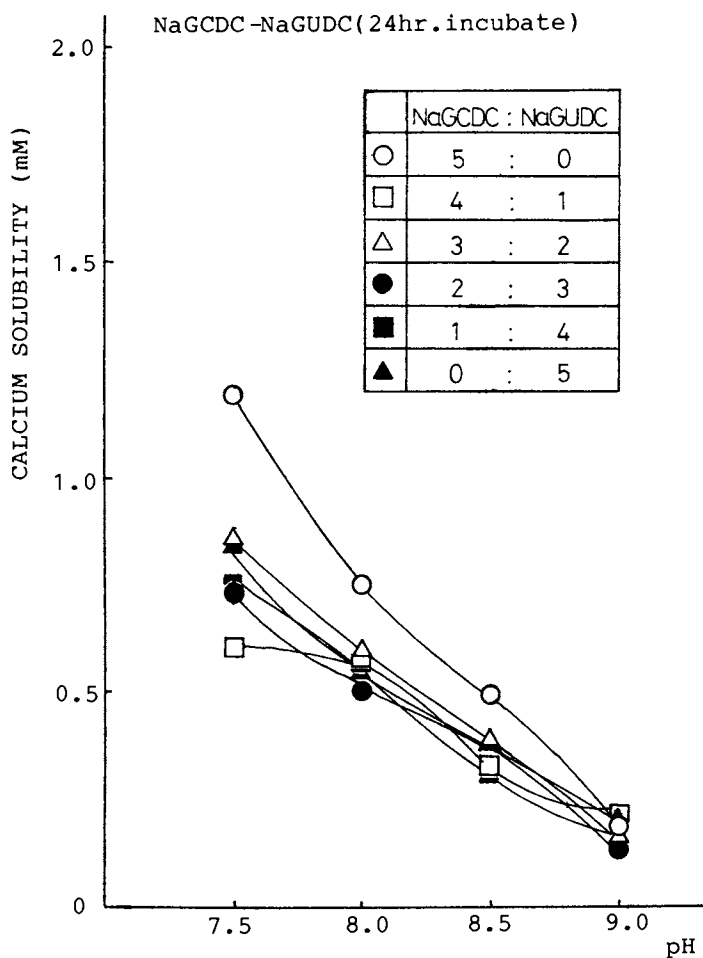
Figure 4   Calcium salt solubility in the mixed system of NaGCDC–NaGUDC as a function of pH.
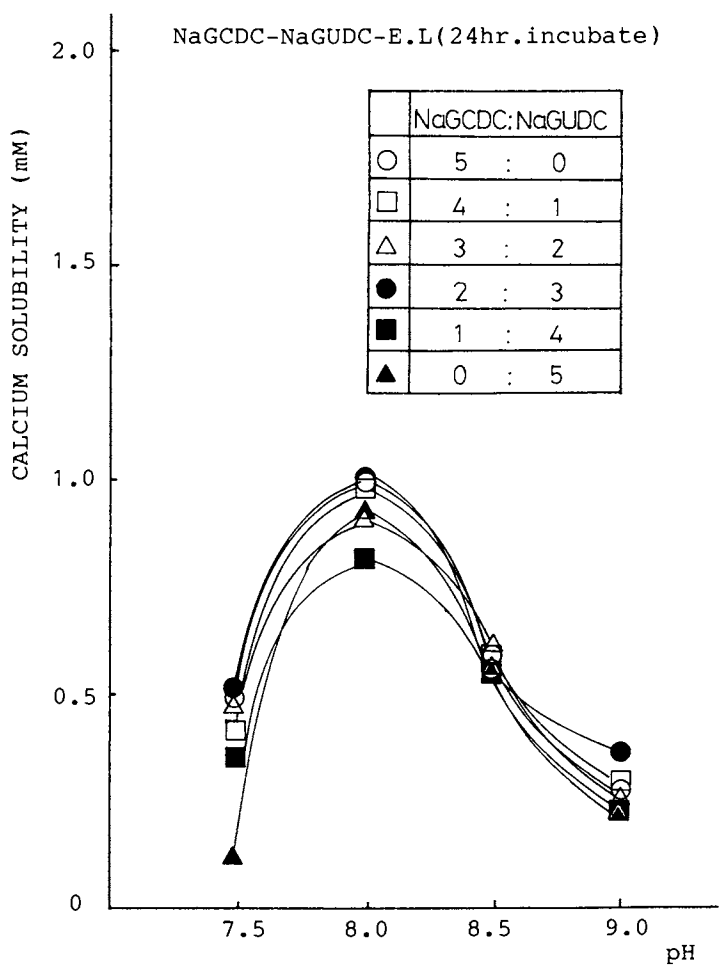
Figure 5   Calcium salt solubility in the mixed system of
NaGCDC–NaGUDC–EL as a function of pH.
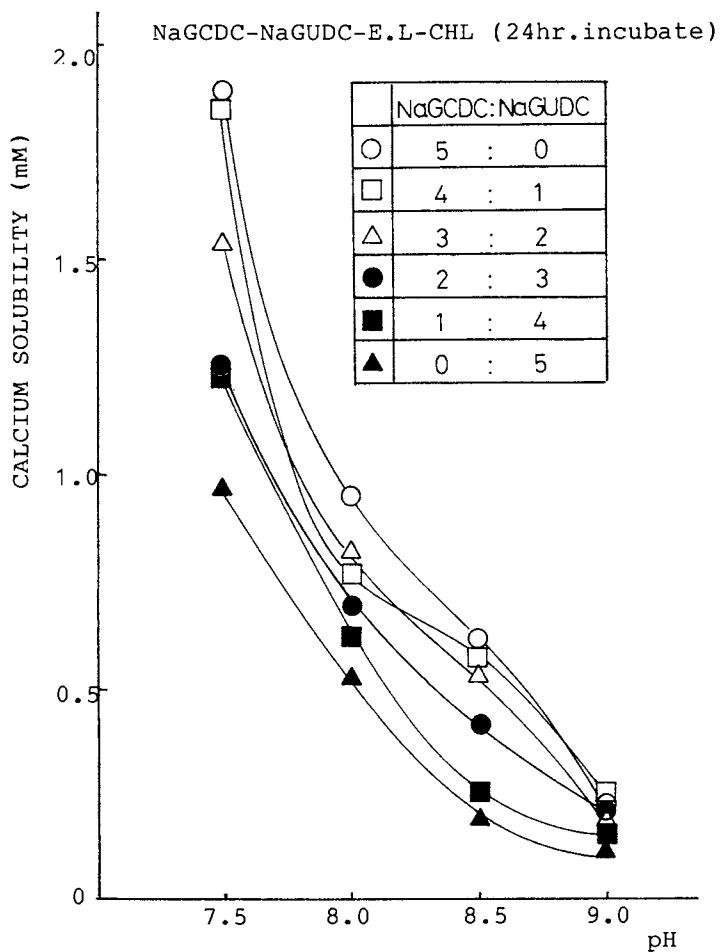
Figure 6   Calcium salt solubility in the mixed system of NaGCDC-NaGUDC-EL-CHLM as a function of pH.

	NaGCDC : NaGUDC		
○	5	:	0
□	4	:	1
△	3	:	2
●	2	:	3
■	1	:	4
▲	0	:	5
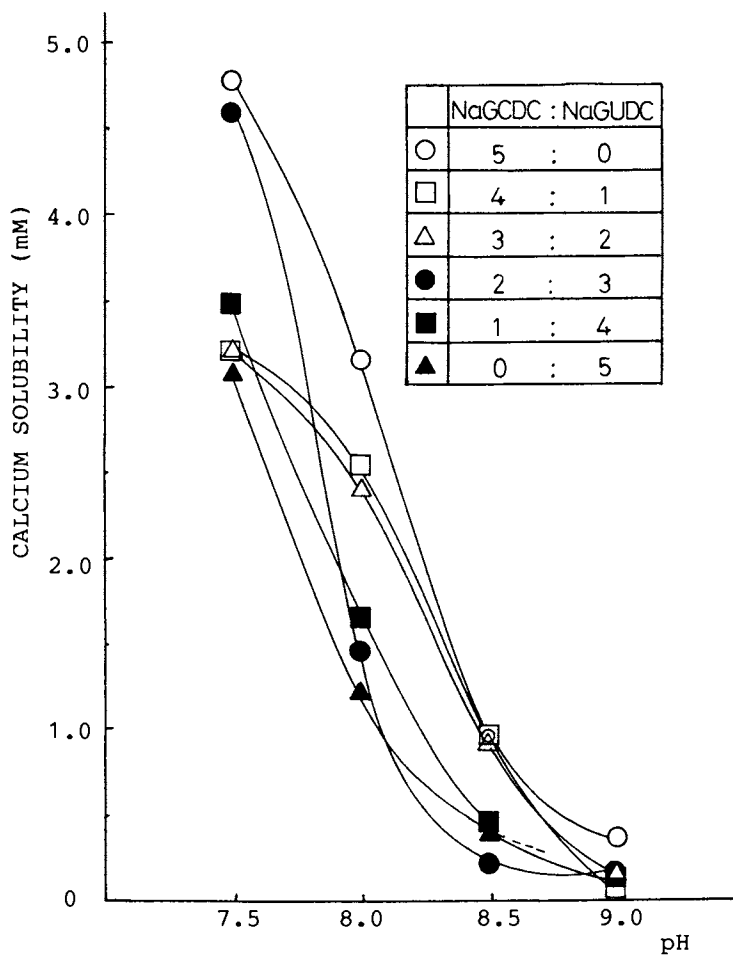
Figure 7   Calcium salt solubility in the mixed system of
           NaGCDC-NaGUDC-EL dipping CHLM. Disk as a function
           of pH after 6 months incubation.

systems of NaGCDC-NaGUDC-EL dipping CHLM disk as a function
of pH after 6 months incubation. This exhibited a tendency
similar to the system with EL and CHLM in Figure 6. This
result suggests that calcification on the CHLM disk is more
liable to occur in the range of higher pH than in the range
of lower pH.

Table 1 shows the numbering of the samples for the
combinations of NaGCDC and NaGUDC.

The results of the calcification on the disks are
summarized in Table 2. The calcification could not be
observed on samples No.4 to 7 at pH 7.5 and disks from No.4
to No.7 were confirmed to dissolve completely.

Carey and Igimi [5] have reported that the dissolution
of CHLM by GUDC is more greatly enhanced in the presence of
EL than GCDC.

Calcification was observed on the surface of disks No.12
to 14 at pH 8.0. At pH 9.0, calcification was observed on
the surface of disks from No.25 to 28.

In all systems rich in NaGUDC, gelation took place on
the disk surface and calcification occured. Corrigan, Carey
[10] and Igimi [11] have reported that GUDC produces a
mesophase during the dissolution of CHLM in the presence of
EL in vitro and also increases the dissolution of CHL by
mesophase formation corresponding to nematic or lamellar
type.

Table 3 shows that liquid crystals are formed in the
mixed systems of NaGCDC-NaGUDC-EL-CHLM after 6 months.

These results are concluded as follows ;
(1) In the lower pH range, liquid crystals were observed
     in the aqueous solutions with concentrations higher
     than 60 mM GUDC.
(2) At higher concentrations of GUDC, the surfaces of
     disks are liable to gelate and liquid crystals were
     observed on the surfaces of all disks.
(3) The higher the pH, the more likely liquid crystals are
     to form.
(4) Calcification took place on the disk surfaces in the
     mixed solutions that produced liquid crystal.
(5) It is noted that dissolution of CHLM by mesophase
     formation means calcification on CHLM disk surface.

These results suggest that calcification may be prevented
by using the combination of GCDC and GUDC to avoid gelation
on the disk surfaces.

Table 1   The numbering of the samples for the combinations of NaGCDC and NaGUDC.

Bile Salt / pH	Blank	100mM (NaGCDC) 0mM (NaGUDC)	80mM (NaGCDC) 20mM (NaGUDC)	60mM (NaGCDC) 40mM (NaGUDC)	40mM (NaGCDC) 60mM (NaGUDC)	20mM (NaGCDC) 80mM (NaGUDC)	0mM (NaGCDC) 100mM (NaGUDC)
7.5	1	2	3	4	5	6	7
8.0	8	9	10	11	12	13	14
8.5	15	16	17	18	19	20	21
9.0	22	23	24	25	26	27	28

Table 2 The solubility of ChLM Disks and Precipitation
of Calcium salts.

No.	1	2	3	4	5	6	7
P.C.	X	X	X	S	S	S	S
No.	8	9	10	11	12	13	14
P.C.	X	X	X	X	X	O	O
No.	15	16	17	18	19	20	21
P.C.	X	X	X	X	O	O	O
No.	22	23	24	25	26	27	28
P.C.	X	X	X	O	O	O	O

```
O  : The precipitation of calcium was observed.
X  : The precipitation of calcium was not observed.
S  : The CHM.DISK was soluble.
```

1-7 : pH7.5, 8-14 : pH8.0, 15-21 : pH8.5, 22-28 : pH9.0,

```
1,8,15,22,  : BLANK (BUFFER-CHM.DISK)
2,9,16,23,  : NaGCDC 100mM, NaGUDC   0mM, E.L, CHM.DISK,
3,10,17,24,: NaGCDC  80mM, NaGUDC  20mM, E.L, CHM.DISK,
4,11,18,25,: NaGCDC  60mM, NaGUDC  40mM, E.L, CHM.DISK,
5,12,19,26,: NaGCDC  40mM, NaGUDC  60mM, E.L, CHM.DISK,
6,13,20,27,: NaGCDC  20mM, NaGUDC  80mM, E.L, CHM.DISK,
7,14,21,28,: NaGCDC   0mM, NaGUDC 100mM, E.L, CHM.DISK,
```

Table 3 Liquid Crystal Formation in Mixed systems of
            NaGCDC-NaGUDC-EL-CHLM after 6 months incubation.

No.	1	2	3	4	5	6	7
L.C.F.	X	X	X	X	O	O	O
No.	8	9	10	11	12	13	14
L.C.F.	X	X	X	O	O	O	O
No.	15	16	17	18	19	20	21
L.C.F.	X	X	X	O	O	O	O
No.	22	23	24	25	26	27	28
L.C.F.	X	O	O	O	O	O	O

O : The liquid crystal was observed.
X : The liquid crystal was not observed.

1-7 : pH7.5, 8-14 : pH8.0, 15-21 : pH8.5, 22-28 : pH9.0,

1,8,15,22, : BLANK (BUFFER-CHM.DISK)
2,9,16,23, : NaGCDC 100mM, NaGUDC   0mM, E.L, CHM.DISK,
3,10,17,24,: NaGCDC 80mM, NaGUDC 20mM, E.L, CHM.DISK,
4,11,18,25,: NaGCDC 60mM, NaGUDC 40mM, E.L, CHM.DISK,
5,12,19,26,: NaGCDC 40mM, NaGUDC 60mM, E.L, CHM.DISK,
6,13,20,27,: NaGCDC 20mM, NaGUDC 80mM, E.L, CHM.DISK,
7,14,21,28,: NaGCDC   0mM, NaGUDC 100mM, E.L, CHM.DISK,

Literature Cited

1) Minoru Ueno : Fragrance Journal No.60, 11 : 56-66, 1983.
2) Raedsch, R., A. Stiehl and P. Czygan : The Lancet, December,5, 1981.
3) Igimi, H., M. Tamesue, Y. Ikejiri and H. Shimura : Life Sci., 21 : 1373-1380, 1977.
4) Salvioli, G., H. Igimi and M.C. Carey * J. Lipid Research, 24 : 701-720, 1983.
5) Igimi, H. and M.C. Carey : J. Lipid Research, 22 : 254-270, 1981.
6) Bateson, M.C., I.A/D/ Bouchier, D.B. Trash, D.P. Mandgal and T.C. Northfield : British Medical Journal, 283(5) : 645-646, 1981.
7) Isao Makino et al : nissyo shi, 80(6) : 1350, 1983.
8) Karl Müller : Biochemistry, 20 : 404, 1981.
9) Edward, W.M., C. Lilian and J.D. Ostward : Gastroentrology, 83(5) : 1079-1089, 1982.
10) Corrigan, O.I., C.C.Su, W.I. Higuchi and A.F. Hofmann : J. Pharm. Sci., 69(7) : 870, 1980.
11) Igimi, H., S. Asakawa, D. Watanabe and H. Shimura : Gastroentrology, 18(2) : 93-97, 1983.

20

The Growth of Molecular Assemblies in Mild Surfactant Solutions

Keishiro Shirahama[1], Koji Takashima[1], Noboru Takisawa[1], Keiichi Kameyama[2], and Toshio Takagi[2]

[1]Department of Chemistry, Faculty of Science and Engineering, Saga University, Saga 840, Japan
[2]Institute for Protein Research, Osaka University, Suita 565, Japan

The size of molecular assembly of six syn-
thetic dialkyl amphiphiles as determined by
a quasi-elastic light scattering is varied
in the presence of nonionic MEGA-n sur-
factants (N-D-gluco-N-methylalkanamide C_n =
7-9).
At high MEGA-n concentration, the size is
as small as a MEGA-n micelle itself sug-
gesting that dialkyl amphiphile is solubil-
ized in the nonionic micelle. At low con-
centration a dialkyl amphiphile vesicle
keeps its size relatively constant and
takes up MEGA-n molecules.
In between, the molecular assembly size
increases with MEGA-n concentration. It is
only this concentration region where the
size shows even more increase on dialytic
removal of MEGA-n surfactant. These phe-
nomena are closely related with the "deter-
gent-removal method" often employed in
phospholipid-mild surfactant systems.

Phospholipids are a major component of living cell mem-
branes. Physical and chemical properties of bilayer
structure composed of phospholipids have been well
studied.([1,2]) One of the intriguing properties of
phospholipids is that they form a closed structure -
hereafter referred to as vesicles. Vesicles have at-
tracted much attention since they are considered to mimic
biocells.
    Preparation methods of vesicles have been known and
employed for various purposes: the ultrasonic irradiation
method, and the injection method, for example. In addi-
tion to them, there has appeared a novel method, which
consists of solubilizing phospholipids in surfactant
solution, and subsequently removing the surfactant by

dialysis or gel chromatography at a temperature higher than the transition point. T_c of the phospholipid, thus called the "detergent-removal method", where the surfactant such as octylglucoside and bile salts, or "mild" surfactant has relatively low surface-activity for easy removal. It is shown that the new method creates a large homogeneous unilamellar vesicle (3-9). It is also claimed that uptake of various substances including very labile biomaterials is feasible without drastic exposures to ultrasonication or organic solvents(10).

A growth of molecular assembly was recognized with mixtures of phospholipid and surfactant even before dialytic removal. Goñi et. al(11,12) have shown that sonication of phospholipid suspension at $T>T_c$ may be required before addition of surfactant in order to obtain the growth of molecular assembly. They also found that the growth is induced with not only mild surfactants but also "hard" surfactants such as SDS and Triton X-100. More recently, Ueno et al. also reported that dodecyl-octa(ethylene oxide) would produce a large homogeneous vesicle(13).

There are several works that have studied more or less the relevant phenomena in a systematic manner(3-13), but little is understood yet. So we thought that it would be informative to change the chemical species that forms the vesicles to some other species. This corresponds to changing "chemical variables" just as one changes physical variables such as temperature and pressure.

Thus, it is expected that not only phospholipids but also dialkyl amphiphiles (Figure 1) can form vesicles with these favorable characteristics by the "detergent-removal method". So we chose synthetic dialkyl amphiphiles which had been reported to form vesicles: dioctadecyldimethylammonium bromide and chloride (DODABr and Cl)(14) didodecyldimethylammonium bromide (DDDABr) (15), N,N-di(dodecanoyloxyethyl)amide derivative (DDdeACl) (16), and 1,3-didodecyl-2-oligoethyleneglycol glycerines with average number of ethyleneglycol, m=13 and 17 (DDGE$_m$)(17). As mild surfactants, N-D-gluco-N-methylalkanamide(18) (Figure 1) were used, since three homologues with reasonable purity were commercially available. It may be possible to see the effect of hydrophile-hydrophobe balance of surfactant by using these compounds. i.e., "another chemical variable".

Quasi-elastic light scattering was employed successfully to estimate sizes of molecular assemblies in terms of hydrodynamic radius, R_H. In the present paper, we concentrated on a "phase diagrammatic" study of molecular assembly size.

EXPERIMENTAL

Materials. Dioctadecyldimethylammonium bromide (Eastman Kodak) and chloride (Tokyo Kasei), didodecyldimethyl-

ammonium bromide (Eastman Kodak), and N,N-(didodecanoyl-oxethyl)amide derivative (donated from Sogo Yakuko Co.) were recrystallized from dried acetone. Didodecyloligo-ethyleneglycol glycerines (kind gifts from Prof. T. Kuwamura, Gunma Univ.) were used as received. MEGA-n surfactants (Dojin Chem.) were recrystallized from dried acetone. The critical micelle concentrations (cmc) were determined from a break point on a III/I ratio (see below) vs. surfactant concentration plot. Purified pyrene was a donation from Dr. K. Nakajima (Nishikyushu Univ.).

Apparatus. A quasi-elastic light scattering measurement system was composed of a light scattering photometer (Union Giken, LS-601) equipped with a single-photon counting unit. Light source was a He-Ne laser (5 mW). Autocorrelation function was derived by a digital correlator (KANOMAX, SAI-43A). All the measurements were carried out at room temperature (22°C) and recorded on a plotter through a microcomputer (Sord, M243).

Emission spectra were recorded on a fluorescence spectrophotometer (Hitachi, MPF-2A) with the excitation wavelength = 337 nm.

Procedures. Dialkyl compound suspension (0.4-4.0mg/ml) was dispersed in water by an ultrasonic irradiator (Branson sonifier cell disruptor 185) for an hour above transition temperature. The suspension was then filtered through a Nucleopore membrane filter (5 μm) to remove titanium dust originating from the sonicator tip. The MEGA-n concentration was varied by one of the following two methods: (1) addition of solid MEGA-n to a vesicle suspension or (2) combining concentrated MEGA-n (usually 50 mg/ml) solution containing a dialkyl amphiphile with the vesicle suspension having the same dialkyl amphiphile concentration as above. The resulting mixture was treated above T_c for more than 10 minutes. Experimental results were the same irrespective of the preparation methods. The sample solution thus prepared was filtered through a Nucleopore membrane filter with an appropriate pore size (0.5-3 μm) prior to quasi-elastic scattering measurements.

Results and Discussion

The hydrodynamic radius, R_H, is plotted against MEGA-9 concentration, C_s, for DODACl in Figure 2 (open circles). The size of the molecular assembly increases at first. and then suddenly falls down to R_H = 5 nm, the size of a MEGA-9 micelle. An aqueous mixture of DODACl and MEGA-9 was dialyzed aginst water at 60°C through a cellulose tubing (cutoff MW = 3,500) for 20 hr. The size of molecular assembly increases even more as shown with closed circles in Figure 2. But this increase depends on amount

(I) DODAX

$$CH_3(CH_2)_{17} \underset{CH_3(CH_2)_{17}}{\overset{+}{N}} \underset{CH_3}{\overset{CH_3}{<}} \quad X^-$$

(II) DDDABr

$$CH_3(CH_2)_{11} \underset{CH_3(CH_2)_{11}}{\overset{+}{N}} \underset{CH_3}{\overset{CH_3}{<}} \quad Br^-$$

(III) DDdeACl

$$\begin{array}{c} O \\ \parallel \\ C_{11}H_{23}-C-O-CH_2CH_2 \\ \\ C_{11}H_{23}-C-O-CH_2CH_2 \\ \parallel \\ O \end{array} \underset{}{\overset{}{>}} N-\overset{O}{\overset{\parallel}{C}}-CH_2-\overset{CH_3}{\underset{CH_3}{\overset{+}{N}}}-CH_3 \quad Cl^-$$

(IV) DDGE$_m$

$$\begin{array}{c} H(CH_2)_{12}OCH_2 \\ \\ H(CH_2)_{12}OCH_2 \end{array} \overset{}{>} CHO(C_2H_4O)_{13 \text{ or } 17}$$

(V) MEGA-n   N-D-gluco-N-methylalkanamide detergents

$$(C_{n-1}H_{2n-1}) \underset{\overset{\parallel}{O}}{\overset{CH_3}{>}} N \underset{}{\overset{OH \ OH \ OH}{-CH_2 - - -}} \underset{OH \ OH}{}$$

		C.M.C.	
n = 8 : MEGA-8	18.5 mg·ml^{-1}	(58 mM)
n = 9 : MEGA-9	5.0	(14)
n = 10 : MEGA-10	1.5	(4)
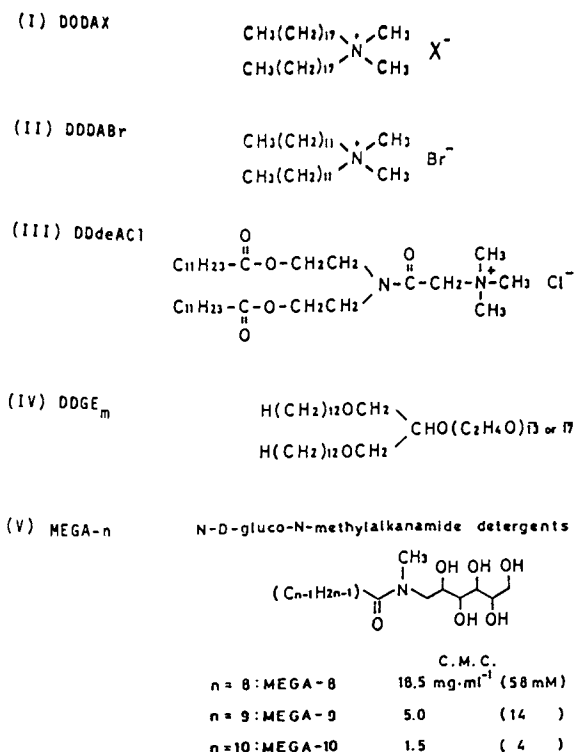
Figure 1.   Dialkyl amphiphiles and MEGA-n surfactants
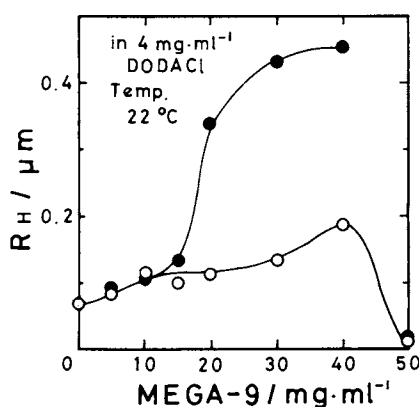
Figure 2.   The hydrodynamic particle radius   of 4mg/ml DODACl in MEGA-9 solution.   ○ : before dialysis, ● : after dialysis (removal of MEGA-9 by dialysis above 60 ℃ for 20h) measurement temperature 22 ℃.

of MEGA-9 present before dialysis: at low MEGA-9 concen-
tration (<10 mg/ml), R_H scarcely augments, and at high
concentration (>50 mg/ml) where MEGA-9 micelles solubil-
ize DODACl, dialysis produced an unstable turbid sus-
pension.

A marked increase in R_H after dialysis was found
only in between.   Figure 3 is an electron micrograph
(negaive-stained with ammonium molybdate) for a sample
dialyzed from the DODACl (4 mg/ml) - MEGA-9 (30 mg/ml)
system.   Single walled structure is seen closed with
comparatively homogeneous size that is compatible with R_H
measured by quasi-elastic light scattering. It is under-
stood that a synthetic dialkyl amphiphile can form a
vesicle with a large homogeneous size by "detergent-
removal method" as claimed for phospholipids.

Figures 4 and 5 show similar results for DODACl in
MEGA-n surfactants having different alkyl lengths (n=8
and 10). It is clear that these systems also behave much
like the MEGA-9 system.   More hydrophobic MEGA-n
surfactants seem to have more size-enhancement effect.
It is noted, however, that the MEGA-10 system takes
longer time to grow to a large vesicle. More hydrophobic
MEGA-10 surfactant would be hard to remove from the
molecular assembly which may be a complex of DODACl and
MEGA-10.

Figure 6 shows the effect of MEGA-8 on R_H of DODABr,
which seems to behave much like its chloride counterpart:
increasing R_H on addition of MEGA-8, and further increase
on dialysis.

Figure 7 displays R_H for DDDABr in MEGA-9 solution.
A gross difference here is that whole changes occur at
lower MEGA-9 concentration as compared with dioctadecyl
analogue seen in Figure 2. Vesicles with shorter dialkyl-
chains may yield to the effect of MEGA-n surfactant much
easier.

Increase of R_H in the presence of MEGA-9 was
confirmed for DDdeACl followed by decrease in R_H down to
ordinary micellar size as seen in Figure 8.

Measurements were extended to nonionic dialkyl
amphiphiles as shown in Figures 9 and 10. The effect of
added MEGA-8 is to increase R_H and then decrease to about
0.2 μm, but not to micellar size. In addition, autocor-
relation function was apparently a double exponential
function, thus indicating the coexistence of small and
large molecular assemblies.   The values of smaller R_H
were designated by dashed circles.   The small R_H is
actually of micellar size.   The effect of ethyleneoxide
length is to lessen the effect of the added MEGA-8: the
peak of R_H appears at MEGA-8 concentration = 10 mg/ml for
average number of ethylene oxide group, m=13, while it
shifts up to 30 mg/ml for m=17.   Parts of MEGA-8 mole-
cules must be trapped in ethylene oxide groups, thus much
MEGA-8 is needed to be delivered into the hydrocarbon
part of vesicles.

It was unexpected that R_H returned back to the
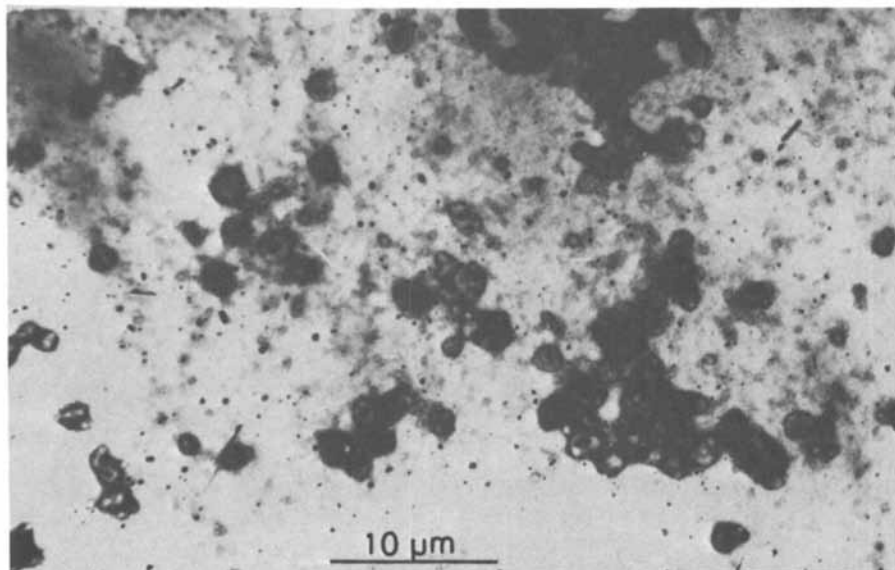
Figure 3. The photograph of the electron microscope (negative stained, ×20,000). The measured sample, 4mg/ml DODACl in 30 mg/ml MEGA-9 was used after dialysis.
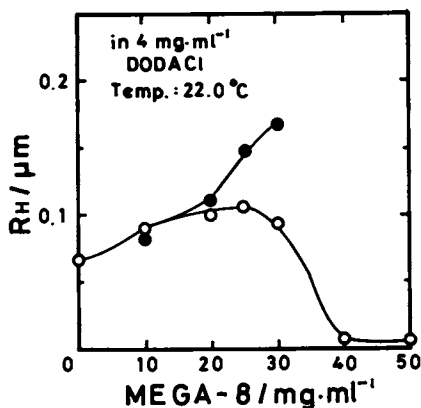
Figure 4. The hydrodynamic particle radius of 4mg/ml DODACl in MEGA-8 solution. ○ : before dialysis, ● : after dialysis (removal of MEGA-8 by dialysis above 60 ℃ for 20h.) measurement temperature 22℃.
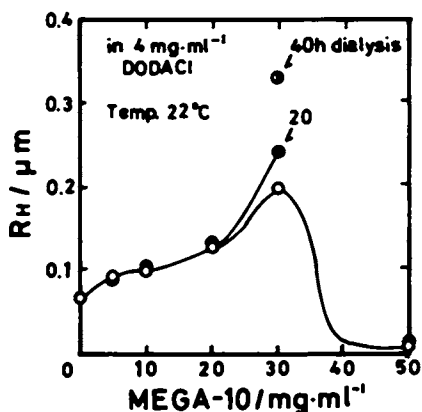
Figure 5. The hydrodynamic particle radius of 4mg/ml
DODACl in MEGA-10 solution. O : before dialysis ● :
after dialysis (removal of MEGA-10 by dialysis above
60 ℃ for 20h.) measurement temperature 22 ℃.
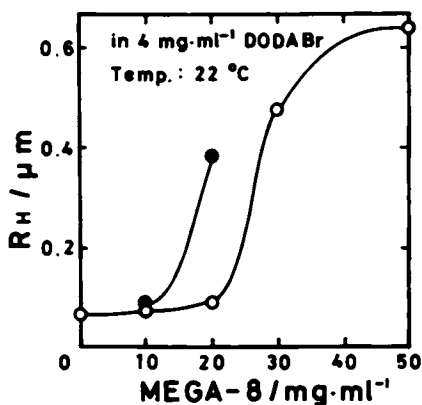
Figure 6. The hydrodynamic particle radius of 4mg/ml
DODABr in MEGA-8 solution. O : before dialysis ● :
after dialysis (removal of MEGA-8 by dialysis above
60 ℃ for 20h.) measurement temperature 22 ℃.
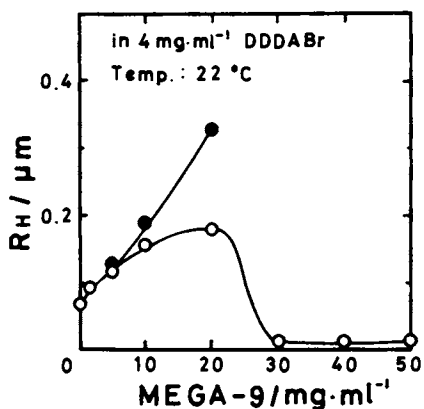
Figure 7. The hydrodynamic particle radius of 4mg/ml DDDABr in MEGA-9 solution. ○ : before dialysis ● : after dialysis (removal of MEGA-9 by dialysis at room temperature for 20h.) measurement temperature 22℃.
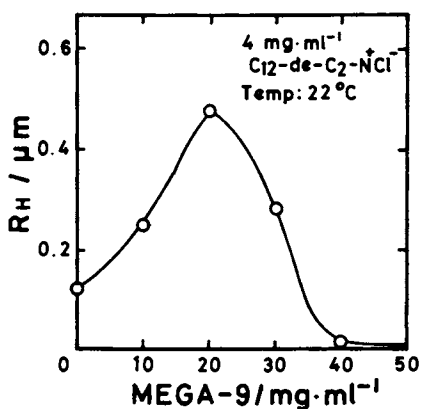
Figure 8. The hydrodynamic particle radius of 4mg/ml DDdeCl in MEGA-9 solution. measurement temperature 22℃.
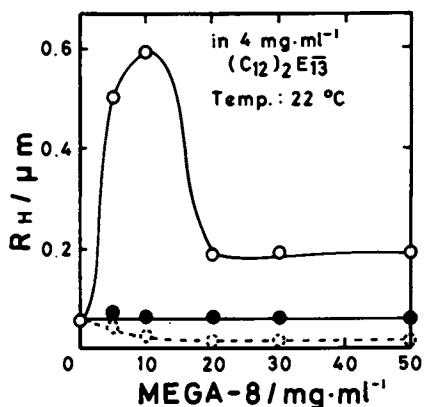
Figure 9. The hydrodynamic particle radius of 4mg/ml $(C_{12})_2E_{13}$ in MEGA-8 solution. $\bigcirc, \circleddash$: before dialysis. $\bullet$: after dialysis (removal of MEGA-8 by dialysis above 60 °C for 20h.) measurement temperature 22°C.
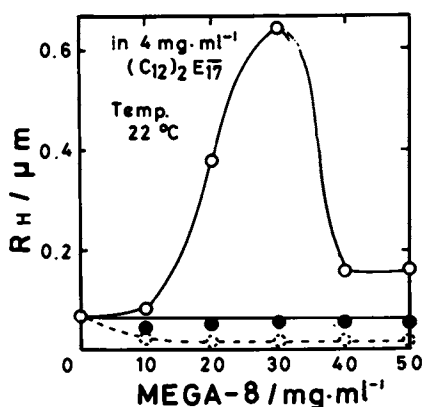
Figure 10. The hydrodynamic particle radius of 4mg/ml $(C_{12})_2E_{17}$ in MEGA-8 solution. $\bigcirc, \circleddash$: before dialysis $\bullet$: after dialysis (removal of MEGA-8 by dialysis above 60 °C for 20h.) measurement temperature 22°C.

original vesicle size after dialyzing out MEGA-8 mole-
cules. The rate of removing MEGA surfactant from these
dialkyl amphiphiles at this experimental condition may be
so slow that vesicle size goes back reversiblly.

Fluorescence spectra of pyrene were employed in
order to see the polarity of the environment given by the
molecular assemblies mentioned so far. The III/I ratio
of vibronic spectra of pyrene, a good measure of micro-
environmental polarity([19,20]), is plotted for the DODACl
systems as a function of MEGA-n concentrations in Figure
11.

At low MEGA-n concentration, the III/I ratio is low
(= 0.84) and almost constant suggesting that pyrene mole-
cules reside in a rather polar environment, which is
however not so polar as in an aqueous phase (III/I =
0.63). It may be considered that the very cohesive nature
of the vesicular bilayer does not allow pyrene molecules
to penetrate deep into the hydrophobic part, and they
stay in peripheral solubilization sites.

On further increasing the MEGA-n concentration,
there appears a sudden kink indicative of some drastic
change in the dispersion state. The III/I ratio steeply
increases and eventually attains a plateau which corre-
sponds to the polarity found in the MEGA-n micelles.

It is above the kink concentration that a large and
homogeneous single-walled vesicle is formed after
dialysis. Some complicated structure other than original
vesicle must be a prerequisite for such a characteristic
vesicle. This unknown structure cannot be a solubiliza-
tion state, since it occurs below the critical micelle
concentration of each MEGA-n. We dare to speculate that
some MEGA-n-saturated bilayer with open structure may be
responsible for the growth.

Dialysis causes a deficiency in MEGA surfactant
which has patched hydrophobic portion of dialkyl amphi-
philic molecular assembly.
Consequently exposed hydrophobic sides are relieved on
collisions by irreversibly forming a closed bilayer
structure - a vesicle([21]).

The vesicular size might go back reversiblly to the
original one in the case of nonionic vesicles (Figures 9
and 10) for which the present removal rate may be too
slow. A similar behavior was reported by Schurtenberger
et al. for their lecithin-bile salt systems: vesicle size
is reduced to the original dimension after dialysis of
bile salt, but remains large when the solubilized
lecithin solution is diluted with the buffer solution
that corresponds to very fast reduction of bile salt
concentration, i.e., fast removal of bile salt([22]).
Weder et al. also described that a large vesicle forma-
tion depends critically on the rate of removal([4,5]).

It has been shown,therefore, that the behavior of
molecular assemblies can be divided into three regions
depending upon the amount of MEGA-n surfactant: (1) at
higher MEGA-n concentration where dialkyl amphiphile is
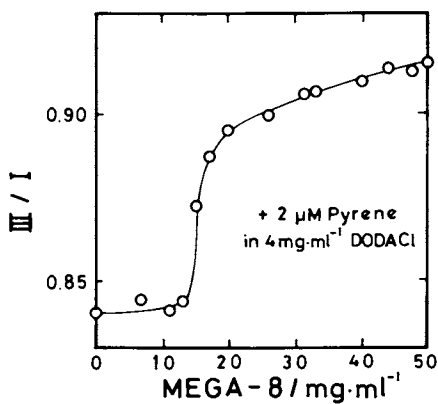
Figure 11. Variation of the III/I ratio of vibronic band intensities of 2μM pyrene as a function MEGA-8 and 9 concentrations in 4 mg/ml DODACl at 22 ℃.

solubilized into MEGA-n micelles, which is rather easy
to understand, (2) at low MEGA-n concentration where the
original vesicle structure is supposedly retained and
MEGA-n molecules are partitioned between the vesicle and
bulk water phases, and (3) the concentration range
between (1) and (2), where what is happening is not known
yet.
    There have been some papers that describe the three
regions in the relevant phopholipid-surfactant mix-
tures(4, 22, 23).
    It seems to be a kind of transition somewhat akin to
such phenomena as phase inversion observed in oil/water/
surfactant systems(24), and critical demixing (25, 26).

Acknowledgments

Literature Cited

1. In "Liposomes: From physical structure to therapeu-
    tic applications"; Knight,C. Ed. Elsevier: New York,
    1981.
2. In "Biological Membranes"; Chapman,D., Ed Academic
    Press: New York, 1982; Vol.IV.
3. Brunner,J.; Skrabal,P.; Hauser,H. Biochim. Biophys.
    Acta 1976. 455. 322.
4. Milsmann,M.; Schwendener,R.; Weder,H-G. Biochim.
    Biophys. Acta 1978, 512. 147.
5. Zumbuehl,O.; Weder,H-G. Biochim. Biophys. Acta 1981,
    640, 252.
6. Rhoden.V.; S. Goldin,S. Biochemistry 1979, 18, 4173.
7. Enoch,H; Strittmatter,P. Proc. Natl. Acad. Sci. USA.
    1979,76, 145.
8. Mimms, L.; Zampighi, G.; Nozaki, Y.; Tanford, C.;
    Reynolds, J. Biochmistry 1981, 20, 833.
9. Parente, R.;Lentz, B.Biochemistry,1984,23,2353.
10. Philyspot. J.; Mutaftschiev, S.; Liautard, J.,
    Biochim. Biophys. Acta 1983, 734, 137.
11. Alonso, A.; Sàez, R.; Villena, A.; Goñi. F.J.
    Membrane Biol. 1982. 67, 55.
12. Villalàin, J.; Goñi,F.; Macarulla, J. Molecular
    Cellular Biochemistry 1982, 49, 113.
13. Ueno, M.; Tanford, C.; Reynolds, J. Biochemistry
    1984, 23,3070.
14. Kunitake, T. ; Okahata, Y. J. Am. Chem. Soc. 1977,
    99, 3860.
15. McNeil, R.; Thomas, J. J. Colloid Interface Sci.
    1980, 73, 522.
16. Kunitake, T.; Asakura, S.; Higashi, N.; Nakashima,
    N. Rep. Asahi Glass Found. Ind. Technol. 1984, 45,
    163.

17. Kuwamura, T.; Kameyama, E. Kogyokagaku Zasshi (in
     Japanese) 1962, 65, 1265.
18. Hildreth, J. Biochemical. J. 1982, 207, 363.
19. Thomas, J., Chem. Rev. 1980, 80. 283.
20. Edwards, H.; Allen, J.,J. Chem. Research (S) 1982,
     179.
21. Lasic, D.,Biochim. Biophys. Acta 1982 692. 501.
22. Schurtenberger, P.; Mazer, N.; Kanzig, W., J. Phys.
     Chem. 89, 1042.
23. Jackson, M.; Schmidt, C.; Lichtenberg. D.; Litman.
     B.; Albert. A..Biochemistry 1982, 21, 4576.
24. In "Surfactants in Solution". Mittal, K.; Lindman,
     B., Eds.; Plenum Press: New York, 1984; Vol. III, p.
     1501- 1921.
25. Zulauf, M.; Rosenbusch, J.,J. Phys. Chem. 1983, 87,
     856
26. Corti, M.; Minero, C.; Degiorgio, V.,J. Phys. Chem.
     1984, 88, 308.

Micellar Solubilization of Methanol and Triglycerides

A. W. Schwab and E. H. Pryde

Northern Regional Research Center, Agricultural Research Service, U.S. Department of Agriculture, Peoria, IL 61604

Micellar and pre-micellar solutions of methanol in triolein were studied with three different surfactant systems using 2-octanol as a co-surfactant. Surfactants evaluated by viscosity, conductivity, density, refractive index and particle size data along with polarizing microscopic examinations were bis(2-ethylhexyl) sodium sulfosuccinate, triethylammonium linoleate and tetradecyldimethylammonium linoleate. Data show phase equilibria regions of liquid crystalline phases as well as micellar solutions. All systems were effective for solubilizing methanol in triolein. The order of effectiveness for water tolerance is: Tetradecyldimethylammonium linoleate> Bis(2-ethylhexyl) sodium sulfosuccinate> Triethylammonium linoleate

Micelles and microemulsions, terms perhaps unfamiliar to the American farmer, are important to his needs for an emergency fuel derivable from agriculturally renewable resources to run his direct injection diesel engine during planting and harvesting seasons. Unfortunately, vegetable oils such as soybean and safflower oils as such are not entirely satisfactory fuels, partly because of their incomplete combustion, but mainly because of their high viscosities (1). Research at the Northern Regional Research Center has been directed toward lowering the viscosity by micro-emulsification of vegetable oil with other materials to form hybrid fuels. Previously, we have reported on triglyceride-aqueous ethanol microemulsions (2) and triglyceride-methanol microemulsions (3). These were nonionic systems, and we have now extended our studies to include ionic and known micellar systems. Micelle formation of bis (2-ethylhexyl) sodium sulfosuccinate in water is well documented. In polar solvents such as methanol, however, it has been generally assumed that micellization either does not

occur or, if it does, the aggregation number is very small ($\underline{4}$).
One of our objectives is to study micellization in both methanol
and 2-octanol. Friberg ($\underline{5}$) has noted that micellar solutions do
not merit the name microemulsions. Among the systems studied were
bis(2-ethylhexyl) sodium sulfosuccinate, triethylammonium linoleate
and tetradecyldimethylammonium linoleate using 2-octanol as a
co-surfactant. This selection represents three different classes
of surfactants. Bis(2-ethylhexyl) sodium sulfosuccinate, commonly
referred to as Aerosol OT, is of the anionic type which carries a
sodium cation. This particular surfactant would not be recommended
for use in a diesel engine because of its potential ash deposit.
Triethylammonium linoleate is also an anionic type surfactant, and
the hydrophobic moiety is derivable from agriculture resources and
the cation is an organic amine which should not create a potential
ash problem. Tetradecyldimethylammonium linoleate was included
because it represents a new class of double-chain surfactants. In
a related study, Ruckenstein ($\underline{6}$) noted that optimum
microemulsification results were obtained with a combination of
single- and double-chained surfactants. Triolein was selected as
a representative triglyceride because its chemistry is closely
related to that of soybean oil, and it is currently available in
high purity. Soybean oil is a likely candidate as an alternate
fuel, since it is an agriculturally renewable product with heat
content of about ninety percent that of #2 diesel fuel.

Materials and Methods[*]

Triolein (tri-$\underline{cis}$-octadecenoin $d^{25} = 0.9091$; $\eta_D^{25} = 1.4662$) was
obtained from Nu Chek Prep., Inc. and was 99+% pure by GLC analysis.
Methanol (99.9+%, HPLC grade) and 2-octanol (98%, $\eta_D^{20} = 1.4234$;
$d^{20} = 0.819$) were acquired from Aldrich and were purified over
type 4A molecular sieves (Union Carbide) and filtered before use.
Karl Fisher titrations for H_2O on both alcohols prior to usage
gave values of <0.01% H_2O. Bis (2-ethylhexyl) sodium sulfosuccinate
was purum grade obtained from Fluka and received no further
purification. Triethylammonium linoleate was prepared by reacting
equimolar quantities of triethylamine (Aldrich, Gold Label, 99+%,
$\eta_D^{20} = 1.4000$) and a commercial grade of linoleic acid (Emersol
315) obtained from Emery Industries. The acid composition by
gas-liquid chromatography (GLC) analysis showed 65.5% linoleic,
19.0% oleic, 10.5% linolenic, 3.5% palmitic and 0.5% stearic acids
plus traces of lauric, pentadecanoic, margaric, myristoleic and
palmitoleic acids. Tetradecyldimethylammonium linoleate was
prepared by reacting equimolar quantities of linoleic acid
(Emersol 315) and tetradecyldimethylamine (ADMA[TM]4) obtained from
Ethyl Chemicals. GLC analysis of the amine shows a composition of
97.0% tetradecyldimethyl, 2.0% dodecyldimethyl and 1.0%
hexadecyldimethyl amines. The amine value is 229 mgKOH/g. The

---

[*]The mention of firm names or trade products does not imply that
they are endorsed or recommended by the U.S. Department of
Agriculture over other firms or similar products not mentioned.

bis(2-ethylhexyl) sodium sulfosuccinate solutions were prepared by weighing calculated quantities of the solid into sample vials and then adding the alcohol. These were shaken gently and then placed in a constant temperature bath at 25.0 ± 0.1°C and allowed to equilibrate. Viscosities were determined using calibrated Cannon-Fenske viscometers in a Scientific Development Co. kinematic viscosity bath at 25.0°C. Tests were conducted by ASTM Standard D 445-74 (7). Densities were determined with a Mettler/Paar DMA 602M oscillating tube precision density meter. Water tolerance determinations were made by the AOCS Official Cloud Point Test (8). Conductivity experiments were performed with a Lab-Line Portable Lectro Mho-Meter, Mark V. GLC analyses were carried out with a 6 ft X 1/8 in. stainless-steel column and a flame ionization detector. For alcohol and hydrocarbon analyses a 15% Carbowax 20M packing was used, and with methyl esters a 10% EGSS-X packing was employed. The methyl esters were prepared for GLC analysis by American Oil Chemists Society (AOCS) method Ce 2-66 (9).

Results and Discussion

The bis(2-ethylhexyl) sodium sulfosuccinate system was initially investigated because its structure of liquid crystalline solution phases and mechanism of solubilization with water had been reported by Rogers and Winsor (10). In our studies, we substituted methanol for water. Table I lists critical micelle concentrations for bis(2-ethylhexyl) sodium sulfosuccinate, triethylammonium linoleate and tetradecyldimethylammonium linoleate in methanol and 2-octanol at 25°C. Literature references for critical micelle concentrations in methanol are sparse, and it has even been suggested that in polar solvents such as ethanol, either micellization does not occur or, if it does, only to a small degree (4). The data of Table I show that micellization occurs in methanol at low concentrations.

We have no measurements of micellar size, since the translation of micelle size into the number of monomers in the micelle is not a simple task and requires assumptions not easily experimentally tested. We are hopeful of extending experimentation in this direction in future research. Table II lists dielectric constants, dipole moments and effective polarities for methanol, 1- and 2-octanol, and water at 25°C.

Comparison of dipole moments shows only small differences in polarity. From these data, it can be reasoned that micellization in methanol is feasible. Dielectric constants and effective polarities (dipole moment/molar volume) support this premise with more divergent values. It is noted that bis(2-ethylhexyl) sodium sulfosuccinate forms micelles readily in water and 2-octanol which have the highest and lowest dielectric constants, respectively, but micelles are formed only at low concentrations in methanol whose dielectric constant is intermediate in value.

Figure 1 is a plot of kinematic viscosity, at 25°C, for varying molar ratios of methanol to bis(2-ethylhexyl) sodium sulfosuccinate. Three distinct regions are observed, and each is denoted by dotted vertical lines and designated as either bound methanol, trapped methanol, or apparently free methanol. Eicke

Table I. Critical Micelle Concentrations of Surfactants

in Methanol, 2-octanol and Water at 25°C[a]

| | Surfactant | | |
Solvent	Triethyl-ammonium Linoleate	Bis(2-ethyl-hexyl) sodium sulfosuccinate	Tetradecyldimethyl-ammonium Linoleate
	Critical Micelle Concentrations[b]		
Methanol	0.016	0.0076	0.002
2-Octanol	16.9	76.2	96.1
Water	0.020	2.5[c]	0.014

[a]Determined Conductometrically by plotting equivalent conductance against $\sqrt{C}$.

[b]Values in moles/liter X 10^3.

[c]P. Mukerjee and K. S. Mysels, "Critical Micelle Concentrations of Aqueous Surfactant Solutions," National Bureau of Standards, Washington, D.C., 1970.

Table II. Dielectric Constants, Dipole Moments and Effective

Polarities for Methanol, Octanols and Water at 25°C

Compound	Dielectric Constant (ε)	Dipole Moment (Debyes)	Effective[a] Polarity $\dfrac{\mu}{\bar{V}}$
Methanol	32.63	1.70	0.0418
2-Octanol	----	1.65	0.0103
1-Octanol	10.34	1.68	0.0106
Water	78.30	1.84	0.1022

[a]Dipole moment divided by molar volume.

(11) noted similar regions in his studies with water and bis(2-ethylhexyl) sodium sulfosuccinate. For molar ratios of less than 5, the methanol appears to be bound in a liquid crystal form with bis(2-ethylhexyl) sodium sulfosuccinate which coexists with phases of neat crystalline bis(2-ethylhexyl) sodium sulfosuccinate and methanol in micellar solution. In the 5 to 20 molar ratio region, the methanol appears primarily to be trapped as a micellar solution along with some of the neat phase. Above the 20 molar ratio, bis(2-ethylhexyl) sodium sulfosuccinate is largely molecularly dispersed. Observations with the polarizing microscope substantiate these data. Figures 2, 3 and 4 are photo-micrographs at 330 magnification of 5, 40 and 90 to 1 molar ratios of methanol to bis(2-ethylhexyl) sodium sulfosuccinate, respectively. All samples show birefringence, and a decrease in crystal size is noted with increasing amounts of methanol. All systems display classical focal conic, fan-shaped and mosaic textures, as well as oily streaks and "batonnets" that are characteristic of a smectic A phase (12). Figure 5 is a Fisher-Taylor-Hirschfelder atom model of a methanol-bis(2-ethylhexyl) sodium sulfosuccinate dimer. This could be a pre-micellar unit which eventually becomes a swollen micelle and then a liquid crystal. It is conceivable that a methanol molecule is associated with the counterion of a bis(2-ethylhexyl) sodium sulfosuccinate molecule. This complex, inturn, is linked to other molecules through hydrogen bonding, thus creating a network structure.

   Figure 6 is a plot of specific conductance against mole ratios of methanol to bis(2-ethylhexyl) sodium sulfosuccinate. Like the viscosity data, there are three regions. In the first region, a rapid rise in conductance occurs, which indicates the formation of a microemulsion. It is in this region that the swollen micellar solution and liquid crystalline phase of methanol in bis(2-ethylhexyl) sodium sulfosuccinate is breaking with the formation of microspheres that constitute the microemulsion (13).
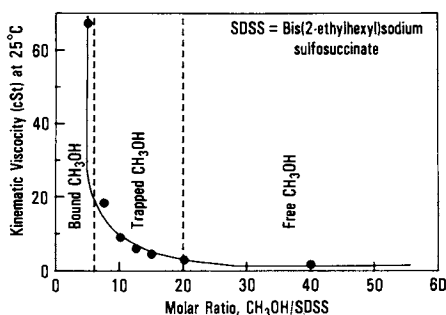
Figure 1.   Plot of kinematic viscosity against amount of solubilized methanol in bis(2-ethylhexyl) sodium sulfosuccinate at 298°K.
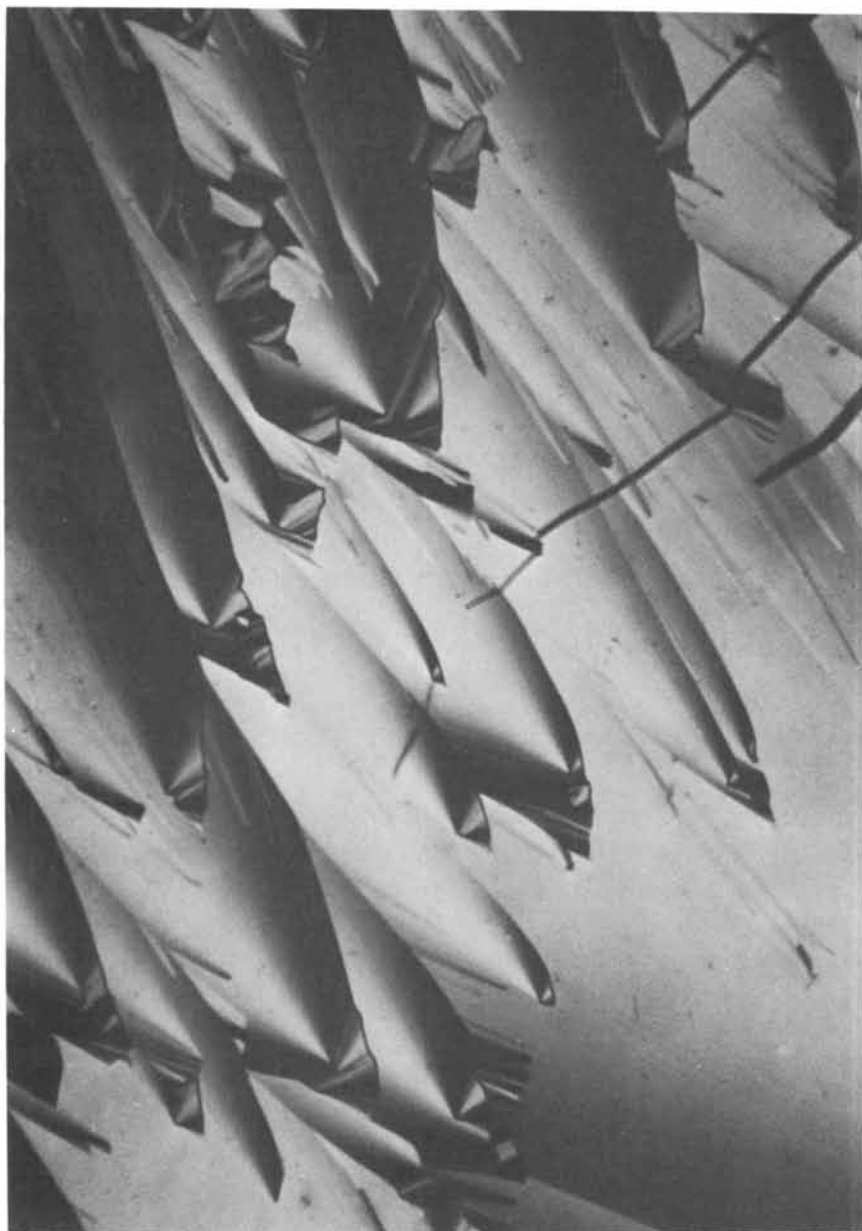
Figure 2. Photomicrograph at 298°K of 5/1 molar ratio CH_3OH/ bis(2-ethylhexyl) sodium sulfosuccinate; magnifications 330X; crossed polaroids.
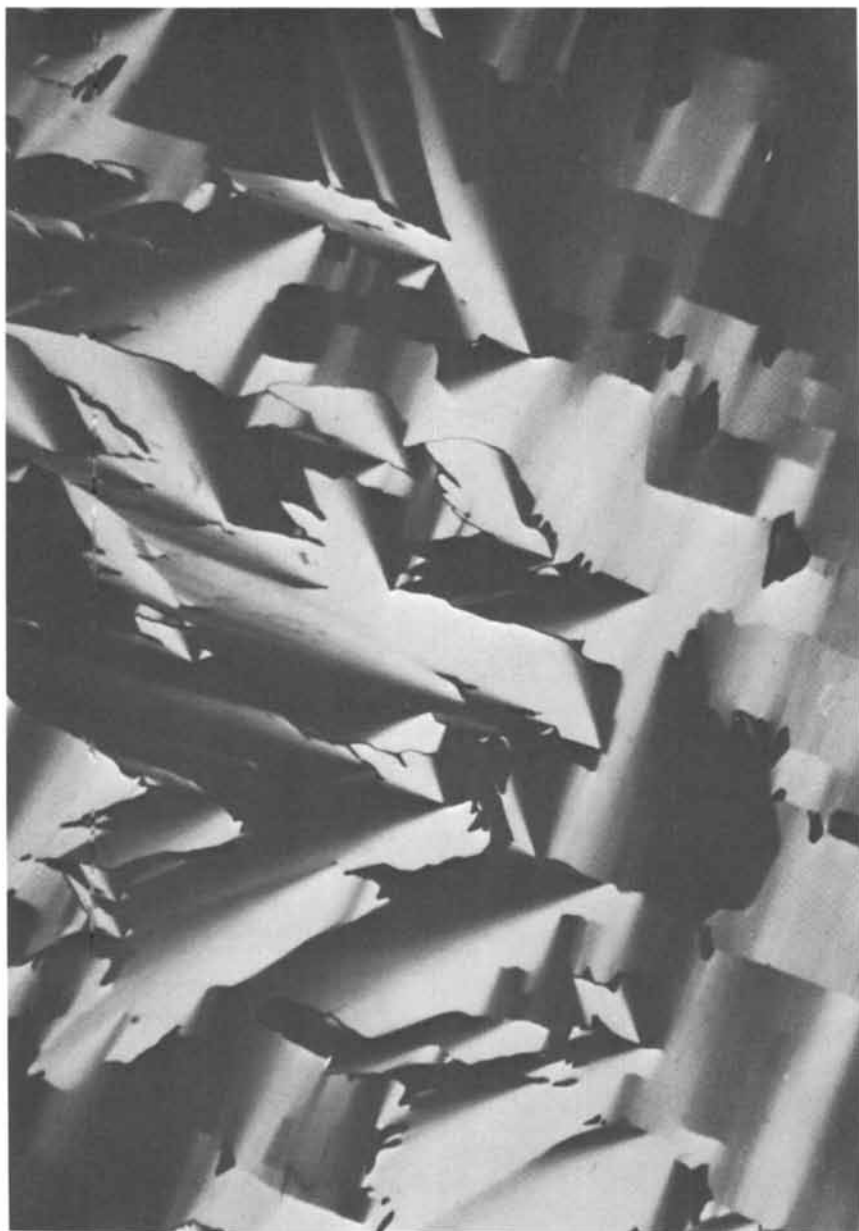
Figure 3.   Photomicrograph at 298°K of 40/1 molar ratio CH$_3$OH/ bis(2-ethylhexyl) sodium sulfosuccinate; magnification 330X; crossed polaroids.

Figure 4. Photomicrograph at 298°K of 90/1 molar ratio $CH_3OH/$ bis(2-ethylhexyl) sodium sulfosuccinate; magnification 330X; crossed polaroids.
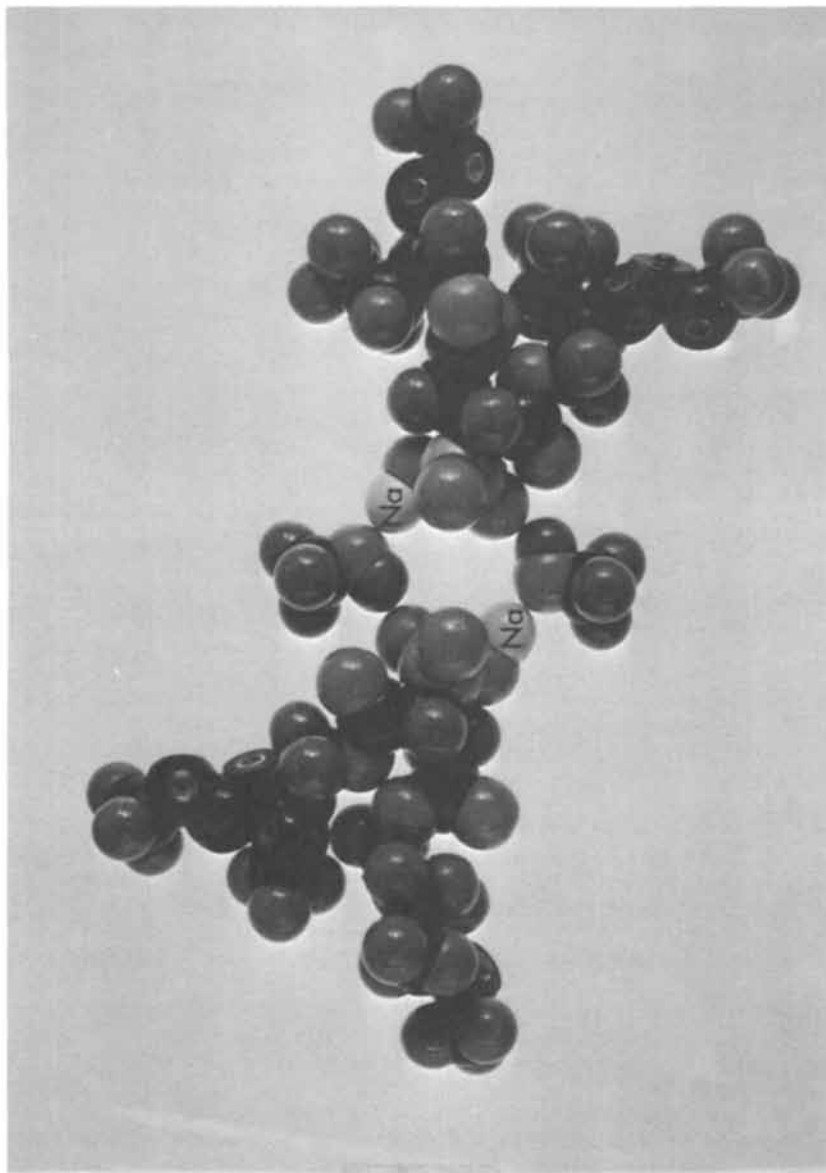
Figure 5. Fisher-Taylor-Hirschfelder atom model of CH_3OH-bis(2-ethylhexyl) sodium sulfosuccinate complex.[3]

The increase in conductivity is due to increase in dissolved
surfactant, and this increase continues until all the crystallites
dissolve. The peak in specific conductance is attained when the
microemulsion is formed and the specific conductance levels off.
The plateau of Figure 6 is often referred to as a "percolation
threshold" (14) and is reached when there is a disordered
interspersion capable of bicontinuous structures (15). Further
addition of methanol results in a lowering of conductivity explained
by the solution eventually approaching the conductivity of methanol.
This is the region of molecular dispersion. These conductivity
curves are similar to those observed by Laguës and Santerey (13)
on a system of water, cyclohexane, sodium dodecylsulfate and
1-pentanol.

Figures 7, 8 and 9 are plots at 25°C of specific conductance
and density versus volume fraction of methanol in 2/1 triolein/
surfactant systems which are 4/1 molar ratios of 2-octanol to
bis(2-ethylhexyl) sodium sulfosuccinate, triethylammonium linoleate
and tetradecyldimethylammonium linoleate, respectively. For each
surfactant system, a maximum for specific conductance and a minimum
for density was observed at the same volume fraction, but this
volume fraction of methanol varied between the three surfactant
systems. At volume fractions of methanol above these abrupt
changes, each system exhibited translucence, and it appears that
gel-like structures form. These data are consistent for
microemulsion structures that are based largely on geometric
considerations (16-18).

Figure 10 is a ternary diagram for the systems Triolein/S/
Methanol, where S is respectively 4/1 molar ratios of 2-octanol to
bis(2-ethylhexyl) sodium sulfosuccinate, triethylammonium linoleate
or tetradecyldimethyl ammonium linoleate at 25°C. Not much
difference is noted between phase areas for the triethylammonium
linoleate and bis(2-ethylhexyl) sodium sulfosuccinate systems.
Both are definitely inferior to the tetradecyldimethylammonium
linoleate which shows the greatest solubilized area of methanol in
triolein at 25°C.

Figure 11 shows a comparison of water tolerances of the three
systems at 25°C for a 6/3/1 volume ratio of triolein/surfactant
system/methanol at 25°C. The test used for this comparison was
the Official Oil Chemists test #Cc6-25 (8). The increased water
tolerance noted by the tetradecyldimethylammonium linoleate system
might be attributed to the double chained surfactant character.
This arrangement leads to increased hydrogen bonding and consequent
methanol tolerance. Both the tetradecyldimethyl and linoleate
moieties are hydrophobic in character, and in a reverse micellar
system, these may be viewed as interfacing with the triolein,
leaving a large inner core for the methanol solubilization. The
double-chained surfactants merit further attention in the
solubilization of methanol in triolein and in the potential use of
these surfactant systems for the development of emergency fuels
from agriculturally renewable resources.
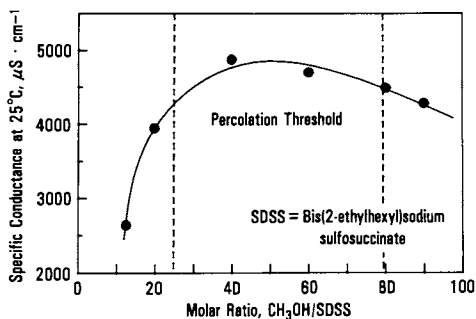
Figure 6.   Plot of specific conductance against amount of
solubilized methanol in bis(2-ethylhexyl) sodium
sulfosuccinate at 298°K.
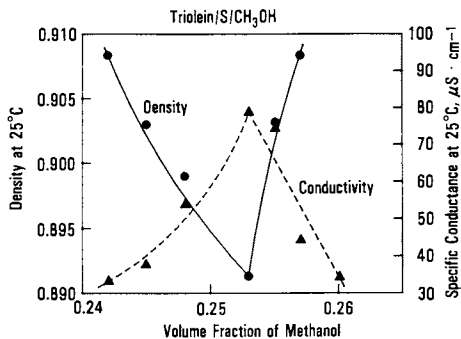
Figure 7.   Plots at 298°K of specific conductance and density
against volume fraction of methanol in a 2/1 triolein/
surfactant system which is a 4/1 molar ratio of
2-octanol to bis(2-ethylhexyl) sodium sulfosuccinate.
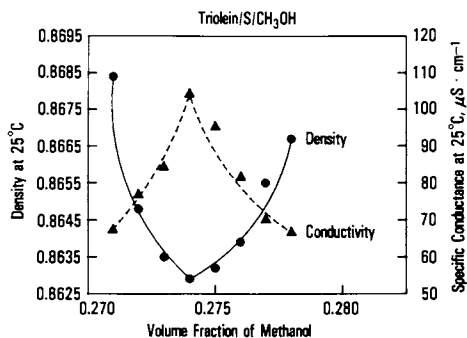
Figure 8. Plots at 298°K of specific conductance and density against volume fraction of methanol in a 2/1 triolein/surfactant system which is a 4/1 molar ratio of 2-octanol to triethylammonium linoleate.
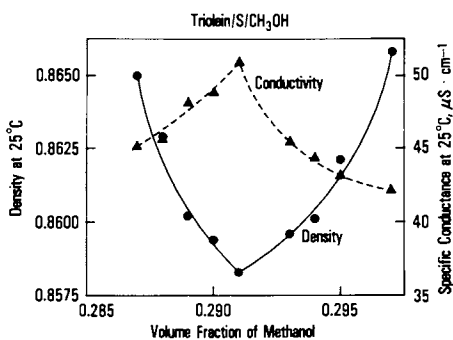
Figure 9. Plots at 298°K of specific conductance and density against volume fraction of methanol in a 2/1 triolein/surfactant system which is a 4/1 molar ratio of 2-octanol to tetradecyldimethylammonium linoleate.
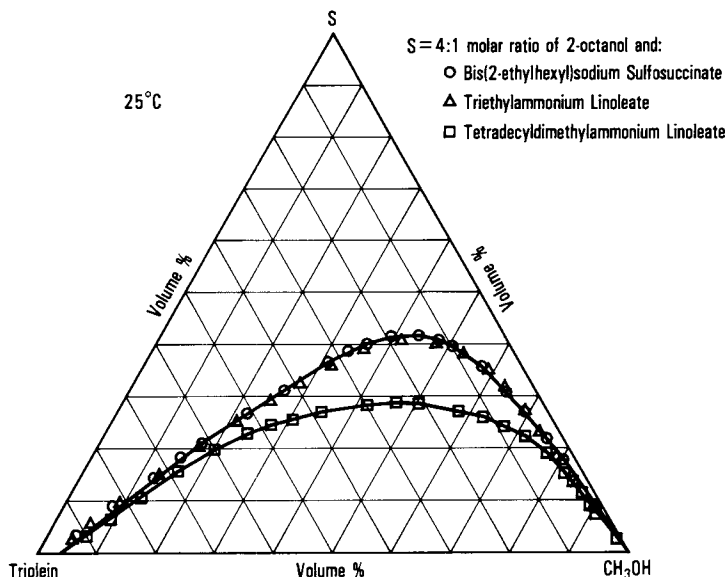
Figure 10. Ternary phase diagram at 298°K for systems of methanol in triolein with surfactant systems of bis(2-ethylhexyl) sodium sulfosuccinate, triethylammonium linoleate and tetradecyldimethylammonimum linoleate with 4/1 molar ratios of 2-octanol as co-surfactant.
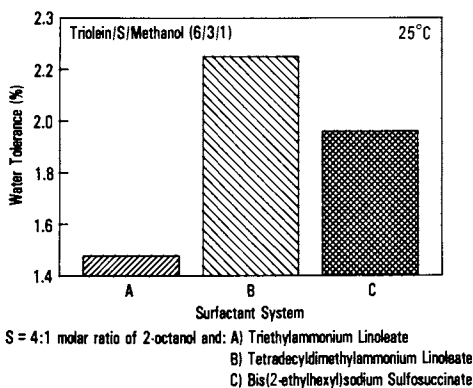
Figure 11. Bar graph of water tolerances at 298°K for triolein/ surfactant/ methanol (6/3/1) systems where surfactant is a 4/1 molar ratio of 2-octanol to either bis(2-ethylhexyl) sodium sulfosuccinate, triethylammonium linoleate or tetradecyldimethylammonium linoleate.

Literature Cited

1. Pryde, E. H.; Schwab, A. W. "Cooperative Work on Engine
    Evaluation of Hybrid Fuels" in "Vegetable Oil as Diesel
    Fuel," U.S. Department of Agriculture, ARM-NC-28, 1983, p.
    90.
2. Schwab, A. W.; Nielsen, H. C.; Brooks, D. D.; Pryde, E. H.
    J. Disp. Sci. Tech. 1983, 4(1), 1-17.
3. Schwab, A. W.; Pryde, E. H. Accepted for Publication in
    J. Disp. Sci. Tech.
4. Rosen, M. J. "Surfactants and Interfacial Phenomena", Wiley-
    Interscience, New York, 1978; p. 89.
5. Friberg, S. E. Progr. Colloid and Polymer Sci. 1983, 68,
    41-47.
6. Ruckenstein, E. "Solubilization and Microemulsification";
    Paper #05D48, Abstracts, International Chemical Congress of
    Pacific Basin Societies, Honolulu, Hawaii, 1984.
7. American Society for Testing Materials, ANS1/ASTM D445-74.
8. AOCS Official and Tentative Methods, 3rd ed, American Oil
    Chemists Society, Chicago, IL 1969 Cc 6-25.
9. AOCS Official and Tentative Methods, 3rd ed, American Oil
    Chemists Society, Chicago, IL 1969, Ce 2-66
10. Rogers, J; Winsor, P. A. J. Colloid Interface Sci. 1969,
    30(2), 247-257.
11. Eicke, H. F. In "Microemulsions"; Robb, I. D., Ed.; "The
    Microemulsion Concept in Nonpolar Surfactant Solutions";
    Plenum Press: New York, 1982; p. 17.
12. Candau, F.; Ballet, F. "Formation and Structure of Four -
    Component Systems Containing Polymeric Surfactants" in
    "Microemulsions"; Robb; I. D.; Plenum Press: New York, 1982;
    p. 59.
13. Lagues, M.; Santerey, J. Phys. Chem. 1980, 84, 3503-3508.
14. Bennett, K. E.; Hatfield, J.C.; Davis, H. T.; Macosko, C. W.;
    Scriven, L. E. In "Microemulsions", Robb, I. D., Ed.;
    "Viscosity and Conductivity of Microemulsions," Plenum Press:
    New York, 1982, p. 77.
15. Scriven, L. E. In "Micellization Solubilization and
    Microemulsions"; Mittal, K. L. Ed.; Plennum Press: New York,
    1977; Vol. II, p. 887.
16. Chen, S. J.; Evans, D. Fennell; Ninham, B. W. J. Phys. Chem.
    1984, 1631-1634.
17. Lissant, K. J. J. Colloid Interface Sci. 1966, 22, 462.
18. Lissant, K. J. "Emulsions and Emulsion Technology", Part I,
    ed. Marcel Dekker, New York, 1974.

Effects of Different Distributions of Lyophobic Chain Length on the Interfacial Properties of Nonaethoxylated Fatty Alcohol

Xia Jiding, Sun Yan, and Zhou Heyun

Department of Chemical Engineering, Wuxi Institute of Light Industry, Wuxi, Jiangsu, People's Republic of China

Fourteen kinds of mixtures with distribution in carbon chain length of nonaethoxylated fatty alcohol (AE9) were prepared. By the pseudo-phase separation model and the regular solution theory, the thermodynamic effects of the distribution of chain length on inter-facial properties of mixed solution are discussed. Experimental results have shown that the nonideal mixing by regular solution theory are reasonable. By adjusting the distribution of carbon length of AE9, the efficiency and effectiveness of surface tension reduction can be increased. The amount of AE9 with carbon chain length longer than C_{16} should be kept to a minimum for wettability considerations and the narrow distribution with the major portion C_{12}-C_{14} is preferred for the stability of castor oil emulsion. The mixtures containing 2-5 compounds of AE9 in normal distribution, with the major portion C_{12}-C_{14} give good detergency performance.

The interfacial phenomena of nonionic polyoxyethylenated fatty alcohols are principally dependent on their chemical structure and characteristic features (1). In our previous work (2) we have shown that the assumption of ideal mixing for homologous mixtures, with different Gaussian distribution in POE chain length (prepared from mono-polyoxyethylene glycol n-dodecyl ether), is reasonable. In order to attain an effective syngergism of the mixed surfactants, the selection of an optimum hydrophobic chain length distribution is an important factor from both theoretical and practical aspects because of the wide distribution of hydrocarbon chain lengths exist-ing in natural or synthetic fatty alcohols.

Present investigation was undertaken to elucidate the relation-ships between the nonaethoxylated fatty alcohols with different distributions of hydrocarbon chain lengths and surface adsorption,

micelle formation, wettability, emulsion formation and other per-
formance criteria of aqueous solutions.

Experimental

Materials. $C_{10}, C_{12}, C_{14}, C_{16}, C_{18}OH$ were Shanghai Chemical Reagent Co.
extra pure materials, purity > 98%. Ethylene oxide was purified
with monoethanol amine to an aldehyde content < 0.03%. Mixed alco-
hols were prepared from individual purified fatty alcohols according
to a Gaussian distribution for 2-5 components. Nonaethoxylated
fatty alcohols (AE$_9$) were synthesized and purified as usual. The
average number of ethylene oxide (CO) groups added (9±0.3) was
determined by HI method (Table I).

Test Methods. Surface tension (γ) measurements were taken by Wil-
helmy method (25±0.1°C). Critical micelle concentrations (cmc) were
obtained from γ-logC curves. Contact angle, Type GI, Japan. Wetting
test, Canvas disk method, CIS,HG-2-380-66. Foam test, Ross-Miles
lather method. Emulsibility was determined by mixing 20 ml of 2.5%
aqueous solution of AE$_9$ with 20 ml castor oil (HLB required = 14) at
a given time. The volume of the emulsifying layer was measured
after the solutions were separated. Detergency was measured by
launderometer in a water hardness of 250 ppm $CaCO_3$ at 45°C. The
whiteness of fabrics was measured (in %) before and after washing.

Results and Discussion

Surface Adsorption of the Mixed Solution. In this system the sur-
face adsorption of AE$_9$ with different hydrocarbon chain length dis-
tributions was found to be related to the efficiency and effective-
ness of surface tension reduction and the change of standard free
energy. By the Gibbs equation, Szyskowski equation $\pi=\Gamma RTLn(K_1C_1 + 1)$
and Langmuir equation of monomolecular adsorption $\Gamma_1=(\Gamma CK_1\alpha_1)/(1 +
\Sigma CK_1\alpha_1)$, the parameter K, amount of excess surface adsorption, Γ_1,
surface area occupied by one molecule A, and the change of adsorp-
tion of free energy ΔG°_{ads}, ($\Delta G^\circ_{ads}=RTLn$ cmc$-\pi_{cmc}A_{min}$) are shown in
Table I, Figure 1,2. This indicates that there is an increased
tendency for surface adsorption (Γ) with the increase of hydrocarbon
chain length of AE$_9$, making G°_{ads} more negative by about 1.2 KJ per
-CH_2- group, but the effectiveness of adsorption appears to be
lowered when the hydrocarbon chain length is longer than C_{14}
(Figure 1).
      For solutions of AE$_9$ with different distributions of hydrocarbon
chain lengths, the γ-log C curves appear to be different than mono-
component system. The surface pressure at critical micelle concen-
tration (π_{cmc}) of AE$_9$ with a long hydrocarbon chain ($C_{16}E_9$) is
increased by adding the short AE$_9$, but the effect is not significant
if the hydrocarbon chain is in a wide distribution (i.g. coconut
fatty radical) (Figure 2,3,4). As for the efficiency of surface
tension reduction $C_{\pi=20}$, there is a synergestic effect for the mixed
solution of AE$_9$. The value of $C_{\pi=20}$ is mostly between 3-4x10^{-6}
mole·L^{-1}, therefore the efficiency of surface tension reduction of
AE$_9$ with short chain may be enhanced after the long chain has been
added, so that the values of ΔG°_{ads} and $C_{\pi=20}$ decrease and the

Table I. $C_{\pi=20}$, $\Delta G°_{ads}$, π_{cmc}, Γ, A of Mixed AE_9 Aqueous Solution

Hydrophobic Chain of AE_9	$C_{\pi=20}\times10^6$ (mol·L⁻¹)			$\Delta G°_{ads}$ (KJ·mol⁻¹)	π_{cmc} (mN·m⁻¹)	$\Gamma\times10^{10}$ (mol·cm⁻²)	A (Å²)
	Measured	Cal'd I(a)	Cal'd II(b)				
C_{10}	87.10			-31.2	38.3	2.69	61.7
C_{12}	11.50			-33.3	39.7	3.67	41.2
C_{14}	2.17			-35.8	39.3	4.58	36.3
C_{16}	2.55			-35.2	31.5	4.84	34.3
C_{10},C_{12}	16.50	20.70	16.50	-33.5	40.0	3.32	50.1
C_{12},C_{14}	3.06	3.81	3.05	-36.2	39.5	3.84	43.2
C_{14},C_{16}	2.18	2.39	2.18	-35.9	36.4	4.64	35.8
C_{12},C_{14},C_{16}	2.19	2.59		-37.2	39.0	4.10	40.5
$C_{10}-C_{16}$	2.54	3.91		-37.0	39.7	3.73	44.5
$C_{10}-C_{18(N)}$ (c)	2.64			-36.0	36.0	3.70	44.9
$C_{10}-C_{18(P)}$ (d)	3.39			-37.1	37.2	3.23	51.4
Coconut fatty alcohol	4.12			-37.3	36.4	3.06	54.3

(a) Calculated on the basis of ideal mixing. (b) Calculated on the basis of non-ideal mixing.
(c) Normal distribution. (d) Poisson distribution.
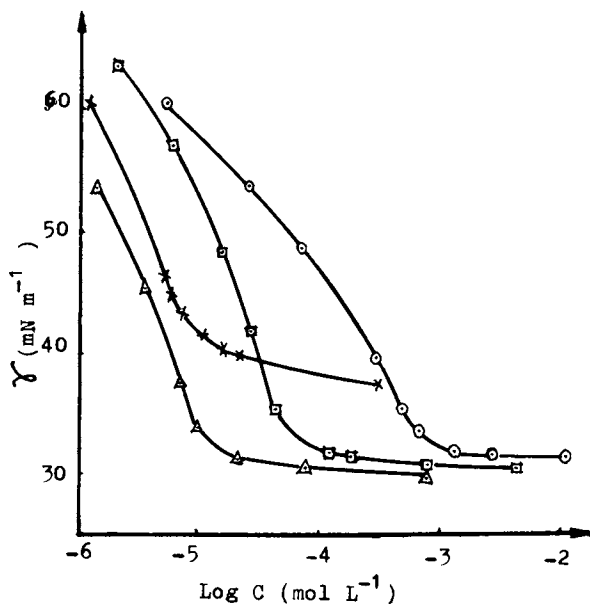
Figure 1. γ-Log C curve of single AE9 aqueous solution
⊙ $C_{10}E_9$, ☐ $C_{12}E_9$,   x $C_{16}E_9$,   Δ $C_{14}E_9$
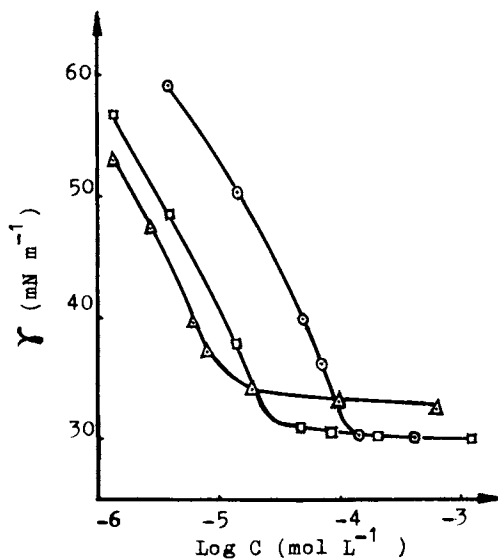
Figure 2. γ-Log C curve of binary mixed AE9 solution
⊙ $C_{10,12}E_9$, ◇ $C_{12,14}E_9$,   Δ $C_{14,16}E_9$
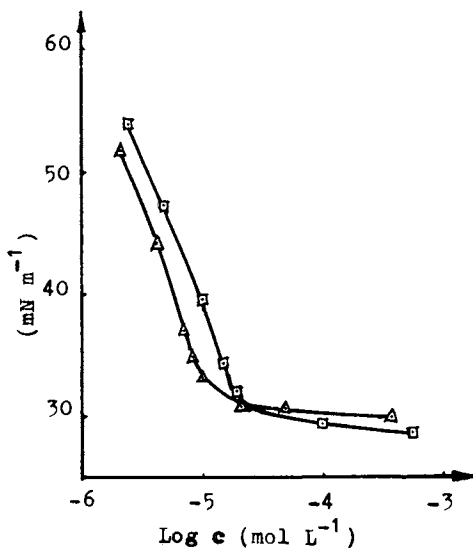
Figure 3. γ-Log C curve of trinary and tetranary mixed AE_9 solution $\square$ $C_{10-16}E_9$, $\triangle C_{12,14,16}E_9$
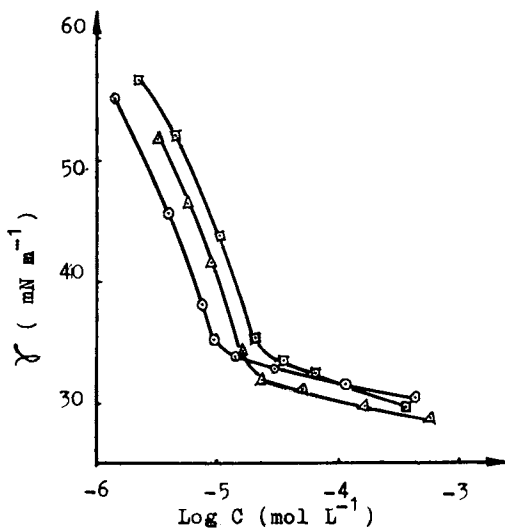
Figure 4. γ-Log C curve of multi-component system of AE_9 solution ⊙ $C_{10-18}(N)E_9$, $\triangle C_{10-18}(P)E_9$, $\square$ coconut alcohol E_9

molecules in the surface layer may be orientated in a closer con-
figuration.

By extending regular solution theory for binary mixtures of AE_9
in aqueous solution to the adsorption of mixture components on the
surface (3,4), it is possible to calculate the mole fraction of AE_9,
X_s, on the mixed surface layer at $\pi=20$, the molecular interaction
parameter, β, the activity coefficients of AE_9 on the mixed surface
layer, f_{1s} and f_{2s}, and mole concentration of surfactant solution,
$C_{\pi=20}$, at surface pressure $\pi=20$ mn$\cdot$m^{-1} ($25\pm0.1°C$). The results from
the following equations are shown in Table I and Table II.

$$\beta_s = \frac{Ln(\frac{C_\pi \alpha}{C_{\pi1}X_{s1}})}{(1-X_{s1})^2} \qquad (1)$$

$$f_{s1} = \exp\beta_s(1-X_{s1})^2 \qquad (2)$$

$$f_{s2} = \exp[\beta_s(X_{s1})^2] \qquad (3)$$

$$C_{\pi=20} = \frac{1}{\frac{\alpha i}{f_{si} \, C_{\pi=20i}}} \qquad (4)$$

Due to competitive adsorption of components in mixed AE_9 solu-
tion, the amount of a strongly adsorbing component, such as $C_{14}E_9$,
on the surface layer is greater than that of a weakly adsorbing com-
ponent and what is in the bulk solution. The calculated values of
$C_{\pi=20}$ coincide with the measured values as can be seen from Table II.
This means that the regular solution treatment of the AE_9 mixture
containing a Gaussian distribution in hydrocarbon chain lengths is
more reasonable than assuming ideal mixing, especially for the mix-
tures with components less than C_{16}.

Formation of Mixed Micelles. The formation of mixed micelles of AE_9
in aqueous solution mainly depends on the standard free energy of
micellization, ΔG_M°. The cmc and ΔG_M° of single AE_9 and mixtures of
AE_9, with hydrocarbon chain length distributions calculated on the
basis of ideal mixing, are shown in Table III. Table IV lists X_{M1},
f_{M1}, f_{M2}, β, and ΔG_M° calculated by regular solution theory. The data
indicate that for the single AE_9, both C_M and ΔG_M° decreases as the
length of the hydrocarbon chain increases. In the range of C_{10}-C_{14},
the lowering of ΔG_M° is about 0.5-0.6 Kcal mol^{-1} per -CH- group, but
appears to have a small effect when the number of carbon atoms in
the straight chain hydrophobic group exceeds C_{14} (Figure 5). Among
all the AE_9, the long chain hydrophobic group seems to have the most
significant action in micellization because the C_M of the mixed
solutions is located near the lower cmc of the individual AE_9.

From data listed in Table IV one sees $\beta < 0$, $f_{M1} < 1$, and $H^E < 0$
which indicate that the micellization of a binary mixture with dif-
ferent hydrocarbon chain lengths is different than the case of ideal

Table II. X_s, β_s, f_{s1}, f_{s2} of Mixed AE_9 Solution During Adsorption

AE_9	α_1 mole fraction	α_2	α_3	α_4	X_{s1} mole fraction	X_{s2}	X_{s3}	X_{s4}	β_s	f_{s1}	f_{s2}
C_{10},C_{12}	0.512	0.488			0.314	0.686			-1.54	0.409	0.917
C_{12},C_{14}	0.512	0.488			0.286	0.714			-1.17	0.526	0.925
C_{14},C_{16}	0.511	0.489			0.574	0.426			-0.29	0.942	0.918
$C_{12,14,16}$	0.168	0.679	0.153		0.074	0.788	0.138				
$C_{10,12,14,16}$	0.086	0.429	0.410	0.075	0.022	0.254	0.634	0.090			

Table III. C_M, ΔG_M° of Mixed AE$_9$ Solution Calculated on the Basis of Ideal Mixing (25±0.1°C)

AE$_9$	$C_M \times 10^3$ (mol·L^{-1}) Measured	Cal'd	ΔG_M° (Kcal·mol^{-1})	AE$_9$	$C_M \times 10^3$ (mol·L^{-1}) Measured	Cal'd	ΔG_M° (Kcal·mol^{-1})
C$_{10}$	10.50		-6.44	C$_{14}$,C$_{16}$	1.21	1.22	-9.08
C$_{12}$	11.40		-7.75	C$_{12,14,16}$	1.42	1.75	-8.98
C$_{14}$	1.73		-8.87	C$_{10}$-C$_{16}$	2.45	2.82	-8.98
C$_{16}$	0.93		-9.23	C$_{10}$-C$_{18}$(N)	2.23		-8.72
C$_{10}$,C$_{12}$	17.20	21.00	-7.51	C$_{10}$-C$_{18}$(P)	3.28		-8.49
C$_{12}$,C$_{14}$	2.86	3.06	-8.57	Coconut Alcohol	3.47		-8.45

Table IV. The Parameters of Micellization of Mixed AE9 Solution Calculated on the Basis of Non-ideal Mixing

AE$_9$	α	X_{M1}	f_{M1}	f_{M2}	β	$C_M \times 10^5$ (mol·L^{-1})	m(a)	ΔG_M° (kcal·mol^{-1})	H^E (b) (Kcal·mol^{-1})
C$_{10}$,C$_{12}$	0.512	0.213	0.395	0.935	-1.50	17.20	11.6	-7.47	-0.62
C$_{12}$,C$_{14}$	0.512	0.180	0.719	0.989	-0.50	2.86	13.6	-8.66	-0.18
C$_{14}$,C$_{16}$	0.512	0.360	0.989	0.996	-0.03	1.20	15.3	-9.10	-0.02

(a) Average carbon number. (b) Excess enthalpy, $H^E = RT(1-X)$.

mixing, especially the mixture of C_{10} and C_{12}, while the mixture of C_{14}, C_{16} begins to approach ideal mixing. The values of ΔG_M^o calculated ($\Delta G_M^o = \Sigma X_{Mi} \Delta G_{Mi}^o$) in Table IV compared to those measured in Table III may reflect that the mixture is only a synergistic effect rather than the formation of a new complex compound. In all cases, the AE9 with the longest hydrocarbon chain, giving a low ΔG_M^o value, may be predominant in the micelle formation.

Wetting, Foaming, Emulsification, and Detergency. The wetting and foaming properties of the mixed AE9 solution with different hydrocarbon chain lengths are shown in Table V. Starting from C_{10} to C_{16} an increase in the length of the hydrophobic group gives an increase in wetting properties, with C_{14} the maximum and a decrease after C_{16} due to the larger hydrophobic group. The mixtures of AE9 containing 2-3 adjacent components, with the exception of $C_{16}E_9$, appear to have a good wettability with cotton fabrics. In this case for AE9 the Poisson distribution seems to be better than Gaussian distribution.
        The foam stability of mixed AE9 with a middle chain length distribution is better than the individual lower one. Among all AE9, the mixed $C_{10,12}E_9$ gives probably the best result on the stability of emulsion to caster oil. Introducing a long hydrocarbon chain in the mixture or a wide distribution in hydrocarbon chain length causes no effect on the emulsion stability (Figure 6).

Solubilization. The amount and position of solubilization mostly depends on the structures and properties of solubilizing agents and solubilizates. In aqueous solutions of AE9 the solubilization of benzene appears to decrease with increase in the hydrocarbon chain length and increase with the number of EO units giving the net result that ΔG_{sol}^o becomes slightly less negative. Benzene molecules entering the outside layer of micelles are polarized by the induction of oxygen in POE groups and solubilized between the polyoxyethylene chains. When the hydrocarbon chain length of AE9 increase, some POE groups nearby the hydrophobic chain appear to lose a portion associated water molecules and the molecules in the micelles become orientated more closely, so that solubilization is decreased. In the same case the solubilization of a mixture of AE9 decreases with increasing average hydrocarbon chain length $(\bar{m})$(Figure 7). It is apparent that the degree of the chain distribution has no effect on the solubilization.

Detergency. The data of detergency of mixed AE9 compared to that of water (ratio R/R_o) are listed in Table VI. The mixtures of AE9 containing shout and long hydrocarbon chains may adjust systematically the wetting, emulsification and solubilization properties and therefore give good washing performance. In general from this work the detergency of the mixed AE9 ranging from $C_{12}-C_{18}$ in a Gaussian distribution, in which $C_{12}-C_{14}$ hydrocarbon group are the main portion, may result in better efficiency.

Table V.   Wetting and Foaming Properties of Mixed AE_9 Solution

AE_9	Wetting Property(a)		Foaming Property(b)	
	Canvas (sec.30°C)	Contact Angle (°)(28°C)	Start (mm)	After 5 min. (mm)
C_{10}	81	48.5	114	62
C_{12}	77	43.9	95	80
C_{14}	54	42.0	70	68
C_{16}	238	55.0	34	32
C_{10}, C_{12}	55	44.8	112	68
C_{12}, C_{14}	59	44.0	89	83
C_{14}, C_{16}	120		43	40
$C_{12,14,16}$	88	54.0	75	75
$C_{10,12,14}$	68	47.8	104	95
$C_{10,12,14,16}$	90	53.5	99	91
$C_{12,14,16,18}$	105	54.4	39	37
$C_{10}-C_{18}$(N)	93	50.0	87	82
$C_{10}-C_{18}$(P)	73	48.1	94	87
Coconut alcohol	90	50.0	92	84

(a) 0.1% solution.   (b) 0.06% solution.
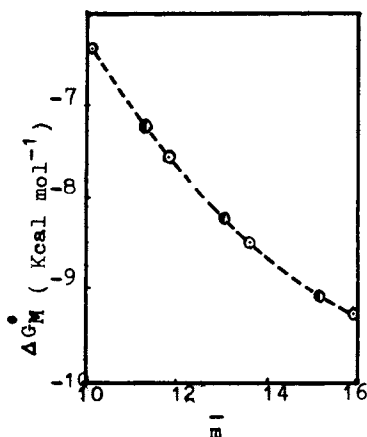
Figure 5. Relationship of ΔG_M^o and average hydrocarbon chain length
($\bar{m}$). The dashed lines are the theoretical value, the
plotted points experimental data, o-single component,
⊙-binary mixture.
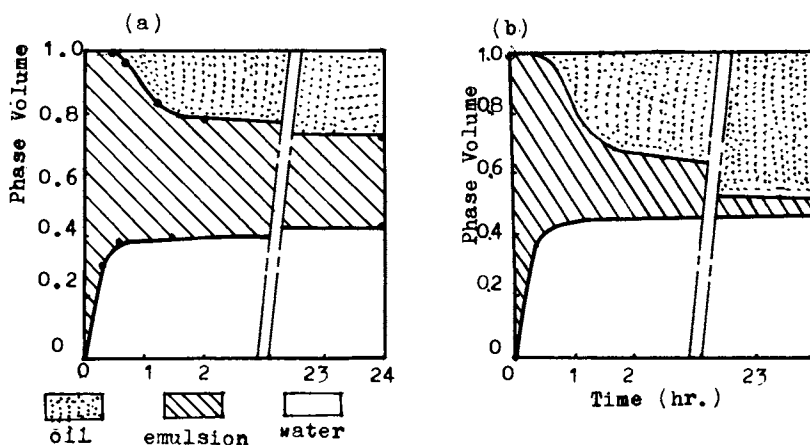
Figure 6. Characteristics of emulsion of AE9 solution.
(a) Single $C_{12}E_9$
(b) Single $C_{16}E_9$
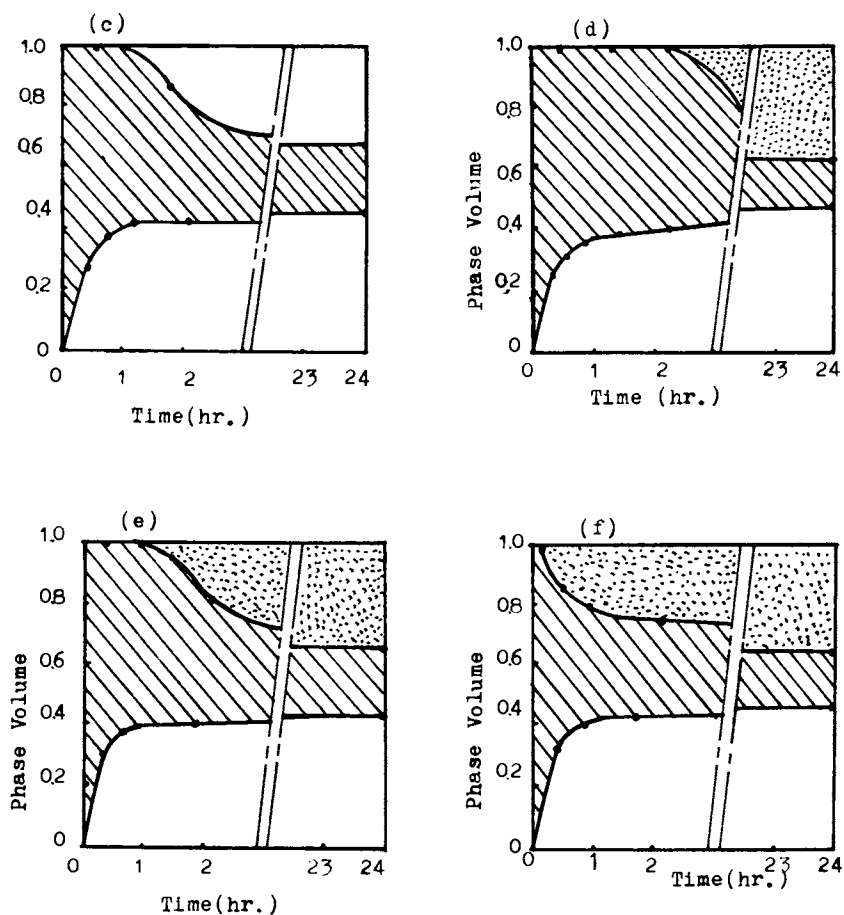
Figure 6. Characteristics of emulsions of AE_9 solutions.
    (c) Single $C_{14}E_9$
    (d) Binary mixed solution of $C_{14,16}E_9$
    (e) Trinary mixed solution of $C_{12,14,16}E_9$
    (f) Tetranary mixed solution of $C_{10-16}E_9$
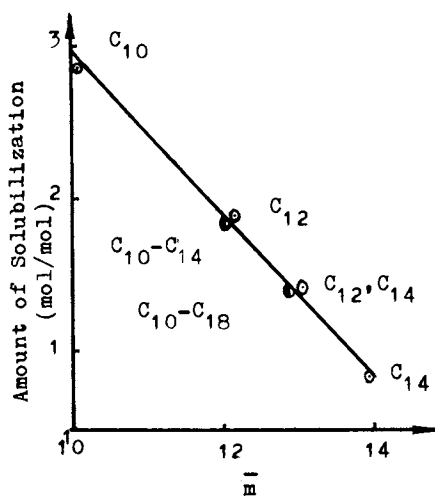
Figure 7. Relationship of solubilization and the average hydrocarbon chain length.

Table VI. Detergency Data of Mixed AE$_9$ Solution (45$\pm$1°C)*

AE$_9$	Cloud Point(°C)	R/R$_\circ$ x100	AE$_9$	Cloud Point(°C)	R/R$_\circ$ x100	AE$_9$	Cloud Point(°C)	R/R$_\circ$ x100
C$_{10}$	92	375	C$_{12}$·C$_{14}$	74	451	C$_{12}$-C$_{18}$	71	393
C$_{12}$	84	413	C$_{14}$·C$_{16}$		356	C$_{10}$-C$_{18}$(N)	79	438
C$_{14}$	71	412	C$_{10}$-C$_{14}$	83	443	C$_{10}$-C$_{18}$(P)	76	350
C$_{16}$	63	338	C$_{12}$-C$_{16}$	82	409	Coconut alcohol	82	401
C$_{10,12}$	78	399	C$_{10}$-C$_{16}$	87	373			

*Concentration of active matter 0.05% (w/v).
R$_\circ$ = 7.43 for water only.

Conclusion

1. The regular solution theory may be applied to surface adsorption and micelle formation of mixed nonaethoxylated fatty alcohols with Gaussian distribution in hydrophobic chain length. Such a system can be treated as an ideal mixture.
2. The strong adsorption components ($C_{14}E_9$) are predominant on the surface adsorbed layer. Long hydrocarbon chain components are preferred in the micelle formation.
3. Good performance may be obtained as follows: wetting property -- less components over C_{16}; Emulsion stability to caster oil -- narrow distribution containing the main portion of C_{10}-C_{12}; solubilization -- decrease with increase of mean carbon number, no effect to hydrocarbon chain distribution; detergency -- binary to pentanary Gaussian distribution of AE_9 in which C_{12}-C_{14} occupy the principal portion.

Legend of Symbols

γ	surface tension
Γ	total amount of excess surface adsorption at surface saturation
Γ_i	adsorbed amount of component i in mixed monolayer
K_i	constant of the Szyskowski equation for the component i
α_i	mole fraction of component i in total mixed solute
C	total concentration of surfactant solution
π	surface pressure
π_{cmc}	surface pressure at cmc
C	mole concentration of surfactant solution at
A	minimum area occupied per molecule at monolayer
X_{s1}, X_{s2}	mole fraction of component 1,2 in mixed monolayer
X_{M1}, X_{M2}	mole fraction of component 1,2 in mixed micelle
β_s	molecular interaction parameter in mixed monolayer
β	molecular interaction parameter in mixed micelle
f_{s1}	activity coefficient of surfactant 1 in mixed monolayer
C_M	critical micelle concentration of surfactant solution
ΔG_M°	standard free energy of micelle formation
ΔG_{ads}°	standard free energy of adsorption
ΔG_{sol}°	standard free energy of solubilization
R/R_o	detergency ratio of surfactant solution to pure water

Literature Cited

1. Rosen, M. J. "Surfactants and Interfacial Phenomena"; John Wiley & Sons Inc.: New York, 1979; p. 149.
2. Xia, J. D.; Hu, Z. Y. "The Effects of Polyoxyethylene Chain Length Distribution on the Interfacial Properties of Polyoxy-ethylenated n-Dodecyl Alcohols" (in press).
3. Rubingh, D. N. In "Solution Chemistry of Surfactants"; Mittal, K. L. Ed.; Plenum Press: New York, 1978; Vol. I, p. 337.
4. Rosen, M. J.; Hua, X. Y. J. Colloid Interface Science. 1982, 86, (1), 164.

23

Mixed Adsorbed Film of 1-Octadecanol and Dodecylammonium Chloride at the Hexane-Water Interface

Yoshiteru Hayami[1] and Kinsi Motomura[2]

[1]Chikushi Jogakuen Junior College, Dazaifu, Fukuoka 818-01, Japan
[2]Department of Chemistry, Faculty of Science, Kyushu University 33, Fukuoka 812, Japan

The interfacial tension of mixed adsorbed films of
1-octadecanol and dodecylammonium chloride has been
measured as a function of temperature at various bulk
concentrations under atmospheric pressure. The
transition interfacial pressure of 1-octadecanol film
has been observed to increase with the addition of
dodecylammonium chloride and then to disappear. The
interfacial pressure vs mean area per adsorbed molecule
curves have been illustrated at a constant mole
fraction of adsorbed molecules. With the aid of the
thermodynamic treatment developed previously, we find
that the mutual interaction between 1-octadecanol and
dodecylammonium chloride molecules in the expanded
state is similar in magnitude to the interaction
between the same kind of film-forming molecules.

Generally, there are two approaches to the investigation of mixed
adsorbed films at an oil/water interface. One way is to study mixed
adsorption of surfactants from the same bulk phase and the other is
to study adsorption from both of the bulk phases. The former has
been done by many workers from the physicochemical viewpoint to
clarify the difference in molecular interaction between the adsorbed
state and the bulk state. The latter has been made mostly from the
practical point of view, e.g., solvent extraction and complex-forming
reactions that take place at the interface, though little is known
concerning the thermodynamic viewpoint (1). The thermodynamic study
is actually useful to elucidate the behavior of film molecules in the
adsorbed state.
  It is interesting to employ the system consisting of mixed
adsorbed film of 1-octadecanol and dodecylammonium chloride because
the former shows the phase transition from an expanded to a condensed
state (2). The interfacial tension was measured as a function of
temperature at various bulk concentrations under atmospheric pressure
and the molecular interaction between film-forming components was
considered.

Experimental

1-Octadecanol was recrystallized from hexane after fractionation by
vacuum distillation, and its purity was checked by gas-liquid
chromatography. Dodecylammonium chloride was recrystallized from a
mixture of ethanol and water, and its purity was confirmed by the
fact that it had no minimum near the critical micelle concentration
on the surface tension vs concentration curve. Hexane was distilled
after passing through an activated alumina column. Water was
distilled from alkaline permanganate solution of distilled water
after refluxing for one day. The purity of hexane and water was
confirmed by the value of the interfacial tension between them.
     The interfacial tension was measured by the pendant drop method.
Detailed description of the apparatus and the method was given
previously ($\underline{3}$).

Results

The interfacial tension γ was measured as a function of temperature
T, molality m_1^O of 1-octadecanol in hexane, and molality m_2^W of
dodecylammonium chloride in water under atmospheric pressure. The
molality m_1^O was increased up to the solubility limit.
     Figure 1 shows the plots of the interfacial tension against
temperature at various m_2^W values for m_1^O = 7.54 mmol kg^{-1}. All the
curves except for the concentrated solution of dodecylammonium
chloride have a break point which represents the phase transition
from the condensed to expanded state. The phase transition
temperature lowers with increasing m_2^W and disappears above a certain
m_2^W value.
     In the present paper, we will discuss only the variation in γ
with the concentrations m_1^O and m_2^W at 298.15 K. In order to apply the
thermodynamics to experimental results, it is required that the
interfacial tension is plotted against the concentrations m_1^O and m_2^W.
Taking the values of γ at 298.15 K from Figure 1, the variation of
γ with m_2^W under the condition that the concentration m_1^O is fixed at
298.15 K is shown in Figure 2. The curve has a higher negative slope
for the expanded state and a lower one for the condensed state. The
m_2^W value of the phase transition point is seen to increase with
increasing m_1^O.
     In the same manner, we can obtain the interfacial tension vs
concentration m_1^O curves at fixed m_2^W value at 298.15 K shown in
Figure 3.
     Contrary to the γ vs m_2^W curves in Figure 2, the curves which
have lower and higher negative slopes in Figure 3 are the expanded
and condensed states, respectively. In addition, it is found that
the slopes of γ vs m_2^W and γ vs m_1^O curves increase with increase in m_1^O
and m_2^W, respectively.

Discussion

Taking into consideration that the solvents are practically
immiscible and that 1-octadecanol and dodecylammonium chloride are
soluble only in hexane and water respectively, the total differential
of the interfacial tension γ can be expressed as a function of
temperature T, pressure p, molality m_1^O, and molality m_2^W as follows
($\underline{4}$) :
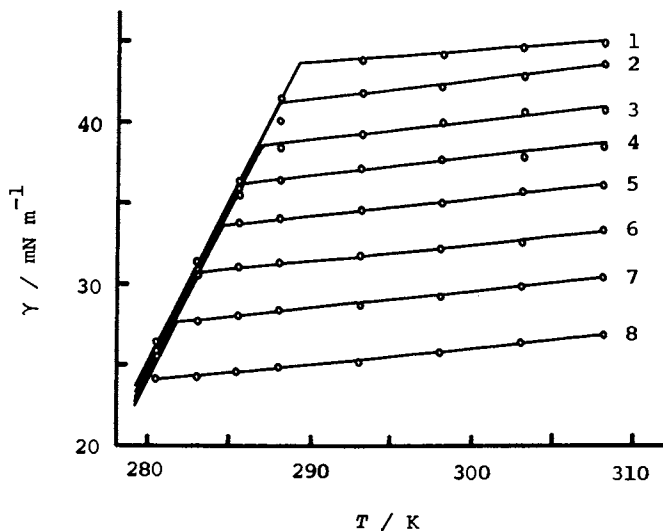
Figure 1. Interfacial tension vs temperature curves at constant m_2^W and $m_1^O = 7.54$ mmol kg^{-1}: (1) $m_2^W = 0$ mmol kg^{-1}; (2) 0.22; (3) 0.53; (4) 0.90; (5) 1.33; (6) 1.82; (7) 2.43; (8) 3.28.
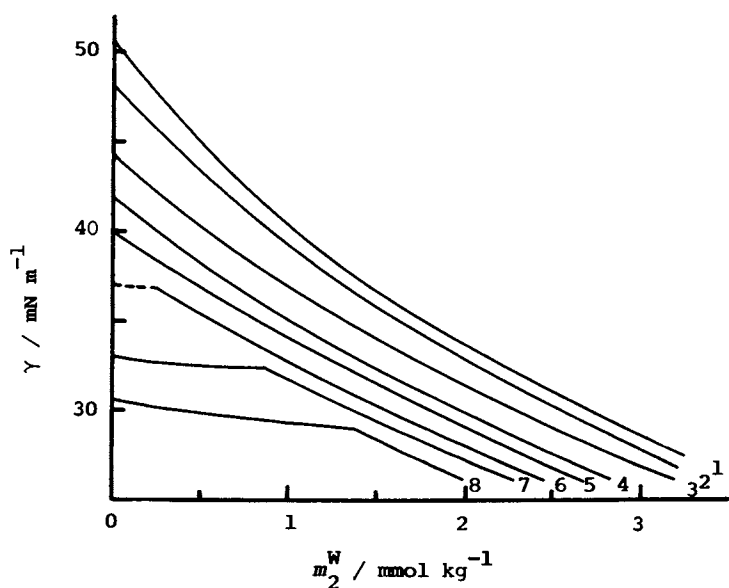
Figure 2. Interfacial tension vs concentration m_2^W curves at constant m_1^O and 298.15 K: (1) $m_1^O = 0$ mmol kg^{-1}; (2) 2.37; (3) 7.54; (4) 13.22; (5) 18.66; (6) 23.89; (7) 29.41; (8) 33.73.

$$d\gamma = - \Delta s dT + \Delta v dp - \Gamma_1^H (\partial\mu_1/\partial m_1^O)_{T,p} dm_1^O - 2\Gamma_2^H (\partial\mu_\pm/\partial m_2^W)_{T,p} dm_2^W \tag{1}$$

where the subscripts 1 and 2 are 1-octadecanol and dodecylammonium chloride, respectively. On deriving Equation 1, we have used the condition of electroneutrality for the interfacial layer.

The interfacial densities of 1-octadecanol Γ_1^H and of dodecylammonium chloride Γ_2^H are evaluated, respectively, by

$$\Gamma_1^H = - (\partial\gamma/\partial m_1^O)_{T,p,m_2^W} /RT\{ [(\partial f/\partial m_1^O)/f] + (1/m_1^O) \} \tag{2}$$

and

$$\Gamma_2^H = - m_2^W (\partial\gamma/\partial m_2^W)_{T,p,m_1^O} /2RT \tag{3}$$

Here, the correction for the activity coefficient f is used in calculating Γ_1^H (5), but not in calculating Γ_2^H because m_2^W is limited to a low concentration range. Application of Equation 3 and Equation 2 to the γ vs concentration curves in Figures 2 and 3 gives the values of Γ_2^H and Γ_1^H as a function of m_2^W and m_1^O, respectively. The results at 298.15 K are shown in Figures 4 and 5. The discontinuous change on the Γ_2^H vs m_2^W curves in Figure 4 and on the Γ_1^H vs m_1^O in Figure 5 express the phase transition from the condensed to the expanded film and from the expanded to the condensed film, respectively. It is found for the expanded film that both the Γ_2^H value at constant m_2^W decreases with increasing m_1^O and the Γ_1^H value at constant m_1^O decreases with increasing m_2^W.

The interfacial pressure Π vs the mean area per adsorbed molecule A curves are useful to make clear the film behavior. By making use of Figures 2 and 4, we can obtain the Π vs A curves at constant m_1^O as shown in Figure 6(a), where Π and A are defined, respectively, by

$$\Pi = \gamma^0 - \gamma \tag{4}$$

and

$$A = 1/N_A (\Gamma_1^H + \Gamma_2^H) \tag{5}$$

In the above equations, γ^0 is the interfacial tension of pure hexane/water interface and N_A is Avogadro's number. All the lowest Π values, except for $m_1^O = 0$, give the Π values of the pure adsorbed film of 1-octadecanol at given values of m_1^O. It should be noted that the curves exhibit the phase change of the adsorbed film from the condensed to the expanded state at the interfacial pressure of the transition when the area decreases.

In a similar manner, the Π vs A curves at constant m_2^W are obtained from Figures 3 and 5 and shown in Figure 6(b). Again, all the lowest Π values, except for $m_2^W = 0$, represent the Π values of the pure adsorbed film of dodecylammonium chloride at given m_2^W values. However, the curves exhibit the phase transition from the expanded to the condensed state.

The Π vs A curve of a mixed insoluble monolayer is generally obtained at a constant composition of film-forming components present
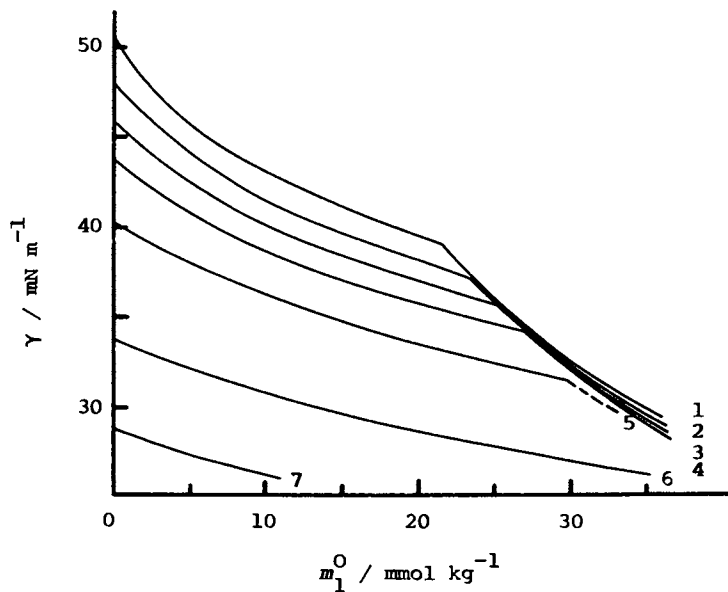
Figure 3. Interfacial tension vs concentration m_1^O curves at constant m_2^W and 298.15 K: (1) m_2^W = 0 mmol kg^{-1}; (2) 0.2; (3) 0.4; (4) 0.6; (5) 1.0; (6) 2.0; (7) 3.0.
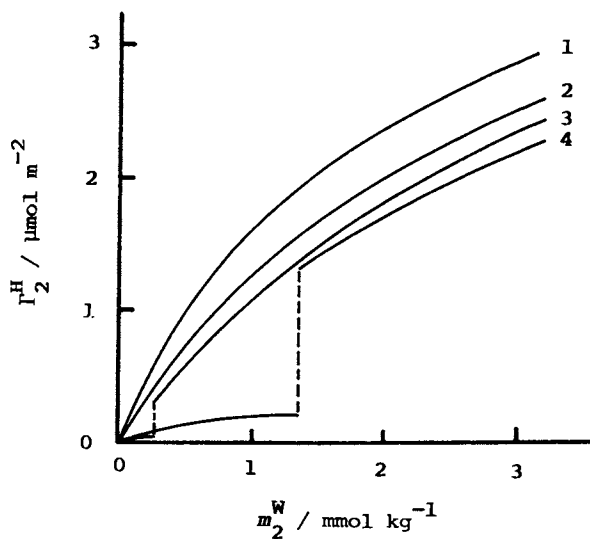
Figure 4. Interfacial density of dodecylammonium chloride vs m_2^W curves at constant m_1^O and 298.15 K: (1) m_1^O = 0 mmol kg^{-1}; (2) 7.54; (3) 23.89; (4) 33.73.
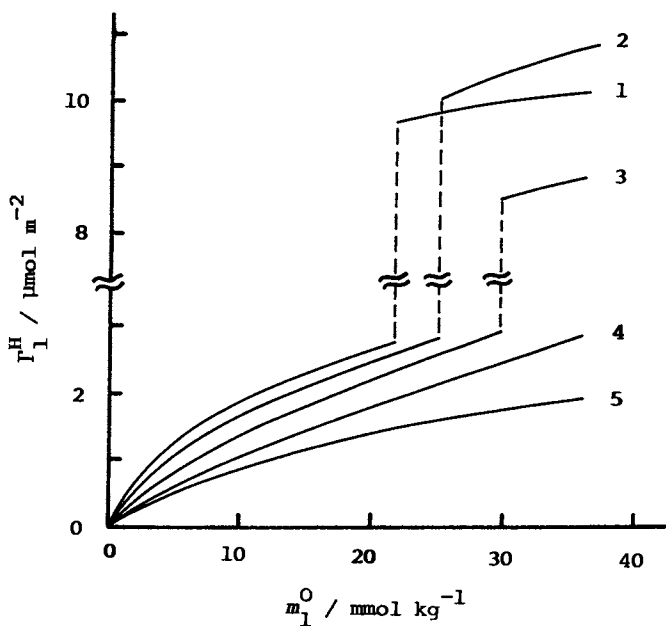
Figure 5. Interfacial density of 1-octadecanol vs m_1^O curves at constant m_2^W and 298.15 K: (1) $m_2^W = 0$ mmol kg^{-1}; (2) 0.4; (3) 1.0; (4) 2.0; (5) 3.0.
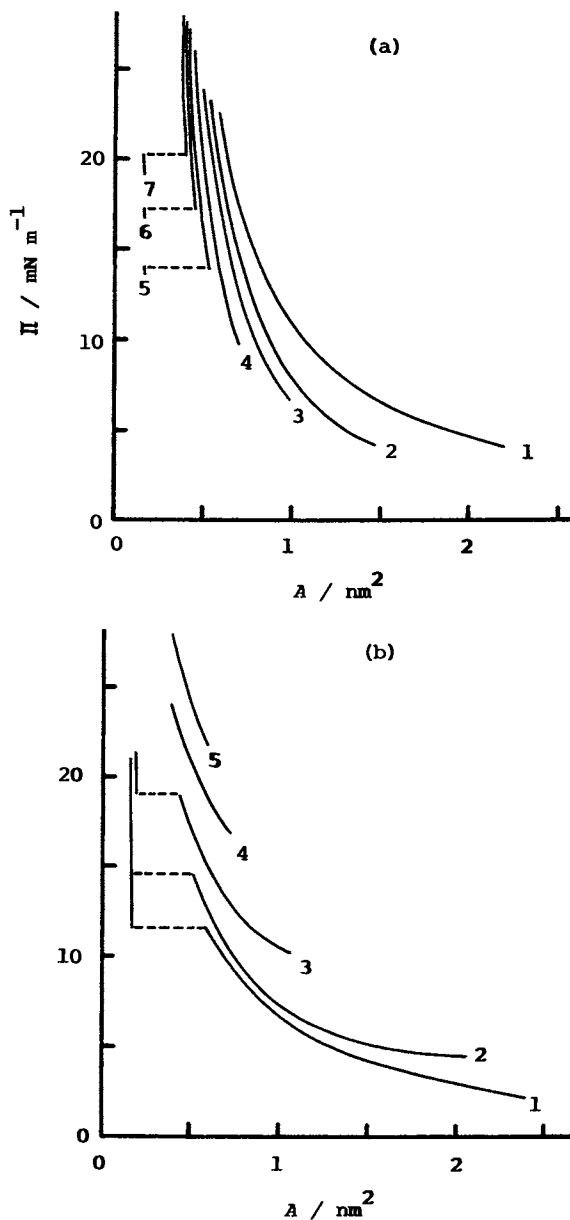
Figure 6. (a) Interfacial pressure vs mean area per molecule curves at constant m_1^O: (1) $m_1^O = 0$ mmol kg^{-1}; (2) 4; (3) 8; (4) 16; (5) 24; (6) 28; (7) 32. (b) Interfacial pressure vs mean area per molecule curves at constant m_2^W: (1) $m_2^W = 0$ mmol kg^{-1}; (2) 0.4; (3) 1.0; (4) 2.0; (5) 3.0.

in the monolayer. The curves of the mixed adsorbed films in Figures 6(a) and 6(b) do not satisfy this requirement. However, we can draw a similar Π vs A curve for the mixed adsorbed film by holding constant the value of the mole fraction of dodecylammonium chloride X_2^H defined by

$$X_2^H = \Gamma_2^H / (\Gamma_1^H + \Gamma_2^H) \tag{6}$$

The Π vs A curves obtained are shown in Figure 7. It is seen that the condensed state is realized in a very small mole fraction range. This might be attributed to the electrostatic repulsion between dodecylammonium ions. The curves in Figure 7 are more appropriate than those in Figures 6(a) and 6(b) for the purpose of thermodynamic considerations at the interface.

We are interested in the behavior of surfactant molecules in the mixed adsorbed film. The nonideal behavior of a mixed adsorbed film is correlated to activity coefficients of surface-active components with reference to the pure adsorbed film of each component. In the same manner as the previous paper (6), we can express the chemical potentials of 1-octadecanol and dodecylammonium chloride in the mixed adsorbed film as follows :

$$\mu_i = \mu_i^i(T,p,\gamma) + RT\ln f_i^\Pi x_i^H. \qquad i = 1, 2 \tag{7}$$

In this equation, μ_i^i is the chemical potential of pure component i in the pure adsorbed film and f_i^Π is the apparent activity coefficient of component i. In addition, an apparent partial molar area is written as

$$\overline{a}_i^\gamma = - (\partial\mu_i/\partial\gamma)_{T,p,X_2^H} \tag{8}$$

Substitution of Equation 7 into Equation 8 results in

$$\overline{a}_i^\gamma = a^i + RT(\partial\ln f_i^\Pi/\partial\Pi)_{T,p,X_2^H} \tag{9}$$

where a^i is the area per mole of pure component i. The mean molecular area A of the expanded film is plotted against the mole fraction X_2^H at constant Π in Figure 8. Taking into account the amplified error inherent in the conversion of the interfacial density into the area per adsorbed molecule at the lower interfacial pressure, all the curves in Figure 8 are said to be fairly linear. Consequently, we find $\partial\ln f_i^\Pi/\partial\Pi$ effectively zero. This result implies that the value of f_i^Π is almost unity and hence the mutual interaction between 1-octadecanol and dodecylammonium chloride molecules in the expanded state is similar in magnitude to the one between the same kind of constituent molecules.
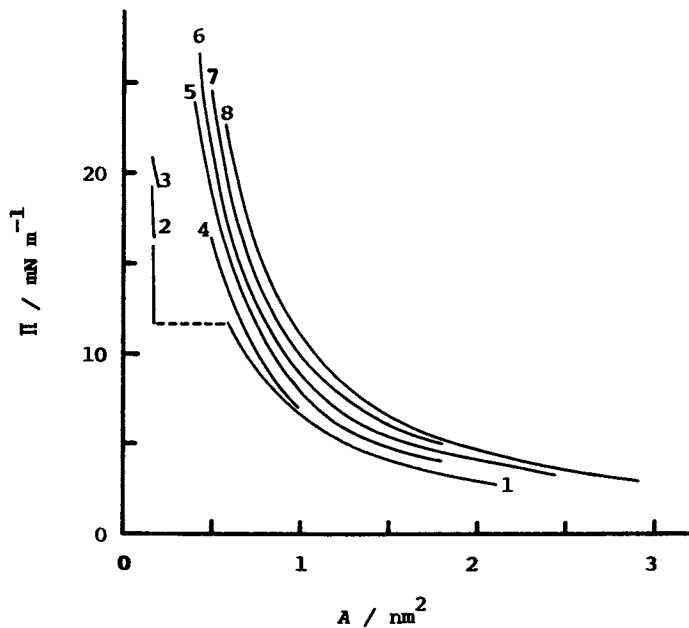
Figure 7. Interfacial pressure vs mean area per molecule curves at constant X_2^H: (1) X_2^H = 0; (2) 0.004; (3) 0.01; (4) 0.2; (5) 0.4; (6) 0.6; (7) 0.8; (8) 1.0.
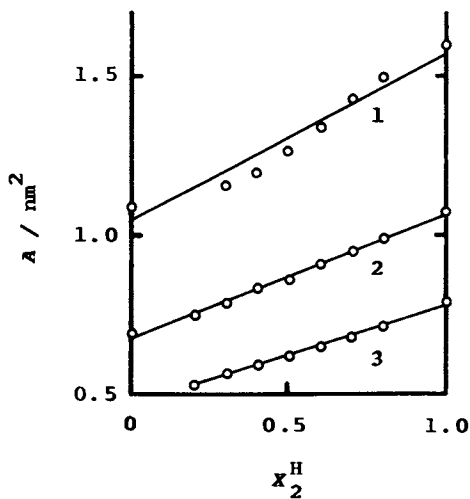
Figure 8. Mean area per molecule vs mole fraction of dodecylammonium chloride curves at constant Π: (1) Π = 6 mN m^{-1}; (2) 10; (3) 15.

Literature Cited

1. Hutchinson, E. J. Colloid Sci. 1948, 3, 521-9.
2. Matubayasi, N.; Motomura, K.; Aratono, M.; Matuura, R. Bull. Chem. Soc. Jpn. 1978, 51, 2800-3.
3. Motomura, K.; Matubayasi, N.; Aratono, M.; Matuura, R. J. Colloid Interface Sci. 1978, 64, 356-61.
4. Motomura, K. Advan. Colloid Interface Sci. 1980, 12, 1-42.
5. Unpublished data.
6. Motomura, K.; Yano, T.; Ikematsu, M.; Matuo, H.; Matuura, R. J. Colloid Interface Sci. 1979, 69, 209-16.

24

Behavior and Applications of Surfactant Mixtures

John F. Scamehorn

School of Chemical Engineering and Materials Science, University of Oklahoma, Norman, OK 73019

Future trends in research into the science and technology of surfactant mixtures is discussed. This is a field rich in opportunities for innovative scientific research and also practical applications. Research in this area will dramatically increase in quantity in the next several decades and great progress in the understanding and utilization of surfactant mixtures is expected.

Research into the chemistry and physics of surfactant mixture behavior has seen a rapid increase in activity over the last decade. New technological applications involving surfactants have evolved, many of which are dependent on the use of surfactant mixtures. There is no reason to doubt that new applications of surfactant mixtures will continue to be discovered and some recently proposed ones will reach large scale commercialization. As a result of the economic driving force and the growing awareness of the wealth of fascinating scientific phenomena occurring in mixed surfactant systems, research into surfactant mixture behavior will also continue to increase in intensity. The next decade or two promise to be times of exciting progress in this field.

Chapter 1 was an overview of this field. In this chapter, I wish to discuss the current focus of work on surfactant mixtures. I will also try to outline the areas in which I believe research is needed in surfactant mixture behavior. As a result, this will be a highly opinionated, speculative, and personal chapter. If some of the discussion stimulates creative thought in other researchers, whether they agree with me or not, a goal of this chapter will have been achieved.

One of the most encouraging aspects of this field is
the increasingly international nature of work in the
area.   The chapters in this book represent contributions
from Australia, Canada, England, Japan, Peoples Republic
of China, United States, Sweden, and West Germany.
     This chapter will be organized into sections dealing
with the various aggregates which surfactants can form.
Applications will be included as part of the discussion
of these other topics.

Micelle Formation

Micelles are often present in surfactant systems.   In
some processes, such as solubilization, they are directly
involved.   Micelles   indirectly   affect   many   other
processes because monomer concentrations or activities of
the surfactant components are dictated by the monomer-
micelle equilibrium at total surfactant concentrations
above the CMC. Therefore, interest in mixed micelle
formation will continue to grow.
     There are some large gaps in our knowledge of mixed
micelles which is seriously impeding progress toward
understanding and quantifying their behavior.   These gaps
are mainly experimental in nature;   i.e., although
improved models are needed, there is little value in
further theoretical development without certain critical
data to compare predictions against.

Surfactant Activity in Micellar Systems.   The activities
or concentrations of individual surfactant monomers in
equilibrium with mixed micelles are the most important
quantities predicted by micellar thermodynamic models.
These variables often dictate practical performance of
surfactant solutions.   The monomer concentrations in
mixed micellar systems have been measured by
ultrafiltration (1), dialysis (2), a combination of
conductivity and specific ion electrode measurements (3),
a method using surface tension of mixtures at and above
the CMC (4), gel filtration (5), conductivity (6),
specific ion electrode measurements (7), NMR (8),
chromatographic separation of surfactants with a
hydrophilic substrate (9) and by application of the
Gibbs-Duhem equation to CMC data (10).   Surfactant
specific electrodes have been used to measure anionic
surfactant activities in single surfactant systems
(11,12) and might be useful in mixed systems .
     None of these methods have been widely adopted
because of their relative complexity or because they are
not generally applicable to any arbitrary surfactant
system.   As examples, the surface tension method (4)
relies on the pure surfactants having substantially
different plateau surface tensions; the ultrafiltration
method (1) requires the micelles of the pure surfactants
involved to have approximately the same size and the

monomeric surfactant components to have similar diffusion
characteristics; the conductivity method (6) works only
with   anionic/anionic   or   cationic/cationic surfactant
systems; and the method using CMC data (10) is only
effective when the pure surfactants have similar CMC
values.

     The need for a simple, universal method of measuring
individual monomer activities in mixed micelle systems is
the   most   pressing problem in this field of research and
deserves substantial attention.

     A   partial   answer   would be   the development   of
commercially available surfactant specific electrodes.
These could provide at least ionic surfactant component
activity.

     Perhaps   the   answer   lies   in   the   introduction of
another process   in   the   system   which relies only on
monomer activities   in   a   known   fashion.   The   surface
tension method already mentioned (4) relies on   the   fact
that   surface   tension   is   determined   solely by monomer
concentrations.   However,   the plateau surface tension is
not   terribly   sensitive   to   monomer composition in many
cases of interest. An aggregate formation process which
can   be   much more sensitive is adsorption of surfactants
on hydrophilic (13-15) or hydrophobic (see Chapter 17)
surfaces.

     As   already   discussed   in   Chapter   1,   the relative
tendency of a surfactant component to adsorb on a   given
surface   or   to   form   micelles   can   vary   greatly with
surfactant structure.   The adsorption of each component
could be measured below the CMC at various concentrations
of   each   surfactant   in   a   mixture.   A   matrix could be
constructed to tabulate the   (hopefully unique)   monomer
concentration   of   each   component   in   the   mixture
corresponding to any combination of adsorption levels for
the   various   components   present.   For   example,   for   a
binary system of surfactants A and B,   when adsorption of
A is 0.5 mmole/g and that of   B   is   0.3   mmole/g,   there
should   be   only   one   unique   combination   of   monomer
concentrations of surfactant A and of surfactant B   which
would result in this adsorption (e.g.,   1 mM of A and 1.5
mM   of   B).   Well   above   the   CMC,   where   most   of   the
surfactant   in solution is present as micelles,   micellar
composition   is   approximately   equal   to   solution
composition   and   is,   therefore,   known.   If   individual
surfactant component adsorption is also measured here, it
would   allow   computation   of   each   surfactant   monomer
concentration   (from   the   aforementioned   matrix)   in
equilibrium with   the   mixed   micelles.   Other   processes
dependent   on   monomer   concentration   or   surfactant
component activities only could also be used in a similar
fashion to determine monomer-micelle equilibrium.

Enthalpies   and Entropies of Mixing in Micelles.   Next to
monomer   activities,   the   most   needed   data   on   mixed
micelles   are   the   enthalpy (heat) and entropy of mixing

upon micelle formation. These measurements will give
great insight into the physical interactions in mixed
micelle formation. They also permit extrapolation of
monomer-micelle equilibrium data to different
temperatures. The test of the ability to describe these
fundamental thermodynamic quantities can permit the
discard of unsound mixed micelle models.

In theory, the temperature dependence of CMC data
can be used to calculate heats and entropies of mixing
(see Chapter 2). However, this temperature dependence is
often so small as to be difficult to measure accurately.
Calorimetry will see much use in this field in the near
future as the method of choice to obtain this much needed
data, as already pioneered by several studies (16,17).

Micelle Size and Shape. The size and shape of mixed
micelles can provide a great deal of information about
the structure and surfactant interactions involved (see
Chapter 1). However, this is generally not a simple
measurement. Interpretation of light scattering data is
controversial and the equipment is expensive and
specialized. Osmometry is difficult to use for the high
molecular weight surfactants of general interest.
Perhaps new methods such as NMR or exclusion
chromatography will be useful in these measurements.
With the advent of new techniques and improvements in
traditional methods, information on mixed micelle
geometry will become more available in the future.

Micelle Transition to Other Aggregates. It is well known
that as such variables as chain length in an homologous
surfactant series or temperature is varied, transitions
from micelles to extended structures such as liquid
crystals and vesicles can occur. This can also occur as
the surfactant composition of a mixed surfactant systems
is varied. For example, Puig et. al. (18) studied a
mixture of a surfactant which forms micelles as a single
component and one which forms liquid crystals as a single
component. This system could form mixed micelles or
mixed liquid crystals when both surfactants are present.
In Chapter 6, Desnoyers discusses a system containing a
mixture of a micelle forming surfactant and a pseudo-
micelle forming species. In Chapter 20 of this book,
Shirahama et. al. study mixtures of a micelle forming
surfactant and a vesicle forming surfactant. It would
aid in the understanding of such phenomena to have a more
thorough knowledge of the thermodynamics of mixing and
the micelle shape and size as transition points are
approached.

Counterion Binding. Counterion binding on mixed micelles
is of crucial importance toward understanding the
structure and electrostatic forces involved in micelle
formation involving ionic surfactants. Specific ion
electrodes are effective at measuring counterion bindings

on mixed micelles (19). Systematic measurements of the
effect of surfactant structure on ionic/nonionic
surfactant counterion binding will be tabulated with
time. Counterion binding on anionic/cationic mixed
micelles will help define the oppositely charged head
group interactions on this micelle surface.

Model Development. There is vast opportunity for
development of fundamentally based models to describe the
thermodynamics of mixed micelle formation. As discussed
in Chapter 1, regular solution theory has yielded useful
relations to describe monomer-micelle equilibrium.
However, the thermodynamic assumptions behind regular
solution theory are incorrect for these systems.
Therefore, the temperature dependence of mixed micelle
properties predicted from it are incorrect and there may
be surfactant mixtures for which it does not even work
empirically. This is a totally unsatisfactory state of
affairs.
     The lack of certain critical data for these systems,
as already discussed, has hampered development of
improved theories. Models of mixed micelle formation
need to be based on the fundamental forces causing
nonidealities of mixing. Some of these have been
discussed in Chapter 1. Chapter 2 by Osborne-Lee and
Schechter is an example of the type of theoretical
analysis which is needed to advance this field. In that
paper, a theoretical model is developed based on
fundamental enthalpic and entropic considerations and
compared to experimental monomomer-micelle equilibrium
and heat of mixing data. Other forces which might be
explicitly included in future models are electrostatic
forces (as done by Rathman and Scamehorn (20)), and
specific chemical interactions between the dissimilar
surfactants, examples of such interactions being given in
Chapter 1. Any useful model must contain a very limited
number of adjustable constants.
     To this point, only models based on the pseudo-phase
separation model have been discussed. Mixed micelle
models utilizing the mass action model may be necessary
for micelles with small aggregation numbers, as
demonstrated by Kamrath and Franses (21). However, even
for large micelles, the fundamental basis for the pseudo-
phase separation model needs to be examined. In
micelles, how much solvent or how many counterions (bound
or in the electrical double layer) should be included in
the micellar pseudo-phase is unclear. The difficulty is
normally surmounted by assuming that the pseudo-phase
consists of only the surfactant components; i.e., solvent
or counterions are ignored. The validity of treating the
micelle on a surfactant-only basis has not been verified.
Funasaki and Hada (22) have questioned the thermodynamic
consistency of such an approach.
     Yoesting and Scamehorn (23) measured activity
coefficients of all components in a mixed coacervate

phase   above   the   cloud   point   containing   anionic
surfactant,   nonionic   surfactant,   water,   and   NaCl.
Application of a thermodynamic consistency test using the
Gibbs-Duhem   equation   showed   that   the   data   were
consistent.   However, when the phase was   treated   as   a
pseudo-phase on a surfactant-only basis,   the data failed
the   thermodynamic   consistency   test.   Similarly,   Haque
(24) analyzed a microemulsion phase consisting of anionic
surfactant, nonionic surfactant, water, octane, and NaCl.
Once again, the actual thermodynamic data was consistent,
but when the microemulsion was treated as a pseudo-phase,
it failed the consistency test.

     Analysis of mixed micellar thermodynamic data in this
way   will   be   a   useful   analysis.   Some   methods   for
obtaining mixed micellar   thermodynamic   data   implicitly
utilize   the   Gibbs-Duhem   equation,   but data from those
that don't (e.g., ultrafiltration- see Chapter 2) should
shed light on this issue.

     An ultimate goal of theory in this field is not   only
to model a given mixed surfactant system,   but to be able
to predict the properties   of   any   arbitrary   system.   A
group contribution method based on measurements from many
systems may be the ultimate means to this goal,   whatever
specific mathematical model is found   most   useful.   Such
systematic   studies   of   surfactant structure as those of
Rosen (see Chapter 11) will provide a data base for   such
correlations.   A   number of important systems have yet to
receive   sufficient   attention.   Examples   of   such
surfactant   pairs   are   ethoxylated   anionic/nonionic,
ethoxylated   anionic/nonethoxylated   anionic,   and
nonethoxylated nonionic/ionic.

<u>Inverted   Micelles</u>.   The   study   of inverted micelles has
received little attention.   The study of these aggregates
can benefit by application of techniques used for   normal
micelles   such   as fluorescence probes as demonstrated by
Jao and Kreuz in Chapter   7.   With   applications   in   oil
recovery and dry cleaning,   this topic will see increased
research activity.

<u>Systems Showing   Positive   Deviation   from   Ideality</u>.   The
study   of   surfactant   systems showing positive deviation
from   ideality   of   mixing   and   those   showing   negative
deviation   from   ideality converge as systems are studied
which   are   fluorocarbon/hydrocarbon (tending   to   show
positive   deviation)   with   hydrophilic groups tending to
show   negative   deviation   from   ideality   (e.g.,
anionic/nonionic).   The   result   of   the   offsetting
tendencies can   provide   insight   into   the   interactions
between   surfactants.   An   excellent example of this type
of study is given in Chapter 14   by   Zhao   and   Zhu.   Any
complete   model   of mixed micellization must ultimately be
able to handle either positive or negative deviation from
ideality.   The   use   of   spectroscopic   probes   in   these
systems, as demonstrated in Chapter 4 by Meguro et.   al.,

will see more application, particularly when positive
deviation is great enough so that two types of micelles
may exist (see Chapter 1).

Monolayer Formation

Micelles and monolayers are analogous in many ways, as
discussed in Chapter 1. Therefore, much of the future
direction of research in the topic will be similar to
that already discussed for mixed micelles. However,
there are some important differences also.

In my opinion, the study of monolayer formation has
less practical importance than the study of micelles.
Yet, the thermodynamics of monolayer formation has seen
substantial study. I think that this is largely due to
the fact that the monomer-monolayer equilibrium can be
unambiguously and relatively easily measured using the
Hutchinson method (25), as exploited by Rosen and Hua
(26), while this cannot be said for monomer-micelle
equilibrium. Therefore, mixed monolayer formation will
be a more fruitful field for model development in the
near future than mixed micelles because of the
availability of a method of obtaining experimental data
for comparison.

At very low surface coverage at the air-water
interface, a phase transition is thought to occur where
the sparsely covered surface forms aggregated structures
on the surface (27). It would be of great scientific
interest to study this transition for mixed surfactant
systems. The surface tension would need to be measured
very accurately and very pure surfactants would need to
be used for this study.

For systems exhibiting positive deviations from
ideality of mixing, aggregate patches of different
composition may form on the surface. If methods (e.g.,
spectroscopic) could be developed to detect the average
size of these distincly different patches, this would
give insight into the monolayer formation process.

Solubilization

In aqueous surfactant solutions, either by
circumstance or design, non-surface active organic
species may be present. Examples are oil recovery, where
crude oil is present, or micellar-enhanced
ultrafiltration, where micelles are being used to effect
a separation of dissolved organic pollutants from water.
The ability of mixed micelles to solubilize organic
solutes has received relatively little study. In
addition, the solubilization of these compounds by
micelles may change the monomer-micelle equilibrium
compositions.

Experimental methods to measure the organic solute
activity in surfactant solutions over a wide range of
activities (not just at saturation) include vapor

pressure (28), semi-equilibrium dialysis (29), micellar-enhanced ultrafiltration (30,31), molecular sieve technique (31), potentiometric titration (32), Raman spectroscopy (33), fluorescence spectroscopy (34), UV spectroscopy (35), and NMR (36). A method to determine surfactant activity in micellar solutions containing a single surfactant component and a solubilizate has also been developed (37).

As our understanding and ability to model monomer-micelle equilibrium in the absence of added solutes evolves, research into the more complex systems will progress. A combination of methods of measuring activities of solubilizable solutes as well as surfactant species in these systems will not only provide information on solubilization capacity of mixed micelles for solute, but also show how solute affects surfactant interaction and mixing in the micelle. Additional information on micelle size and shape in the presence of solute would provide an even more complete picture of the mixed micelle and solubilization therein.

Solutes which solubilize in the micellar core might be a probe which could give information on micellar core size, or at least the sum of the inverse of the radii of curvature of the core, through the effect of Laplace pressure (38) on solubilization. Solutes which solubilize outside of the hydrocarbon core in the mixed micelle could interact with the different hydrophilic groups. Both solubilization and surfactant mixing thermodynamics could be affected by the simultaneous presence of the dissimilar surfactant hydrophilic groups and the solute in the same region. Systematic studies of solubilization of a range of polar solutes in micelles containing surfactant mixtures, which exhibit negative deviation from ideality of mixing in the absence of solute, over a range of solute activities from the Henry's Law region to saturation are needed. An even more challenging prospect for the future is solubilization of mixed solutes into mixed micelles. Nagarajan et. al. (39) has studied solubilization of mixed solutes into single component micelles.

Adsorption on Solids

The formation of mixed aggregates on solid surfaces (admicelles) has only in the last decade been addressed in systematic fashion. The surface has only been scratched in this important topic.

Most work which has been done has used metal oxides as the adsorbent. There is a need for more work on more hydrophobic surfaces (such as that in Chapter 17). Most systematic studies on metal oxides have used fairly homogeneous surfaces. For practical application to situations where adsorption on more heterogeneous surfaces is of interest (e.g., detergency, flotation, enhanced oil recovery), more study must be done on these

surfaces. Examples of such surfaces are clays such as
kaolinite or montmorillonite. When mixed admicelles form
on heterogeneous surfaces, the composition of the surface
patches   may   vary.   It   is   crucial   to   verify   this
experimentally in order   to   understand   and   model   this
phenomena.   For   example,   anionic   surfactant   adsorbs
strongly on alumina (at low or medium pH) (13), but   not
significantly   on   silica (14),   while nonionic surfactant
adsorbs on silica (14),   but not significantly on alumina
(13).   Kaolinite   is   composed   of   alternating layers of
Gibbsite (alumina) and silica.   Both anionic and nonionic
surfactants,   and their mixtures adsorb strongly on   this
mineral   (13).   Are   the   mixed   admicelles formed fairly
uniform   in   composition,   or   do   those   formed   on   the
Gibbsite layer consist mainly of anionic surfactant while
those   on   the   silica   layer   consist of mainly nonionic
surfactant?   This question should be one of the key   ones
for researchers in this field in the near future.
      The same thermodynamic quantities   needed   for   mixed
micelle formation (already discussed) are also needed for
mixed   admicelle   formation.   Luckily,   the   monomer-
admicelle equilibrium   data   can   be   fairly   easily   and
unambiguously   obtained   (e.g.,   see   Chapter   15).   This
should be combined with   calorimetric   data   for   a   more
complete   thermodynamic   picture   of the mixed admicelle.
As with micelles, counterion bindings on mixed admicelles
also   need   to   be   obtained   in   order   to   account   for
electrostatic   forces   properly.   Only   one   study   has
measured   counterion   binding   on   single-component
admicelles (40), with none reported for mixed admicelles.
      A comparison of the degree   of   nonideality   between
mixed   admicelles   and   mixed   micelles   of   the   same
composition   will   be   fascinating   and   should   lead   to
greater   understanding   of both mixed aggregate formation
processes.   The   importance   of   the   influence   of   the
surface   on   interactions   between   dissimilar surfactant
components in the admicelle is not   well   understood.   If
the   surface   only   needs   to   be there to "nucleate" the
process by forcing a   high   enough   density   of   adsorbed
surfactant   to   initiate   admicelle   formation,   and   has
little influence on intersurfactant   interaction   in   the
mixed   admicelle,   then mixed micelle surfactant activity
coefficients,   heat of mixing etc.   should be similar   to
those   of   mixed   admicelles.   There   is limited evidence
that that is not the case (see Chapter 15).   If there   is
a difference, then a great deal of study needs to be done
to determine surface affects on aggregate thermodynamics.
The   adsorption   of   the   surfactants   above   the   CMC is
determined   by   the   competition   between   micelle   and
admicelle   formation   (see   Chapter   1).   This   is   an
important   quanitity   in   enhanced   oil   recovery,   for
example,   so   the   understanding of the relative tendency
for micelle and   admicelle   formation   is   of   more   than
academic interest.
      There   has   been   limited spectroscopic investigation

into the aggregation number of admicelles for single-
surfactant systems (41). This would be of great value in
the study of mixed admicelles.
    It would be of scientific interest to study the
adsorption of mixed surfactant systems showing positive
deviations from ideality, as has been discussed for mixed
micelles and monolayers.
    In the real world, soluble organic materials may be
present in the aqueous surfactant system. As with
micelles, it is important to know how these affect mixed
admicelle formation and how well these organics are
solubilized in the admicelle (adsolubilized).
    In the oil field applications, the reservoir can act
as a giant chromatographic column, causing separation of
components in the injected slug during an operation
(chromatographic separation). Given an adsorption
isotherm for a mixed system, this effect can be modeled
if the system is at equilibrium (42). However, little
work has been done to experimentally study rate
(diffusion, non-equilibrium adsorption) effects for
inclusion into a model. Since these may be important in
actuality, this combination of adsorption thermodynamics,
transport in porous media equations, and rate studies for
surfactants should not only be interesting and
challenging to develop, but will be of economic
importance as well.

Surfactant Precipitation

Studies of surfactant precipitation have concentrated on
predicting the precipitation phase boundaries (i.e., the
amount of added electrolyte necessary to cause
precipitation). On the phase boundary, only an
infintesimal amount of precipitate is formed, and the
precipitate generally contains only one type of crystal.
This phase boundary has been modeled for ionic/nonionic
surfactants where monovalent salt is the added
electrolyte (43), but no such model is available to
predict hardness tolerance, which is of even more
practical importance. Systematic experimental hardness
tolerance data on mixed ionic/nonionic surfactant systems
needs to be obtained and a model developed to describe
it.
    Systems in which surfactant precipitate is present in
substantial quantities in equilibrium with micelles and
monomer are of interest. For example, in a technique for
improving mobility control in oil reservoirs, surfactant
is purposely precipitated in the permeable region of a
reservoir to plug it (44). When substantial precipitate
is present, crystals of different composition can be in
simultaneous equilibrium. Experimental study and
modeling of these systems where several K_{sp} relationships
are simultaneously satisfied will be a challenging task.
    The kinetics of crystallization is an important
phenomena. Whether the surfactant system has exceeded

the precipitation phase boundary in a washing machine
with a residence time of 30 minutes may be irrelevant if
20 hrs are required for substantial precipitation to
occur. Systematic studies of the rate effects are needed
for both single and multicomponent surfactant systems.
    The size of surfactant precipitate structures may
vary widely, from colloidal precipitate, too small to be
seen visually, to large crystals. This is an important
property, because some deleterious effects of surfactant
precipitation could be minimized or beneficial effects of
precipitation could be negated if the precipitate were of
colloidal dimensions. Examples of the importance of
precipitate structure and size include the aforementioned
oil field process and recovery of surfactant from
surfactant-based separations via precipitation-filtering.
Effects of using surfactant mixtures on precipitate
structures would be useful to know.

Cloud Point Phenomena

The cloud point phenomena as a lower consolute solution
temperature is becoming better understood in terms of
critical solution theory and the fundamental forces
involved for pure nonionic surfactant systems. However,
the phenomena may still occur if some ionic surfactant is
added to the nonionic surfactant system. A challenge to
theoreticians will be to model these mixed ionic/nonionic
systems. This will require inclusion of electrostatic
considerations in the modeling.
    As the temperature of a mixed surfactant system is
increased above its cloud point, the coacervate
(concentrated) phase may go from a concentrated micellar
solution (e.g., 1 weight % surfactant) to ca. 30 weight %
surfactant. For mixed ionic/nonionic systems, it would
be of interest to measure thermodynamic properties of
mixing in this coacervate as this temperature increased
to see if the changes from micelle to concentrated
coacervate were continuous or if discontinuities occurred
at certain temperatures/compositions. The similarities
and differences between the micelle and coacervate could
be made clearer by such an experiment.

Miscellaneous

The discussion so far has focused predominately on
individual aggregation processes. However, as discussed
at length in Chapter 1, these processes often do not
occur in isolation, but several are often present
simultaneously. Also, advantage can be taken of
simultaneous multiaggregate formation for practical
applications by the surfactant technologist. Therefore,
the study of systems with several aggregates present
simultaneously, on other than an empirical basis, will
become more frequent over the next few decades. As an
adjunct to this, the comparative study of the formation

of   different   surfactant   aggregates   for   the   same
surfactant system will be seen more   frequently   also   in
mixed   surfactant   investigations.   This   is   now   being
commonly done for micelles and   monolayers,   as   seen   in
Chapters 11-14.
     There   are   a number of processes which have not been
discussed   (because   of   space)   in   which   mixture   of
surfactants   are   important.   Among   these   are   foaming,
emulsion   formation,   liquid   crystal   formation,
microemulsion   formation,   adsorption   as   liquid-liquid
interfaces, and phase partitioning of surfactants between
immiscible liquid   phases.   These   areas   will   also   see
increased interest in the use of surfactant mixtures.

Summary

This chapter has attempted to point   out   some   areas   in
which   this   author   feels   research   is needed and where
research will   tend   to   concentrate   in   the   surfactant
mixtures   field.   I hope that this chapter has stimulated
some speculative thought on research   needed   to   advance
knowledge in this important area.

Acknowledgments

Literature Cited

1.   Osborne-Lee,   I.W.;   Schechter,   R.S.   J.   Colloid
Interface Sci. 1985, 108, 60.
2.   Rubingh, D.N. In "Solution Chemistry of Surfactants";
Mittal, K.L., Ed.; Plenum Press: New York, 1979; Vol.   I,
p. 337.
3. Nishikido, N. J. Colloid Interface Sci. 1977, 60, 242.
4. Funasaki, N.; Hada, S. J. Phys. Chem. 1979, 83, 2471.
5. Tokiwa, F.; Ohki, K.; Kokubo, I. Bull. Chem. Soc. Jpn.
1968, 41, 2845.
6.   Mysels, K.J.; Otter, R.J.   J.   Colloid Sci. 1961, 16,
462.
7.   Shedlovsky, L.; Jakob, C.W.; Epstein, M.B.   J.   Phys.
Chem. 1963, 67, 2075.
8. Inoue, H.; Nakagawa, T. J. Phys. Chem. 1966, 70, 1108.
9.   Schechter, R.S., presented at 59th Annual ACS Colloid
and Surface Science Symposium, Potsdam,   New York,   June,
1985.
10.   Nguyen,   C.M.;   Rathman,   J.F.;   Scamehorn, J.F.   J.

Colloid Interface Sci., In Press.
11. Cutler, S.G.; Meares, P.; Hall, D.G. J. Chem. Soc. Faraday Trans. 1 1978, 74, 1758.
12. Koshinuma, M.; Sasaki, T. Bull. Chem. Soc. Jpn. 1975, 48, 2755.
13. Scamehorn, J.F.; Schechter, R.S.; Wade, W.H. J. Colloid Interface Sci. 1982, 85, 479.
14. Scamehorn, J.F.; Schechter, R.S.; Wade, W.H. J. Colloid Interface Sci. 1982, 85, 494.
15. Gao, Y.; Yue, C.; Lu, S.; Gu, W.; Gu, T. J. Colloid Interface Sci 1984, 100, 581.
16. Holland, P.M. In "Structure/Performance Relations in Surfactants"; Rosen, M.J., Ed.; ACS Symposium Series: Washington, D.C., 1984; p. 141.
17. Hey, M.J.; MacTaggart, J.W.; Rochester, C.H. J. Chem. Soc. Faraday Trans. 1 1985, 81, 207.
18. Puig, J.E.; Franses, E.I.; Miller, W.G. J. Colloid Interface Sci. 1982, 89, 441.
19. Rathman, J.F.; Scamehorn, J.F. J. Phys. Chem. 1984, 88, 5807.
20. Rathman, J.F.; Scamehorn, J.F. Langmuir, submitted.
21. Kamrath, R.F.; Franses, E.I. J. Phys. Chem. 1984, 88, 1642.
22. Funasaki, N.; Hada, S. J. Phys. Chem. 1980, 84, 736.
23. Yoesting, O.E.; Scamehorn, J.F. Colloid Polym. Sci., In Press.
24. Haque, O., M.S. Thesis, University of Oklahoma, 1985.
25. Hutchinson, E. J. Colloid Sci. 1948, 3, 413.
26. Rosen, M.J.; Hua, X.Y. J. Colloid Interface Sci. 1982, 86, 164.
27. Aratono, M.; Uryu, S.; Hayami, Y.; Motomura, K.; Matuura, R. J. Colloid Interface Sci. 1984, 98, 33.
28. Tucker, E.E.; Christian, S.D. J. Colloid Interface Sci. 1985, 104, 562.
29. Christian, S.D.; Smith G.A.; Tucker, E.E.; Scamehorn, J.F. Langmuir 1985, 1, 564.
30. Dunn, R.O.; Scamehorn, J.F.; Christian, S.D. Sep. Sci. Technol. 1985, 20, 257.
31. Aboutaleb, A.E.; Sakr, A.M.; El-Sabbagh, H.M.; Abdelrahman, S.I. Pharm. Ind. 1980, 42, 940.
32. Donbrow, M.; Rhodes, C.T. J. Pharm. Pharmacol. 1975, 17, 258.
33. Shih, L.B.; Williams, R.W. J. Phys. Chem., In Press.
34. Abuin, E.B.; Lissi, E.A. J. Colloid Interface Sci. 1983, 95, 198.
35. Mukerjee, P.; Cardinal, J.R. J. Phys. Chem. 1978, 82, 1620.
36. Stilbs, P. J. Colloid Interface Sci. 1982, 87, 385.
37. Christian, S.D.; Tucker, E.E.; Smith, G.A.; Bushong, D.S. J. Colloid Interface Sci., In Press.
38. Mukerjee, P. In "Solution Chemistry of Surfactants", Mittal, K.L., Ed.; Plenum: New York, 1979; Vol. 1, p. 153.
39. Nagarajan, R.; Chaiko, N.A.; Ruckenstein, R. J. Phys. Chem. 1984, 88, 2916.

40.   Bitting, D.; Harwell, J.H. <u>Langmuir,</u> submitted for
publication.
41. Levitz, P.; Van Damme, H.; Keravis, D. <u>J. Phys. Chem.</u>
1984, 88, 2228.
42.   Harwell, J.H.; Schechter, R.S.; Wade, W.H.   <u>AICHE J.</u>
1985, 31, 415.
43.   Stellner, K.L.; Scamehorn, J.F. <u>J. Am. Oil Chem.</u>
<u>Soc.,</u> submitted for publication.
44.   Arshad,   S.A.;   Harwell, J.H.   SPE Paper No.   14291,
Presented at the 60th Annual Technical Conference of the
Society of Petroleum Engineers, Las Vegas, September,
1985.

Author Index

Abe, Masahiko, 68
Alexander, D. M., 133
Aratono, Makoto, 163
Asano, H., 256
Barnes, G. T., 133
Chang, David L., 116
Cui, Jun-Gang, 172
Desnoyers, Jacques E., 79
Dobias, Bohuslav, 216
Esumi, Kunio, 61
Franses, Elias I., 44
Harwell, Jeffrey H., 200
Hayami, Yoshiteru, 312
Heyun, Zhou, 297
Holland, Paul M., 102
Jao, Tze-Chi, 90
Jiding, Xia, 297
Kameyama, Keiichi, 270
Kamrath, Robert F., 44
Kreuz, Kenneth, 90
Kronberg, B., 225
Kwak, Jan C. T., 79
Lindstrom, M., 225
Matsukiyo, Hidetsugu, 163
McGregor, M. A., 133
Meakin, Brian J., 242
Meguro, Kenjiro, 61
Morton, Frank S., 242

Motomura, Kinsi, 163,312
Muto, Yasushi, 61
Ogino, Keizo, 68
Okai, T., 256
Osborne-Lee, Irvin W., 30
Perron, Gerald, 79
Pouton, Colin W., 242
Pryde, E. H., 283
Roberts, Bruce L., 200
Rosano, Henri L., 116
Rosen, Milton J., 144
Sakurai, Fujio, 61
Scamehorn, John F., 1,200,324
Schechter, Robert S., 30
Schwab, A. W., 283
Shirahama, Keishiro, 270
Stenius, P., 225
Takagi, Toshio, 270
Takashima, Koji, 270
Takisawa, Noboru, 270
Ueno, M., 256
Wakerly, Mark G., 242
Walker, K., 133
Yamashita, Fumitaka, 79
Yan, Sun, 297
Zhao, Guo-Xi, 172,184
Zhu, Bu-Yao, 172,184

Subject Index

A

Absorption wavelength, maximum,
    determination for mixed
    surfactants with azo oil dyes, 70
Activity coefficients
  based on the regular solution theory
      model, 31
  direct relationship with composition
      between micellar and
      pseudophase, 106
  direct relationship with mole
      fractions, 106
  micellar phase, mixed micelle
      formation, 34
  nonethoxylated alcohols, 302
  representing the mixture critical
      micelle concentration, 31
Admicelles
  adsorption, positive deviations from
      ideality discussed, 206-214

Admicelles--Continued
  definition, 201
  formation on heterogeneous
      surfaces, 332
  formation on solid surfaces, 331-333
  importance of surface influence on
      components, 332
  mixed
    adsorption on alumina, 206
    materials used in formation
        thermodynamics study, 203
    nonideality compared to mixed
        micelles, 332
    predicted adsorption isotherms
        from ideal solution
        theory, 206
    theory, 203-205
  surfactants tendency to form, 17-18
  theory and development history, 203
Adsorption
  anionic surfactants on metal oxide
      surfaces, 201

338

Author Index

Abe, Masahiko, 68
Alexander, D. M., 133
Aratono, Makoto, 163
Asano, H., 256
Barnes, G. T., 133
Chang, David L., 116
Cui, Jun-Gang, 172
Desnoyers, Jacques E., 79
Dobias, Bohuslav, 216
Esumi, Kunio, 61
Franses, Elias I., 44
Harwell, Jeffrey H., 200
Hayami, Yoshiteru, 312
Heyun, Zhou, 297
Holland, Paul M., 102
Jao, Tze-Chi, 90
Jiding, Xia, 297
Kameyama, Keiichi, 270
Kamrath, Robert F., 44
Kreuz, Kenneth, 90
Kronberg, B., 225
Kwak, Jan C. T., 79
Lindstrom, M., 225
Matsukiyo, Hidetsugu, 163
McGregor, M. A., 133
Meakin, Brian J., 242
Meguro, Kenjiro, 61
Morton, Frank S., 242

Motomura, Kinsi, 163,312
Muto, Yasushi, 61
Ogino, Keizo, 68
Okai, T., 256
Osborne-Lee, Irvin W., 30
Perron, Gerald, 79
Pouton, Colin W., 242
Pryde, E. H., 283
Roberts, Bruce L., 200
Rosano, Henri L., 116
Rosen, Milton J., 144
Sakurai, Fujio, 61
Scamehorn, John F., 1,200,324
Schechter, Robert S., 30
Schwab, A. W., 283
Shirahama, Keishiro, 270
Stenius, P., 225
Takagi, Toshio, 270
Takashima, Koji, 270
Takisawa, Noboru, 270
Ueno, M., 256
Wakerly, Mark G., 242
Walker, K., 133
Yamashita, Fumitaka, 79
Yan, Sun, 297
Zhao, Guo-Xi, 172,184
Zhu, Bu-Yao, 172,184

Subject Index

A

Absorption wavelength, maximum,
    determination for mixed
    surfactants with azo oil dyes, 70
Activity coefficients
  based on the regular solution theory
      model, 31
  direct relationship with composition
      between micellar and
      pseudophase, 106
  direct relationship with mole
      fractions, 106
  micellar phase, mixed micelle
      formation, 34
  nonaethoxylated alcohols, 302
  representing the mixture critical
      micelle concentration, 31
Admicelles
  adsorption, positive deviations from
      ideality discussed, 206-214

Admicelles--Continued
  definition, 201
  formation on heterogeneous
      surfaces, 332
  formation on solid surfaces, 331-333
  importance of surface influence on
      components, 332
  mixed
    adsorption on alumina, 206
    materials used in formation
        thermodynamics study, 203
    nonideality compared to mixed
        micelles, 332
    predicted adsorption isotherms
        from ideal solution
        theory, 206
    theory, 203-205
  surfactants tendency to form, 17-18
  theory and development history, 203
Adsorption
  anionic surfactants on metal oxide
      surfaces, 201

338

E

Electrical work, micelle
    formation, 186
Electron microscope, photograph, 275f
Emulsification properties, mixed
    nonaethoxylated alcohol
    solution, 305
Emulsion
  characteristics of nonaethoxylated
      alcohol solution, 307-308f
  droplets, binary surfactant
      systems, 247t
  preparation under controlled
      conditions, 243
Enthalpies of
    dilution, 1-butoxyethanol, 82t
Enthalpies of transfer
  1-butoxyethanol from water
      to sodium decanoate, 86
  sodium decanoate from water to
      1-butoxyethanol, 86
Enthalpy
  micellization for nonylphenol
      ethoxylates, 42t
  mixing decylbenzene sulfonate
      micelles with nonylphenol
      ethoxylate micelles, 42t
Entropy, micellization for nonyl-
    phenol ethoxylates, 42t
Equilibrium constant, mixed micelle
    formation, 34
Excess free energy of mixing, mixed
    surfactant systems, 31-32

F

Fading rate, examined for azo oil dyes
    in mixed surfactant systems, 74-77
Fisher-Taylor-Hirschfelder atom model
  methanol-bis(2-ethylhexyl) sodium
      sulfosuccinate complex, 291f
  methanol-bis(2-ethylhexyl) sodium
      sulfosuccinate dimer, 287
Flotability, related to surfactant
    adsorption layer, 218
Flotation recovery
  barite as dependent on sodium
      alkysulfate
      concentration, 221f,222f,223f
  fluorite, as dependent on sodium
      dodecylbenzene sulfonate
      concentration, 220f
  quartz, as dependent on
      cetylpyridinium chloride
      concentration, 221f
Fluorescence intensity
  ANS probe in aqueous single
      surfactant solution, 62

Fluorescence intensity--Continued
  ANS probe in fluorocarbon
      surfactant solution, 63
  concentration of
      surfactant, 64f
Fluorescence probe
  characterization tool, 90
  instrumentation used in calcium
      alkarylsulfonate study, 91
  limits of application, 90
  1-pyrene carboxaldehyde, 95
Fluorescence spectra,
    dioctadecyldimethylammonium
    chloride, 280f
Fluorocarbon surfactants,
    characteristics, 184
Foaming, mixed nonaethoxylated
    alcohol solution, 305
Free energy
  adsorption
    binary surfactant systems, 231
    single surfactant systems, 230-231
  calculated for mixed micelles, 41t
  gain, when hydrocarbon part of
      surfactants transferred from
      aqueous to hydrocarbon
      environment, 231-232
  micellization, single
      surfactant systems, 231
  mixing, surface phase
      for surfactant mixtures, 229-230

G

Gibbs adsorption equation, case of
    mixed aqueous solution, 174
Gibbs equation
  nonionic monolayer and an ionized
      surfactant application, 134
  surface adsorption of binary mixed
      systems, 188
Glycoursodeoxycholate, gallstone
    treatment method, 256
Gouy-Chapman theory, discussed, 129

H

Head group interactions, surface
    properties of mixed surfactants
    altered, 129
Heat capacities
  sodium decanoate, 82
  sodium decanoate solutions, 83f
Heat capacities of
    transfer, 2-butoxyethanol
    solutions, 83f

Micelles--Continued
    equation, 180-181
    nonaethoxylated
        alcohols, 302-305
    polyoxyethylene carboxylate and
        alkyl poly(oxyethylene)
        ether systems, 72
    synergism, 152-153
free energy, calculated for, 41t
interaction parameter
    obtained, 153
model predictions and measured
    value differences
    explained, 40-43
monomer activity measurement
    activity measurement methods,
        40-43
    concentration of a binary
        mixture, 4
        phase chemical potentials, 33
    negative deviation from
        ideality, 7-9
    nonideal description, 11
    polyethoxylated surfactants
        examined, 10
    positive deviations from
        ideality, 12
    surfactant interaction described
        by solution theory, 7
    synergism in formation, 153t
    thermodynamic models, experimental
        conditions, 34-35
    thermodynamics of formation, 33-34
practical processes, example, 2
size and shape, 327
solubilization, 15
transition to other aggregates, 327
Micellization
    azeotropes
        calculated for MAM, 49
        pseudophase separation model, 51
    descriptive equations, 185-187
    feasibility in methanol, 286
    fluorocarbon and hydrocarbon
        surfactants, 184-198
    mixed, new mathematical
        models, 44-59
    standard free energy, relationship to
        average hydrocarbon chain
        length, 307f
    thermodynamic properties for various
        surfactants, 35t
Minerals
    adsorption, electrokinetic, and
        flotation properties above the
        CMC, 216-224
    flotation basis, 216
    hydrophobicity, 216
    materials and methods used in
        flotation properties study, 217
Mixed absorbed films, investigation
    approaches at oil-water
    interface, 312

Mixed monolayer model, nonideal, based
    on the pseudo-phase separation
    approach, 102-113
Model development, mixed micelle
    formation, 328
Molecular assemblies
    behavior of dialkyl
        amphiphiles, 279-281
    growth
        apparatus used in study, 272
        materials used in study, 271-272
        mild surfactant solutions, 270-281
        procedures used in study, 272
    polarity examined by fluorescence
        spectra, 279
Monolayers
    equilibrium studies of surfactant
        penetration outlined, 134
    formation
        definition, 13
        mechanism, 13-14
        phase transition at low surface
            coverage at the air-water
            interface, 330
        thermodynamic interest
            examined, 330
    history of surfactant
        interactions, 133-134
    mixed
        interaction parameters defined,
            equation, 146
        studied for octadecyldimethylamine
            oxide-sodium octadecyl sulfate
            system, 121
    penetration by surfactants, 133-141
    properties, materials and
        preparations in
        experiment, 117-118
    theory of surfactant
        penetration, 134-136
Monomer
    activities, concentration
        determination discussed, 325-326
    concentrations, surfactants, binary
        system, total, 8t
Monomer-micelle equilibrium
    description, 3
    measurement of surfactant
        species, 331
    surfactant systems, 6f
Mutual phobicity
    existence between hydrocarbon and
        fluorocarbon chains, 179
    interaction parameter
        influenced, 180

                            N

Nonaethoxylated fatty alcohols
    effects of different distribution of